Cloud point extraction of proteins and characterisation by liquid chromatography and mass spectrometry

Dissertation

zur Erlangung des akademischen Grades
doctor rerum naturalium (Dr. rer. nat.)
der mathematisch-naturwissenschaftlichen Fakultät
der Universität Rostock

vorgelegt von
Dipl.-Chem. Ria Fritz

Rostock 2013

urn:nbn:de:gbv:28-diss2014-0113-4

Eingereicht am 04.11.2013

Verteidigung: 01.04.2014

Die vorliegende Arbeit wurde im Zeitraum von September 2008 bis Oktober 2013 am Institut für Chemie der Universität Rostock angefertigt.

Danksagung

Ein großes Dankeschön gilt vor allem Herrn Prof. Dr. Udo Kragl, der mir mit Vergabe dieser Arbeit die Möglichkeit geboten hat, mein fachliches Interesse in der Arbeitsgruppe „Technische Chemie“ weiter zu verfolgen. Auch für den fachlichen Beistand mit anregenden Diskussionen, die mir immer einen frischen Blickwinkel auf meine Ergebnisse erlaubt haben sowie für die Möglichkeiten, meine Arbeit auf internationalen Konferenzen und Tagungen zu präsentieren, möchte ich mich herzlich bedanken.

Mein Dank gilt auch ganz besonders Herrn Prof. Dr. Dr. Jens Pahnke für diese Dissertation die zentrale Problemstellung lieferte. Außerdem möchte ich mich bei Dr. Markus Krohn aus der AG Pahnke dafür bedanken, dass er die drei Mäusehirne, die ich in meiner Arbeit untersucht habe, präparierte und mir alle benötigten Aβ relevanten Proben und Standards bereitgestellt hat. Des Weiteren bin ich auch dankbar für die zuverlässige Beantwortung aller medizinischer Fragen die ich im Bezug auf Alzheimer’s hatte.

Danke auch an Herrn Dr. Ruth, dem ich nicht nur meine solide analytische Ausbildung, sondern auch die umfangreiche praktische Erfahrung mit LC-MS Geräten verdanke. Auch sein großer Erfahrungsschatz half mir oft über methodische Stolpersteine.

An dieser Stelle möchte ich auch der Universität Rostock und dem Graduiertenkolleg „Nachhaltigkeit in Katalyse und Technik“ für die finanzielle Unterstützung meiner Arbeit danken.

Vielen, vielen Dank auch an den Rest der AG Kragl! Abgesehen vom guten Arbeitsklima wurde es nie wirklich langweilig über den Tag. Ob große Kreuzworträtselrunden, Kickertuniere, WM Tipp-Spiele oder leckeres Waffelbacken, irgendwas hat meinen Tag immer bereichert. Besonders danken möchte ich Jenny und Anett, die immer ein offenes Ohr und alternative Ideen für meine analytischen Probleme hatten und das Arbeiten im Büro aufgelockert haben. Auch dem Rest der Mittagstruppe; Steffi, Sabine, Anne, Daniela, Regina und Frau Freitag möchte ich meinen Dank für die Gesellschaft in Mittags- und Kaffeepausen ausdrücken. Der guten Seele Frau Freitag möchte ich auch nochmal gesondert danken, für ihre konstante Hilfe und dem unerschöpflichen Wissen, wo alles steht.

Nicht zuletzt gilt mein Dank meinen Freunden und meiner Familie. Meinen Eltern dafür, dass sie mir diesen Weg überhaupt ermöglicht haben. Meinem kleinen Bruder dafür, dass er auch aus der Ferne immer für eine Unterhaltung und vor allem Ablenkung zu haben ist und mir das Gefühl gibt, das ich mit gutem Beispiel voran gehe. Meinem Verlobten und meiner „Zweitfamilie“ Arno, Karin, René und Yvonne möchte ich auch aus tiefstem Herzen für die Unterstützung in den letzten Jahren danken.

1. Gutachter Prof. Dr. Udo Kragl, Universität Rostock

2. Gutachter Prof. Dr. Ralf Zimmermann, Universität Rostock

Für Maik.

“And, as always happens, and happens far too soon, the strange and wonderful becomes a memory and a memory becomes a dream. Tomorrow it's gone.” – *Terry Pratchett*

Abstract

In Alzheimer's disease soluble protein oligomers of amyloid β 42 have been implicated as toxic species leading to degeneration and cell death of neurons. Standard enzyme-linked immunosorbent assays rely on specific antibody-antigen reactions but can not discern between different oligomeric species. For this work, cloud point extraction using Triton X-114 as non-ionic detergent component was chosen to extract hydrophobic proteins and possible Aβ42 species into the detergent phase formed upon temperature induced phase separation. Extracted proteins were identified following SDS PAGE by LC-MS/MS data analysis and characterised based on the relation of grand average hydropathicity index (GRAVY) to extraction phase, cellular location and function. Phase extraction behaviour was found to be far more dependent on cellular location and function than hydropaticity alone. Micelles appeared to emulate natural lipid bi-layer design, leading to a preferred extraction of membrane-related proteins into the detergent phase (~53 %) while cytoplasm-associated proteins were predominant in the aqueous phase (57-61 %).

CPE proved to be very beneficial for the isolation of Aβ oligomer species, significantly expanding the range of ELISA sample preparation protocols. Investigation of Aβ42 monomer phase separation behaviour revealed a probable low mass cut-off of Triton X-114 micelles and strong undesirable matrix interactions. A size exclusion chromatography – mass spectrometry method was developed with the prospective aim of providing simultaneous detection of multiple oligomeric species using characteristic charge state distributions. Optimisation efforts led to signal improvements of nearly +700 % for Aβ with a preliminary lower detection limit of 0.1 mg/mL Aβ42 monomer.

Publication

Fritz, R., W. Ruth, et al. (2009). "Assessment of acetone as an alternative to acetonitrile in peptide analysis by liquid chromatography/mass spectrometry."
Rapid Communication in Mass Spectrometry **23**: 2139-2145

Oral presentation

Fritz, R. (07.09.2010). "Detection of amyloid-β peptides by SEC-HPLC-MS"
30th International Symposium on the Separation of Proteins, Peptides and Polynucleotides, Bologna/Italy

Poster presentation

Fritz, R., W. Ruth, et al. (01.-04.09.2009). "Applying altenative solvents to analysis of proteins by liquid chromatography-mass spectrometry"
18th International Mass Spectrometry Conference, Bremen/Germany

I. Index

II. Index of figures

III. Index of tables

IV. Abbreviations

Aβ40, Aβ42	amyloid β protein with 40 or 42 amino acid sequence
AA	amino acid
amu	atomic mass unit
ATPS	aqueous two phase system
ATPMS	aqueous two phase micellar system
AD	Alzheimer's disease
APP	amyloid precursor protein
ADP	adenosyldiphosphate
ATP	adenosyltriphosphate
aq	aqueous phase
ACN	acetonitril
BSA	bovine serum albumin
BBB	blood brain barrier
bar	unit of pressure
°C	degree celsius
CPE	cloud point extraction
CBB	Coomassie Brilliant Blue
CID	collision induced dissociation
CP	cloud point
CMC	critical micelle concentration
CSD	charge state distribution
CSF	cerebral spinal fluid
CNS	central nervous system
CoA	coenzyme A
$CHCl_3$	chloroform
CNBr	cyanogen bromide
DMSO	dimethylsulfoxide
DNA	desoxyribonucleic acid
DC	direct current
Da	Dalton
EBI	European Bioinformatics Institute
E. *coli*	*Escherichia coli*
ESI	electrospray ionisation
ELISA	enzyme-linked immunosorbent assay
FCA	formic acid
FTICR	fourier transform ion cyclotron resonance
g	gram, unit of mass
x g	times gravitational force
GABA	γ-aminobutyric acid
GRAVY	grand average of hydropathicity index
h	hour, unit of time

HCl	chloric acid
k	kilo, 10^3
LC/MS	liquid chromatography mass spectrometry
LC-MS/MS	liquid chromatography tandem mass spectrometry
LCQ	LCQ Deca ion trap mass spectrometer
LTQ	linear trap quadrupol mass spectrometer
LMCO	low mass cut off
L	liter
LLE	liquid-liquid extraction
LDS	lithium dodecylsulfate
m	milli, 10^{-3}
µ	micro, 10^{-6}
M	$mol \cdot L^{-1}$
MALDI-TOF	matrix-assisted laser desorption ionisation time-of-flight
min	minute, unit of time
MS	mass spectrometry
MeOH	methanol
MRFA	peptide (methionine – arginine – phenylalanine – alanine)
MES	2-(*N*-morpholino)ethanesulfonic acid
m/z	mass to charge ratio
Δ m/z	mass difference between MS signals
n	nano, 10^{-9}
N_2	nitrogen
NH_4COOH	ammonium formate
NaCl	natrium chloride
NCBI	National Center of Biotechnological Information
NADH, NAD^+	nicotinamide adenine dinucleotide
O_2	oxygen
P	protein probability
P_i	inorganic phosphate
PBS	phosphate buffered solution
PEG	polyethylenglycol
PFF	peptide fragment fingerprinting
pI	isoelectric point
PICUP	photochemical induced cross-linking of unmodified proteins
PIR	Protein Information Resource
PMF	peptide mass fingerprinting
PONPE	polyoxyethylene nonyl phenyl ether
ppm	parts per million
®	registered trademark
r_0	size of ion trap, distance center ion trap to electrodes

RF	radio frequency
RI	refractive index
RNA	ribonucleic acid
R_f	relative mobility value
RPLC	reverse phase liquid chromatography
RP-HPLC	reverse phase high pressure liquid chromatography (= RPLC)
SDS PAGE	sodium dodecylsulfate polyacrylamide gelelectrophoresis
SEC	size exclusion chromatography
S_p	primary score
SRF	search results file
S, P	supernatant, precipitate
TBP	tri-n-butylphosphate
TCA	trichloroacetic acid
TIC	total ion current
tris	tris(hydroxymethyl)aminomethane chloride
U	direct current potential
UV	ultraviolet, detection method
UV/Vis	ultraviolet/visible light spectrum, detection method
V	volt, unit of voltage
V_0	void volume, SEC
V_t	elution volume
W	Watt
X	detergent phase
X in AA sequence	oxidised methionine
X-114	Triton X-114
1mer	monomer, monomeric protein species
2mer	dimer, dimeric protein species
3mer	trimer, trimeric protein species
4mer	tetramer, terameric protein species
5mer	pentamer, pentameric protein species
6mer	hexamer, hexameric protein species
7mer	Septamer, septameric protein species
8mer	octamer, octameric protein species
9mer	nonamer, nonameric protein species
10mer	decamer, decameric protein species
11mer	undecamer, undecameric protein species
12mer	dodecamer, dodecameric protein species

1. Introduction

Proteins are essential in the control and execution of countless biological processes in all living organisms. The intricate system can however be impaired by genetic diseases causing overproduction, damaging or altered processing of specific proteins. Especially neurodegenerative diseases have been associated with such imbalances leading to the progressive loss of structure and function of nerve cells. Table 1-1 summarizes common diseases as well as the corresponding proteins and deposits leading to the cognitive decline typical for these diseases.

Table 1-1 Neurodegenerative diseases (Taylor, Hardy et al. 2002)

Disease	Protein deposits	Toxic protein
Alzheimer's disease	Extracellular plaques	Amyloid β
	Intracellular tangles	Protein tau
Parkinson's disease	Lewy bodies	α-synuclein
Prion disease	Prion plaque	PrP
Polyglutamine disease (e.g. Huntington's disease)	Nuclear and cytoplasmic inclusions	Polyglutamine containing proteins
Tauopathy	Cytoplasmic tangles	Protein tau
Familial amyotrophic lateral sclerosis	Bunina bodies	SOD1

The symptoms and progression of Alzheimer's disease as a leading cause of dementia have first been described by the German physician Alois Alzheimer in 1906. During his practice at a mental facility in Frankfurt am Main he came across the now famous case of Auguste Deter who had developed severe memory impairment, became irrationally paranoid and could no longer recognize persons well known to her. Over the years Auguste stayed in the asylum her condition got increasingly worse. Even after his departure from the institution Alzheimer was interested in the causes of her illness and asked to study her brain post-mortem (Alzheimer 1911; Goedert and Ghetti 2007).

While Alzheimer was only able to visualize abnormal deposits (plagues and tangles) in the affected brain, the identity of involved components was only discovered 70 years later. Tangle filaments accumulate in nerve cells and consist of tau proteins; neuritic plagues are formed extracellular and mainly consist of the peptide amyloid β with 38 to 42 amino acids (Masters, Simms et al. 1985; Grundke-Iqbal, Iqbal et al. 1986).

The identification of the main components led to the formulation of the *amyloid cascade hypothesis* that proposed the deposition of amyloid β protein (Aβ) as a major component of plaques triggers the neurofibrillary tangles, neuron cell death, vascular damages and dementia (Hardy and Higgins 1992). Over the years that hypothesis has been thoroughly questioned since some experimental data was not in complete agreement with the theory. Abundance of amyloid plaques could not successfully be correlated to the observed degree of cognitive impairment. Levels of impairment correlate better with the concentrations of oligomeric soluble Aβ species (Klein, Krafft et al. 2001; Hardy and Selkoe 2002; Lesne, Koh et al. 2006; Townsend, Shankar et al. 2006; Haass and Selkoe 2007; Moore, Rangachari et al. 2009).

Amyloid β proteins are produced naturally by enzymatic degradation of a specific transmembrane protein (amyloid precursor protein, APP). Three enzymes are responsible for bioprocessing of APP on two different pathways (Fig 1-1). On the non-amyloidogenic

pathway (A) α-secretase degrades APP producing soluble, but non-toxic fragments. The amyloidogenic pathway (B) involves β- and γ-secretase to produce amyloid beta fragments of 38 to 42 amino acids. The length of the resulting peptide depends on various factors, many still unknown. An overproduction of the 42 amino acid species leads to accumulation into oligomers and plaque formation (Haass and Selkoe 2007).

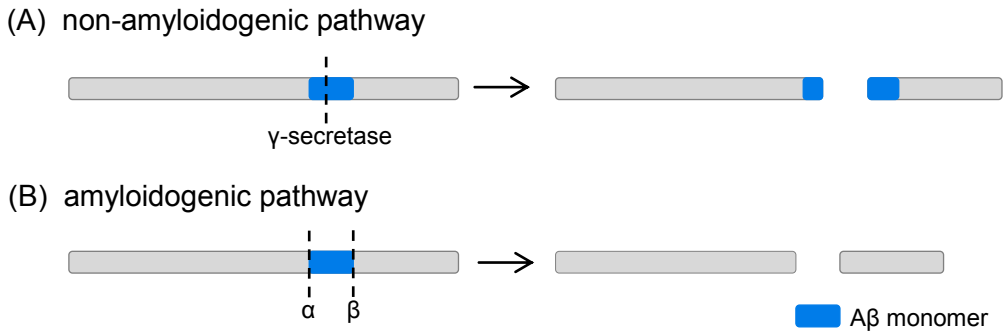

Figure 1-1 Processing pathways of amyloid precursor protein APP

Events that trigger an imbalance in amyloid β monomer levels and the onset of the disease could not yet be assigned to one specific cause but to several environmental risk factors and genetic preconditions have been identified. The major risk factor is age as the probability to develop AD doubles every five years from 65 years onwards. Occurrence of Alzheimer's disease is also more likely if one or more family members are or were affected. The onset familial AD is thought to be linked to a combination of environmental factors and risk genes (e.g. apolipoprotein APOE-e4, chromosome 19). Only in very rare cases (≤ 5%) Alzheimer's is directly caused by deterministic genes that guarantee the development of illness. Variations in genetic information for amyloid precursor protein (APP, chromosome 21), presenilin-1 (PS-1, chromosome 14) and presenilin-2 (PS-2, chromosome 1) lead to the onset of typical symptoms already at the ages 30 to 40 (Maurer and Hoyer 2006; Alzheimer's-Association 2012).

Even minute amounts of natural Aβ oligomers impede synaptic function significantly presumably by disrupting primary steps of signal transduction cascades between neurons involved in memory forming processes (Townsend, Shankar et al. 2006). Lesné et al studied mice that produced an APP variant associated with human AD but no tangles of tau protein and found that the Aβ42 monomer (4.5 kDa) could not solely be responsible for the observed cognitive decline and investigated soluble oligomeric species and proposed Aß56* (dodecamer, ~56 kDa) as most likely candidate for a potential pre-clinical detection of AD (Lesne, Koh et al. 2006).

Characterisation of the oligomerisation process and the involved soluble oligomeric species may prove to be the key to unlock the neurotoxicity mechanism and find new directions for medical treatments to inhibit or reverse the disease's progression. Structural studies have been performed with synthesised amyloid β species 40 and 42 in buffered solutions. To observe the formation process as well as metastable intermediates *photochemical induced cross-linking of unmodified proteins* (PICUP) was used to "freeze" oligomeric mixtures. A valuable insight was gained by analysis of such mixtures by ion mobility mass spectrometry that allowed accurate determination of oligmer cross-sections. Bernstein et al. used the data to propose a mechanism for oligomerisation and subsequent plaque formation confirming the occurrence of toxic dodecamers of Aβ42 (Bitan and Teplow 2004; Bernstein, Dupuis et al. 2009).

The analysis of oligomeric Aβ species is therefore of importance in the examination of the disease's progression and could provide indicators for early diagnosis and allow the development of medical approaches for treatment. The biggest challenges in the analysis of brain proteins lie in the biological matrix itself and the low concentration of the toxic protein species requiring sample preparation methods suitable to cope with the extraordinary high fat content of the tissue while providing stable extraction conditions for proteins.

Mass spectrometric detection of peptides and proteins is a uniquely sensitive and flexible detection method. A mass spectrometer can act as a general detector for unusual chromatographic techniques like size-exclusion separating biomolecules like soluble Aβ species by molecular size or provide extensive chromatographic and mass spectrometric data of protein digests to identify unknown proteins to characterize protein extracts. The ability to respond not only to a specific property of a protein is required for very sensitive standard approach of immune-based detection methods like ELISA but also to record additional data allowing the simultaneous detection and characterization of other sample components and multiple oligomer species (SEC-MS).

A combination of a sample preparation method designed to extract hydrophobic molecules like soluble amyloid β species (cloud point extraction) and mass spectrometric detection has the potential to broaden the insight into brain tissue extracts.

2. Scope of the work

The aim of this work is the investigation of possible alternative analytical methods to immunology based methods for the detection of the small protein fragment amyloid β implicated in the pathology of Alzheimer's disease. The workflow is schematically expressed in figure 2-1.

The application of liquid chromatography-mass spectrometry is the central focus in method research and development. Since typical extraction methods used to isolate amyloid β from brain tissue entail the use of concentrated and buffered salt solutions incompatible with the sensitive instrumentation, an extraction method is needed to isolate monomeric and ideally oligomeric forms of amyloid β while keeping the ionic strength as low as possible.

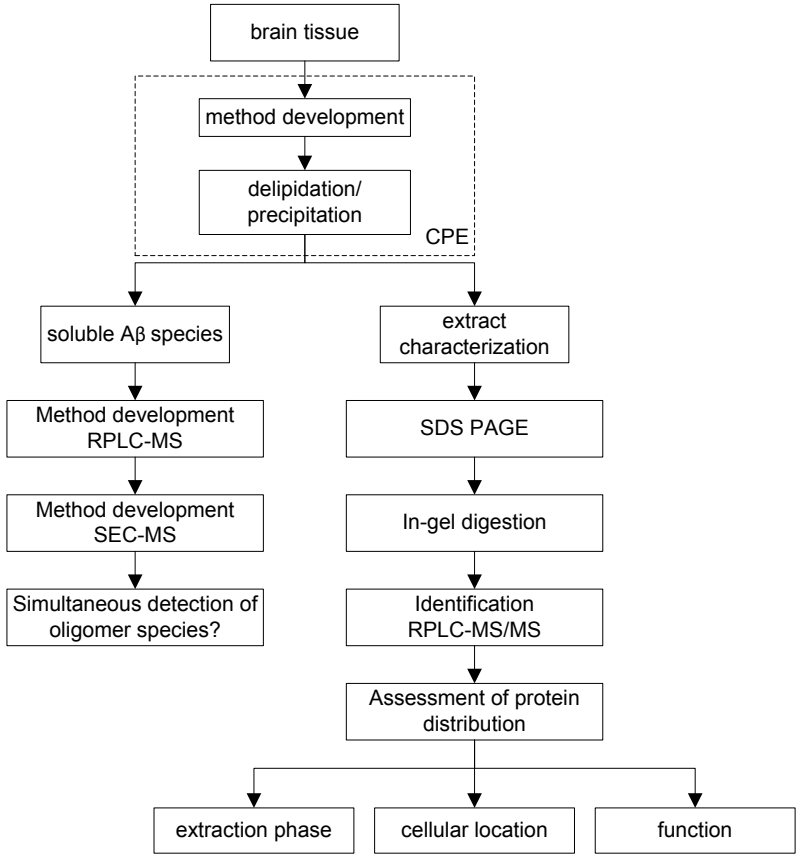

Figure 2-1 Schematic work flow diagram

Cloud point extraction incorporating a water/detergent system was chosen based on the advantageous property that the system can be switched from a homogenous aqueous solution with detergent micelles to a two-phase system by raising the temperature over a specific cloud point temperature separating proteins between a hydrophilic aqueous phase and hydrophobic micelle-rich phase. Existing publications were to be developed to fulfil the task of extracting hydrophobic proteins from mouse brain tissue by determining the

best sample preparation strategy (Bordier 1981; Shevchenko, Sjodin et al. 2010). Various extraction solution compositions as well as precipitation and delipidation methods are tested to optimise the extraction process. Successfully extracted protein samples are then subjected to two alternate examination approaches.

On the one hand the focus will be laid on the detection of amyloid β species with chromatographic and mass spectrometric methods. In comparison to immunology based methods that rely on very specific antibodies to identify amyloid species but cannot discern between monomeric and oligomeric forms mass spectrometric methods offer the identification of mass-to-ratio (m/z) patterns common to the various species.

Starting from traditional separation of proteins by reversed-phase chromatography involved parameters will be optimised to ensure the confident detection of Aβ42. Established parameters will be applied in the subsequent method development of a size exclusion chromatography method that would allow a separation of proteins in dependence of molecular weight-related size and the simultaneous mass spectrometric identification of amyloid β related peaks corresponding to soluble monomers and oligomers.

The characterisation of both extraction phases was on the other hand equally important for the assessment of the extraction process and possible prediction of extraction behaviour based on available data regarding cellular location and function as well as properties derived from amino acid sequences. Especially the relative hydropathicity index – an amino acid sequence based value theoretically determining a protein as hydrophilic or hydrophobic – will be used to examine CPE under the aspect of a "hydrophobic" extraction method for proteins. Samples of both extractions phases will be analysed by performing denaturing gel electrophoresis, tryptic digests of proteins bands, LC-MS/MS analysis and identification of detected proteins using the BioWorks^{TM} software. The electrophoretic separation and analysis of enzymatic digests will also provide confirmation if monomeric and oligomeric species of amyloid β are extracted.

3. State of the art review

This chapter describes analytical techniques and theoretical backgrounds of the methods chosen for this work to analyse and identify proteins and divided into two parts. The first part of the chapter focuses on sample preparation, separation and technical aspects of protein identification by liquid chromatography mass spectrometry. In addition, the merits of using size exclusion chromatography-mass spectrometry to analyse oligomeric protein species are highlighted. The second part of the chapter details cloud point extraction in non-ionic detergent aqueous two-phase micellar systems as a sample preparation method to extract hydrophobic proteins.

3.1 Protein analytics by LC-MS/MS

3.1.1 Liquid chromatography mass spectrometry of protein digests

The sheer number of proteins present after extraction and precipitation requires further sample preparation steps before they can be successfully identified by tandem mass spectrometry. Gel-based electrophoretic methods are able to separate complex protein samples according to molecular weight (one dimensional, 1D) and their isoelectric point (pI, two-dimensional, 2D). Subsequent degradation of immobilized proteins within the gel matrix produces peptides suited for liquid chromatography and the mass spectrometric detector mass range (Granvogl, Plöscher et al. 2007).

Sodium dodecylsulfate polyacrylamide gel electrophoresis (SDS-PAGE)

Proteins gain their specific properties and functions from the unique amino acid composition and their sequence within the molecule. Folding and twisting into intricate quaternate structures to enable enzymatic and metabolic functions relies predominantly on non-covalent bonds between amino acid side chains and covalent disulfide bridges between sulphur containing amino acids (cysteine C, methionine M) in close local vicinity in the folded protein. The ability of amino acids to act as both acid and base due to their functional groups and various side chains is reflected in the amphiphilic nature of proteins (see appendix A.3 for amino acid structures). The pH value at which a protein becomes charge-neutral is characteristic for each amino acid sequence and called *isoelectric point* or pI. Sample preparation in protein analytics is usually carried in buffered systems around physiological pH values (6-8) causing the majority of extracted proteins to retain charged moieties. Electrophoretic methods rely on the mobility of charged proteins in electric fields depending on their charge density and shape of the folded protein to achieve separation (Shapiro, Vinuela et al. 1967; O'Farrell 1975).

Fundamental advantages of modern electrophoretic methods stem from the utilisation of polymer matrices as separation media. Effects that would impair separation in solution, convection and diffusion, are minimised and analytes can be fixated within the matrix until the next sample preparation step. While natural polymers like agar gels find their application in standard DNA separations for DNA fingerprinting (Brdicka and Nurnberg 1993), most electrophoretic methods for protein separation use polymerization of

acrylamide with cross-linking agents like bis-acrylamide (N,N'-methylenebisacrylamide) to create gel matrices of varying acrylamide concentrations (5-25%) best suited for the required separation. Resulting three-dimensional net structures also act as molecular sieves further improving protein separation during electrophoresis. Lower acrylamide concentrations are best suited for proteins of high molecular weights while high percentages result in very fine sieve structures ideal for the separation of small proteins. Additional improvement can be obtained by gels with gradually increasing acrylamide concentrations, extending resolution and mass range.

As a purification technique *native electrophoresis* is performed on proteins while preserving their natural charge distribution and form to isolate active enzymes or protein complexes. While mobility in the electric field and the gel matrix is dependent on multiple factors, impurities can be easily removed if the separation behaviour of the isolated protein is known. The major disadvantage is the unpredictability of the separation process for unknown protein mixtures since charge distribution and molecular diameter of the folded native proteins are controlled by the specific amino acid sequence leading to the paradox that a smaller (molecular weight, shorter AA sequence) protein of elongated quaternary structure moves slower through the matrix than a significantly larger molecule of a more compact structure in a similar charge state. The apparent molecular weight of the smaller protein is perceived as higher than for the larger molecule. Similar effects occur for proteins of comparable molecular weights and structures but differing charge distributions (Schagger, Cramer et al. 1994).

To limit the number of factors influencing electrophoretic mobility, proteins are denatured by heat, detergents and reducing agents like dithiothreitol (DTT) to produce amino acid sequences in their primary structures as linear chains with consistent charge distributions. For *sodium dodecylsulfate polyacrylamide gel electrophoresis* (SDS-PAGE) the eponymous ionic detergent binds headfirst to the amide bond backbone in the constant ratio of 1.4 : 1, overlaying individual charges of each protein with a uniformly negative charge (Reynolds and Tanford 1970). Sulphur-containing reducing agents break up eventual disulfide bridges that would withstand denaturation by heat alone. Thusly prepared protein samples are separated solely based on their molecular weight. Simultaneous separation of standard mixtures with known molecular weights allows a rough estimation of molecular weights (Shapiro, Vinuela et al. 1967; Weber and Osborn 1969; Neville 1971).

Visualisation of proteins in gel after electrophoresis is the most important step to evaluate the separation quality and designate protein bands for further analysis and identification. Various dyes are available to stain proteins within the gel matrix. *Silver staining* relies on binding of silver ions to sulfhydryl and carboxyl groups at low pH values, colouring protein bands distinctively black by reducing silver under basic conditions. Despite being highly sensitive (0.5 ng per band) the required and time consuming removal of silver as well as possible inhibition of enzymatic digestion prior to LC/MS diminishes its practical application (Heukeshoven and Dernick 1985; Merril and Pratt 1986; Richert, Luche et al. 2004).

In an attempt to achieve high sensitivity and compatibility to mass spectrometric methods *fluorescent dyes* where developed. Complexes of organic compounds and heavy metal components or purely organic dyes bind to proteins enabling excitation at defined wavelengths and detecting the resulting fluorescent signal. The need for expensive equipment, the non-permanent nature of light sensitivity and invisibility of stained proteins to the naked eye renders fluorescent dyes relatively impractical for manual

excision of protein bands for in-gel digestion (Berggren, Chernokalskaya et al. 2000; Candiano, Bruschi et al. 2004).

Coomassie dyes, developed in 1963 by Fazekas et al, are generally preferred over more sensitive dyes due to the method's simplicity, reliability and compatibility with subsequent treatments for MS experiments. Binding to proteins via ionic or hydrophobic association, favourably to the basic amino acids lysine (Lys, L), histidine (His, H) and arginine (Arg, R), in a constant ratio (1.4 mg dye per 1 mg protein) the Coomassie dyes Brilliant Blue R-250 and G-250 dyes are able to detect down to 30 ng protein per band (Fazekas, Webster et al. 1963; Tal, Silberstein et al. 1985; Neuhoff, Arold et al. 1988; Patton 2002). Traditional staining protocols can be time consuming (15 hours) and entail the use of trichloroacetic acid, acetic acid and methanol to fixate and stain as well as remove excess stain from the gel matrix. In recent years commercially available staining methods have been developed with the aim of reducing the use of toxic solvents and incubation times in favour of environmentally friendly staining solutions, heat and colloidal dyes. Implementing microwave procedures to aid fast heating and the permanent fixation of proteins within the matrix has reduced the overall time consumption of the procedure to less than 1 hour (Nesatyy, Dacanay et al. 2002).

In-gel digestion of proteins

Degradation of proteins into smaller peptides while still fixated within the gel matrix is essential for mass spectrometric data generation and protein identification. Cleavage can be chemically or enzymatically induced, the extent controlled by the chosen agent.

Two prominent examples for the less frequently used chemical cleavage are strong acids and cyanogen bromide (CNBr). The idea of acid hydrolysis can be related to digestive conditions in stomachs. Unfortunately, the method shows limited cleavage specificity leading to very complex peptide and amino acid mixtures unfit for protein identification algorithms. Cyanogen bromide cleaves specifically at methionine (met, M) under highly acidic conditions ($\geq$ 70% trifluoroacetic acid). The statistically low abundance of methionine in protein sequences however leads to large peptides that are difficult to extract from the gel (Gobom, Mirgorodskaya et al. 1999; Hollemeyer, Heinzle et al. 2002; Quach, Li et al. 2003; Granvogl, Plöscher et al. 2007).

Enzymatic digestion of proteins offers both predictability of resulting peptides and high probability of molecular weights within the desired ranges for mass spectrometry. General procedure based on improvements to original method first described in 1992 by Rosenfeldt et al for an in-gel enzymatic digest is depicted in figure 3-1 (Rosenfeld, Capdevielle et al. 1992; Granvogl, Plöscher et al. 2007).

After electrophoretic separation and staining, proteins are trapped inside the three dimensional structure of the gel (1). To prepare the proteins for digestion, residual Coomassie dye (Coomassie Brilliant Blue – CBB) has to be removed by incubation with acetonitrile-water mixtures (2). The net structure preventing proteins from diffusing out of the matrix limits the size of applicable proteolytic enzymes (proteases). Based on the idea that dehydration of the gel piece entrapping a protein and rehydration with protease solution gives the protease a directional pull into the matrix a respective step is included in the majority of enzymatic digestion methods (3). Though it has been argued that the low diffusion coefficient within the gel matrix negates any positive effect on digestion only increasing solvent absorption (Granvogl, Gruber et al. 2007).

Incubation temperature and duration depends on the chosen protease, but is traditionally performed overnight. Several attempts to optimise the lengthy process by accommodating

specific requirements such as pH value, incubation temperature, sample volume and surface-to-volume ratio of gel pieces have shown that complete digestion can be achieved within 30 minutes (Havlis, Thomas et al. 2003). Alternative ways of introducing energy into the enzymatic reaction system have also been investigated. By replacing incubation at constant temperatures for several hours with microwave irradiation for a few minutes or an ultrasonic field for one minute, comparable digestion results have been obtained (Juan, Chang et al. 2005; Lopez-Ferrer, Capelo et al. 2005; Vesper, Mi et al. 2005; Sun, Gao et al. 2006).

Peptides are small enough to be extracted from gel matrix by diffusion (4). To account for varying physicochemical properties a sequential extraction of hydrophilic peptides with dilute formic acid and hydrophobic peptides with solutions containing high amounts (30-50%) organic solvent, most often acetonitrile is necessary (Feick and Shiozawa 1990; Castellanos-Serra, Ramos et al. 2005).

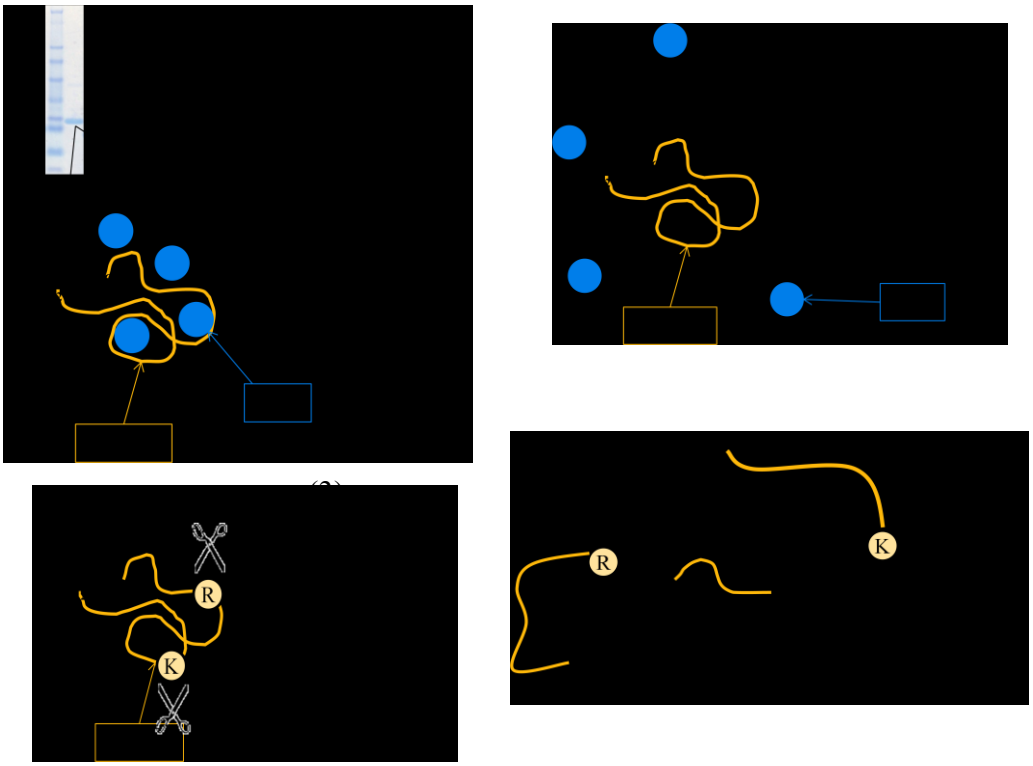

Figure 3-1 General procedure for in-gel enzymatic digestion for trypsin (from Granvogl et al. 2007)

Even minute amounts of anorganic salt have highly negative effects on the electrospray ionisation process and have to be removed prior to LC-MS analysis by evaporation. Ammonium bicarbonate as a volatile buffer salt is removed as ammonia and carbon dioxide (Espada and Rivera-Sagredo 2003).

Scissor symbols in fig. 3-1 represent the serine endopeptidase trypsin, the most commonly used enzyme for in-gel digestions. Cleavage of peptide bonds occurs specifically after lysine (Lys, K) and arginine (Arg, R). The substrate binding site within the enzyme is deep, narrow and possesses a negatively charged aspartate moiety at its bottom to bind basic amino acids via ionic interactions. Following the lock and key principle of enzyme catalysis target amino acids have to exhibit long side chains and the ability to hold a positive charge. Of the proteinogenic amino acids (appendix A-2) only lysine and arginine fulfil these requirements. The combined statistical distribution of both amino acids generally guarantees an optimal mass range of resulting peptides.

Deviation from this routine often originates in demands of the analysed protein and mass spectrometric detection. Smaller peptides are produced by proteases with lower specificities like pepsin (specific for phenylalanine F, methionine M, leucine L and tryptophane W). Sequential digestion by proteases that cut C- or N-terminally after one specific amino acid is helpful in determination of unknown primary sequences. Endoproteases like Lys-C, Glu-C (aspartate D and glutamic acid E) as well as Asp-N (aspartate D) are used in separate digestions of the same protein. Peptide sequence information from mass spectrometric analysis overlaps ensuring complete coverage of the protein (Scheler, Lamer et al. 1998; Michalski and Shiell 1999; Choudhary, Wu et al. 2003; Reinders, Lewandrowski et al. 2004).

Liquid chromatography mass spectrometry

The number of peptides generated by chemical or enzymatic digestion can range from very low for small proteins to fairly high for large proteins and if more than one protein is present in the protein band. Introducing such complex mixtures directly into a mass spectrometer may prove disadvantageous for protein identification. While in theory all peptides can be observed and submitted to fragmentation by tandem mass spectrometry (see chapter 3.1.2), in reality they stand in direct competition during the ionisation process causing data loss especially for peptides in low abundance (Cech and Enke 2001ab).

By coupling *high performance liquid chromatography* (HPLC) to mass spectrometry peptides are retained by apolar interactions with the stationary C18 phase (reverse phase conditions) dependent on amino acid composition and are detected separately (Gekko, Ohmae et al. 1998). Peptides introduced directly or eluting from a chromatographic column are contained in solution or mobile solvent phase that has to be vaporized to transfer charged analytes into gas phase before entering the mass spectrometer.

In the late 1980s John B. Fenn realized the potential of *electrospray ionisation* (ESI) as a gentle, non-destructive ionisation method for non-volatile, polar biomolecules like proteins and peptides at atmospheric pressure (Fenn, Mann et al. 1989). Peptides eluting from the column are transported to the ESI interface through a fine quartz capillary. The mobile phase is sprayed into fine droplets by a high voltage (3-5 kV) applied between the capillary opening (ESI needle) and a heated (200-300°C) transfer capillary at the mass detector entrance supported by sheath gas (N_2). The resulting electric field gradient leads to charge separation at the surface of the mobile phase, causing the liquid to form a "Taylor cone" (Fig 3-2).

Charge accumulation on the surface increases the effect of coulomb repulsion to equal or slightly surpass the surface tension of the liquid (Rayleigh limit) maintaining the cone. Droplets containing solvent, analyte molecules and an excess of positive or negative charges detach from the tip and are accelerated by the electric field (1). Droplets moving towards the detector loose solvent rapidly through evaporation and acquired charges concentrate on their surface until coulomb repulsion again surpasses surface tension and in a process called "coulomb explosion" the droplets burst into a series of even smaller, less charged droplets (2). The cycle of evaporation and coulomb explosion is repeated until only charged "naked" molecules remain in the gas phase (3) and enter the mass spectrometer (delaMora 1996; Cech and Enke 2001b).

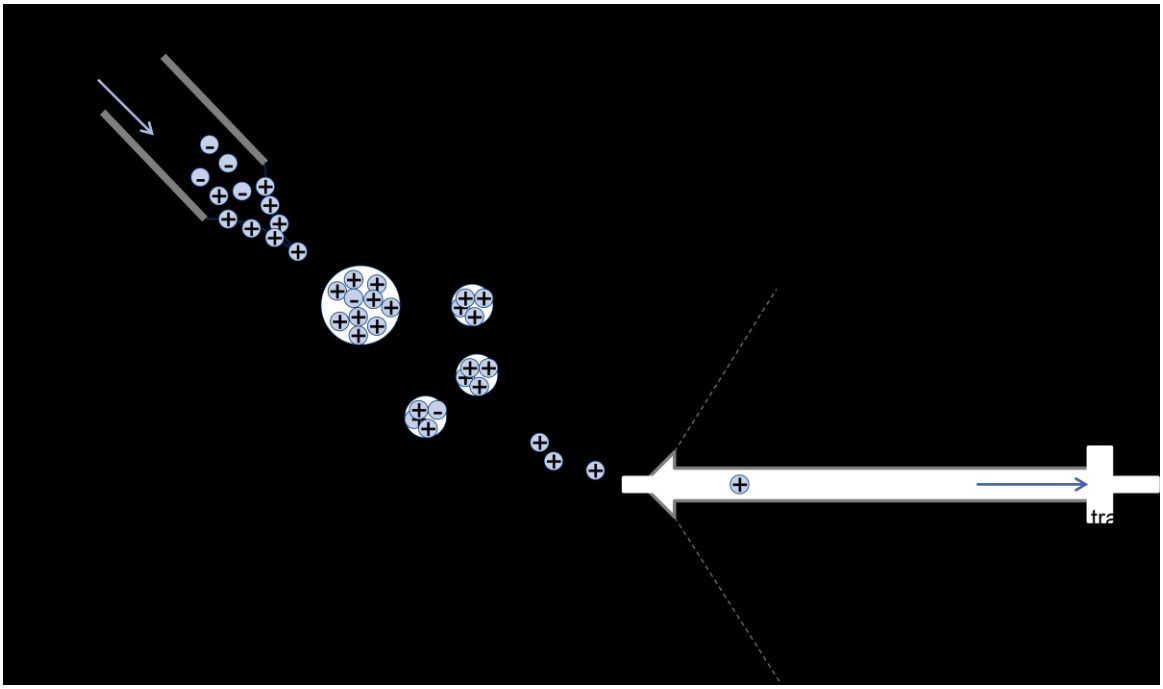

Figure 3-2 Electrospray ionisation. Formation of a Taylor cone (1) and subsequent coulomb explosions (2) leading to "naked" ions (3).

Ions enter the mass spectrometric system at atmospheric pressure but the actual detection in the ion trap occurs at very low pressures. The interface connecting the atmospheric pressure ionisation region to the low pressure detection system of the *linear trap quadrupole* (LTQ) from Thermo Finnigan consists of a heated metal capillary. High temperatures aid the further desolvation of ions as well as the separation of charged species from clusters with neutral species by collisions (Schwartz, Senko et al. 2002).

While charged ions, accelerated through the system by a series of quadrupoles and octapoles (*ion optics*) through compartments of decreasing pressure regiments, reach the ion trap as a focussed ion beam, neutral species and clusters of ions and neutral species are not affected by the electrical fields and are ejected through the vacuum system.

3.1.2 Data-dependent tandem mass spectrometry

Generating data sets for a maximum number of peptide ions during a chromatographic run is highly important for subsequent data analysis. While the resolution and mass accuracy of linear quadrupole ion trap mass spectrometers as the LTQ (Thermo Scientific) are limited in comparison to time-of-flight or quadrupole mass detectors their ability to hold a very high number of ions simultaneously and their fast scan rates allow the real time gathering of high resolution scans (ZOOMScans) and collision induced dissociation (CID) fragmentation data (Yates 2004).

Linear quadrupole ion trap data acquisition

All necessary steps to generate mass spectrometric data for both peptide and fragment ions can be conducted within the trap (*tandem in space*). Isolation, excitation and ejection are managed by dipole excitation with auxiliary alternating current voltages on the X-rods (Douglas 2005). In 2002 the design of a linear ion trap constructed by four hyperbolic

rods cut into three sections of 12, 37 and 12 mm with mass selective radial ejection was patented by Schwartz, Senko and Syka for Thermo Finnigan (Fig 3-3).

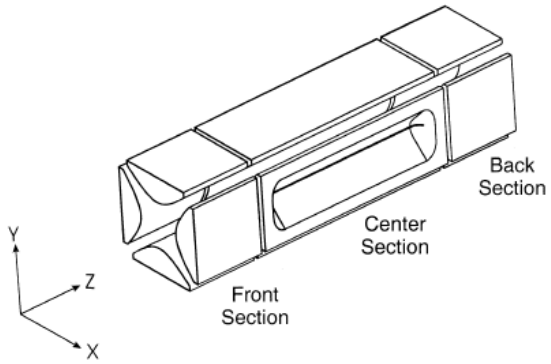

Figure 3-3 Basic design of linear quadrupole ion trap (Schwartz, Senko et al. 2002)

Application of a potential to the hyperbolic rods generates a quadrupole field forming a trapping potential well in the centre of the ion trap.

Ion traps are categorized as "dynamic" mass analysers since ion trajectories during the analysis are influenced by time-dependent forces and are therefore harder to predict than for "static" sector field instruments. Mathematically, the movement of ions within a quadrupole field can be described by Mathieu Equations (Eq. 3-1). Originally intended to investigate the mathematics of vibrating stretched skins, Mathieu provided the foundations to describe ion trajectories and their stability limits in 1868. Ions are confined on stable trajectories radially within the center section by applying radio frequency (RF) voltages and axially by direct current (DC) voltage on the end sections. Both rods along the x axis have a 30 x 0.25 mm slots as ejection paths, doubling the ion detection efficiency with conversion dynodes and electron multipliers on either side. A potential field created by quadrupoles (in contrast to hexa- or octapole) is uncoupled; enabling a separate determination of the involved forces on the ion for the x, y and z coordinates (Mathieu 1868; March 1997).

$$\frac{d^2x}{d\xi^2} + (a_x - 2q_x \cos 2\xi)x = 0 \qquad \textbf{Equation 3-1}$$

$$\xi = \frac{\Omega t}{2}$$

$$a_x = -\frac{8eU}{mr_0^2\,\Omega^2}$$

$$q_x = \frac{4eV}{mr_0^2\,\Omega^2}$$

$e -$ electric charge of ion
$\Omega -$ radial frequency, $\Omega = 2\pi f$
$U -$ direct current potential
$V -$ radio frequency potential
$r_0 -$ size of ion trap, distance centre ion trap to electrodes
$m -$ mass to charge ratio ion (m/z)

The influences of both the m/z ratio and the applied potentials are represented by the stability parameter a_x and q_x in equation 3-1. Most commercial ion trap mass detectors do not offer the application of direct currents (U) to the centre section of the quadrupole electrodes, rendering the influence of a inconsequential in predicting ion trajectory stabilities ($a_x = 0$).

Solutions of the Mathieu Equation are either periodic, but unstable and form boundaries of unstable regions within a stability diagram (Fig. 3-4), corresponding to the parameter β; or periodic and stable determining ion motion within stable regions of the diagram. The trapping parameter β, describing the boundaries at which ion trajectories become uncontrolled is connected to ion oscillation and a complex function of a and q. Figure 3-4 shows a simplified representation of plotting a_x vs. q_x to visualize the stability regions in which ions are contained on stable trajectories. The point at which the stability boundary $\beta_x = 1.0$ intersects with the axis at $a_x = 0$ has the q_x value of 0.908. It defines the lowest m/z ratio that can be stored within the trap at a given set of parameters and represents the "working point" for mass selective ion detection.

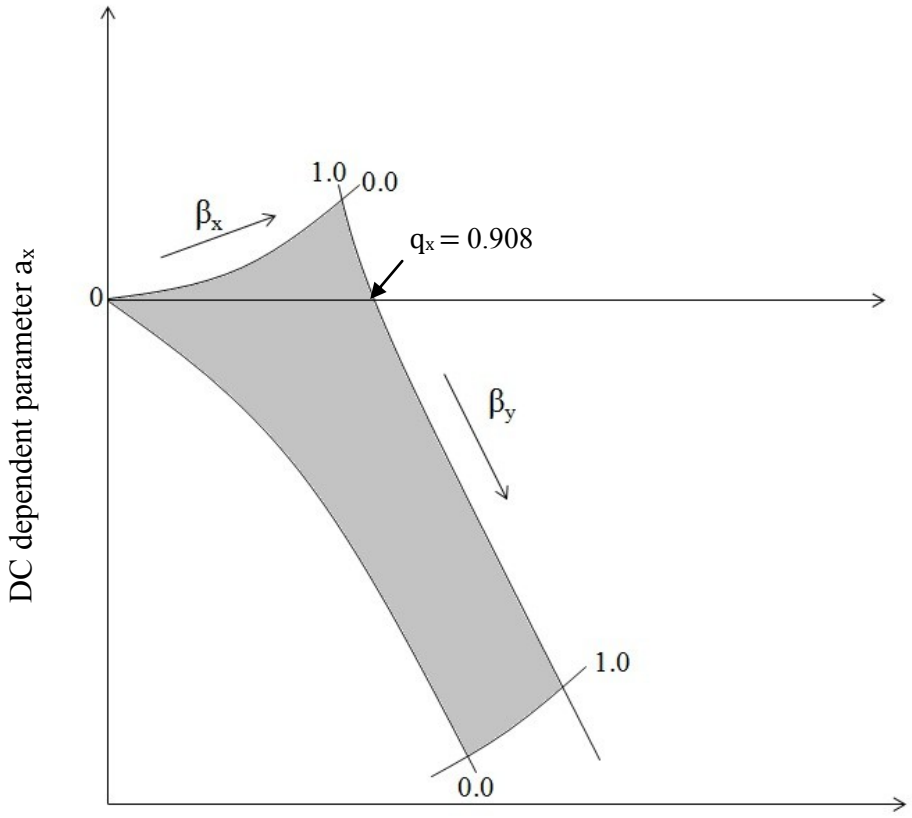

Figure 3-4 Schematic stability diagram for ion trajectories in linear quadrupole fields (March 1997)

After being accelerated through the ion optics of the mass spectrometer ions reaching the linear trap are gathered in the potential well at an initial RF voltage V_0 and radial frequency Ω defining both the low mass cut off (LMCO) and the mass range of the mass spectrometric experiment. To circumvent ion loss due to collisions with the electrodes, ions are "cooled down" and focussed to the centre section of the trap through collisions with helium buffer gas atoms (March 1997).

Each ion species is assigned a q_x value on the $a_x = 0$ axis; ions with high m/z ratios have lower q_x values nearer the origin whereas q_x values for low m/z ratio species extend towards the $q_x = 0.908$ stability boundary (Fig 3-5).

A "ramping" of the RF potential amplitude causes the q_x values of all ions to increase throughout the ramp. Once q_x reaches 0.908, the trajectories of ions at one specific m/z ratio become unstable and the ions are ejected axially through the electrodes generating a signal on the conversion dynode and secondary electron multiplier proportional to the number of ions ejected. Following the RF potential ramp of this "analytical scan" or "FullScan" all ions within the trap are ejected in ascending order of their mass-to-charge ratios. In data-dependent data acquisition FullScans serve as basis for the software to decide (according to user set parameters) which masses to subject to further isolation and fragmentation.

Peptide ions are often multiply charged during electrospray ionisation, leading to more than one corresponding mass signal in a FullScan. Typically the three to five most intensive signals of an analytical scan are selected for isolation and fragmentation. The probabilities of generating several fragmentation spectra for one peptide as well as the coverage of coeluting peptide ions are high.

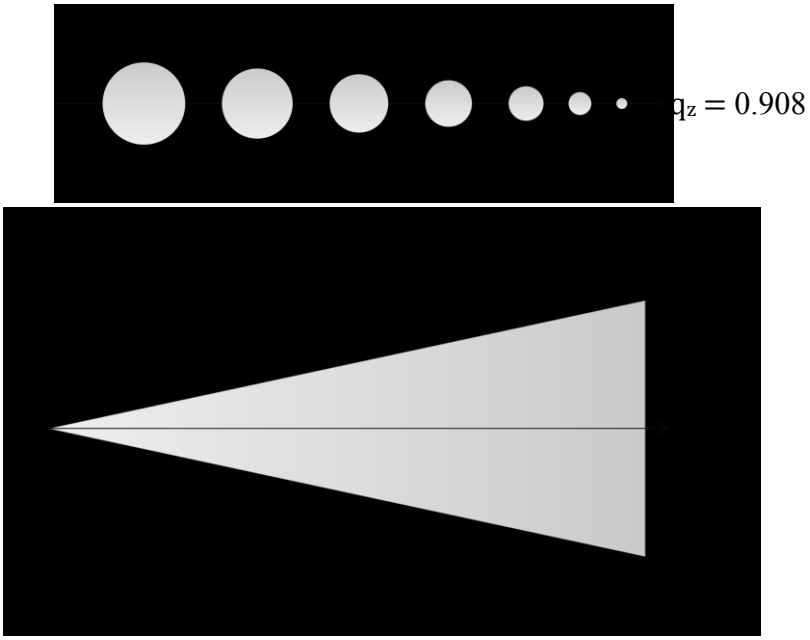

Figure 3-5 Ion distribution in stability region and schematic RF voltage amplitude ramp for analytical scans

Isolation of specific m/z ratios is similar to the performance of an analytical scan, but instead of destabilising all ions in the trap, the RF amplitude ramp exhibits a notch at the frequency of the target ions (Fig 3-6).

Two sets of information can be obtained from the isolated ions. In a high resolution scan of the very narrow m/z window, a so called "ZoomScan", the charge state of a peptide ion can be determined with the help of ^{13}C isotope signals. The apparent mass difference Δ m/z between the ^{12}C and ^{13}C signal is indirectly proportional to the charge state z. For a singly charged ion Δ m/z should be 1 amu, a difference of 0.5 amu indicates the presence of a doubly charged ion. An optional inclusion of ZoomScans into the data-dependent experiment provides the identification software with more accurate data regarding the correct molecular weight of the peptide.

Figure 3-6 Ion isolation in linear quadrupole

The most essential part of tandem mass spectrometry is the fragmentation of isolated peptide ions by *collision induced dissociation* (CID). Following the refocusing of trapped ions in the centre at q_x values of 0.25 to 0.35 a small supplementary oscillating potential at the secular frequency of the isolated ion species leads to resonant excitation and altered trajectories expanding the trapping field towards the end sections of the trap. With greater distance to the centre, ions are constantly accelerated and accumulate kinetic energy. Through subsequent momentum-exchanging collision with helium atoms the internal energy of the ions is incrementally raised until fragmentation occurs. Precise control of the CID process is necessary to achieve good fragmentation data. The time difference for kinetic energy (µs scale) and internal energy (ms scale) to affect ions in the trap has to be carefully balanced, so that ions are allowed to accumulate internal energy and fragment but the remaining intact ions are not ejected from the trap (March 1997; Douglas, Frank et al. 2005). After applying the CID process on the isolated ions for a defined amount of time, a second FullScan is performed to eject the fragment ions from the trap in order of their m/z ratios, resulting in the MS/MS spectrum for the isolated peptide ion.

Peptide fragmentation and nomenclature

The fragmentation of peptide molecules during the CID in the ion trap is not a random process. Parameters of the trap and sequence specific properties like number of charges (ESI = high probability of multiply charged peptide ions in trap) influence the fragmentation patterns (Hunt 1986; Paizs and Suhai 2005). Bond dissociation prevalently occurs at amide bonds between amino acids within the peptide ions resulting in characteristic fragment ions that subsequently allow the identification as well as the sequencing of the peptide. While the intensity and probability of the possible fragment ions is not yet predictable and varies with sequence and CID parameters, the fragmentation along the amide bond "backbone" of peptides was recognized as a predictable outcome by Roepstorff and Fohlmann in 1984 who suggested a nomenclature for these fragments (Roepstorff and Fohlman 1984; Huang, Tseng et al. 2008).

Under consideration of the three most likely locations for bond dissociation the potential fragment ions were named A, B (amide bond) and C ions, if the resulting charge is localized C-terminally and X, Y and Z for N-terminal charges. Tuinman and Pettit introduced the switch from capital letters to lower-case letters to prevent confusion of peptide fragment ions with the one letter code for amino acids. Figure 3-7 depicts the now standardized peptide fragmentation nomenclature (Tuinman and Pettit 1990).

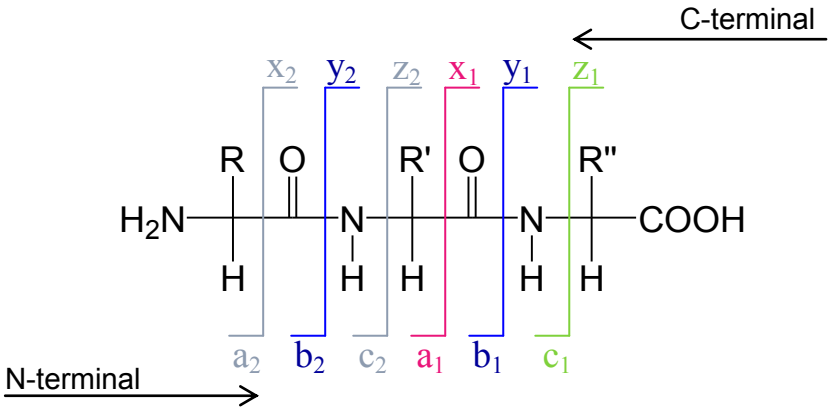

Figure 3-7 Peptide fragment ion nomenclature according to Tuinman et al. (1990)

Despite the apparent simplicity of peptide fragmentation during CID not every possible pair of b/y ions is observed in the fragmentation mass spectra. Not yet fully understood fragmentation processes lead to higher intensities of certain fragment ions (Johnson, Martin et al. 1988). Possible fragmentation mechanisms have been extensively investigated in hope of a clearer picture of the involved pathways and the influence of amino acid sequences on ion formation preferences.

Through statistical evaluation of MS/MS spectra of peptide fragmentations Tabb et al. found that prolin (Pro, P) within the peptide sequence favoured N-terminal amide bond dissociation resulting in increased formation of b ions. Peptides containing histidin (His, H) seem to prefer C-terminal bond dissociation, portrayed by high intensities for the corresponding y ions (Tabb, Smith et al. 2003).

By correlating peptide fragmentation to specific properties like amino acid sequence the prediction of favoured fragmentation pathways and the resulting ion intensities in mass spectra should be possible. Peptides could then not only be identified by comparing theoretical fragmentation patterns to measured spectra, but also by correlating observed ion intensities to predictions adding another identifying component to data analysis. Theorized fragmentation pathways can be classified as either *charge-remote* or *charge-induced* mechanisms. The parameters of collision-induced dissociations in ion trap mass spectrometers promote the fragmentation of the majority of ions via charge-induced pathways. The migration of "mobile" protons acquired during electrospray ionisation towards the amide nitrogen causes two effects. On the one hand the amide bond is weakened through and the carbon atom of the protonated amide group is vulnerable to nucleophilic attacks either from the oxygen of the adjacent N-terminal amide bond (b_x-y_z pathways) or the nitrogen of the N-terminal amino group (diketopiperazin pathways). Further rearrangements lead to the formation of the typical b and y ions (Johnson, Martin et al. 1988; Paizs and Suhai 2004; 2005).

3.1.3 Data analysis software and algorithm

Protein identification and characterisation using mass spectrometry can, in theory, be achieved from two directions. In the "top-down" approach the exact molecular weight and gas phase fragmentation of intact proteins is observed to gain insight into post-translational modifications and structural characteristics. Aside from the need for very accurate instrumentation (preferably FTICR mass detectors) the lower efficiency in protein identification, sensitivity and throughput and the not yet well-controlled

fragmentation within the ICR cell are the causes for the preference of the alternative approach to protein identification (Canas, Lopez-Ferrer et al. 2006). The "bottom-up" or "shotgun" approach entails the analysis of proteins on the peptide level. Enzymatic digestion generates specific peptide mixtures that are analysed by mass spectrometric experiments (Yates 2004).

Different algorithms and tools have been developed to analyse data generated from bottom-up experiments. Strategies to identify peptides and their corresponding proteins depend on the experimental set up. For *peptide mass fingerprinting* (PMF) the enzymatic digest of a protein is directly introduced into a mass spectrometer, often *matrix-assisted laser desorption ionisation* devices with *time-of-flight* mass analysers (MALDI-TOF), creating unique peptide mass maps of the digests. Through the correlation to *in silico* digests of proteins in a sequence database and their theoretical peptides, the most fitting results are assigned to the data sets (James, Quadroni et al. 1993; Pappin, Hojrup et al. 1993).

Identification via sequence information gathered through fragmentation of peptide precursor ions and the collection of MS/MS data is called *peptide fragment fingerprinting* (PFF). PFF data sets are most frequently analysed using Mascot (with the MOWSE scoring algorithm) or Sequest, implementing a scoring algorithm of the same name. In Mascot scoring possible matches to experimental data is based on the statistical evaluation of matches between experimental and theoretical peptide fragment ions rather than cross correlation that is the basis of Sequest score assignment (Perkins, Pappin et al. 1999).

Protein identification in this work was achieved by using the Sequest algorithm implemented in the software "BioWorks™" (Thermo Scientific). Figure 3-8 on the following page shows a general overview of the protein identification process for one peptide in correlation to the experimental data set.

All protein identification programs and their algorithms need protein sequence data to be able to compare experimental MS data to theoretical masses and fragments. The achievements in proteomic projects like the human genome project are providing ever growing numbers of protein sequences from genomic data that are publicly available and constantly updated. Protein databases can be downloaded from various organisations like the Protein Information Resource (PIR) or the European Bioinformatics Institute (EBI) (Barker, Garavelli et al. 1999; Venter, Adams et al. 2001; Wu, Apweiler et al. 2006).

UniProt is one of the best known protein databases and is regularly expanded with new or updated entries. The database in its original form encompasses all known protein sequences for a vast field of organisms that have been studied. To reduce processing time and also the probability of a significant identification of a protein the database has to be reduced by creating a subset of data, specified by certain parameters like organism or species. The protein information is stored in the FASTA file format. Protein sequences and information are listed in text format, the sequence amino acids are represented by single letter code.

The first step in the data analysis process is the extraction of relevant data from liquid chromatography mass spectrometry data sets. Searching the chromatogram from left to right, each scan is examined to find possible peptide ions. If a peptide ion is found, the general process of data extraction is stopped and subsequent scans are examined for peptide ions of the same mass. The collective data from FullScans, ZoomScans and MS/MS experiments for the peptide ion is summarised in an input file (.dta) containing the molecular weight of the protonated peptide, the charge state (from optional ZOOMScans) as well as the combined MS/MS spectra of all relevant scans.

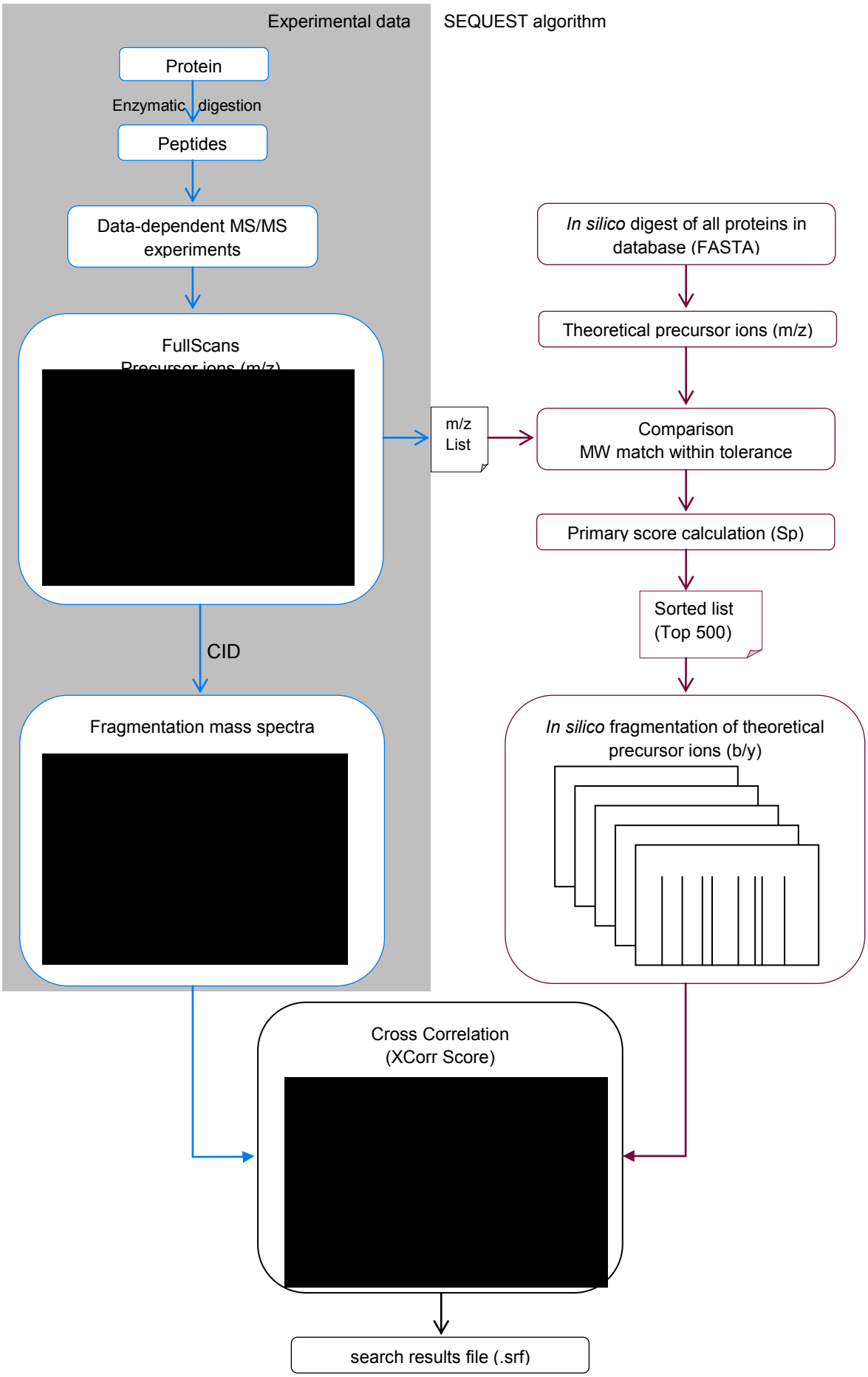

Figure 3-8 Scheme for data analysis by SEQUEST algorithm, according to (Thermo Scientific 2008)

The DTA files for every extracted peptide ion are combined into a search result file (.srf) that is submitted to the identification algorithm.

Analogous to the parameters of the applied protein cleavage method (enzymatic or chemical) a digest of all proteins in the chosen database is performed *in silico*. The resulting list of theoretical peptide ions and their calculated molecular masses is compared to the first peptide in the srf file. A new list of all matches within a preset mass tolerance (X Da) is created and sorted according to the primary score Sp. To calculate the primary score, observed masses of b and y ions are compared to the theoretical fragment ions of the listed peptides. Fragment ion intensity in the experimental MS/MS spectra is ignored for the primary score. The higher the number of matched fragment ions the higher the primary score. Sorted by their decreasing primary score the top 500 matches are submitted to the cross correlation analysis.

To correlate theoretical fragmentation data to observed fragmentation mass spectra virtual mass spectra are constructed from the theoretical fragment ion masses. The XCorr scores are then determined by comparing the virtual fragmentation spectra for every peptide in the primary score list to the observed fragmentation patterns. Matches are sorted by decreasing XCorr score, the highest ranking matches are saved as results and summarised in an output file (.out) that is added to the original search result file. The identification process is repeated for all extracted peptide data sets within the search result file.

BioWorks™ sorts the identification results for the data set according to the proteins matched and lists the corresponding peptides and scoring information. Along with the cross correlation and primary score, several indicators for the significance of a match are displayed.

3.1.4 Size exclusion chromatography-mass spectrometry

An alternative method to gather analytical information from protein mixtures is the chromatographic separation according to their molecular hydrodynamic volume by size exclusion chromatography (SEC). In contrast to the majority of chromatographic separation mechanisms, SEC does not rely on specific interactions with the stationary phase. The principle of the method was first discovered by Porath and Flodin 1959 who developed cross-linked dextran gels to separate proteins by molecular weight leading to the term *gel filtration chromatography* for the separation of biopolymers in aqueous solutions. Today the method is primarily used for purification purposes and the determination of organic polymer molecular weight distributions (*gel permeation chromatography*) (Porath and Flodin 1959).

To elucidate the separation mechanism geometric and thermodynamic models have been devised. Geometric models offer good practical explanations by considering molecules as spherical spheres and assuming simplified pore geometries (conical or cylindrical). Retention of molecules depends on the relative size ratio of molecule size and pore diameter. Molecules larger than the pore diameter cannot penetrate into the pore, travel straight through the column and elute first. The pore diameter dictates the upper limit of size resolution for a column and has to be chosen carefully for the respective polymer mass range. All analytes exceeding the pore diameter are not retained and elute together in the void volume V_0. With decreasing hydrodynamic volume partial diffusion into the pores increases, prolonging the time needed to pass through the column. The lower limit of the separation range is reached if the molecules can diffuse freely in and out the pores (Fig. 3-9). Molecules below this limit also elute at the same time (V_t) since they are

equally retained. Since SEC is a relative chromatographic method a careful calibration has to be performed to successfully correlate elution times or volumes to molecule size.

Like for most other chromatographic methods a range of detectors can be used to observe the separation process. For protein samples UV- and light scattering-detection are standard methods. In recent years the coupling of size exclusion chromatography to mass spectrometric detectors has been employed to various problems to expand the information depth with characteristic mass spectra. One of the biggest challenges in connecting both methods originates from the incompatibility of normally buffered mobile phases of SEC separations and the low salt content tolerance of the detector.

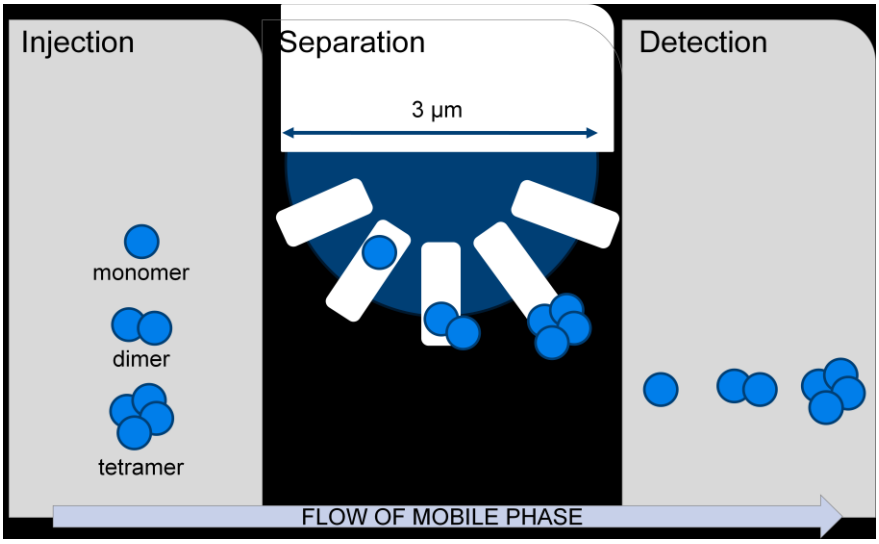

Figure 3-9 Principle of size exclusion chromatography

The advantages of SEC-MS have mainly been acknowledged for bioanalytical applications in aqueous solutions. Nylander et al. identified peptide fragments (0.1-7 kDa) to investigate the physiological role of the prodymorphin system in rat stratia (subcortical part of the forebrain) on a Superdex column (Nylander, Tanno et al. 1995). The miniaturisation of the electrospray ionisation unit (µESI-SEC) was employed to investigate the effects of various inhibitors on the quaternary structure and function of alcohol dehydrogenase (Shen, Benson et al. 2001). Deery et al. investigated the potential of coupling SEC to an ion trap mass spectrometer to characterise polysaccharides as an alternative to the favoured MALDI-TOF route. Replacing the need for time consuming fraction collection and offline analysis the group also found that data qualities were equal to MALDI-TOF data and could be expanded by additional structural data information by tandem mass spectrometry (Deery, Stimson et al. 2001). SEC-MS on an ESI-TOF system was compared to the molecular weight determination of antibodies by reversed phase LC/MS by Brady et al. and significantly higher signal intensities were achieved (Brady, Valliere-Douglass et al. 2008). By optimising the size exclusion chromatography and ESI-TOF analysis of intact arsenic binding proteins was proven superior to SEC-UV methods (Schmidt, Fahlbusch et al. 2009).

Studies into the oligomerisation of amyloid beta peptides already employ SEC separation to characterise the fibrillogenesis process (Walsh, Lomakin et al. 1997). The addition of mass spectrometric data could simplify the correct assignment of peaks to oligomeric species.

3.2 Cloud Point Extraction

3.2.1 Liquid-liquid extraction in sample preparation

Sample preparation is often a crucial step in the analysis of biomolecules. Especially the analysis of proteins requires methods to be as non-altering and as suited as possible to guarantee optimal extraction from the biological sample and allow a sophisticated analysis during the following steps. Depending on the analytical methods applied these steps could either be further purification of one desired target biomolecule or the detailed analysis of an extracted range of biomolecules by gel electrophoretic separations and mass spectrometric experiments.

The highly complex composition and sensitivity of biological matrices leads to demanding requirements for the sample preparation method. A variety of inorganic and organic substances have to be removed without damaging or altering the analytes. An elegant and frequently used method is *liquid-liquid extraction* (LLE), the partitioning of analytes between immiscible or partially soluble liquid phases that can subsequently be isolated to continue the preparation. Due to advantages like simplicity of the method, low costs and ease of scale up and integration into continuous processes in comparison with traditional steps like dialysis or chromatography for purifications, LLE has also been successfully implemented in industrial processes (Gordon, Moore et al. 1990; Silva and Franco 2000; Mazzola, Lopes et al. 2008).

Traditional water-organic solvent two phase systems can seldom be applied to the extraction of proteins from biological samples since most proteins are irreversibly denatured by or poorly soluble in the organic phase. To create more compatible environments, alternative *aqueous two-phase systems* (ATPS) have been investigated. Numerous variants have been invented and applied in biotechnological purification processes. Aqueous two-phase systems can be formed by combining either two incompatible polymers (e.g. polyethylene glycol PEG and dextran) or one polymer and a salt (e.g. PEG and a phosphate salt) in aqueous solutions. Even though ATPS undergo phase separation both phases maintain their aqueous nature offering non-destructive environments while still creating sufficient driving forces to enable partitioning. Increasingly popular variants of ATPS are systems created by ionic liquids. Advantages of these systems for protein extraction or purifications are mild process conditions, fast phase separation, high interfacial phase contact due to the aqueous nature of both phases as well as stabilising and even enhancing effects on bioactivity (Albertsson 1956; Dreyer and Kragl 2008; Freire, Louros et al. 2011; Oppermann, Stein et al. 2011).

3.2.2 Non-ionic detergent aqueous two-phase micellar systems

The use of aqueous surfactant solutions instead of polymers or salts leads to the formation of *aqueous two phase micellar systems* (APTMS). Depending on the surfactant these systems are homogeneous mixtures of sample and surfactant micelles that undergo spontaneous phase separation into two aqueous phases, the lower phase rich in surfactant micelles, the upper micelle-poor, when the temperature is raised (Figure 3-10). The solutions become turbid at a specific temperature, the cloud point (CP), indicating the aggregation of surfactant molecules into large units that scatter visible light. The phase separation stems from the competition between entropy (favouring miscibility of micelles in the system) and enthalpy (favouring separation of micelles from water). Their

respective contributions vary with the temperature and type of surfactant (Quina and Hinze 1999).

The inverse relationship between temperature and the appearance of two phases can be attributed to the reversible dehydration of polar head groups. Dehydration leads to micelle-growth and the development of a water insoluble phase that precipitates as a second, micelle-rich phase (Bordier 1981; Quina and Hinze 1999; Shevchenko, Sjodin et al. 2010). Micelles are present in both phases but the micelle-rich, lower phase offers a more favourable environment for hydrophobic molecules than the upper phase. Partitioning of proteins is dependent on their physical-chemical properties, foremost their hydrophobicity as well as their pI, concentration, pH and the type and concentration of salts present (Liu, Nikas et al. 1996; Mazzola, Lopes et al. 2008).

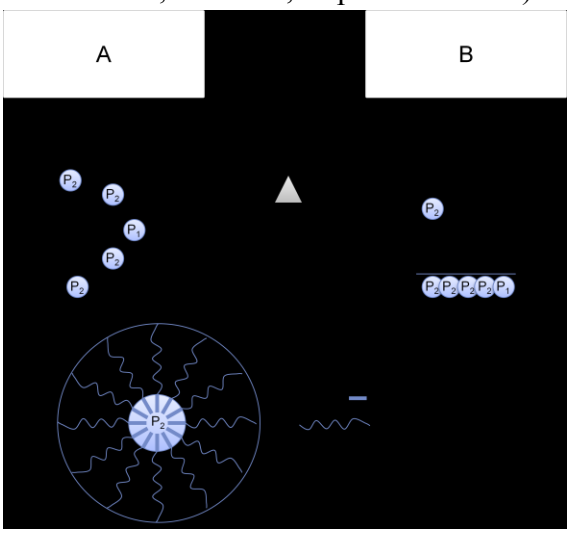

Figure 3-10 Temperature induced (Δ) phase separation of hydrophilic (P_1) and hydrophobic (P_2) proteins in aqueous two phase micellar systems and schematic micelle assembly.

The concept of using CPE for the isolation of hydrophobic molecules was pioneered by Watanabe and co-workers in 1978. Water-soluble Zn(II) chelate complexes were extracted from aqueous solutions by means of a polyoxyethylene nonyl phenyl ether (PONPE-7.5) two phase micellar system. With publishing his findings in 1981 Clément Bordier established the application of non-ionic detergents, namely Triton X-114, for the extraction of hydrophobic biomolecules (Watanabe and Tanaka 1978; Bordier 1981).

Cloud point extraction (CPE) performed with variants of octylphenol ethoxylates that are commercially known as Triton$^{(R)}$ surfactants has since become a valuable tool in bioanalytical sample preparation. Figure 3-11 shows the general structure of the Triton detergents. Table 3-1 lists Triton X species and properties regarding their use for cloud point extractions. Only three species, Triton X-100, X-102 and X-114, possess the ability to form aqueous two phase micellar systems within a reasonable temperature range for aqueous systems. Cloud point temperature as well as critical micelle concentration (CMC) increase with the averge number of oxyethylene units n.

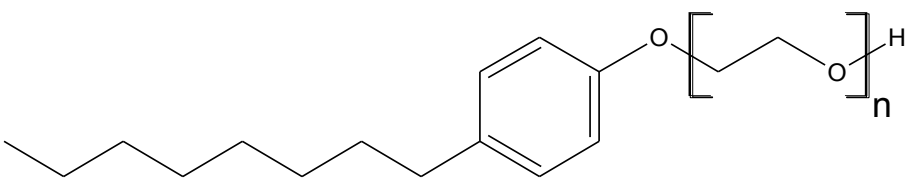

Figure 3-11 Structure of octylphenyl ethoxylate (Triton X) detergents

While Triton X-100 is a commonly used detergent in laboratories for cell lysis and can be used to emulate biological cell systems to study for example antioxidant dimerisation, the cloud point temperature of 66 °C limits its application for protein extractions (Liu and Guo 2008).

Table 3-1 Triton detergents and characteristics

Name	n (avg.)	CP [°C](1)	Appearance(2)	CMC [ppm, 25 °C]
X-15	1.5	insoluble		Insoluble
X-35	3	insoluble	yellow liquid	Insoluble
X-45	4.5	dispersible		136
X-100	9.5	66		189
X-102	12	88		267
X-114	7.5	25	pale yellow liquid	120
X-165*	16	>100		570
X-305*	30	>100		1916
X-405*	35	>100		2442
X-705*	55	>100		3585

* 70 % solution (DOW), (1) 1 % wt aqueous solution, (2) at 25°C

Triton X-114 on the other hand displays several beneficial properties with regard to protein sample preparation. Stable two phase systems are formed above 25 °C allowing very mild extraction conditions with low risk of denaturation or precipitation. The physical-chemical environment within the X-114 micelles allows interaction with hydrophobic and amphiphilic proteins that would otherwise be poorly soluble in aqueous solutions alone. Hydrophilic proteins show little to no hydrophobic interaction with X-114, are not influenced during the extraction and will mostly remain in the upper, micelle-poor phase (Bordier 1981; Liu, Nikas et al. 1996).

The low critical micelle concentration of Triton X-114 (120 ppm, ~0.22 mM) makes the non-ionic detergent preferable to ionic detergents with significantly higher CMCs. Reported critical micelle concentrations for the popular anionic surfactant sodium dodecylsulfate range around 8 mM. Considering the purpose of CPE as an extraction and preconcentration step within the sample preparation process, this proves to be advantageous since only small amounts of pure non-ionic surfactant need to be added, minimizing the volume of the resulting micelle-rich phase (Mandal, Nair et al. 1988; Quina and Hinze 1999).

The unique phase separation behaviour of ATPMS has been implemented in numerous extraction methods. A few reviews have been published that summarize the multiple applications of aqueous two-phase micellar systems as either sample preparation or purification methods. Hinze and Quina review the use of surfactant-mediated cloud point extractions as environmentally benign alternatives to conventional LLE systems with organic solvents and focus on the extraction of organic compounds from water and soil samples (Hinze and Pramauro 1993; Quina and Hinze 1999). Mazzola and co-workers dedicated a part of their review of liquid-liquid extraction methods for biomolecules to aqueous two-phase micellar systems (Mazzola, Lopes et al. 2008).

Cloud point extraction with Triton X-114 has been investigated as a method to remove endotoxins (e.g. liposaccharides), major contaminants in commercial proteins and biologically active extracts. The surfactant facilitates the dissociation of endotoxins from

proteins at low temperatures and can be easily removed by raising the temperature. Liu et al. found that CPE was superior even to affinity chromatography in removing 99 % endotoxins from large-scale *E. coli* recombinant protein purifications (Aida and Pabst 1990; Liu, Tobias et al. 1997).

The method was also applied to the targeted extraction of a range of hydrophobic proteins. Zhang et al. isolated a reduced form of pyruvate oxidase, a peripheral membrane flavoprotein from crude *E. coli* preparations in a single step and lowered the overall preparation time from three weeks to one day (Zhang and Hager 1987). Other conventional but time consuming multi-step protein extractions have been optimised by replacing chromatographic separations with one CPE step. Nisin, a novel natural food preservative with antibacterial properties can be purified from commercial mixtures with Triton X-114. Additionally positive effects on nisin activity were observed (Jozala, Lopes et al. 2008).

Cloud point extractions show particularly high potential for proteins that can rarely be extracted from biological samples by conventional methods. Especially the extraction of membrane proteins that are partially or completely embedded in lipid bilayers allows insights into important metabolic processes. Among their numerous essential cellular functions is the regulation of cell-cell interactions, recognition, migration, adhesion and signal transduction. The simultaneous disruption of cell membranes due to the detergent and the extraction into the hydrophobic environment of the micelles enables detailed studies of this important subproteome. In 1985 Lewis isolated and characterised glycoprotein antigens in lysosomal membranes from rat liver (Lewis, Green et al. 1985). Mast et al. extracted developing Monterey pine compression wood to investigate the contribution of membrane proteins to cell wall and wood formation by LC-MS (Mast, Peng et al. 2010).

Neuropathological diseases like Alzheimer's and Parkinson's disease disrupt neuronal and synaptic signal transmission processes mediated by membrane proteins in the brain. Triton X-114 extractions of brain samples (porcine, mouse, human post-mortem) and their analysis with mass spectrometric methods could help to gather clues for treatment and drug development (Shevchenko, Sjodin et al. 2010; Wetterhall, Shevchenko et al. 2011; English, Manadas et al. 2012).

4. Results and discussion

4.1 Chromatographic separation of amyloid β 42 peptides

The aim of this work was to investigate alternative analysis methods to characterise oligomeric species of amyloid β peptides that are practically indistinguishable to established methods based on antibody-antigen responses. Preliminary experiments were performed to assess already existing extraction methods for enzyme-linked immunosorbent assays performed by the collaborating working group of Prof. Dr. Jens Pahnke and their compatibility to mass spectrometric methods. Furthermore the potential of size exclusion chromatography – mass spectrometry for the separation and simultaneous detection of oligomeric amyloid β species was explored

4.1.1 Reversed phase chromatography - mass spectrometry

Separation on reversed phase columns depends on partitioning coefficients between the stationary highly hydrophobic alkylsilane (C18) phase and the aqueous mobile phase with gradually increasing organic solvent content. Proteins and peptides elute from the column in the approximate order of their hydrophobicity. For unknown protein samples RP-HPLC coupled to a mass spectrometer is the most popular option to obtain general informations.

Among the first samples examined was an Aβ42 ELISA standard (1000 ng/mL), the supernatant as well as the resolvated protein pellet solution of an already analysed mouse brain sample. Figure 4-1 shows the total ion current (TIC) chromatogram for the Aβ42 standard originally intended for ELISA experiments (see appendix A.1.1). Mass detection allowed the application of non-UV transparent acetone in the mobile phase to utilize its superior elution properties in reversed phase chromatography of protein and peptides (Fritz, Ruth et al. 2009).

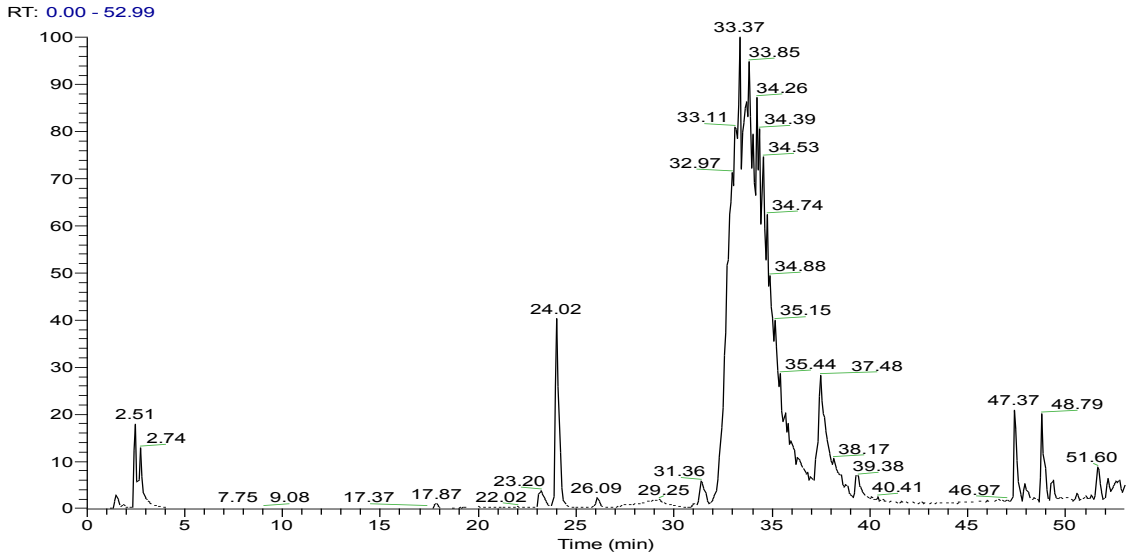

Figure 4-1 Chromatogram of Abeta 1-42 standard solution (1000 ng/mL). Selected time range 0-53 min; BasePeak mass range 300-2000 amu (+); Intensity level 7.42E5 (100%). Gradient elution 5 to 80 % acetone.

One advantage of a mass sensitive detector in comparison to common UV/Vis detection lies within the mass spectrometric information in addition to a sole concentration and wavelength dependent signal.Each data point composing the chromatogram in fig. 4-1 represents a FullScan mass spectrum allowing further analysis and the identification of the correct peaks. Mass spectra corresponding to the largest peak in the spectrum (~32 – 37 min) show a characteristic charge state distribution profile for a large intact protein (Fig. 4-2). ESIprot, a free and easily online accessible software tool developed by Robert Winkler in 2010, was used to determine a rough estimate of the molecular weight as well as the charge states of the molecule from up to nine m/z ratios in ascending order selected as input for the program (Winkler 2010).

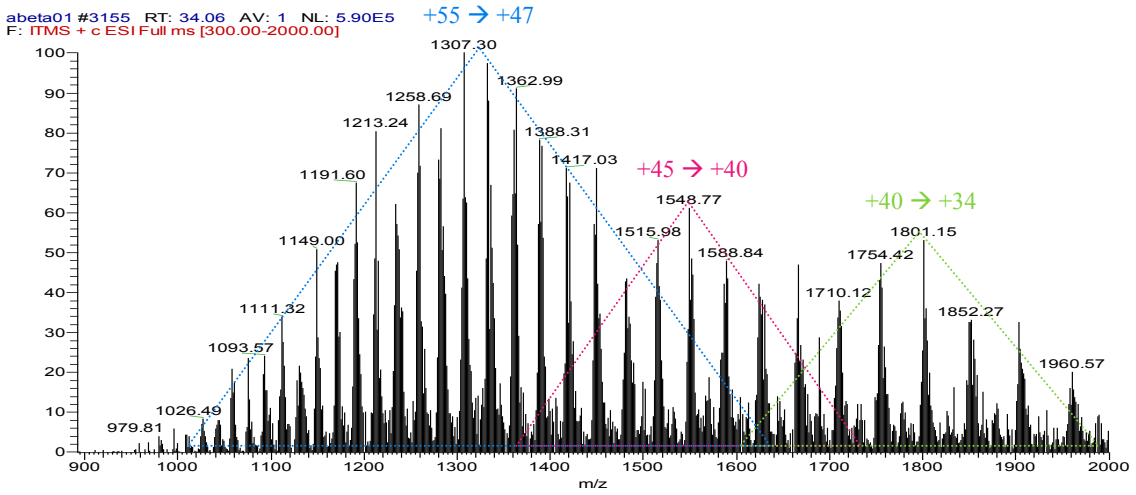

Figure 4-2 Mass spectrum at 34.06 min, showing characteristic charge envelopes of large intact proteins. Average molecular weight 66615.81 Da (ESIprot)

Charge state distribution (CSD) is dependent on several factors like molecular conformation, acid-base behaviour in solution and in the gas phase during ionisation, solvent composition and instrumental factors. They reflect solution-phase conformations of proteins and can indicate degrees of folding (lower charge states, fewer protonation sites accessible) or denaturation (higher charge states, opening of structure increases protonation). Coexistence of different conformations leads to the phenomenon of charge envelopes in the mass spectrum (Iavarone, Jurchen et al. 2001). Three such envelopes can be observed in fig. 4-2, marked by coloured triangles. Six to nine central mass to charge ratios were selected for each and analysed with ESIprot. Calculated molecular weights and charge states were summarised in table 4-1. The estimated weight of ~66.6 kDa pointed to the identity of the protein as bovine serum albumin (BSA, 66432.9 Da; UniProt P02769 [25-607]) that is often added to low concentrated protein standard solutions to prevent inactivation and loss due to absorption to vessel walls during storage (Thermo Scientific 2009).

Fully denaturated BSA contains 100 basic residues that could theoretically by protonated during the electrospray ionisation process (Schnier, Gross et al. 1995). The comparatively low charges in the spectrum indicate at least partially folded structures restricting access to protonation sites. Apart from weak non-covalent bonds stabilising folded conformations, the numerous disulfide bridges preserve basic structural elements.

Table 4-1 Molecular weight and charge state determination by ESIprot

envelope	Selected $[M+H]^+$	MW [da]	charges (z)
(1) blue	1213.24	66602.04 ± 77.10	+55
	1232.38		+54
	1258.69		+53
	1281.06		+52
	1307.30		+51
	1331.61		+50
	1362.99		+49
	1388.31		+48
	1417.03		+47
(2) red	1482.36	66631.72 ± 49.77	+45
	1515.98		+44
	1548.77		+43
	1588.84		+42
	1625.25		+41
	1666.86		+40
(3) green	1666.86	66613.67 ± 31.75	+40
	1709.80		+39
	1752.86		+38
	1801.15		+37
	1852.27		+36
	1903.08		+35
	1960.57		+34

All peaks with clear protein patterns were analysed with the ESIprot tool to discern possible molecular weights and the amyloid β 42 peak. Molecular weights and charge ranges are summarised in table 4-2, the selected m/z values for each data set is listed in appendix A.2 (table A-21).

Table 4-2 Molecular weight determination for peaks in fig. 4-1 by ESIprot

retention time [min]	MW [Da] (ESIprot)	charge states
23.20	(1) 8458.81 ± 1.93	+11 to +6
	(2) 8585.44 ± 4.06	
	(3) 8788.24 ± 1.05	
24.02	8773.19 ± 2.16	+11 to +5
26.09	8947.55 ± 2.09	+11 to +6
27.6 – 29.8	14305.68 ± 0.51	+12 to +8
31.36	3886.49 ± 0.29	+7 to +4
33.3 – 35.9	(1) 66602.04 ± 77.10	+55 to +47
	(2) 66631.72 ± 49.77	+45 to +40
	(3) 66613.67 ± 31.75	+40 to +34
37.48	66921.86 ± 56.64	+52 to +44

None of the peaks directly correspond to expected Aβ42 m/z ratios within the mass range of the FullScan (300 to 2000 amu). Based on the amino acid sequence of amyloid β 42 (Uniprot ID P05067 [672-713]) the theoretical molecular weight of the peptide is 4514.1 Da and detectable charge states range from +3 ($[M+3H]^{3+}$ = 1505 amu) to +15 ($[M+15H]^{15+}$ = 301 amu).

Calculated weights for the first three peaks ranged from 8458.81 Da to 8947.55 Da and were significantly lower than expected for amyloid β 42 dimers (~ 9030 Da). The decrease could indicate partial degradation due to prolonged storage time. The actual

degree of oligomerisation could not be estimated from the data alone since multiplication of the amino acid sequence also multiplies protonation sites and results in similar charge state distributions. Final confirmation of the calculated charge states was not possible with the resolution of the chosen scan mode. The most abundant and presumably stable species, based on peak height and area, calculated as 8773.19 Da, eluted at 24 min with one set of mass signals.

While the provided amyloid β standard solution was intended for immune reaction-based methods and additional components not disclosed by the manufacturer, reversed phase chromatography of the solution showed it to be a mixture of stabilising agents (BSA, lysozyme) and possibly degraded dimers or oligomers unsuited for further mass spectrometric analysis.

In addition to the ELISA amyloid β standard a provided sample set of extracted mouse brain consisting of supernatant (soluble Aβ species) and redissolved protein pellet (insoluble species) was analysed (fig. 4-3). The high salt content of both solutions (~ 5 M guanidine HCl) required was not directly compatible with sensitive mass spectrometric instruments. Proteins were precipitated with acetone prior to the experiments.

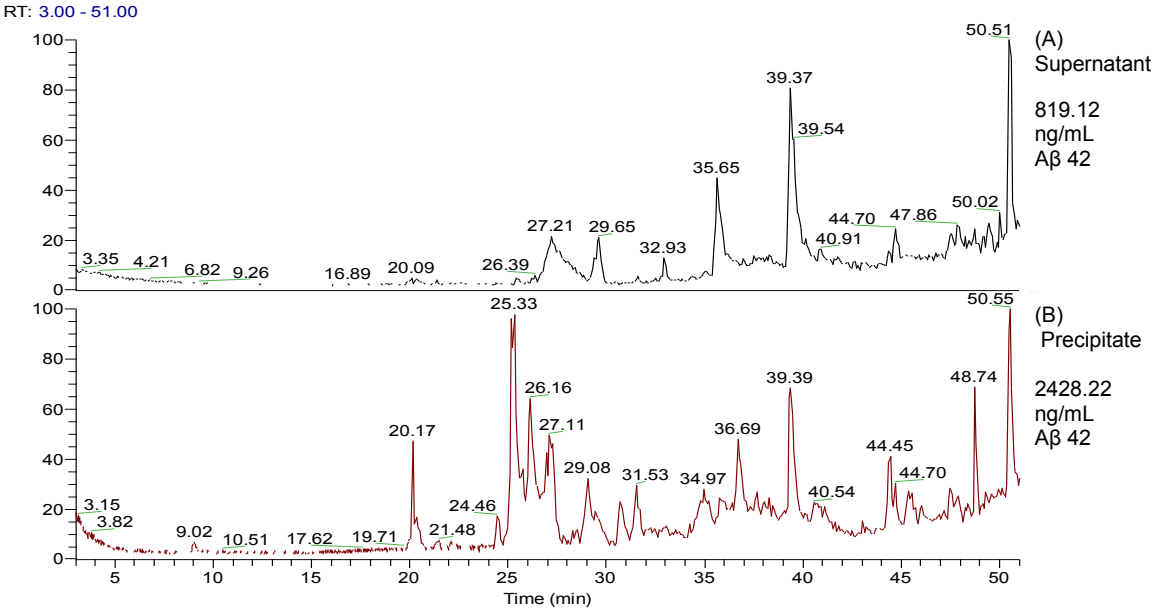

Figure 4-3 Chromatograms of extracted mouse brain samples prepared for ELISA tests. (A) Supernatant; 1.74 mg/mL total protein; 470.76 ng Aβ42 per mg protein (ELISA) (B) Resolvated precipitate; 1.92 mg/mL total protein; 1264.7 ng Aβ42 per mg protein. Gradient elution 5 to 80 % acetone

Even based on optical comparison alone differences between supernatant and precipitate were very distinct. Since the samples have similar total protein concentrations (1.74 mg/mL (A) and 1.92 mg/mL (B)) the appearance of additional peaks in chromatogram (B) was attributed to the sample preparation process optimised for the isolation of soluble and insoluble amyloid β species. Visible peaks with distinct charge state distribution were again submitted to ESIprot (see appendix A.2, tables A-22 and A-23) to estimate molecular weights and charge states (table 4-3).

The absolute number of peaks was higher for the precipitate than for the supernatant (15 vs. 10) but especially within the time frame from 20 to 30 minutes several peaks correspond to very similar molecular weights and charge states. Apart from the peaks at 25.42 min (A) and 25.33 min (B) indicating a molecule of ~14 kDa the calculated weights

were a little higher than expected for a monomer (~ 5 kDa) and lower than a dimeric or indistinguishable oligomeric species (~8.6 kDa). Though the charge state distributions and the resulting molecular weights for the 8.6 kDa species were similar to the observed species in the ELISA Aβ42 standard (see table 4-2) they eluted with a higher organic solvent content pointing towards more hydrophobic molecules (~23-24 min vs. 29-30 min). Reasons for the shift could lie in the complex nature of the sample. While the extraction was performed with the goal to isolate a maximum amount of soluble and insoluble amyloid β species, other proteins and matrix components were also extracted.

Additional peaks in both chromatograms indicated mostly smaller proteins (~9 – 24 kDa) and one larger protein of 68 kDa in the supernatant.

Table 4-3 Molecular weight determination with ESIprot 1.0 from supernatant (A) and precipitate (B) chromatograms in fig 4-3

Supernatant			Precipitate		
retention time [min]	**MW [Da] (ESIprot)**	**charge states**	**retention time [min]**	**MW [Da] (ESIprot)**	**charge states**
			20.00	24054.19 ± 57.18	+31 to +24
20.09	4964.17 ± 1.22	+8 to +4	**20.17**	4964.63 ± 0.87	+8 to +5
20.27	5062.57 ± 0.96	+8 to +5	**20.36**	5062.98 ± 0.99	+8 to +5
			21.48	9159.24 ± 42.71	+13 to +9
			24.46	17498.88 ± 59.02	+27 to+20
25.42	14206.64 ± 81.74	+21 to +13	**25.33**	14135.32 ± 5.8	+23 to +15
			26.16	13830.68 ± 13.89	+21 to +14
27.21–28.4	12725.92 ± 216.09	+11 to +7	**27.29**	10076.32 ± 1.31	+12 to +8
29.39	(1) 8562.62 ± 8.17	+12 to +7	**29.08**	(1) 8566.08 ± 0.79	+12 to +7
	(2) 8448.64 ± 4.92	+12 to +8		(2) 8449.01 ± 5.71	+12 to +7
29.65	8663.09 ± 1.49	+12 to +6	**29.44**	8644.51 ± 47.36	+12 to +7
			30.80	9893.72 ± 106.34	+13 to +9
31.57	14926.43 ± 393.72	+17 to +10	**31.53**	10979.90 ± 17.29	+14 to +10
32.93	14322.26 ± 2.08	+13 to +8			
			34.97	13130.36 ± 154.43	+17 to +10
35.65	68252.72 ± 116.79	+50 to +42			
			36.69	9620.50 ± 0.81	+13 to +8
			40.54	16795.24 ± 16.41	+14 to +9
47.54	7673.23 ± 57.77	+15 to +12			
47.86	5989.06 ± 89.63	+14 to +10			

ELISA results for the Aβ42 content of both samples corresponded roughly to a ratio of 1 : 3 (supernatant : precipitate). A signal occurring in both data sets mirroring this ratio could identify a visible amyloid β peak in the chromatograms. The area for the most likely candidates was determined with the QualBrowser analysis software embedded within XCalibur™ and summarised in table 4-4.

As only the first peak at 20.09/20.17 min showed a similar increase in signal intensity and area it could be assumed that the peaks related to the main amyloid β species detected by ELISA. A decline in the perceived ratios was attributed to loss during the necessary protein precipitation with acetone.

Table 4-4 Peak areas for selected candidate peaks (ICIS integration algorithm)

retention time [min] **S/P**	**isolated** **mass range [m/z]**	**Supernatant** Signal intensity Area	**Precipitate** Signal intensity Area	**Ratio (Area)** **S:P**
20.09/20.17	710	2.95E03 33987	3.89E03 69477	1 : 2
20.27/20.36	724	1.54E03 66342	2.42E03 68762	1 : 1
25.42/25.33	786	2.05E03 71020	1.65E04 623718	1 : 9
29.39/29.08	953	7.23E03 171184	5.51E03 141686	1 : 0.8

Since the standard mixture used for ELISA experiments to determine amyloid β concentrations was not suitable for further mass spectrometric detection, a synthesised monomeric standard (> 95 %) was provided by Pahnke et al. (see appendix A.1.1). A 1 mg/mL solution in 50 % DMSO was analysed by RPLC-MS (fig. 4-4) to characterise the sample and gather basic mass spectrometric information on the protein.

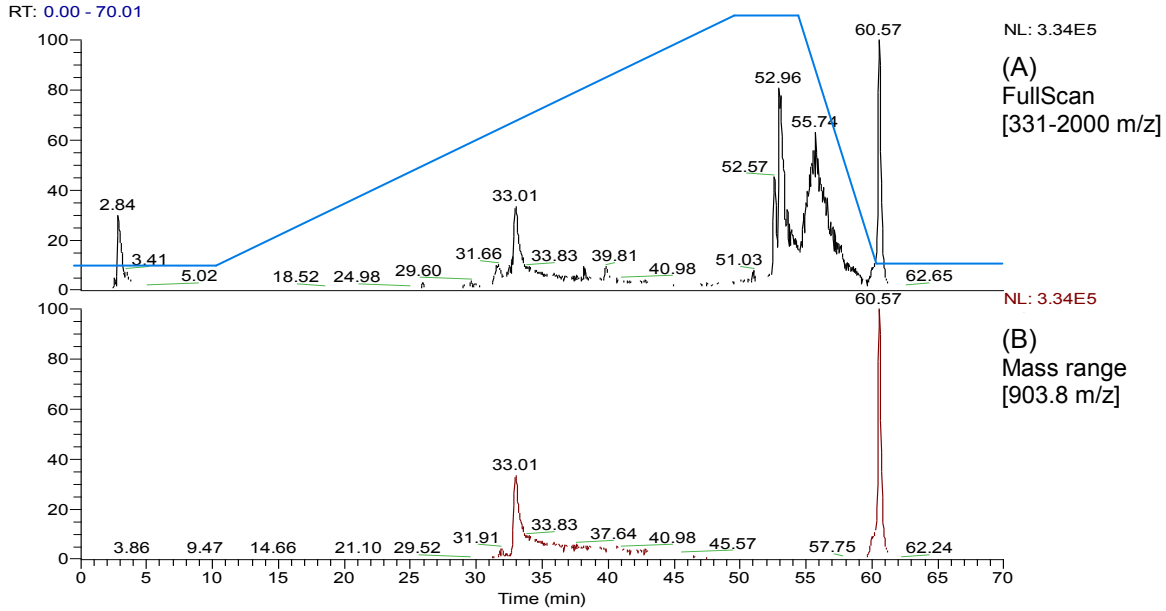

Figure 4-4 Chromatogram of 1 mg/mL Aβ42 in 50 % DMSO; 3 µL; FullScan, 25 °C. BasePeak chromatogram +ESI (A) and mass range chromatogram [903.8 ± 0.5 m/z] (B). Gradient elution 5-80 % acetone

The high maximum concentration of acetone in the applied gradient elution of 80 % (indicated in fig. 4-4 by blue line) leads to the accumulation of unrelated system peaks from 52 to 55 minutes.

Mass spectra of the monomer detected at 33.1 min showed a distinct charge state distribution (fig. 4-5). By defining a mass range filter (903.8 m/z) the software extracts all spectra containing the m/z ratio and plots the respective intensities as a clearer chromatogram with two peaks instead of only one that was expected (B).

Several pieces of information were gained from the data set. (I) the shape of the first peak at 33 min confirmed the high hydrophobicity of the Aβ42 monomer as it eluted from the column with an acetone content of approx. 48 % and showed very strong tailing of up to

15 min after the actual peak indicating a gradual release with increasing acetone content of the mobile phase. (II) Calculating the molecular weight with ESIprot based on the mass spectrum in fig. 4-5 as 4514.02 ± 1.07 Da supported the positive assignment of the peak to the monomeric species of Aβ42 with a theoretical molecular weight of 4514.1 Da (P05067 [672-713]). Detected charge states (+6 to +3) were annotated in the spectrum.

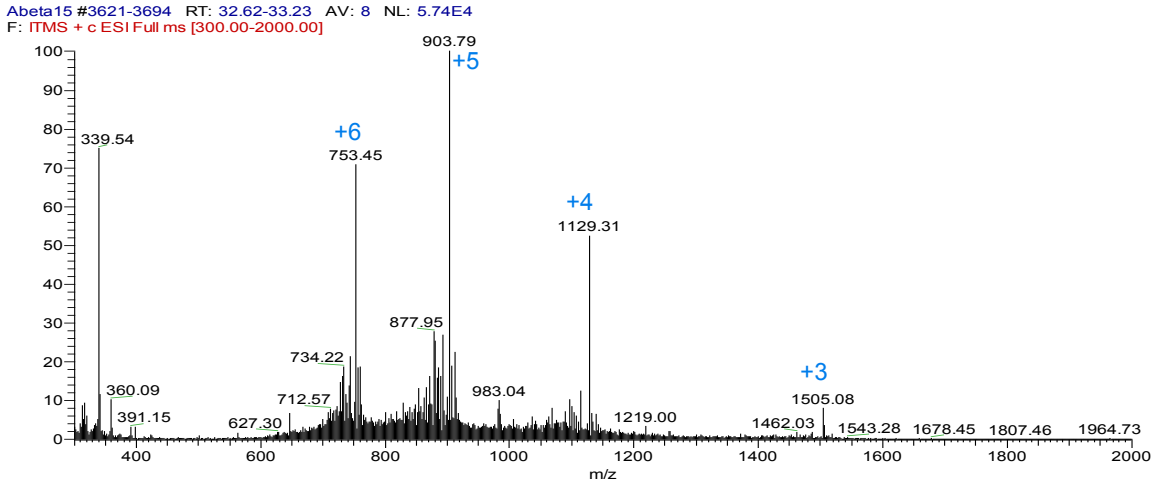

Figure 4-5 FullScan of amyloid β 42 monomer, molecular weight (ESIprot) 4514.02±1.07 Da

(III) A smaller peak shortly before the monomer peak (31.66 min) contained similar CSDs to the Aβ42 monomer with slightly shifted masses. Three sets of masses were again selected for molecular weight determination with ESIprot (fig. 4-6). The first data set (1) consists of relatively weak signals but indicates the presence of a very small amount of the Aβ40 peptide (P05067 [672-711] 4329.8 Da), probably a remnant of the production process of the standard. The strongest set of signals (3) can be assigned to oxidised Aβ42 (mass difference of 16 Da).

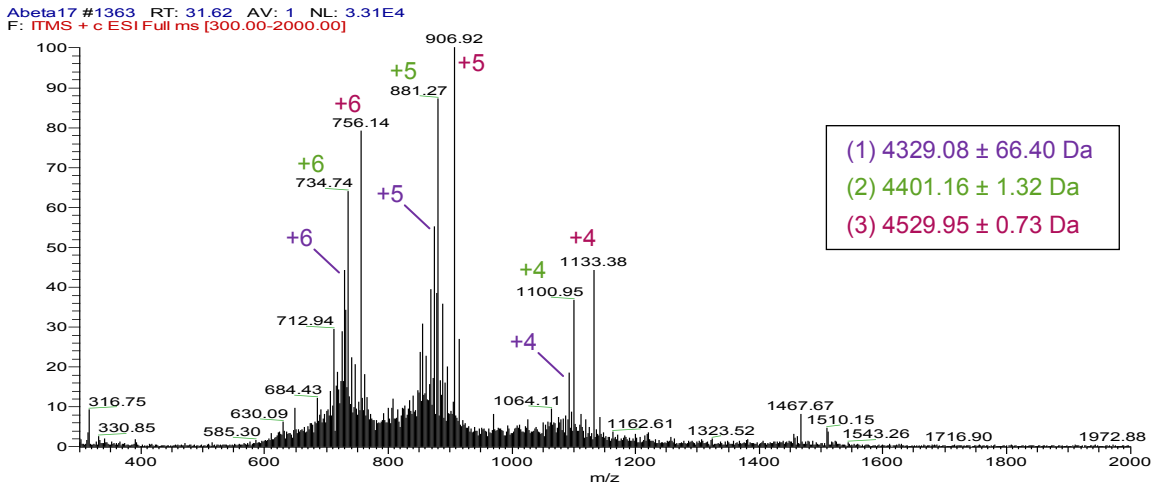

Figure 4-6 FullScan mass spectrum at 31.62 min. Data sets for ESIprot marked (1) violet, (2) green, (3) pink.

Closer examination of the second peak (IV) in the mass range chromatogram showed an identical charge state distribution to the 33.1 min peak. Since the appearance of one analyte at two different points (time and mobile phase composition) during the

chromatographic separation was improbable, further mass spectroscopic experiments were performed to investigate the exact nature of the apparent second Aβ42 peak.

The instrument method was modified to contain high resolution scans of the m/z ratio 903.8 during the elution times of the peaks (see appendix A.1.2.4). By isolating masses in a narrow window of ± 2.5 amu a more precise measurement of the respective m/z ratios of the protein was possible. Still, a distinction between the two species was not achieved even at the highest resolution available. Figure 4-7 represents mass spectra recorded during the UltraZOOM scans (for chromatograms and spectrum for 60.57 min peak see appendix A.4.1).

Based on the molecular weight of Aβ42 the charge state of 903.8 m/z ions should be +5 and the theoretical mass difference between isotopic peaks Δ m/z ~ 0.2 amu. Throughout both peaks a mass difference of Δ m/z ~ 0.1 amu was dominating the high resolution scans with only a low number of scans showing the expected mass differences for the +5 species.

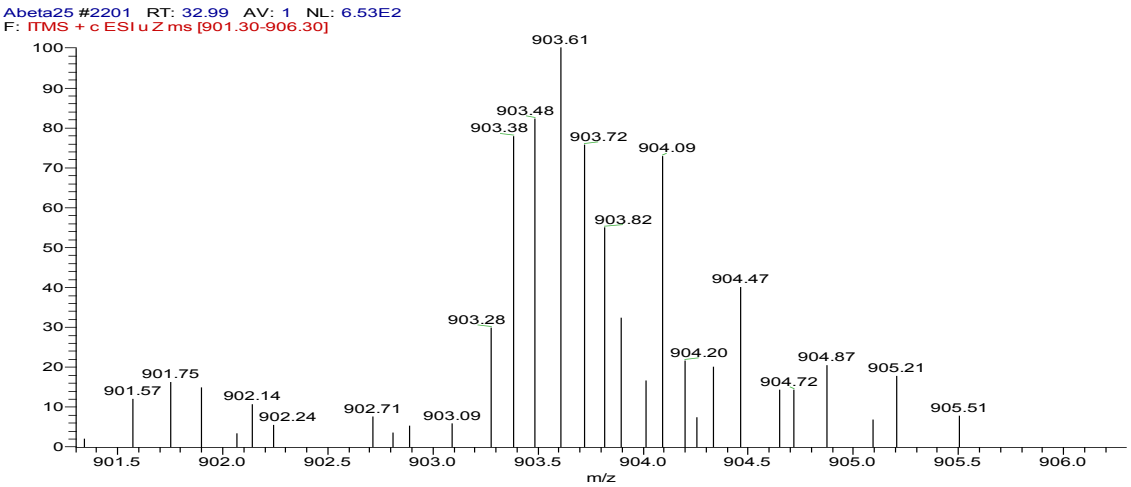

Figure 4-7 UltraZOOM scan on m/z = 903.8 ± 2.5 amu detected at 32.99 min

Analogue scans at both retention times led to the assumption that both peaks correspond to the same Aβ42 species with a main charge state of +10. They underline the aforementioned difficulties to discern between monomer and oligomer species of the protein by reversed-phase chromatography with limited mass resolution detection techniques like ion trap devices. Even exhausting the available resources the actual charge states and oligomeric nature of one or maybe both species were estimated as too low.

Other factors influencing the two peaks are sample concentration and column temperature. Figure 4-8 and 4-9 show the mass range chromatograms (903.8 m/z) of an Aβ42 dilution series of 1 mg/mL (A) to 0.1 µg/mL (E) at 25 °C and 40 °C, respectively.

At the lower temperature both peaks are present for all concentration levels and the peak at 60.5 min remains the strongest signal. With decreasing concentrations the peak shape at ~32.8 min improved as the extended tailing was reduced. The persistence of the later peak probably stemmed from the hydrophobic character of the protein, eluting shortly after the acetone maximum plateau (80 %) of the gradient. Clear chromatograms extracted from the mass spectrometric data with mass range filters for all concentrations proved the sensitivity of MS detection for amyloid β 42 as a basis for alternative chromatographic separation techniques.

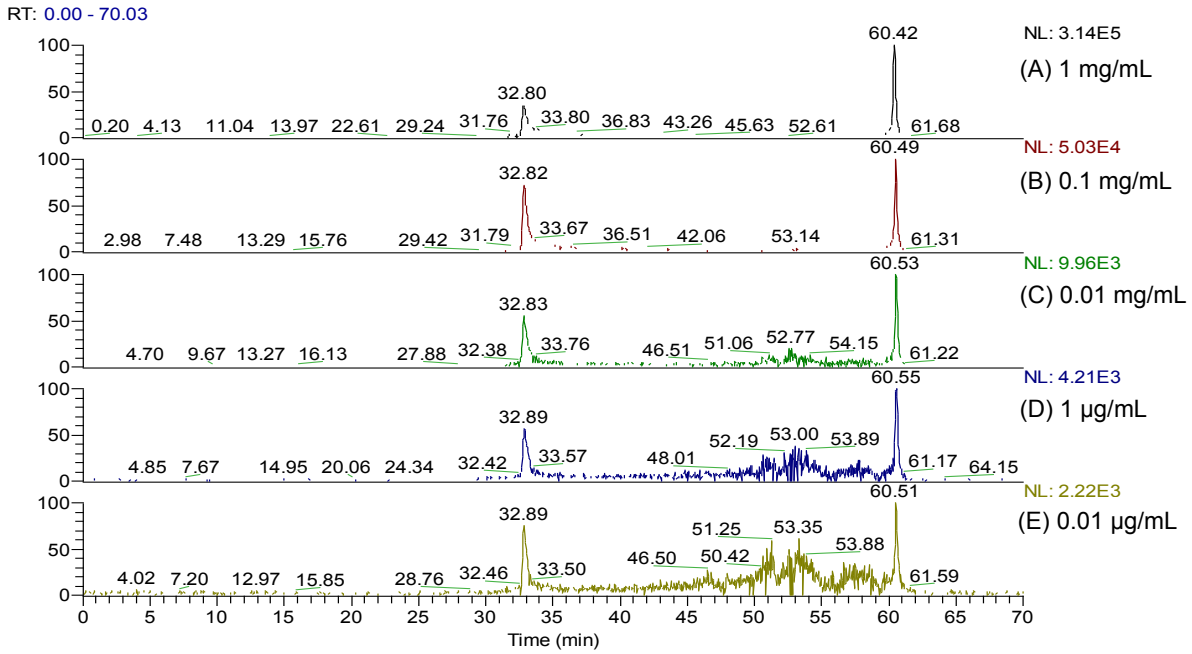

Figure 4-8 Dilution series of Aβ42 standard at 25 °C column temperature, mass range [903.8 ± 0.5 amu]

Raising the column temperature to 40 °C mostly eliminated the occurrence of the second peak while a retention time shift towards 31.2 min, nearly 2 min earlier was observed for the first (fig. 4-9). Peak shapes improved even for the highest concentration of 1 mg/mL but despite the near disappearance of the 60.5 min peak at 40 °C, peak area and height of the main peak did not increase accordingly.

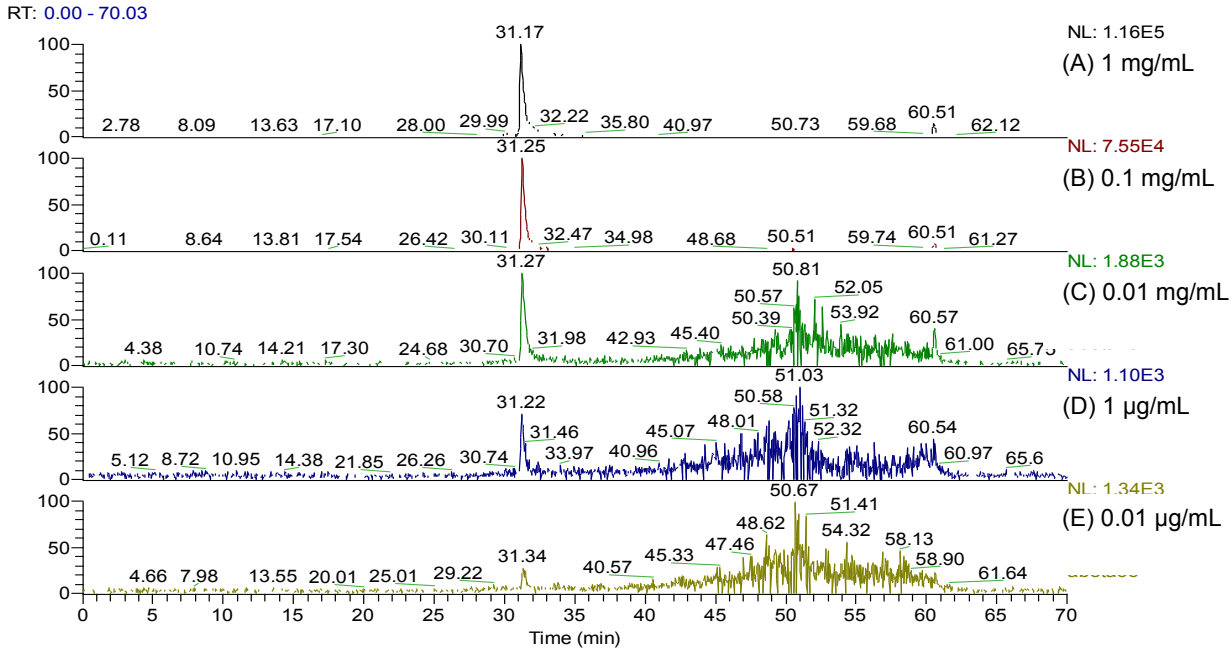

Figure 4-9 Dilution series of Aβ42 standard at 40 °C column temperature, mass range [903.8 ± 0.5 amu]

Another noticeable difference was the more pronounced decline in peak area in comparison to 25 °C, again attributed to strong hydrophobic interactions of the protein

with the stationary phase. Closer examination of blanks between the individual sample runs (25 °C) revealed the tendency of the protein to "stick" to the column adding to the analyte response for the following concentration, even if two blank runs were performed. The effect was minimised by the higher temperature providing more accurate data for the dilution series.

Column temperature influence on the retention of an analyte is described by the decrease in retention factor *k* in the van't Hoff equation and, to a smaller extent, mobile phase viscosity. Increasing temperature affects the partitioning equilibrium between analyte in the mobile phase and the stationary hydrophobic phase accelerating the retention process. To further explore the effect an additional experiment was performed at 70 °C with the 0.1 mg/mL concentration level (fig. 4-10). Peak shape improvement, diminishing of the 60.5 min peak as well as reduction of retention time became even more pronounced.

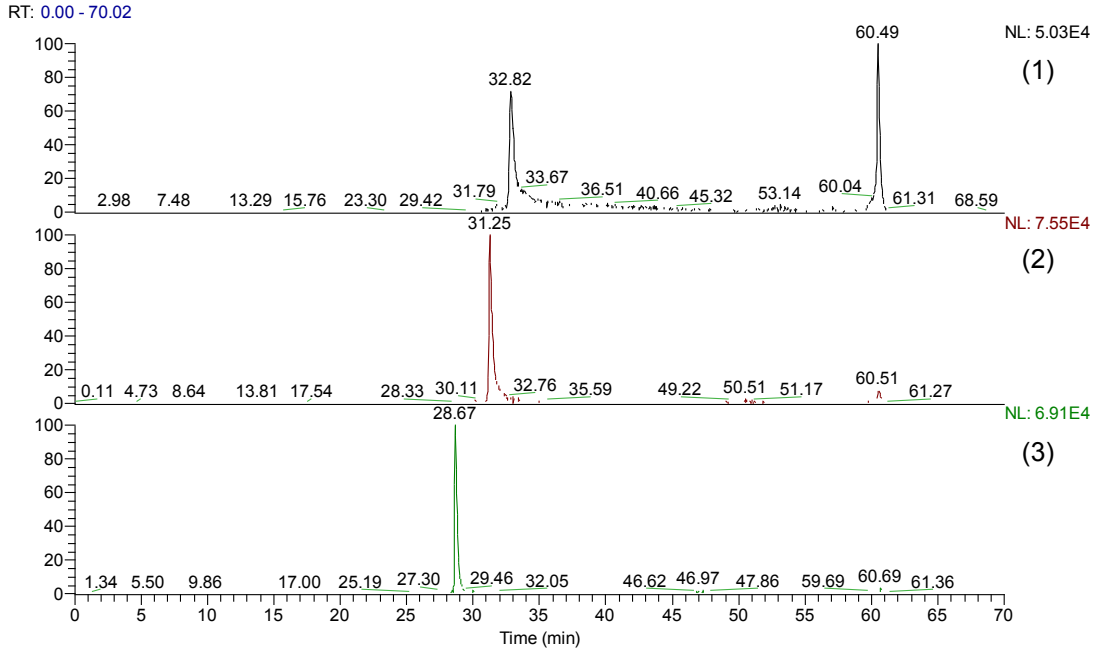

Figure 4-10 Temperature influence on chromatographic separation of 0.1 mg/mL Aβ42, mass range chromatograms [903.8 ± 0.5 amu] at 25 °C (1), 40 °C (2) and 70 °C (3)

The retention time of the second peak most prominent at 25 °C was not influenced by the temperature change. Its appearance seems to be influenced by the acetone gradient and the strong hydrophobic character alone, supporting its classification as an artefact peak as opposed to a potential amyloid β oligomeric species.

4.1.2 Size exclusion chromatography-mass spectrometry

Coupling a size exclusion column to a mass spectrometer is considerably more complex than for established reverse-phase methods. Typical SEC methods focus on maintaining favourable and non-denaturing environments for proteins during separation. Size exclusion chromatography utilises isocratic elution ensuring consistent conditions throughout the experiment and standard detection of proteins and peptides. UV/Vis or RI detection is fairly tolerant in regard to mobile phase composition as long as absorption is not affected. The presence of most commonly used buffer systems containing phosphate and alkaline salts to maintain isotonic conditions however, has a disruptive impact on the electrospray ionisation process. Non-volatile compounds are precipitated in the ESI orifice upon vaporization of the liquid phase, blocking the needle and the continued spray process. Volatile buffer systems like ammonium formate and acetate are compatible with the ionisation process but concessions in total salt content of the mobile phase have to be made to ensure sufficient separation and high MS data quality (Iida and Murata 1990).

The maximal tolerable ion strength for both available mass spectrometers (LCQ and LTQ, Thermo Scientific) was provided by the manufacturer as 50 mM. To minimise ion suppression due to competition between buffer and analyte ions the initial concentration of tested buffer systems with varying degrees of organic solvent content (ACN) was set at 10 mM ammonium formate. Acetonitrile was added to the mobile phase to suppress unintentional interactions between the stationary phase and proteins preventing separation by size exclusion alone. Ultimately the percentage of organic solvent is mostly dependent on the hydrophobicity of the separated proteins. Since amyloid β proteins were classified as hydrophobic based on its amino acid sequence (GRAVY index) the content of ACN in the mobile phase was set at 20 % (v/v).

Prerequisites for SEC columns in HPLC-MS applications were stability of the packing material against high backpressures caused by typical flow rates for analytical separations, a fitting inner diameter and consistent pore sizes defining the separation range of the column. A BioSEC column (4.6 x 300 mm; 150 Å, 3 µm, 500-150000 Da) manufactured by Agilent was selected for the intended experiments.

Column specifications limited the maximum pressure at 240 bar and applicable flow rates to a range from 100 to 400 µL/min. While the flow rates are typical for columns with analytical inner diameters the tolerance for high pressures is lower than for conventional reverse-phase columns (~ 400 bar). The performance optimum was stated in terms of backpressure instead of flow rates. To determine the corresponding flow rate for the LC/MS system various flow rates were applied and the respective pressure values observed (see appendix A.1.3.2). The intersection of the optimal pressure (137 bar) and the resulting linear function indicated the optimal flow rate of roughly 270 µL/min that was set for all subsequent SEC experiments (see appendix A.4.2).

To assess the actual compatibility of SEC with a buffered mobile phase with mass spectrometric detection of proteins, specifically Aβ42, preliminary tests with standard proteins were performed. The first protein examined by SEC-MS using an isocratic mobile phase of 10 mM ammonium formate and 20 % ACN was pepsin (P00791 [60-385] 34509.8 Da; GRAVY 0.072) as a readily available and low priced standard. The characteristic charge state distribution for the intact protein is depicted in figure 4-11.

In comparison to other CSD spectra already shown only approximately half of the charge envelope fell into the mass range of the FullScan method (331 – 2000 amu). Entering the most prominent masses into ESIprot resulted in a calculated molecular weight of 34660.33 ± 37.98 Da for charge states from +18 to +22. Slightly higher than the

theoretical mass of pepsin it points towards a modified protein whose nature was not further investigated.

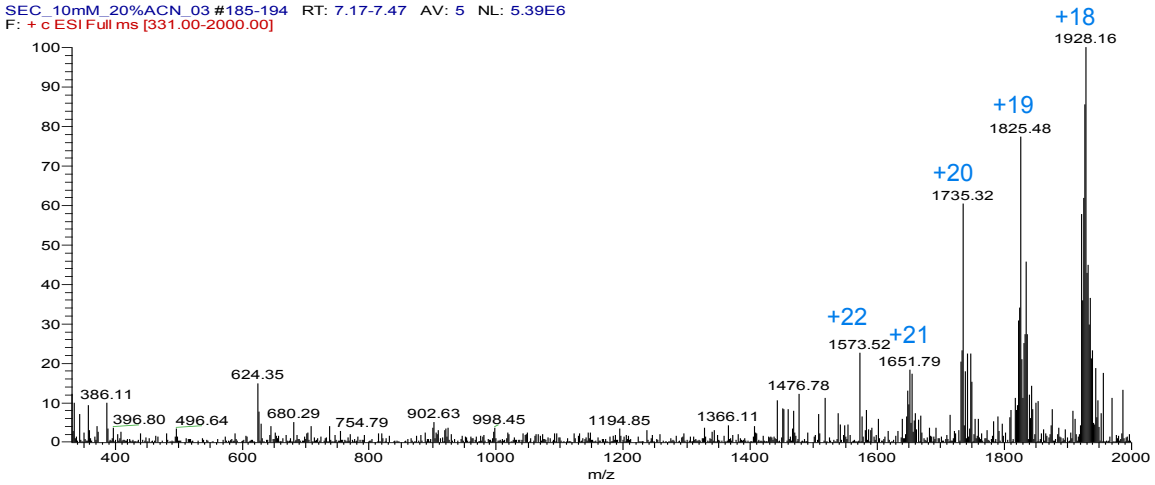

Figure 4-11 Charge state distribution of pepsin (0.5 mg/mL). FullScan chromatograms (averaged) mass range [331-2000 amu]. ESIprot calculation with noted m/z: 34660.33 ± 37.98 Da.

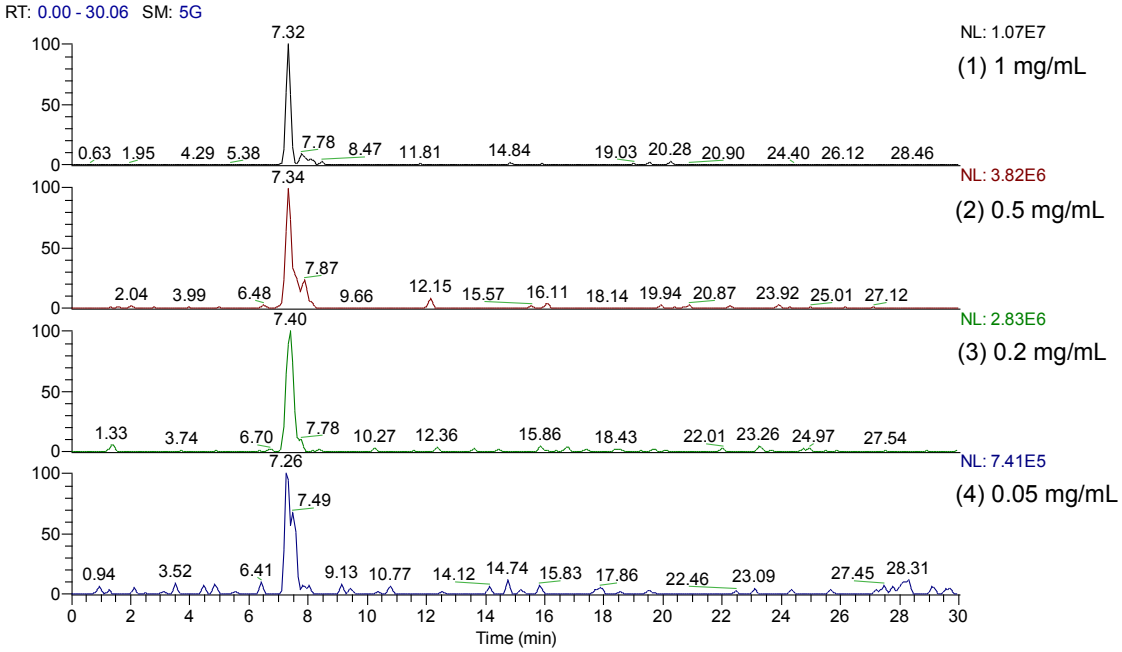

Figure 4-12 SEC-MS chromatograms of pepsin dilutions (1) 1 mg/mL; (2) 0.5 mg/mL; (3) 0.2 mg/mL and (4) 0.05 mg/mL; mass range [1928.16 ± 0.5 amu]

Figure 4-12 shows mass range chromatograms [1928.16 ± 0.5 amu] of samples with decreasing pepsin concentrations. Pepsin served as an orientation point in developing the analytic method to detect amyloid β oligomers. Even for the lowest level of 0.05 mg/mL examined a clear peak around 7 to 8 min was detected.

Based on the successful detection of pepsin, a 1 mg/mL Aβ42 monomer solution was subjected to the method. In comparison to the pepsin chromatograms, the peak in figure 4-13 was broader and lower. The retention time from 14 to 15 minutes suggested a significantly smaller molecule than the 34.5 kDa protein at 7-8 min.

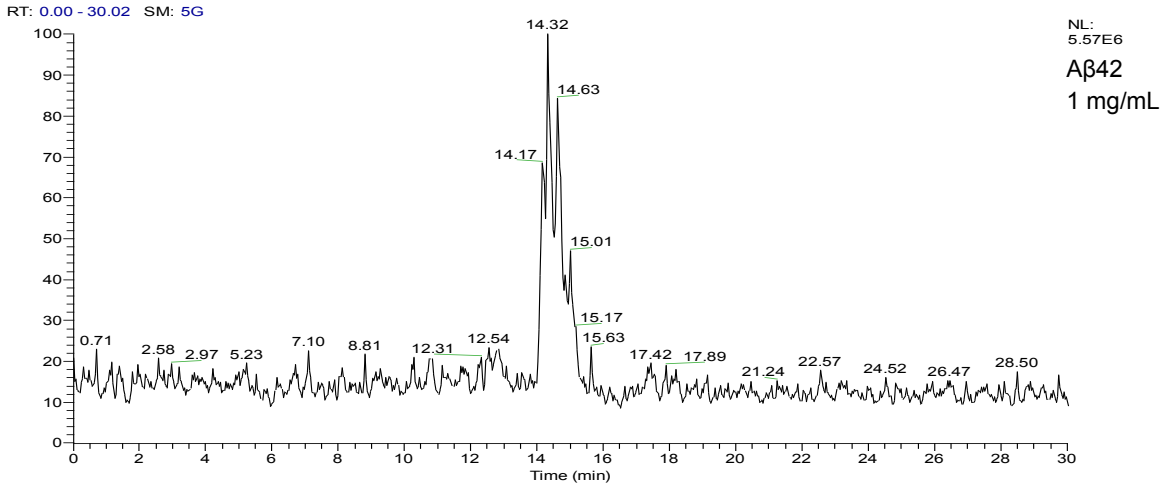

Figure 4-13 BasePeak SEC chromatogram of 1 mg/mL Aβ42 standard solution; mobile phase: 10 mM ammonium formate 20 % ACN

The mass spectrometric data did however not allow a positive assignment of the peak to the amyloid β 42 protein (fig. 4-14). None of the previously observed CSDs (see chapter 4.1.1) of the protein and its variants could be discerned in the averaged mass spectrum of the peak.

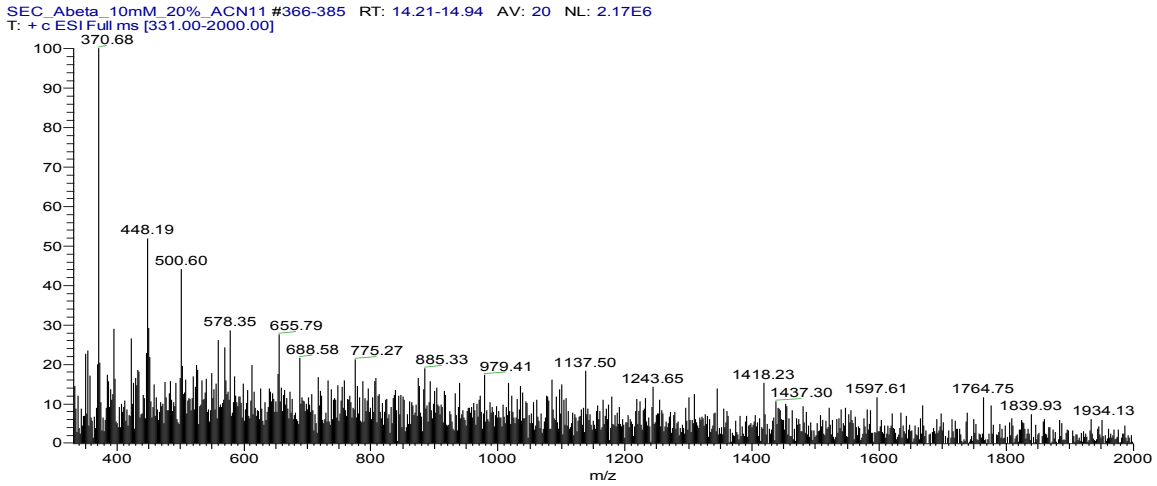

Figure 4-14 FullScan [331-2000 amu] data for SEC-MS of Aβ42; mobile phase: 10 mM NH_4COOH, 20 % ACN

Several factors influence the electrospray ionisation process and subsequently the data quality of mass spectra. Varying parameters in the tune method of the mass spectrometer, defining and controlling the conditions of the ionisation, can improve the efficiency for more difficult target analytes (see appendix A.1.3.4).

Raising the capillary temperature can improve ion transfer efficiency, separation and further desolvation of ion clusters. Sheath gas flow rate aids the spraying process while sweep gas is used to minimise adduct formation and to remove neutral gas phase components before entering the mass spectrometer. Initial modifications of the tune method originated in the high water content of the mobile phase and the observation of condensation within the ESI source.

Starting from a slightly modified version of the general tune method generated from an annual tuning with specific standards, transfer capillary temperature and gas flow rates

were customised to amplify data quality. Table 4-5 summarises changed parameters for three adapted tune files.

Table 4-5 Tune parameters for tune methods 1-3

tune parameter	method 1	method 2	method 3
T, transfer capillary [°C]	275	275	300
Sheath gas [units]	30	40	40
Sweep gas [units]	5	20	20
total signal intensity (NL)	7.31E05	3.16E05	1.29E05

To exclude possible effects of ammonium formate in the mobile phase, adapted tune methods were tested without the column using a piece of tubing and a mobile phase consisting of 80 % water and 20 % ACN with 0.1 % formic acid.

Tune mass spectra of the mobile phase are displayed in the appendix (see A.4.3). Ideally these spectra should have a low total intensity (NL value) and appear mostly "empty" aside from known and reoccurring masses (e.g. softening agents from polymer parts of the system, minute contaminants from mobile phase components).

The combination of higher gas flow rates and the increase in transfer capillary temperature offered the best conditions for the planned experiments. With each customisation the total intensity of the mass spectra decreased, reaching a minimum for method 3 by showing a relatively even distribution of signal intensities. Increasing the capillary temperature had the biggest effect on protein ionisation and MS data quality.

Methods 2 and 3 were applied to the detection of a haemoglobin solution (1 mg/mL) to investigate their compatibility with large biomolecules. For this set of experiments, haemoglobin replaced pepsin as standard protein to ensure the observation of a complete charge envelope within the mass range of the detector. The heightened gas flow rates of tune method 2 were however insufficient to improve ionisation and provide usable mass spectra (fig. 4-15).

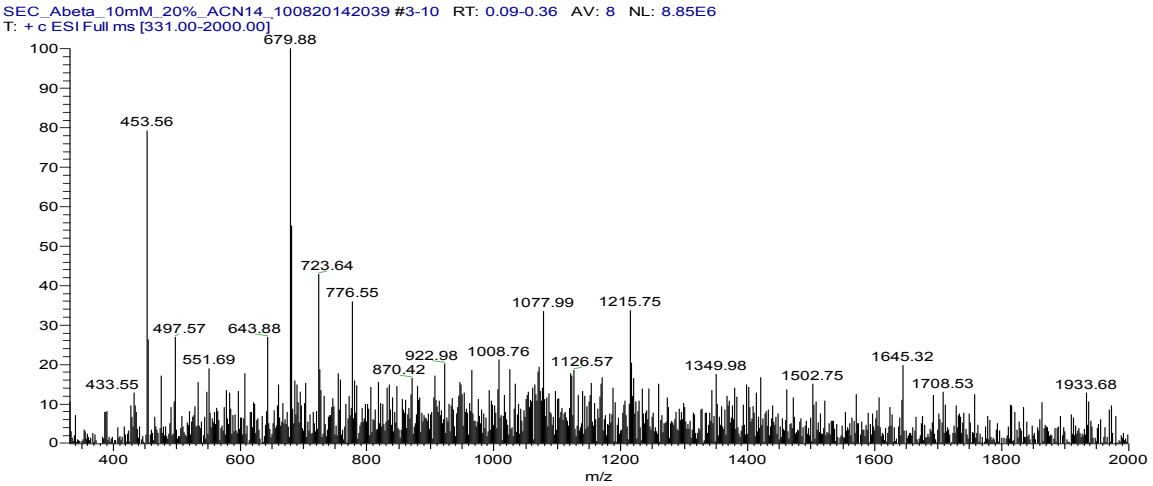

Figure 4-15 FullScan spectra of haemoglobin (1 mg/mL, 5 µL injection volume) [331-2000 amu]; tune method (2); mobile phase: 80/20 H_2O/ACN with 0.1 % FCA

Repeating the experiment applying the parameter setting of method 3 showed a significantly better CSD for haemoglobin (fig. 4-16). Though the data quality was still not

at its optimum, m/z ratios from 887.04 to 1141.27 amu led to an estimated molecular weight of 16023.84 ± 75.92 Da (+18 to +14) correlating roughly with the theoretical molecular weight of haemoglobin β (P02070 [1-145] 15954.3 Da; GRAVY -0.004). Haemoglobin occurs in natural systems as a tetrameric complex of α and β haemoglobin subunits. Mass signals for the α chain (P01699 [2-142] 15053.1 Da, GRAVY 0.014) could not be found in the mass spectrum.

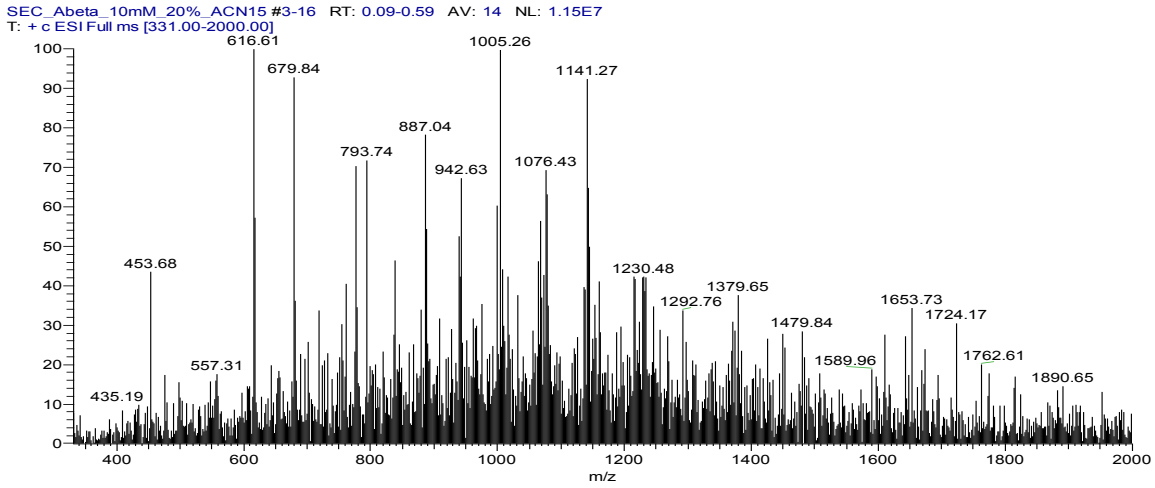

Figure 4-16 FullScan spectra of haemoglobin (1 mg/mL, 5 µL injection volume) [331-2000 amu]; tune method (3); mobile phase: 80/20 H_2O/ACN with 0.1 % FCA

Repetition of the experiment with the initial mobile phase composition of 10 mM ammonium formate in 20 % ACN showed the suppressing impact of the salt on the ionisation process effectively negating improvements achieved by prior optimisation efforts (fig. 4-17).

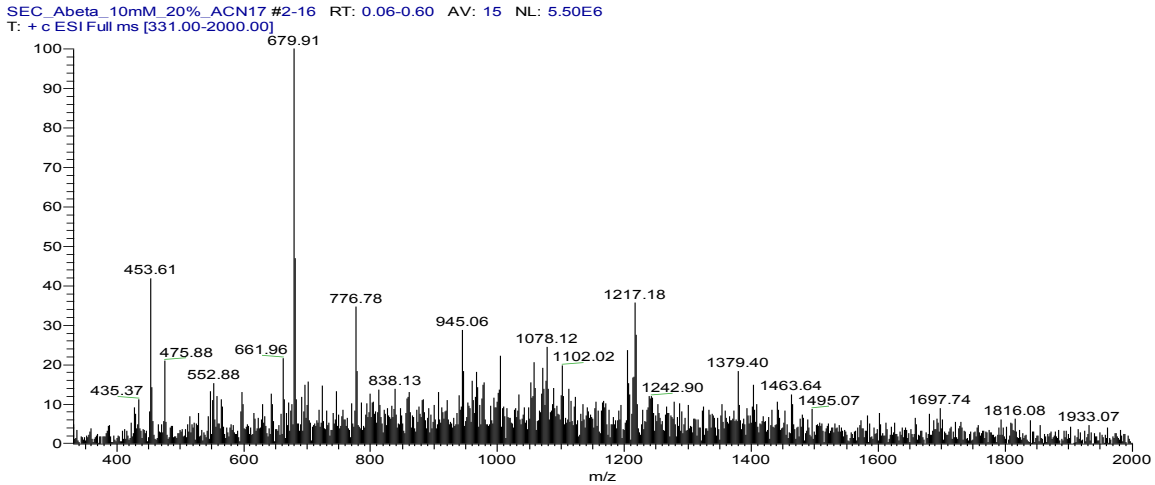

Figure 4-17 FullScan spectra of haemoglobin (1 mg/mL, 5 µL injection volume) [331-2000 amu]; tune method (3); mobile phase: 10 mM NH_4COOH, 20 % ACN

In conclusion the use of ammonium formate for size exclusion – mass spectrometry experiments was dropped in favour of an isocratic mobile phase of 80 % H_2O with 0.1 % formic acid and 20 % acetonitrile with 0.1 % FCA.

To get a sense of manageable concentration limits the newly adopted changes were applied first to dilution series of myoglobin (P68082 [2-145] 16951.4 Da, GRAVY -

0.396) and lysozyme (P00698 [19-147] 14313.1 Da, GRAVY -0.472). The experiment served two purposes; on the one hand the proteins possessed similar molecular weights offering insight into the separation qualities of the column, on the other hand their different amino acid compositions influencing the signal response of the mass spectrometer provided data on the flexibility of the method.

Dilution levels of 0.5 mg/mL – 0.05 µg/mL were analysed (table 4-6). Only the highest concentration of myoglobin resulted in a fairly broad peak (~ 11-14 min), a smaller peak at 15.86 min and similar mass spectra for both (for both chromatographic and MS data see appendix A.4.4). Detection of myoglobin signals earlier than for lysozyme contrary to the expected results indicated non-desired interactions between the stationary phase and myoglobin delaying elution of the theoretically larger protein.

Table 4-6 Summary of positively detected myoglobin and lysozyme by SEC-MS

Protein concentration	Myoglobin	Lysozyme
(A) 0.5 mg/mL	✓ (11-14 min)	✓(10-11 min)
(B) 0.05 mg/mL	-	✓(10-11 min)
(C) 5 µg/mL	-	✓(10-11 min)
(D) 0.5 µg/mL	-	-
(E) 0.05 µg/mL	-	-

The results also suggested a high dependence of signal response on the specific nature of the analyte regulated by amino acid composition. Signal intensity (1.69E08 vs. 4.88E07 for 0.5 mg/mL), peak shape and lowest concentration detectable were superior for lysozyme indicating the protein as a more suited protein standard for further SEC experiments.

Applying the optimised parameter set of method 3 as well as the altered mobile phase composition to a 0.1 mg/mL solution of Aβ42 allowed an assessment of the suitability to the ultimately intended target protein (fig. 4-18).

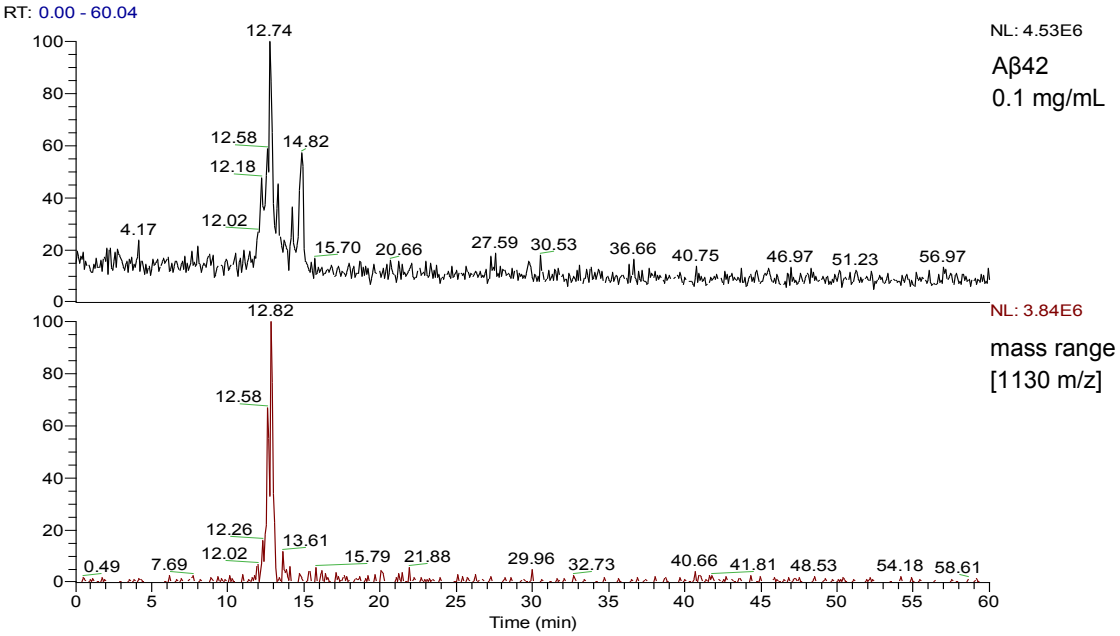

Figure 4-18 SEC-MS chromatogram of 0.1 mg/mL Aβ42 standard solution; tune method (3); mobile phase: 80 % H_2O/20 % ACN with 0.1 % FCA

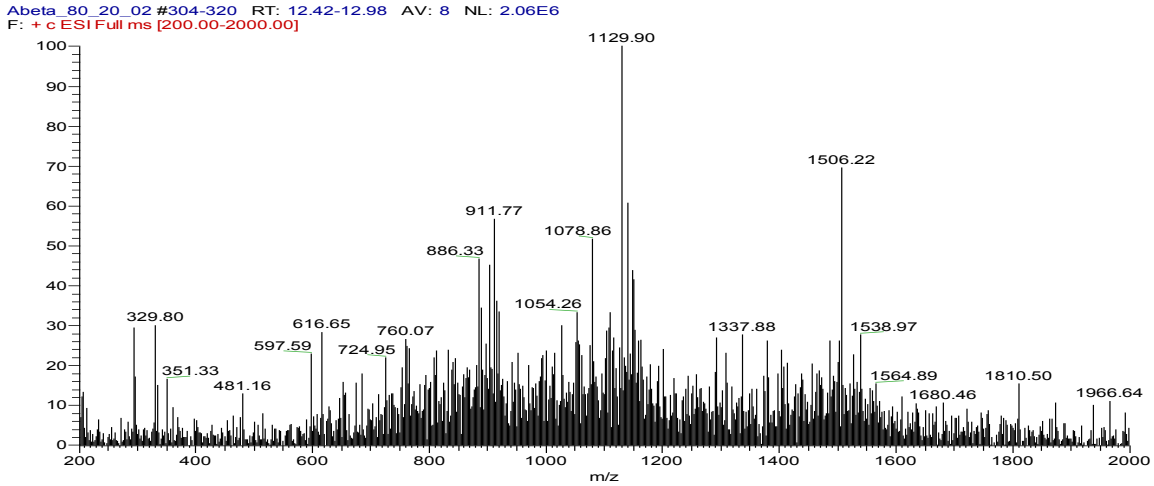

Figure 4-19 FullScan spectra (averaged) [200-2000 amu] for SEC-MS of 0.1 mg/mL Aβ42; tune method (3); mobile phase: 80 % H_2O/20 % ACN with 0.1 % FCA

The previously longer retention could indicate unintentional interactions with the column material in 10 mM ammonium formate, 20 % ACN adding to the time needed for the molecule to move through the system. Since the organic component in the mobile phase was added to SEC separations to prevent or at least reduce these non-favourable interactions yet another modification was tested to improve amyloid β separation and detection. The acetonitrile content was raised to 30 % and a 0.1 mg/mL Aβ42 standard solution was again subjected to SEC (fig. 4-20). The quasi identical chromatogram proved that the heightened hydrophobicity of the mobile phase had no additional effects on the retention mechanism of Aβ42.

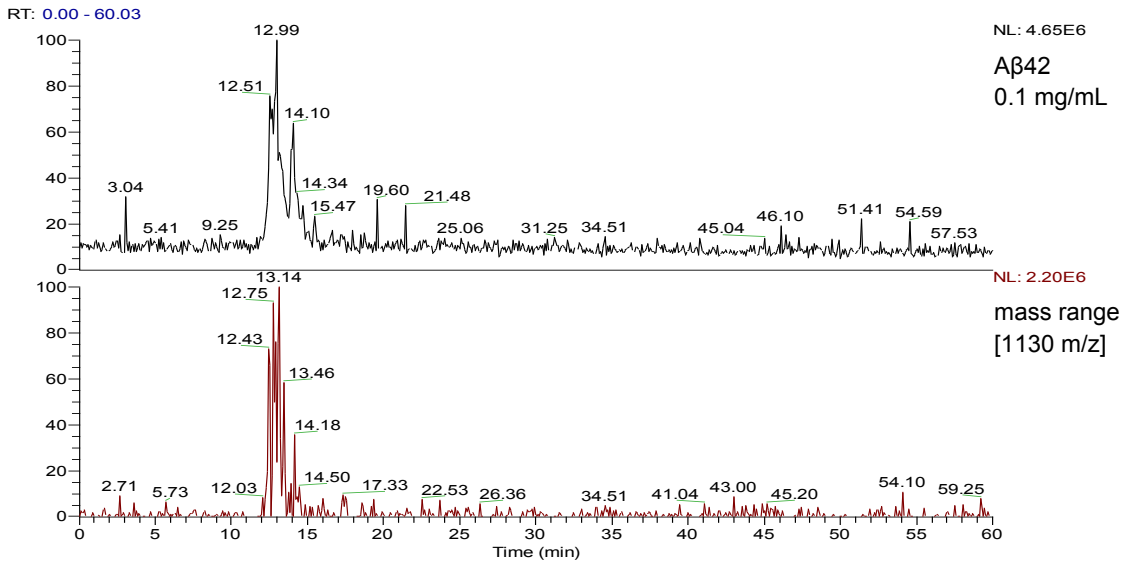

Figure 4-20 SEC-MS chromatogram of 0.1 mg/mL Aβ42 standard solution; tune method (3); mobile phase: 70 % H_2O/30 % ACN with 0.1 % FCA

Reviewing the mass spectrometric data revealed a startling decrease in spectrum quality (fig. 4-21). The characteristic m/z ratios nearly disappeared in the background noise of the mass spectrum rendering the normally useful extraction of a specific mass range ineffective.

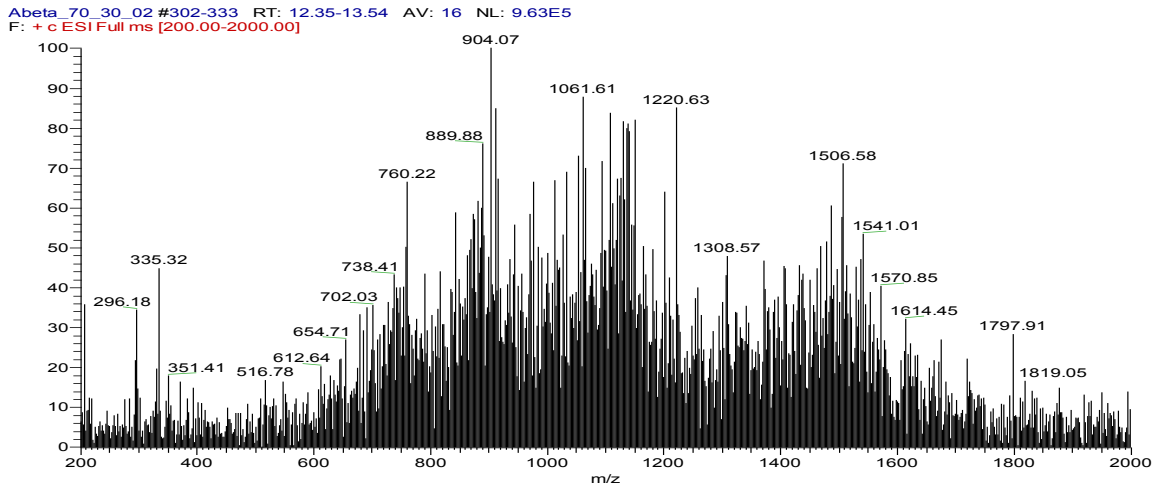

Figure 4-21 FullScan spectra (averaged) [200-2000 amu] for SEC-MS of 0.1 mg/mL Aβ42; tune method (3); mobile phase: 70 % H_2O/30 % ACN with 0.1 % FCA

Concluding that with removing ammonium formate from the mobile phase and optimising gas flow rates to aid the ionisation process as well as adjusting the transfer capillary temperature an optimum for external factors of separation and ionisation was found. The focus was then shifted towards optimising the coordination of electronic components of the mass spectrometer. An analyte specific tuning, software-controlled, was performed using an amyloid β 42 monomer standard solution to generate a tune method tailored for the protein. While altering these parameters from the general method may lead to loss in signal response for other proteins, the detection of amyloid proteins would be significantly improved (see appendix A.1.3.6).

Two new tune methods were created by selecting characteristic m/z ratios of Aβ42 for signal optimisation (table 4-7). Focussing on the highest observed mass to charge ratio (1505 amu, z = 3) first, an overall change in signal, the measurable response of the mass spectrometer for the m/z, grew by 578.3 %. Seeing that the quintuply charged ion has been the most intensive signal observed in mass spectra of Aβ42 an additional tune was performed on the m/z ratio of 904 amu. Compared to the 1505 amu tune method the signal response could be raised even higher (+112.2 %).

Table 4-7 Detection parameters optimised by automatic tune using characteristic Aβ42 masses

		tune focus	
optimised parameter	**method 3 [V]**	**1505 amu [V]**	**904 amu [V]**
capillary voltage	3	45	40
tube lens offset	45	15	0
second octapole offset	-10	-5	-6
first octapole offset	-3	-4	-4
inter octapole lens	-16	-20	-20
change in signal	-	+578.3	+112.2

Almost identical, but opposite changes in capillary voltage and tube lens offset were necessary to improve the detection of amyloid β. The capillary voltage was raised from 3 V to 45/40 V aiding the passage of the larger ions into the mass spectrometer. The tube lens offset is normally applied to separate neutral components entering the mass

spectrometer from charged ions. Functioning as entrance into the sensitive octapole lens and ion trap system the tube lens is set slightly off centre in relation to the transfer capillary (Thermo Scientific 2008).

Charged ions are guided through the lens by applying a specific voltage influence their trajectory while neutral gas phase components are not affected and "miss" the opening. Strong reduction of the tube lens offset from 45 V to 15 and 0 V indicated a negative influence on amyloid β 42 ion trajectories and the successful transfer towards the trap using the parameter set of tune method 3.

Implementing the optimised tune parameters into separate instrument methods their efficiency was tested by analysing a 0.1 mg/mL Aβ42 standard solution (fig. 4-22 to 4-25). Figure 4-22 shows the base peak and isolated mass range (903.8 ± 0.5 amu) chromatograms for the 1505 amu method.

In comparison to the chromatogram in fig. 4-18 the protein also elutes in the time frame of 12-14 min albeit with a faintly shifted peak maximum of 13.24 min. The overall signal intensity was increased by one magnitude confirming the improved detection parameters of the method.

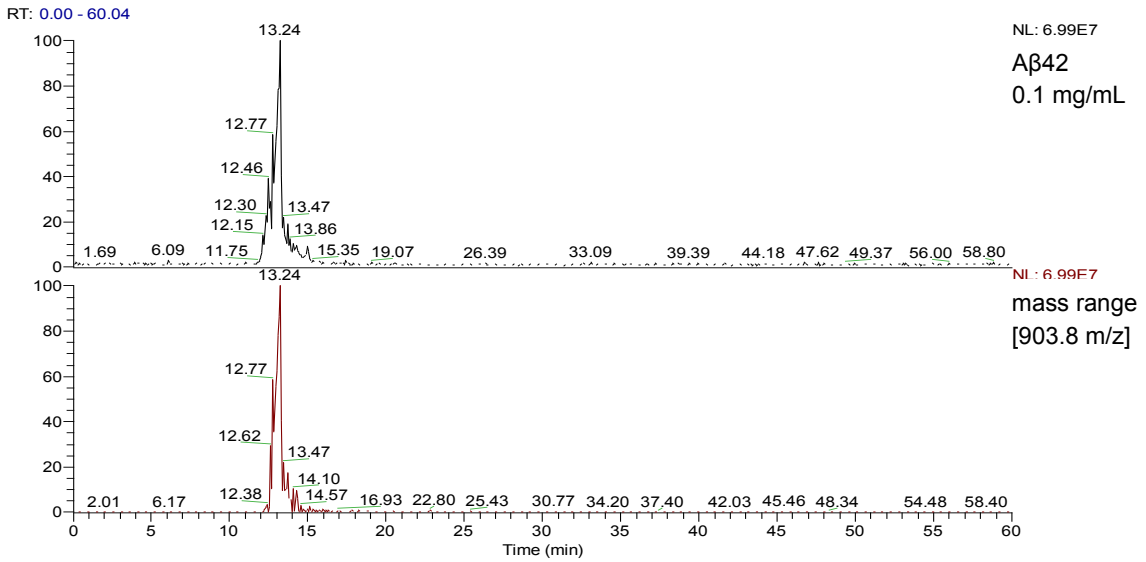

Figure 4-22 Chromatographic data for 0.1 mg/mL Aβ42, base peak and mass range [903.8 ± 0.5 amu]; tune method optimised for Aβ42 (1505 amu): capillary temp. 300 °C, sweep gas 40 units, aux. gas 20 units; mobile phase: 80 % H_2O/20 % ACN with 0.1 % FCA

Averaged mass spectra for the peak showed the charge distribution for Aβ42 (z = +6 to +3) with a cleaner background than in the previous separations (fig. 4-23). The data did not reach the quality of spectra observed for the standard acquired for reversed-phase chromatography. The decline was attributed to the use of a three-dimensional ion trap (LCQ) for size-exclusion method development as opposed to a superior linear trap (LTQ) and isocratic instead of gradient elution. Even though the tune method was customised by focussing on 1505 amu the strongest signal in the spectrum was still 904.14 amu (z = 5) while the intensity actual target ion nearly sinks to background levels.

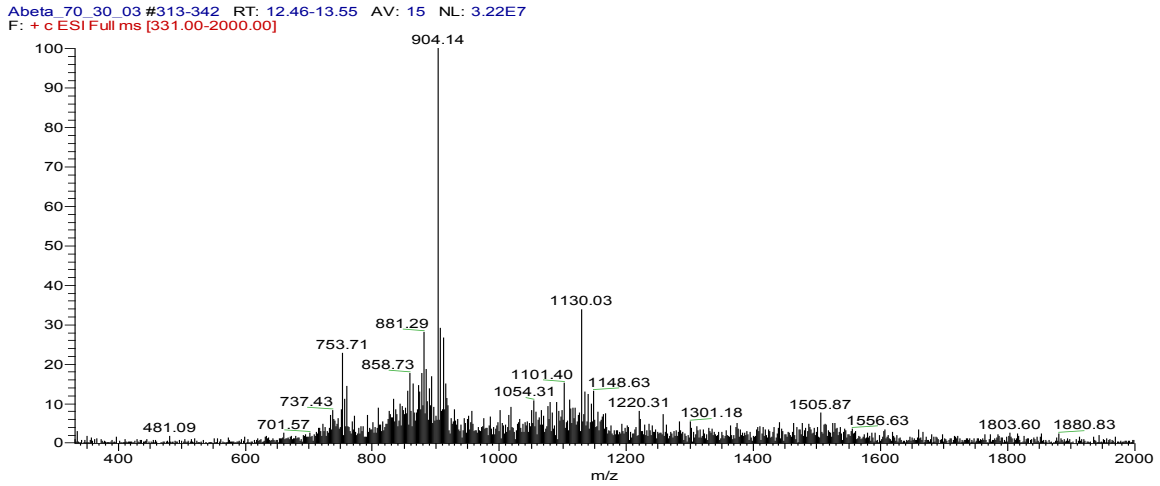

Figure 4-23 FullScan spectra (averaged) [331-2000 amu] for SEC-MS of 0.1 mg/mL Aβ42; tune method optimised for Aβ42 (1505 amu): capillary temp. 300 °C, sweep gas 40 units, aux. gas 20 units; mobile phase: 80 % H_2O/20 % ACN with 0.1 % FCA

The experiment was repeated using the second optimised tune method focussed on 904 amu (z = 3, fig. 4-24). Small changes in peak shape and peak maximum were noticeable and the overall intensity was lower.

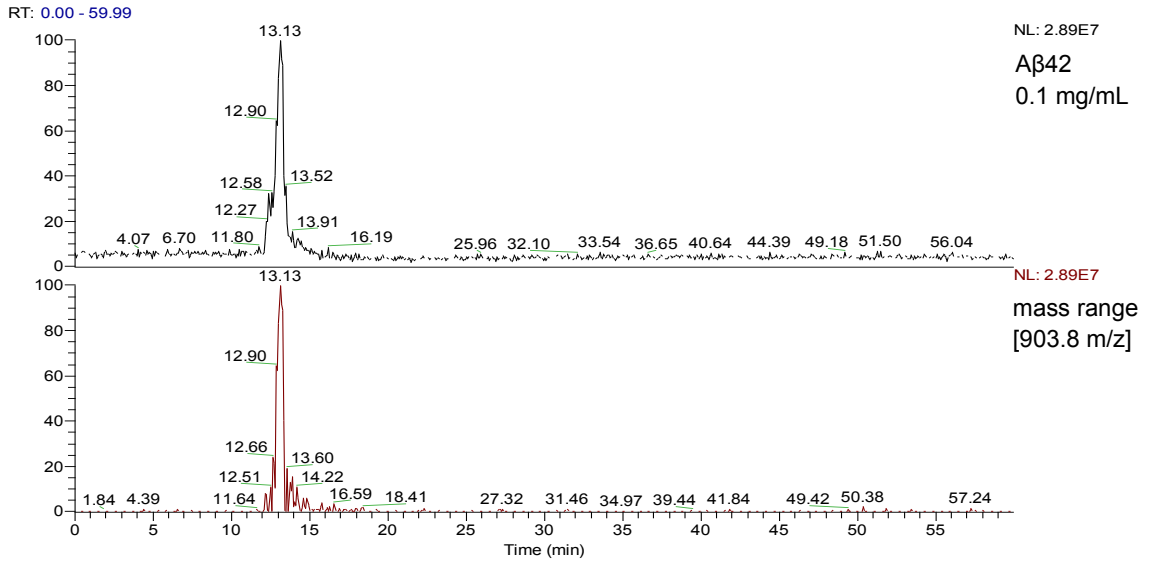

Figure 4-24 Chromatographic data for 0.1 mg/mL Aβ42, base peak and mass range [903.8 ± 0.5 amu]; tune method optimised for Aβ42 (904 amu); capillary temp. 300 °C, sweep gas 40 units, aux. gas 20 units; mobile phase: 80 % H_2O/20 % ACN with 0.1 % FCA

The mass spectrometric data showed a similar charge distribution to the 1505 method data, alluding to the charge states z = +3 to z = +6. Contrary to the previous data set the triply charged molecule could not be clearly distinguished from the background and the relative abundance of z = +6 (753.67 amu) and z = +4 (1129.73 amu) in reference to the most intensive signal was increased by approx. 10 % (fig 4-25).

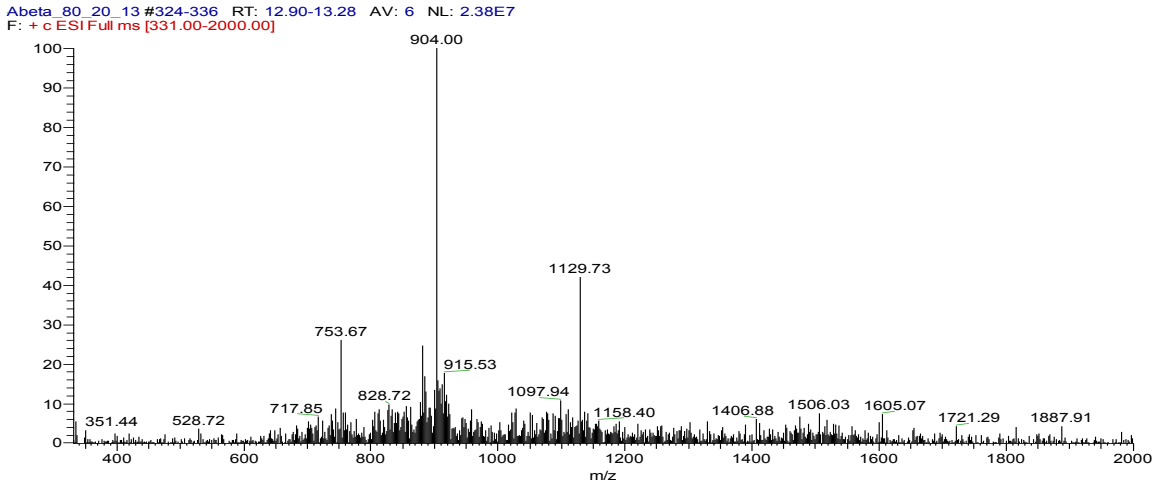

Figure 4-25 FullScan spectra (averaged) [331-2000 amu] for SEC-MS of 0.1 mg/mL Aβ42; tune method optimised for Aβ42 (904 amu): capillary temp. 300 °C, sweep gas 40 units, aux. gas 20 units; mobile phase: 80 % H_2O/20 % ACN with 0.1 % FCA

A dilution series of amyloid β 42 was analysed by SEC-MS using the instrument method based on the 1505 amu tune method (fig. 4-26). Aβ42 could now be detected from a 0.01 mg/mL level upwards and identified through the characteristic charge state distribution in the mass spectra.

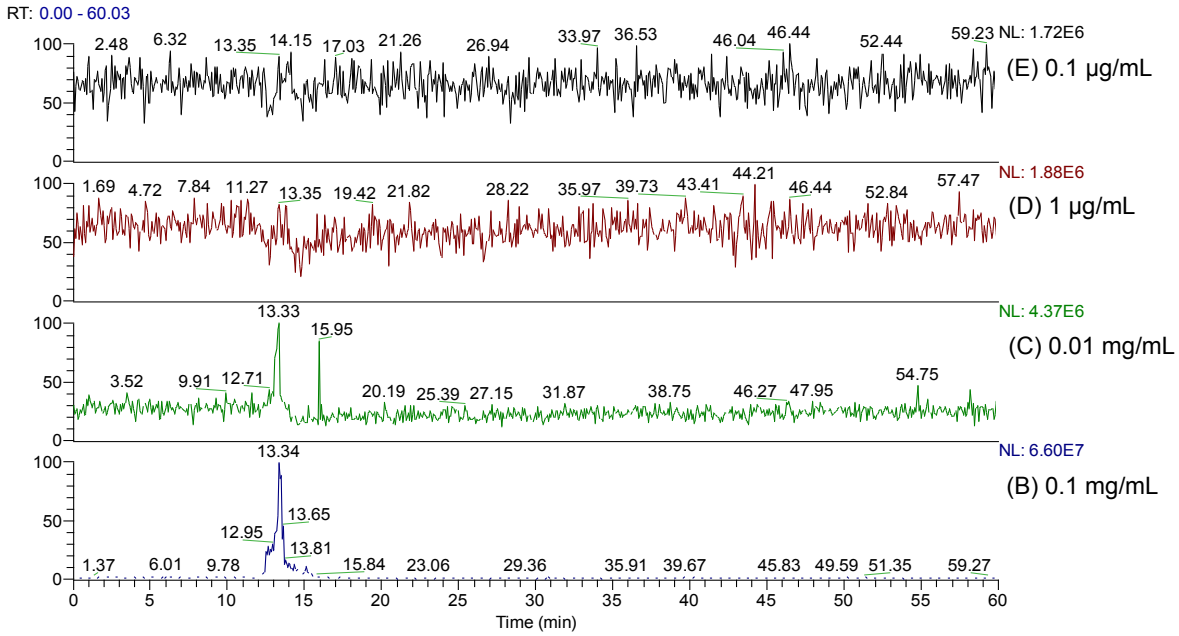

Figure 4-26 Dilution series for Aβ42 (E) 0.1 µg/mL to (B) 0.1 mg/mL, base peak chromatograms; tune method optimised for Aβ42 (1505 amu): capillary temp. 300 °C, sweep gas 40 units, aux. gas 20 units; mobile phase: 80 % H_2O/20 % ACN with 0.1 % FCA

The peak shape for the highest concentration showed fronting, probably caused by an additional amyloid β species. Here, the choice for a mass spectrometric detector instead of established UV/Vis devices proved its advantages. By selecting the fronting section of the peak, evaluating the mass spectra (fig. 4-27) and applying a mass range filter isolating the strongest signal (907.26 amu ± 0.5 amu) a peak otherwise suppressed by the main signal around 13.3 minutes (fig. 4-28) was revealed.

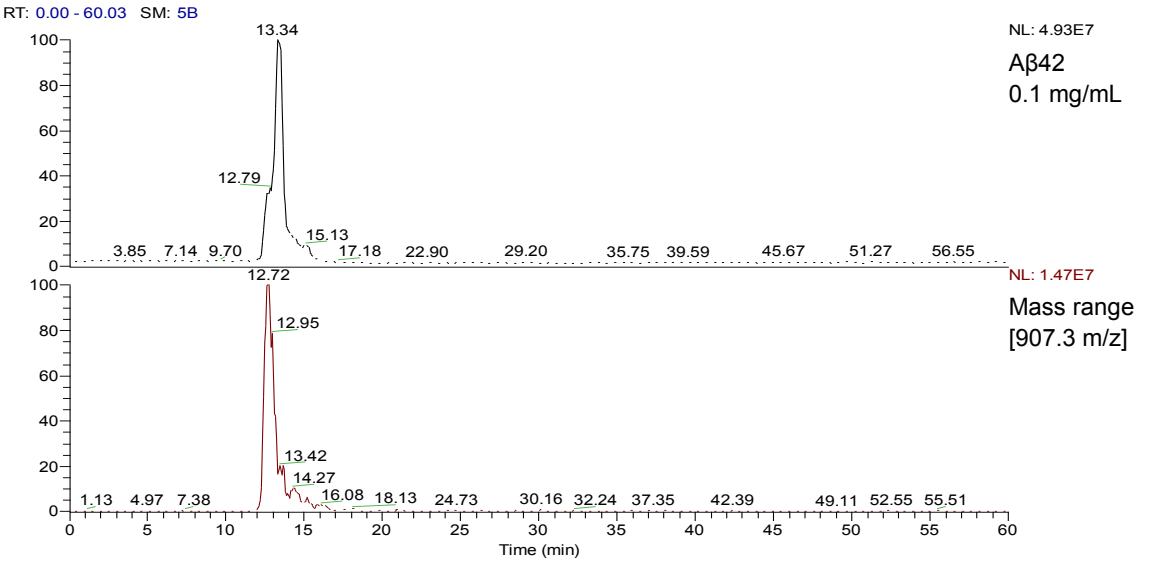

Figure 4-27 Chromatographic data for 0.1 mg/mL; Base peak and mass range chromatogram [907.3 ± 0.5 amu]

The charge state distribution detected in the mass spectra was already familiar from previous data sets gained during the reversed phase chromatography of Aβ42 (see fig. 4-6). Mass to charge ratios for z = +6 to +4 were entered into ESIprot to calculate a molecular weight of 4531.61 ± 0.98 Da. The reoccurring mass difference of 16 amu suggested a methionine-oxygenated species of Aβ42.

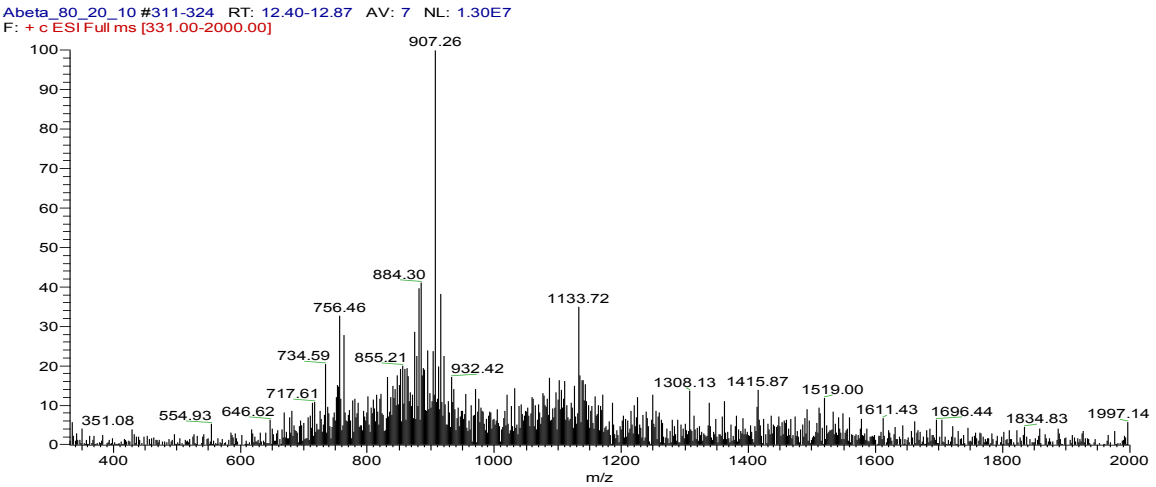

Figure 4-28 FullScan spectra (averaged) [331-2000 amu] for SEC-MS of 0.1 mg/mL Aβ42 corresponding to RT 12.4 – 12.87 min. Oxygenated species of Aβ42 suggested by molecular weight of 4531.61 ± 0.98 Da (ESIprot)

Throughout the method development for SEC-MS detection of amyloid β other standard proteins were examined, enabling a very rough estimation of the apparent molecular weight based on retention time. Even though most proteins had to be excluded due to either poor sample quality (haemoglobin) or non-ideal separation behaviour (myoglobin), clear signals for pepsin and lysozyme were used to get an idea about the relation of observed retention times to molecule size in terms of molecular weight.

Since both proteins are larger than an amyloid β 42 monomer, an additional reference point at the low end of the molecular mass scale was needed. A small peptide (524 Da)

named after the four amino acid sequence MRFA (methionine, arginine, phenylalanine and alanine) normally used during the annual tuning process was submitted to the method. Barely inside the separation range of the column (500 – 150,000 Da), the peptide marked the maximum retention time for the system. Analytes detected beyond 14.6 min were not separated while travelling through the column and were indistinguishable by separation mechanism alone.

Molecular weights of the chosen proteins and peptides were plotted against their corresponding retention times (peak max, fig. 4-29). Since only three reference points were plotted, the quadratic regression function chosen was very accurate (R^2 = 1.0000) but not necessarily the correct function describing the separation process along the SEC column. Conclusions regarding the molecular weight or hydrodynamic diameter, respectively of the amyloid β 42 can therefore only be careful estimations.

Both peak maximum (black line) and peak width (grey area) were considered for the calculations. The time frame of the peak covered a molecular weight range of 2.9 to 7.9 kDa while the peak maximum corresponded to an almost spot on estimate of 4.6 kDa for the amyloid β 42.

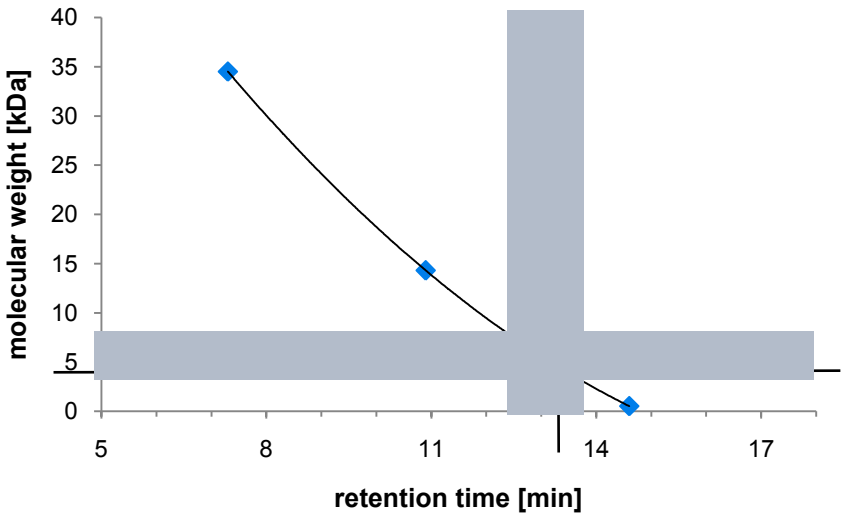

Figure 4-29 Plot molecular weight [kDa] vs. retention time [min] for pepsin (34.5 kDa), lysozyme (14.3 kDa) and MRFA (0.524 kDa). Regression: $y = 0.2586\ x^2 - 10.3179\ x + 96.0389$, R^2= 1.0000. Peak width (gray area) and maximum (black line) of Aβ42

With additional proteins, suited for the sensitive detection method and highly purified for as narrow peaks as possible, a calibration over the full separation range of the column would be possible. By isolating mass ranges of characteristic m/z ratios for Aβ proteins the method has the potential to simultaneously observe monomeric and oligomeric species in sample solutions. In comparison to immunoassays size-exclusion chromatography – mass spectrometry can differentiate between the species, providing insight into prevalent soluble oligomeric species thought to be essential in the progression of Alzheimer's disease and a trigger in neuronal cell death responsible for the decline in cognitive functions.

The major weakness of SEC, regardless of the specific detection method, is the stability of the column material itself. Since the separation mechanism does not rely on interactions with the solid phase, any damage generally caused by air bubbles

inadvertently forced through the column at high pressures influences separation efficiency. Channels created by air bubbles facilitate easier passages for proteins circumventing diffusion into pores and reducing actual retention times. Unfortunately the column used to develop the detection method described in this work was similarly affected before further experiments with oligomeric Aβ42 molecules or actual protein extracts from mouse brain samples could be performed within the available time frame. As a result, alternative pathways were explored to characterise amyloid β samples and protein extracts from mice brain tissue containing amyloid species.

4.1.3 Interims summary I – chromatographic separation of Aβ42

As a standard method used in protein analytics, preliminary reverse phase chromatography – MS of amyloid β 42 containing samples showed both the promise of MS detection and the limitations of RP chromatography for this separation problem.

- Additional MS data in chromatogram enabled partial protein identifications through calculated molecular weights from charge state distributions (ESIprot).
- Aβ 42 could not be doubtlessly identified in ELISA standard or provided protein extracts, but calculated weights pointed towards partial degradation and possible oligomerisation due to prolonged storage times.
- Separation of a synthesised monomeric Aβ42 standard provided essential MS data sets of Aβ42, Aβ40 and an oxygenated Aβ42 species for further method developments.
- Experiments proved Aβ 42 species as highly hydrophobic, eluting with high acetone contents in the mobile phase.
- Limitations of C18 stationary phase due to inability of underlying separation mechanism to differentiate monomeric and oligomeric species.
- Limitations of MS due to restricted resolution range preventing accurate charge state determination and estimation of oligomerisation.

Size exclusion chromatography – mass spectrometry was successfully established to provide an alternative for the separation and simultaneous detection of amyloid β oligomers. Obstacles in method development mainly originated from incompability of traditional buffered mobile phases and highly salt content sensitive electrospray ionisation process.

- Mobile phase optimisation led to a buffer-free mobile phase of 80 % H_2O and 20 % ACN with 0.1 % FCA.
- Method development focussed on optimisation of ion detection for standard proteins (pepsin, haemoglobin, myoglobin, lysozyme, MRFA) and amyloid β 42 and included basic ionisation parameters (T, auxiliary gas flow rates).
- Software-controlled tuning of the mass spectrometer led to signal improvement of nearly 700 % for Aβ42 detection.
- Lowest detected concentration 0.01 mg/mL at RT coinciding with molecular weight of ~4.6 kDa, confirming monomeric species.
- High potential as oligomer analysis method, limitations due to sensitive column material.

4.2 Protein extraction from mouse brain tissue and delipidation

Transition from source material to analysable sample represents a crucial step in sample preparations. For this work a method was needed to extract proteins from mouse brain tissue, mainly consisting of fats and water. Detecting and analysing amyloid β species was the main objective requiring extensive research into extraction methods that would preferably offer the isolation of low concentrations of hydrophobic proteins from overly abundant, hydrophilic proteins like immunoglobulins, albumins and matrix components.

Cloud point extraction using the non-ionic detergent Triton X-114 was chosen as the most suitable extraction method. This chapter describes the development of a sample preparation method based on a published CPE method for porcine brains to extract hydrophobic proteins from mouse brain tissues. Two avenues were pursued to achieve optimal results in extraction efficiency and the subsequent analytical examinations, namely choice of precipitation and delipidation method and influence of extraction medium composition on sample quality.

4.2.1 Protein precipitation and delipidation

Brain tissue is a very complex matrix that prevents method development approximated by buffered protein solutions alone. Investigations into the optimisation of the extraction and sample preparation process have to be performed using the actual biological matrix. The general composition of a human brain is summarised in table 4-8 in comparison to muscle tissue. Especially the combination of low protein concentration (8 %) and heightened lipid content (10-12 %), two thirds caused by protective myelin layers of neurons alone, complicates the extraction process, successful phase separation and subsequent sample preparation for electrophoretic separations and analysis (McIlwain and Bachelard 1985).

Table 4-8 General composition of human brain tissue

component	content in skeletal muscle [%]	content in whole brain [%]
water	75	77-78
lipids	5	10-12
protein	18-20	8
carbohydrate	1	1
soluble org. substances	3-5	2
inorganic salts	1	1

Protein precipitation is a very common purification step designed to separate proteins from other matrix components. Depending on the specific task, either purification of a target protein or precipitation of favourably all extracted proteins, various approaches are available to decrease protein solubility and cause precipitation.

Considering the high lipid content of the mouse brain, precipitation of extraction phase samples by addition of organic solvents (e.g. acetone) was chosen to not only lower the dielectrical constant of the solution causing proteins to aggregate and precipitate due to electrostatical interactions but also offer a medium preferable to both the non-ionic detergent and lipid molecules. Findings published by Shevchenko et al. concerning the

extraction of hydrophobic membrane proteins from porcine brains suggested possible delipidation methods for brain tissue (table 4-9).

Table 4-9 Applied protein precipitation and delipidation method

delipidation method	solvent composition/system
A	acetone, ice-cold
B	MeOH, H_2O, $CHCl_3$ two phase system
C	acetone: MeOH (8:1), ice-cold
D	Tri-n-butylphosphate: acetone: MeOH (1:12:1)

To assess each precipitation method 100 µL aliquots of a mouse brain protein sample extracted by cloud point extraction with a 1 % X-114 solution in a buffer system similar to the publication (buffer 1, see chapter 4.2.2 table 4-10) were treated according to the respective protocols. Resulting precipitates were redissolved in electrophoresis sample buffer containing lithium dodecylsulfate (LDS), incubated for 10 min at 70 °C and analysed by 1D SDS-PAGE.

Figure 4-30 shows the coomassie stained gel for the hydrophobic (A-C) and the hydrophilic (A'-C') phases on the left and the respective lanes for the fourth method (D/D') on the right. The latter samples were run on a separate gel depicted in chapter 4.2.2 fig. 4-31.

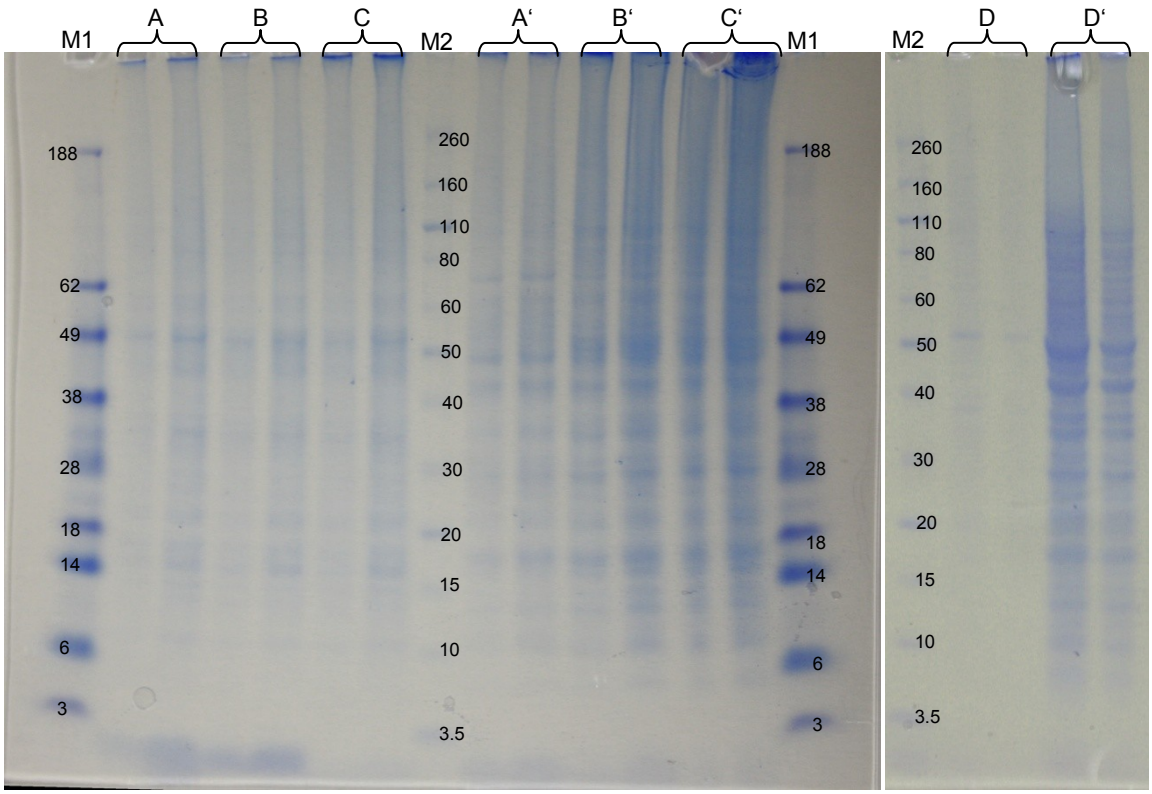

Figure 4-30 SDS-PAGE (4-12 %, A-C/A'-C' non-reducing cond., D/D' reducing cond.) of protein extracts using buffer system 1. M1 – SeeBlue prestained marker, M2 – Novex Sharp unstained marker. Sample volume 7.5 µL (**left**) and 15 µL (**right**) for A-C/A'-C'; 8 µL and 4 µL for D/D'

Differences between the precipitation methods were already observable during sample preparation for electrophoresis. Precipitates gained from the aqueous phases of method A' and to a lesser extent B' could not be completely redissolved in the electrophoresis buffer.

The incubation at 70 °C in the presence of the ionic detergent lithium dodecylsulfate (LDS) should lead to protein denaturation and the formation of uniform negatively charged protein-detergent complexes highly soluble in the buffer. Incomplete resolvation of precipitates A' and B' could have been caused by several factors. Using acetone alone may not be effective enough to remove the high lipid content present in both phases due to the lipophilic environment provided by Triton X-114 micelles. Lipids may bind to hydrophobic regions of proteins and interfere with their precipitation or resolvation in the aqueous electrophoresis buffer. Another phenomenon known to occur during protein precipitation is the often irreversible aggregation of proteins into insoluble conglomerates by electrostatic attraction (Wessel and Flügge 1984; Harris and Angal 1995).

The amount of dry precipitate was visibly lower for hydrophobic phases in comparison to aqueous phases. Photometric experiments using the 660 nm protein assay confirmed a ratio of ~1 mg/mL protein in hydrophobic phases to ~3 mg/mL in aqueous phases (see appendix A.5). Overall protein concentration in the extract phases could also have been a contributing factor in protein aggregation.

Examining the lanes corresponding to the individual delipidation methods allowed a qualitative assessment based on number of visible protein bands, intensity of the stain, resolution of protein bands and the general quality of the electrophoretic separation.

Precipitation with ice-cold acetone (A) was the least effective method tested. While there were some protein bands for the hydrophobic phase (A) visible and the intensity of the Coomassie blue stain was similar to other hydrophobic phases, the method proved to be almost ineffective regarding the aqueous phase (A'). Due to effects described above only a fraction of the actual proteins precipitated was redissolved in the sample leading to the faint bands observed for A' even in the maximum sample volume of 15 µL.

Method B utilised proteins precipitating as an interphase during the formation of a two-phase system between a water/methanol phase and a chloroform/methanol phase (Wessel and Flügge 1984). Major differences to acetone precipitation were visible for lanes belonging to the aqueous phase (B'). By subjective, visual assessment a larger amount of protein precipitate was redissolved during the electrophoresis sample preparation than for method A. The heightened intensity of the stained bands as well as the appearance of a higher number over an extended mass range (< 6 kDa to ~110 kDa) confirmed the increased concentration. Separation quality however, was worse for this delipidation method. Vertical streaking caused protein bands above 50 kDa to be difficult to distinguish from the overly stained background. Precipitation and delipidation using the methanol/chloroform/water system was eventually discarded due to the relatively complex sample preparation procedure and the low resolution and light vertical streaking in comparison to method D.

Combining acetone and methanol (8:1) led to a slightly increased protein concentration on the gel for the hydrophobic phase (C), judging by the colour intensity of the stained proteins. Band distribution followed a similar pattern to the alternative delipidation methods. The method proved to be the least suitable for the hydrophilic phase. While the intensity of the coomassie blue stain was high for both sample volumes (C') the quality of the separation, represented by a noticeable thinning of the lane confinements (left lane) and intensive vertical streaking was the worst of all investigated methods. Already during the electrophoresis the well structure was deformed most likely by insoluble protein aggregates and contaminants in the sample, unable to enter the gel matrix but still subjected to the current and trying to move in direction of the anode. Method C was therefore also discarded as a suitable precipitation and delipidation method.

By far the best results were achieved using a combination of organic solvents capable of accommodating high amounts of lipids (acetone, methanol) and the defoaming agent tri-n-butylphosphate (TBP). Method D was used by Mastro et al. to simultaneously delipidate black tiger prawn eggs containing a high amount of lipids (20 %) and produce a protein precipitate suitable for two-dimensional electrophoretic analysis (Mastro and Hall 1999). The group also found the method to be superior to the delipidation by organic solvents alone (acetone/methanol, 8:1).

Based on a visual evaluation the last set of hydrophobic lanes (D) in figure 4-34 it seemed as if precipitation by a mixture of tri-n-butylphosphate, acetone and methanol (1:12:1) was less effective for the hydrophobic phase. But as a consequence of streaking and deformation observed for the other three methods, sample volumes applied to the gel were reduced from 7.5/15 µL to 8 and 4 µL. The general pattern for the few visible protein bands remained unchanged but the light vertical streaking was reduced. The small number of protein bands for all detergent phases was mainly caused by smaller precipitation yields. By optimising the extraction buffer composition and the volume of electrophoresis buffer redissolving the precipitates, number and intensity of protein bands could be increased (see chapter 4.2.2).

More remarkable however were improvements observed for the aqueous phase (D'). The high resolution in both lanes emphasised the good quality of the protein precipitate. Even for the reduced sample volumes the intensity of the coomassie stain exceeded the alternative methods while displaying only a minimal degree of streaking. A small portion of the heightened resolution was attributed to the switch to reducing electrophoretic conditions. Dithiothreitol was added to the electrophoresis sample buffers to sever possible disulfide bonds and sharpen protein bands.

The high quality of samples prepared according to Mastro et al. (1999) using the combination of organic solvents commonly applied in protein precipitations and TBP was determined as the most effective method to gain high quality protein samples from cloud point extracts of mouse brains. A crucial factor for successful protein precipitation from a solution combining high lipid concentrations and non-ionic detergent was the addition of the defoaming agent tri-n-butylphosphate, as both acetone alone (A) and in combination with methanol (C) were insufficient.

4.2.2 Influence of extraction medium on cloud point extraction

The first published method to extract proteins with a non-ionic detergent from the Triton family was based on simple buffered 2 mg/mL protein solutions. Bordier et al. used 0.06 % Triton X-114 in a mild buffer (10 mM Tris pH 7.4, 150 mM NaCl) to observe the partitioning behaviour of hydrophilic and hydrophobic proteins by 1D SDS-PAGE. All hydrophilic proteins (e.g. BSA [GRAVY -0.475], catalase [-0.630], myoglobin [-0.396], cytochrome c [-0.426]) were exclusively found in the aqueous phases while hydrophobic and amphiphilic proteins (e.g. acetylcholinesterase [-0.212], bacteriorhodopsin [0.708], cytochrome c oxidase [+0.500]) were enriched in the detergent phase but could still be detected in the aqueous phase (Bordier 1981).

Based on a publication by Shevchenko et al. (2010) who used cloud point extraction with Triton X-114 to extract proteins from porcine brain material for bottom-up mass spectrometric identification of membrane proteins, the detergent content for extraction media was set at 1 %, ensuring a phase volume capable of containing a maximum concentration of hydrophobic proteins. To investigate a possible influence of buffer

composition on the separation three systems of varying complexity were employed (table 4-10).

Table 4-10 Extraction buffer compositions

component		concentration [mM]			function
		buffer 1	buffer 2	buffer 3	
Tris-HCl		10	10	-	stable pH 7.4
NaCl	PBS	~150	150	-	isotonic cond.
KCl	PBS	2.65			non-denaturing cond.
$Na_2HPO_4 \cdot 2\ H_2O$	PBS	8.12	-	-	stable pH
KH_2PO_4	PBS	2.44			
Triton X-114		1 %	1 %	1 %	hydrophobic extraction

Tris - tris(hydroxymethyl)aminomethane, PBS – phosphate buffered solution

Protein extraction from biological materials often requires mild and non-toxic conditions to preserve conformations and biological activities of target molecules. Isotonic phosphate buffered saline (PBS) systems are therefore broadly applied to protein extractions and purifications. Tris(hydroxymethyl)aminomethane chloride (Tris) is added as an additional buffer system to cope with spontaneous pH shifts caused by dissolution of cell membranes releasing the contents of various cell organelles (buffer 1). The second buffer system tested was originally used by Bordier et al. (1981) and lacked the buffering capacity of the phosphate system. As an alternative option pure water with 1 % X-114 was explored to investigate the actual necessity of a buffered system since such systems were designed with hydrophilic proteins in mind and the presence of inorganic salts can influence the cloud point temperature and phase partitioning (Weckstrom 1985; Lopes, Garcia et al. 2007).

The addition of a protease inhibitor cocktail to all solutions prior to the extraction prevented protein degradation due to the disruption of various cell compartments and the release of a range of proteolytic enzymes. Three trans-genetically modified APPPS1 mice, expressing mutated amyloid precursor protein and presenilin-1 variants were provided by the collaborating working group of Prof. Dr. Pahnke (see appendix A.1.1 table A-3).

After performing cloud point extractions (see chapter A.4) with each buffer system, 100 µL of each phase were precipitated by a mixture of tri-n-butylphosphate, acetone and methanol (1:12:1) determined to be the most suitable method by previous optimisation efforts (see chapter 4.2.1) and the resulting protein solutions separated by gel electrophoresis (fig. 4-31). On the basis of separation quality as well as the number of visible protein bands for each sample an assessment of the impact of buffer choice on the extraction efficiency and quality was possible.

The least successful extraction result was observed for the original isotonic Bordier tris buffer system (2) as only the aqueous phase (aq) resulted in protein bands detectable by the Coomassie Brilliant Blue stain. Apparently, no significant amounts of hydrophobic proteins were extracted into the hydrophobic detergent phase (X). While this occurrence could also stem from errors in sample preparation, the overall lack of visible bands for the X-114 phase eliminated the second buffer system from further application in this work.

Buffer system 1, favoured by Shevchenko et al. (2001) showed slight improvements in comparison to system 2. Weak protein bands were visible for the detergent phase (X) indicating at least small amounts of proteins extracted into the hydrophobic phase. The faint blue colouring of most of the bands represented low concentrations in the sample.

Figure 4-31 depicts only a photograph of the actual gel and finer details and definition of single protein bands were better distinguishable when handling the gel itself. Mass distributions for the aqueous phases of buffer 1 and 2 appeared quite similar, showing a slightly improved resolution, stain intensity and clearer background for the phosphate buffered saline extraction.

Astonishingly the most effective extraction solution was the simple water/detergent system (3) tested at the off-chance at less complex extraction medium. Numerous protein bands were visible from ~110 kDa to ~15 kDa for the 8 µL sample volume of the detergent phase (left lane for 3 (X)). Some mirrored the more abundant bands found in the aqueous phase indicating partitioning of higher concentrated proteins while other bands were found only in the hydrophobic phase.

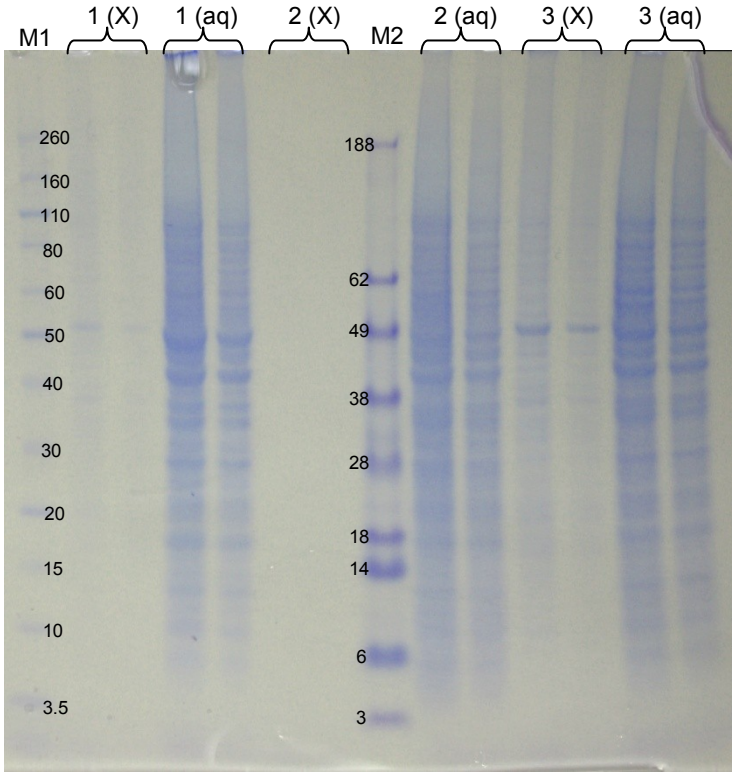

Figure 4-31 SDS-PAGE (4-12 %, reducing cond.) of protein extracts using buffer systems 1-3. M1 – Novex Sharp unstained marker, M2 – SeeBlue marker. Sample volume 8 µL (**left**) and 4 µL (**right**) for each phase respectively.

Examining the 4 µL sample volume results for the aqueous phases of all three extraction methods led to the conclusion that the simple water system was also the most suitable for hydrophilic proteins extracted from mouse brain tissue; bands were more defined and intensive, distributed over a large molecular weight range from ~110 kDa to less than 6 kDa.

During the sample preparation process it became apparent that the absolute amount of precipitate was always significantly lower for detergent phases than for hydrophilic phases. Photometric assays using the 660 nm protein assay (see appendix A.1.5.1) of protein extracts confirmed a general ratio of protein concentrations in the X-114 to the aqueous phase as 1 mg/mL: 3 mg/mL (table 4-11 and appendix A.5).

Table 4-11 Protein concentrations determined by photometric assay (660 nm, Pierce) at 10.5 °C

		concentration [µg/mL]	
extraction medium	**tissue mass [wet]**	X-114 phase	aqueous phase
buffer 1	~ 140 mg	1141.7	2664.2
buffer 2	~ 157 mg	1069.6	2712.1
buffer 3	~ 160 mg	1126.4	3094.5

To somewhat alleviate the gap, another set of samples was prepared for gel electrophoresis with reduced resolvation solution volumes (40 µL instead of 100 µL) for hydrophobic phases (fig. 4-32).

For all X-114 samples the number of visible protein bands increased, albeit in lesser extent for the Bordier buffer system (2) that showed no bands in the previous gel than for the other two extraction media. A closer look at the 2 (X) lane confirmed the decreased extraction efficiency of the isotonic tris-buffered solution. As an example, the relatively intensive protein band present in all other sample lanes around 49 kDa was not observed most likely due to poor phase partitioning.

The lower graphic resolution of the image in figure 4-32 in comparison to fig. 4-31 and light background staining for all samples hinder a clear distinction of less concentrated protein bands in the picture, nearly levelling the optical differences between the aqueous sample lanes.

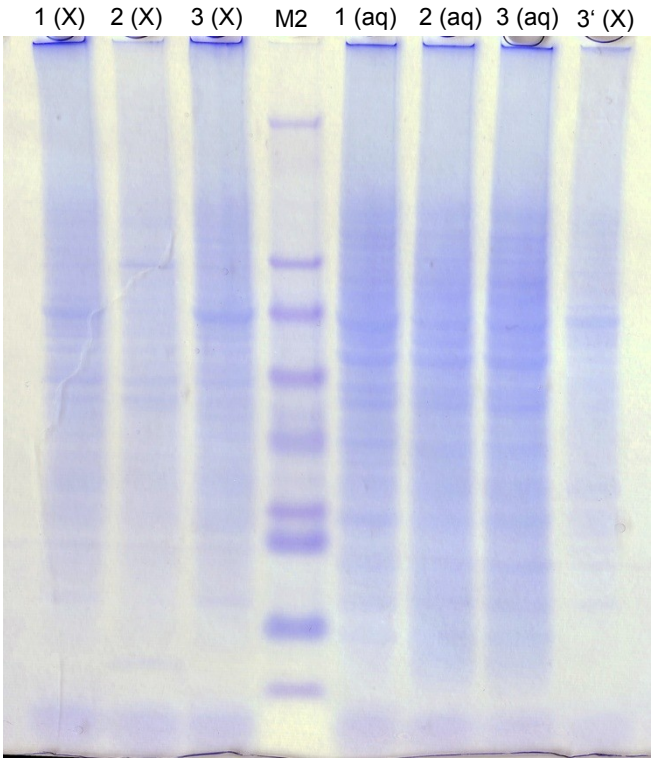

Figure 4-32 SDS-PAGE (4-12 %, reducing cond.) of protein extracts using buffer systems 1-3. M2 – SeeBlue marker. Detergent phases (**left of marker**) 40 µL resolvation solution, aqueous phases (**right**) 100 µL

An additional lane of the gel was used to run the detergent phase sample from the prior gel electrophoresis 3’ (X) again, allowing a direct assessment of the effect of the reduced volume 3 (X). As expected the colour intensity increased enabling the identification of

less abundant protein bands. The general distribution of protein bands was identical in both lanes.

Blue residue atop the wells illustrated the still incomplete transition of proteins from the electrophoresis sample buffer into the gel matrix, most likely caused by irreversibly denatured/precipitated proteins. Both gel electrophoresis experiments confirmed the high suitability of the simplest extraction system consisting of 1 % Triton X-114 in pure water. Samples prepared from both the detergent and aqueous phase yielded numerous clear protein bands suitable for in-gel digestions.

4.2.3 Interims summary II – protein extraction and delipidation

The extraction of proteins from mouse brain tissue and subsequent sample preparation steps represented a crucial part of this work. Four precipitation/delipidation methods published in literature were investigated.

- Photometric assays (660 nm assay) revealed protein content ratio of aqueous to detergent phases as approx. 3 : 1 mg/mL.
- Gel electrophoresis of prepared samples determined sample quality (number of protein bands, resolution, background staining) and mass ranges of extracted proteins.
- Superior precipitation/delipidation was achieved by combining tolerance for high lipid concentration in brain tissue and non-ionic detergent found in a mixture of methanol, acetone and the defoaming agent tri-n-butylphosphate (1:12:1).

Furthermore the influence of extraction medium composition in the cloud point extraction process on sample and gel electrophoresis quality was explored. The three buffer systems tested declined in complexity from a phosphate buffered saline with an additional Tris buffer system, an only Tris buffered system to ultrapure water.

- Simple system of 1 % Triton X-114 in ultrapure water containing a standard protease inhibitor cocktail surprisingly emerged as optimal extraction environment.
- The unconventional and uncomplicated system produced highest sample quality and broadest mass range of detected protein bands (110 kDa to 15 kDa).
- Gel electrophoresis results of detergent phases was improved by taking relative protein concentration of aqueous and detergent phases into account, leading to reduction of resolvation volume of precipitates from hydrophobic phases.
- High quality of electrophoretic separation yielded numerous clear protein bands for tryptic in-gel digestion and identification by LC-MS/MS.
- Still optimisation potential in slightly incomplete resolvation of protein precipitates prior to SDS PAGE.

4.3 Assessment of protein partitioning in cloud point extraction

To evaluate cloud point extraction with Triton X-114 as a suitable sample preparation method for mouse brain tissue with a focus on amyloid species, proteins were identified using BioWorks™ software and their occurrence in relation to various parameters investigated. The distributions of detected proteins corresponding to elevated capillary voltage as well as specific cellular locations and functions were studied to assess protein partitioning behaviour.

Since the tested chromatographic separation methods for intact proteins were insufficient (RPLC-MS) or halted before a reliable analysis method could be established (SEC-MS), for a thorough characterisation of protein partitioning behaviour, protein bands separated and fixed by SDS-PAGE were subjected to tryptic digestion and identification by reversed phase liquid chromatography and two-dimensional mass spectrometry of the resulting peptides (see appendices A.1.5.2 and A.1.5.4).

In total 260 bands were selected from five prepared gels with varying sample preparation parameters. Excision of bands was decided based on multiple criteria. The initial main focus was the examination of potential amyloid β oligomer bands. Plotting retention factor R_f (ratio of travelled distance protein to an unretained substance) against their logarithmic molecular weights of marker proteins (M1 or M2) allowed the calculation of theoretical distances covered by oligomeric species in each gel. Protein bands roughly matching the values of monomers (~4.6 kDa) to dodecamers (~55.2 kDa) were further analysed by LC-MS/MS (see appendix A.1.5.5). With progressing insight into analysed samples and the aim of characterising extracts the selection of protein bands was expanded to include non-oligomer candidate bands for samples both from the aqueous and detergent phases.

To identify proteins in excised protein bands from various extraction approaches described in chapter 4.2.2 generated mass spectrometric data sets were analysed using BioWorks™ software and Sequest algorithm (see appendix A.1.5.6). Closer examination of each compiled search result file provided multiple protein matches for peptides detected during the respective chromatographic runs. Performance and examination were optimised by limiting the number of database entries. While using the universal UniProt database would cover all the bases and provide results, it also contains all known proteins and a high number of analogues found in various organisms amounting to over 30.3 million entries. To improve the probability of correct results and reduce the extremely high time demands, an organism specific sub-database was created using the FASTA database tool of the BioWorks™ software. Selecting the latin genus [mus] as the deciding parameter for proteins to be included resulted in a significantly smaller database of nearly 92,000 entries that automatically included all mouse species, mainly the ordinary house mouse that was the basis for the genetically altered laboratory animals (Mus musculus). Additionally some non-related organisms like bacteria and other animals whose latin names or protein names inadvertently included the letter combination. Further specification of the selection parameter to [Mus musculus] would have resulted in an even slimmer data set (~ 81,000) but the inclusion of random organisms served as an additional indicator for reliable protein identifications.

The FASTA database format only allows for the most basic protein information to be included. Usually an entry consists of a one line description detailing name, database ID and organism followed by the protein amino acid sequence in one letter code. BioWorks™ calculates composite values like pI and molecular weight from the sequence

information. Any additional information regarding functions and specific cellular location in the organism has been accessed online using the UniProt platform.

Cloud point extraction creates a two phase environment that allows the separation of proteins according to their hydrophobic character. An indicator of this particular protein property is the grand average of hydropathicity index (GRAVY), based on the relative hydrophobicity or hydrophilicity of amino acid residues in protein sequences (Kyte and Doolittle 1982). The indices are freely accessible online using the ProtParam tool provided by the Swiss Institute of Bioinformatics (SIB) by entering either six character UniProt database IDs or organism specific acronyms. GRAVY indices are not displayed in BioWorks^{TM} search result files and had to be looked up manually for each valid protein match (see appendix A.1.5.7).

Individual pieces of information were summarised in table form to evaluate the extracted proteins based on different parameters. In addition to basic informations – protein name, UniProt ID, molecular weight and pI – the individual GRAVY indices were added and the affiliation to one or both extraction phases as well as their detection with either the initial (capillary voltage 18 V) or altered (43 V) instrument method was noted for each protein. Considering CPE is generally favoured for the extraction of membrane or membrane-bound proteins available cellular location information and a basic categorisation based on specific protein functions (e.g. transport, metabolism, cell cycle etc.) was also included for each protein.

Since the extraction relied on hydrophobic interactions of proteins with Triton X-114 micelles, sorting the established table by their GRAVY indices allowed assessments based on the number and properties of proteins detected according to the various parameters while simultaneously observing the influence of the calculated hydropathicity on partitioning behaviour.

4.3.1 Partitioning according to extraction phase

A crucial point of interest was the characterisation of both extraction phases in relation to the hydrophobicity of detected proteins. Based on the extraction mechanism an accumulation of proteins found in aqueous phases was expected mostly for negative GRAVY indices and mainly positive for detergent phases.

Diagrams displayed in figure 4-33 gave an overview of the number of proteins detected using a capillary voltage of 18 V (above) representing a routine analysis method for tryptic digests with the linear trap quadrupole (LTQ) mass spectrometer or using an altered capillary voltage of 43 V (below) to implement insights gained from optimisation efforts in the detection of the hydrophobic amyloid β 42 protein (see chapter 4.2). Both figures show the total number of proteins detected within defined narrow GRAVY index ranges spanning the absolute value of 0.125 composed of the respective fractions found in either one or both extraction phases.

Though minor differences are noticeable, general trends concerning protein distribution in the extraction phases and in relation to protein hydropathicity were similar for both settings. Of 441 identified proteins with 18 V, 234 (53.1 %) were exclusive to the aqueous phase, 100 (22.7 %) to the detergent and 107 (24.3 %) were found in both phases. For 43 V (374) capillary voltage 55.1 % (206) were detected in the aqueous phase, 24.3 % (91) in micelle-rich phases and 20.6 % (77) in both. The observed overlap indicated a good phase separation as it reflected published results of overlaps of 16 to 23 % for CPE of mouse brain tissue (Wetterhall, Shevchenko et al. 2011).

The majority of proteins were detected in the GRAVY range of -0.750 to 0.125 with the highest number of proteins occurring from -0.375 to -0.250 for both methods. For 18 V this fraction also represented the maxima for each extraction phase and proteins belonging to both extraction phases. The diagrams show similar trends in the correlation of the number of proteins detected and their GRAVY indices hinting at natural distributions within the tissue; the largest portions being very hydrophilic to lightly hydrophobic. Extreme ends of the GRAVY scale were less abundant due probably to higher efforts necessary to create and maintain suitable environments in the cellular structure.

The quantity of detected proteins was lower for 43 V; to an extent because the altered instrument method was only implemented starting from the 81th excised band.

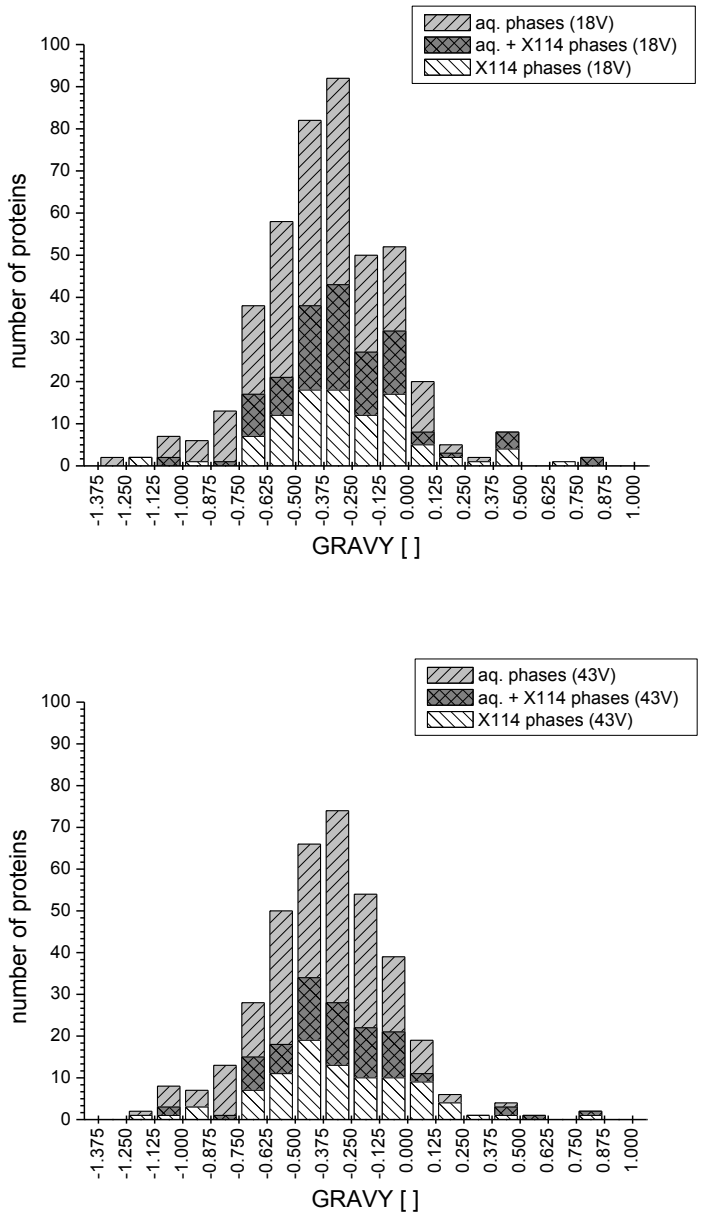

Figure 4-33 Plot of all detected proteins for aqueous and Triton-X114 rich phases vs. GRAVY index ranges of [0.125]. Total height equals total number of proteins assigned to the GRAVY range, composed of marked areas representing number of proteins found in each or in both phases. Capillary voltage: 18 V (**above**) and 43 V (**below**).

Of 236 proteins identified in the first 80 bands, 160 (~68 %) were also detected with the higher capillary voltage in later samples. A high ratio of proteins exclusive to the 80 bands (76, ~ 32 %) had relatively high probabilities (P > 0.1) indicating either low quality matches, very low abundance of the detected peptides or problems during ionisation due to specific peptide properties. Reliable matches in BioWorks™ search result files were indicated by low values of the probability P that the reported match was false. The threshold to include a protein match for extract characterisation was defined as $P \leq 0.5$; representing a 1:2 chance that the suggested protein is false. Additionally, examining the remaining 180 protein bands also showed a high number of proteins exclusively detected with capillary voltages of 18 V or 43 V, lessening the significance of the first 80 runs not repeated with the altered 43 V settings.

Figure 4-34 illustrates the correlation of the quantity of detected proteins and the applied instrument methods defined by capillary voltage. A high percentage in each GRAVY range could be detected with both instrument methods showing a similar distribution to proteins found in both extraction phases (fig. 4-33); rising and falling with the total number of proteins detected.

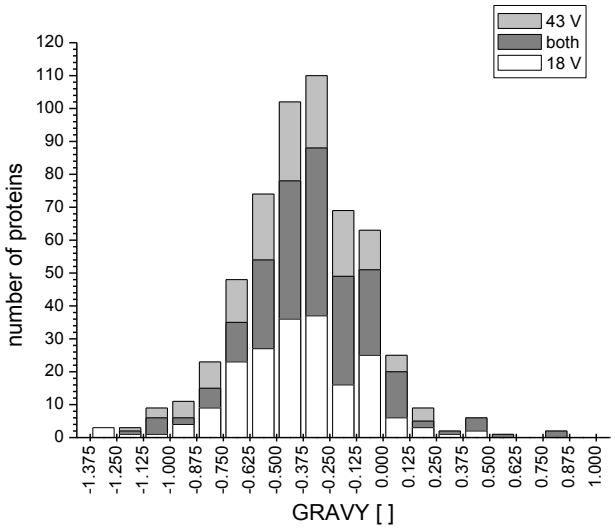

Figure 4-34 Protein distributions vs. GRAVY indices using capillary voltages of 18 or 43 V

The ratio of proteins exclusively detected with the standard 18 V method was often higher than with 43 V. Overall 35.5 % (194) of all identified proteins (546) were detected with 18 V and 23.3 % (126) with 43 V. The overlap between the two capillary voltage settings was 41.4 % (226).

However, increasing capillary voltage expanded the detection range and allowed a more thorough characterisation of the extracts. Additional proteins were identified for index ranges up to 0.250 with a maximum of 24 new proteins in the -0.5 to -0.375 range. An investigation into protein identities, cellular locations and functions in connection to the capillary voltage is discussed in chapter 4.3.2. Increasing the capillary voltage had only a small impact on the detection of very hydrophobic proteins (GRAVY > 0) adding just nine protein matches from 0 to 0.250.

The protein identification strategy used relies on peptides produced by the proteolytic enzyme trypsin. Any effect observed for the raised capillary voltage was therefore not necessarily associated with the overall relative hydropathicity of indicated matches but primarily reflects on the electrospray ionisation process and ion transfer into the mass

spectrometer defined by parameter sets implemented in instrument methods. As soon as peptide bonds within the protein molecule are severed, properties known and associated with the intact protein become obsolete. Instead, numerous peptides are formed each with unique and sequence specific properties that influence chromatographic retention and, more importantly, the ionisation process.

The fairly even distribution of additionally detected proteins over the observed GRAVY range suggests a generic, positive impact on the ionisation process based on peptide properties that have not been included in this characterisation and assessment of cloud point extractions. Statistical examinations of peptides assigned to protein matches may provide further insights into sequence specific properties influencing the ionisation process at higher capillary voltages.

Looking at the protein distributions in the extraction phases separately (fig. 4-35) slight differences between aqueous and detergent-rich phases were evident. Instead of the expected distinct confinement to the negative (aq. phases) or positive (X114 phases) GRAVY indices, both extraction phases encompassed a broad range on the scale. Yet, tendencies related to the expected phase separation behaviour were still noticeable.

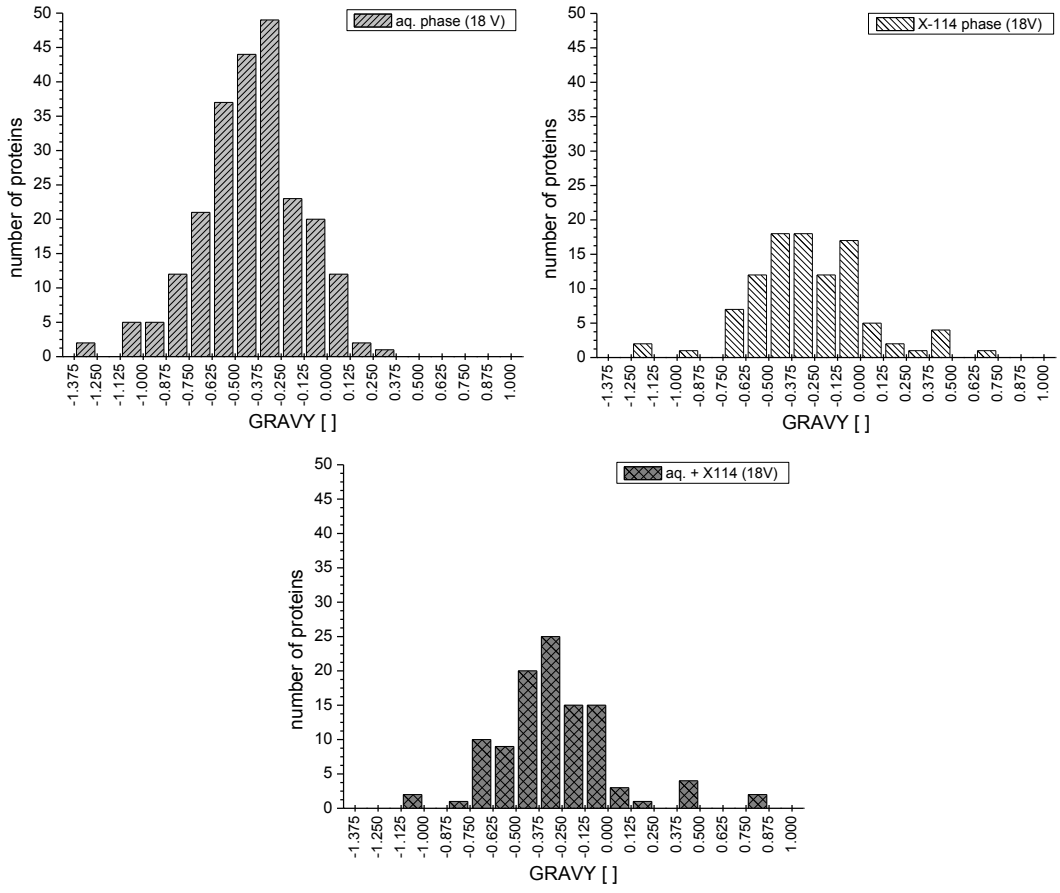

Figure 4-35 Number of proteins vs. GRAVY indices for 18 V capillary voltage for aq. phases (**top left**), detergent phases (**top right**) and both (**bottom**).

Only three proteins were assigned in the highly hydrophilic GRAVY range of -1.375 to -0.75 for Triton X-114 phases in comparison to 24 detected in their aqueous counterparts, confirming a preference of highly hydrophilic proteins for the aqueous extraction environment. The opposite end of the observed scale provided a similar picture for the

detergent phases, where only three proteins were detected in the range of 0.125 to 0.375 for aqueous samples while eight were found in detergent-rich phases with GRAVY indices of up to 0.750 indicating improved solubilities for highly hydrophobic proteins in Triton X-114 micelles during the extraction.

Differences between the extraction phases were also visible in the general appearances of the distributions. For aqueous phases the slope for increasing and decreasing protein numbers was quite steep within a range encompassing GRAVY indices from -1.334 to 0.355. Proteins extracted into the detergent phase showed a lower and broader distribution reaching less than half the protein quantities found in the aqueous phase. The overlap between both phases displayed partial characteristics of each separate phase, concentrated within the most frequent GRAVY ranges (-0.750 to 0.000) with sporadic occurrences of highly hydrophilic (-1.000 to -1.125) and hydrophobic (0.375 to 0.500; 0.750 to 0.875) proteins. Only a few were common to both extraction phases outside the range from -0.750 to 0, demonstrating that cloud point extraction of brain tissue using Triton X-114 was indeed a partitioning process between detergent micelles and aqueous solution. The overlap between both phases was most likely favoured for proteins in higher concentrations within the favoured GRAVY range.

The protein distributions for each extraction phase and proteins found in both detected with the elevated capillary voltage of 43 V followed similar patterns to the 18 V method (see appendices A.7.4 to A.7.6). Major differences lay in the smaller number of proteins detected in the preferred hydrophilic GRAVY ranges from -0.750 to 0.000 and a slight shift in the distribution of hydrophobic proteins detected (0.000 to 0.500). Some of the proteins included in the diagram were exclusive to the altered instrument setting but the distribution still confirmed the detection of a natural protein distribution patterns within the extracted tissue.

The most hydrophobic proteins found in the mouse brain tissue extracts according to their GRAVY indices – Claudin-11 (UniProt ID Q60771, GRAVY 0.854, MW 22.1 kDa, pI 8.23), a transmembrane protein involved in calcium-independent cell adhesion and the protoheme IX farnesyl transferase (A0LTZ0, GRAVY 0.824, 33 kDa, pI 10.98), an enzyme involved in the porphyrin metabolism – were detected in both phases at 18 V capillary voltage. For 43 V only the farnesyl transferase was detected in both phases, Claudin-11 could only be detected in digest samples from the detergent phase.

Proteins with the lowest GRAVY values differed for the methods. The two lowest indices were found only for 18 V in the range from -1.375 to -1.25 in comparison to -1.25 to -1.125 for 43 V. With a GRAVY index of -1.334 stathmin (P54227, 17.1 kDa, pI 5.76), a cytoplasmic protein involved in regulation of the microtubule filament system and possibly required for axon formation during neurogenesis, was the most hydrophilic protein detected with 18 V capillary voltage during this study. The second protein was identified as PRKR-interacting protein 1 (Q9CWV6, GRAVY -1.28, 21.5 kDa, pI 9.44) found in nuclei and able to bind double stranded RNA. Both proteins were exclusive to aqueous extraction phases.

The hydrophilic range for the higher capillary voltage extended to minimum of -1.233 for the aqueous phase with calreticulin (P14211, 46.3 kDa, pI 4.33), a calcium-binding chaperone that promotes folding, oligomeric assembly and quality control of proteins in the endoplasmatic reticulum. The lowest GRAVY index for the detergent phase for 43 V was myelin basic protein (P04370, GRAVY -1.198, 27.2 kDa, pI 9.58), representing a group of protein isoforms that belong to the most abundant protein components of myelin membranes in the nervous system and are structural constituents of myelin sheaths of neurons.

A prediction of partitioning behaviour in cloud point extractions with Triton X-114 based on amino acid sequences and the resulting relative hydropathicity tendencies was eventually rated as not reliable. As a composite parameter based on individual amino acid values it can only be considered as a preliminary inclination towards a possible partitioning behaviour during phase separation. Other protein specific properties apparently played larger roles as driving forces than originally assumed in the premise of this work.

4.3.2 Partitioning according to cell component location

The theory behind the application of cloud point extraction with Triton X-114 to the extraction of hydrophobic proteins from brain tissue was the assumption that detergent micelles formed in the aqueous solution emulate a bilipid layer-like environment. Proteins adapted to conditions near and within a membrane should prefer the similar environment provided by the micelles and be consequently extracted into the detergent phase.

In addition to the very insightful general information obtainable by searching the UniProt online database, each entry also contains, if known, basic biological data. A point of interest in the characterisation of the cloud point extraction samples was the assessment of detected proteins in relation to their respective cellular locations in the tissue. The accumulation of membrane bound and membrane associated proteins in the detergent phases and subsequently an excess of proteins originating from cytoplasm in aqueous extraction phases was expected, based on published results (Bordier 1981; Shevchenko, Sjodin et al. 2010; Wetterhall, Shevchenko et al. 2011).

Only proteins with definite location data were included in the following examinations. Entries with specified cell compartments but without clear indications whether the protein is typically found in cytoplasmic or membrane environments were exempted. Even with the high degree of fully characterised proteins for the house mouse due to its common use as laboratory animal for medical studies, some matches showed, as of march 2013, incomplete or empty data sets preventing a complete classification of all detected proteins. Proteins excluded from the assessment represented just a small fraction of each GRAVY range and did not significantly influence the trends observed.

Analogous to distribution diagrams compiled for the extraction phases in chapter 4.3.1., the cellular origin of extracted proteins was plotted against their GRAVY indices subdivided into smaller steps of 0.125 units. Figures 4-36 and 4-37 display the resulting bar charts for each extraction phase and 18 V capillary voltage as well as pie charts summarising the overall ratios corresponding to each location.

In comparison to the previous observations of GRAVY distributions of proteins found in either the aqueous or detergent phase that was unable to confirm CPE as a hydrophobic extraction method judged by the indices alone, the assessment by cellular location showed clear tendencies for both phases. More than half (53.2 %) or two thirds (67.5 %), counting proteins also credited to cytoplasm, of proteins extracted into the micelle rich phase were associated to membranes while merely a third (32.5 %) or less than half (46.8 %) originated from cytoplasmic environments (fig. 4-36, right).

The trend was reversed for the aqueous phase. Even from the bar chart alone it was obvious that significantly larger portions of identified proteins originated from various cytoplasmic compartments. Merely a fifth (21.4 %) or 38.5 % were related to membranes, 61.4 % were associated solely to the cytoplasm and 17.1 % were common to both (fig. 4-37, right).

For detergent phases the prevalence of membrane proteins was especially apparent for GRAVY indices higher than -0.500. Below that value the number of proteins credited to the cytoplasm was higher. The majority of membrane related protein matches was concentrated in the GRAVY range from -0.500 to 0.125. Proteins in the GRAVY range from -0.125 to 0.125 were predominantly membrane related and somewhat reinforced the general connection between the relative hydropathicity index and membrane associated proteins. The more hydrophobic detected proteins became, the less they were found in the cytoplasm alone. Similar to the distributions based on the extraction phases the most hydrophobic proteins were linked to both locations.

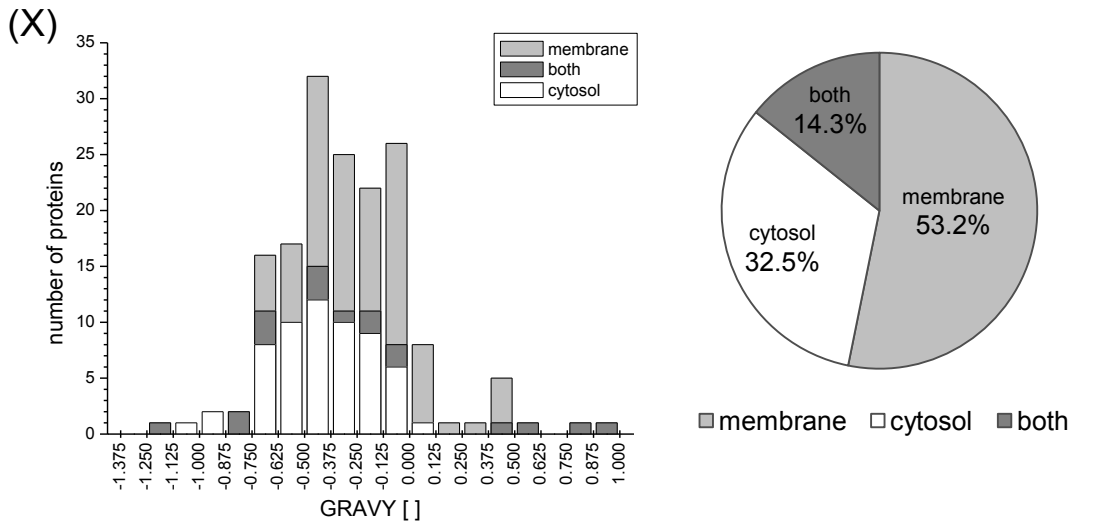

Figure 4-36 Protein distribution according to cellular location vs. GRAVY for proteins detected in the detergent phases and with 18 V capillary voltage.

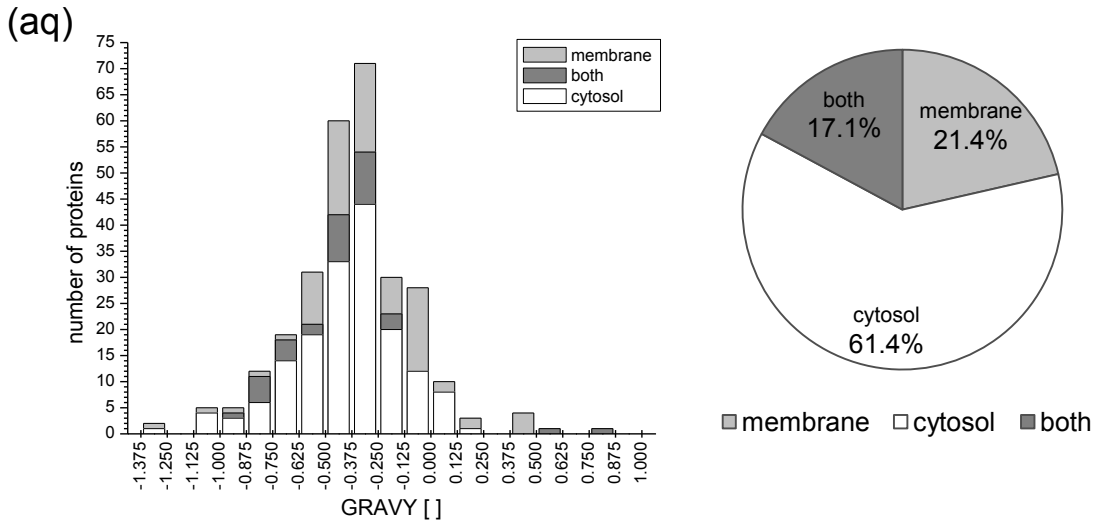

Figure 4-37 Protein distribution according to cellular location vs. GRAVY for proteins detected in the aqueous phases (aq) and with 18 V capillary voltage

Based on the protein distribution in the aqueous phase in fig. 4-37 it became clear that while CPE with Triton X-114 was successful in extracting portions of membrane proteins regardless of their relative hydrophobicity from the aqueous phase into the micelle-rich phase, a significant portion of membrane proteins remained. An explanation may be found in the limited phase volumes of the detergent phase during the extraction. Micelle concentration and consequently the detergent phase volume were limited by the percentage of Triton X-114 in the extraction solution. The chosen content of 1 % was already considerably higher than originally published by Bordier (0.06 %) to ensure both high micelle concentration and counteract competition for the favourable hydrophobic environment between proteins and lipid molecules present in fatty brain tissue.

The number of membrane proteins credited to the aqueous phase (54) seemed nearly equal to the detergent phase (61). In relation their overall distribution however, the fraction of membrane proteins in the aqueous phase decreased distinctively. The excess of

proteins related to cytoplasmic cellular locations followed the progression of the trends observed for GRAVY ranges from -1.375 to 0.250.

Visually a distinction between the extraction phases can be exemplified by comparing the transitions from lightly hydrophilic [-0.125 to 0.000] to hydrophobic [0.000 to 0.125] indices. In the micelle-rich phases the first range represented the highest number of membrane (18 + 2) proteins detected in a GRAVY range while the ratio in the slightly hydrophobic range marked the highest ratio to cytoplasmic proteins (7:1). For the aqueous phase the number of membrane proteins for the first range was still among the highest detected (16) but the ratio to cytoplasm related proteins was significantly higher (M/C 4:3). In the following positive range it was flipped in comparison to the detergent phase, with a ratio in favour of the cytoplamic fraction (1:4).

Patterns observed for the instrument method employing the lower capillary voltage of 18 V were largely repeated for the higher setting of 43 V. Diagrams summarising the data are shown in figures 4-38 and 4-39 below.

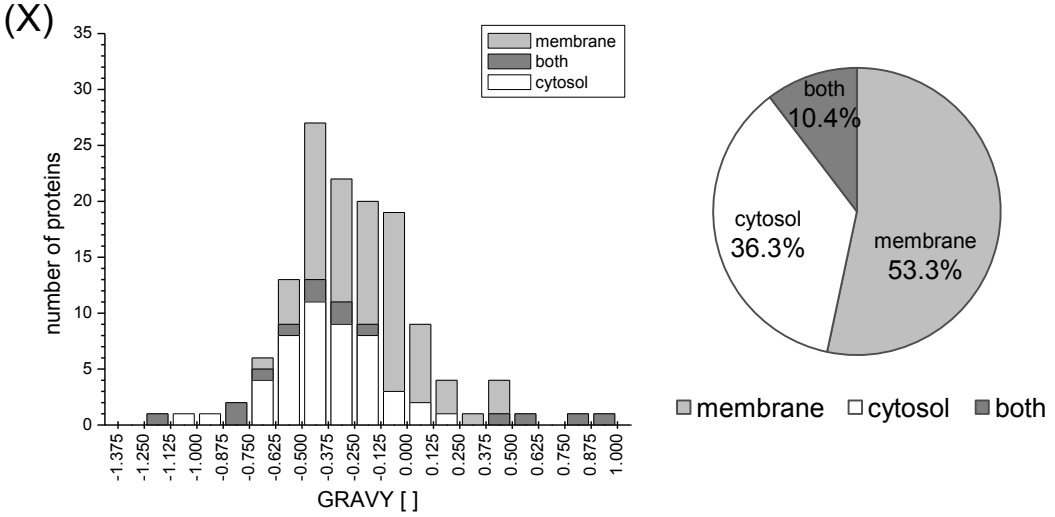

Figure 4-38 Protein distribution according to cellular location vs. GRAVY for proteins detected in the detergent phases and with 18 V capillary voltage

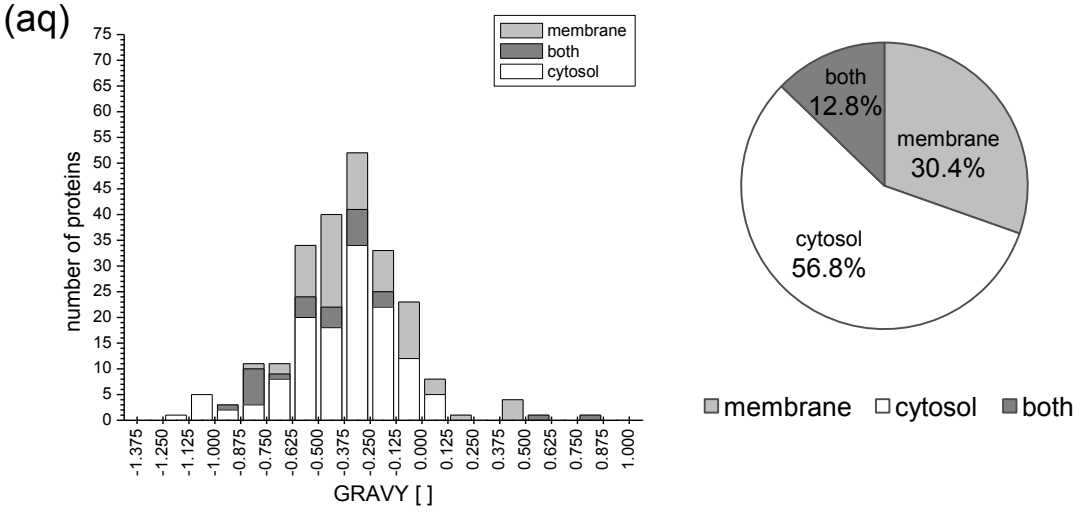

Figure 4-39 Protein distribution according to cellular location vs. GRAVY for proteins detected in the aqueous phases and with 43 V capillary voltage

The protein distribution in the detergent phase was only slightly altered for the 43 V capillary experiments. Despite decreased overall numbers the ratio of membrane proteins identified in the micelle-rich phase remained constant at 53.3 %. Proteins linked to cytoplasm increased by approximately 4 % and covered the broader GRAVY range from -1.125 to 0.250. Proteins originating from membrane environments on the other hand were mainly detected in the narrower range from -0.625 to 0.5. The ratios of membrane proteins across the ranges were more evenly balanced from -0.500 to -0.125 but then abruptly increased with increasing GRAVY values. In both instrument settings the maximum number of proteins was detected for GRAVY indices from -0.500 to -0.375 (32 and 22, respectively). The detection of the most hydrophilic as well as hydrophobic proteins was unaffected.

Increasing the capillary voltage had a considerably larger impact on the aqueous phase distribution. The fractions of cytoplasm related and overlapping proteins decreased to 56.8 % and 12.8 % in favour of membrane proteins increasing by 9 % to 30.4 %. The change was also visible in the uneven rise and fall of protein numbers per GRAVY range resulting in a less smooth distribution compared to 18 V. The lowest relative hydropathicity detected was represented by one cytoplasmic protein in the -1.250 to -1.125 range (Calreticulin, P14211, -1.233).

Still, the altered setting offered similar observations to characterise the aqueous extraction phase. The percentages of proteins from cytoplasmic environments were mostly dominant over a range from -1.250 to 0.250, the highest number of cytoplasmic proteins was again found in the GRAVY range from -0.375 to -0.250 despite the decreased overall number (72 to 52) and most hydrophobic protein (both locations) was detected in the range from 0.750 to 0.875 (protoheme IX farnesyltransferase, A0LTZ0, 0.824).

Comparable to the 18 V distributions, the distinction between extraction phases was especially clear at the transition from the hydrophilic to the hydrophobic section of the GRAVY axis. For the detergent phase (X) the slightly hydrophilic range from -0.125 to 0 contained the peak number of membrane related proteins detected (16) as well as the highest ratio in relation to cytoplasm related proteins (16:3) for 43 V. The ratio was considerably higher than the 3:1 (M/C) ratio for the lower capillary voltage and nearly reached the highest ratio in the 18 V distribution of the Triton X-114 phase observed in the 0 to 0.125 range. The ratio observed for [-0.125 to 0] in the aqueous phase shifted slightly in favour of cytoplasm related proteins from 4:3 (M/C, 18 V) to 11:12 (43V).

Any ratio determined had to be cautiously evaluated in regard to the small number of proteins detected, especially for quantities below 10 the impact of one added or subtracted protein on the result was misleading. For the detergent phase the apparent leap in the ratio for the mildly hydrophobic range [0 to 0.125] from 7:1 (18 V) to 3.5:1 (43 V) was re-examined in relation to the detected protein numbers and served as a good example of that effect. Visually the resemblance for both capillary voltage settings was obvious; the addition of one cytoplasm related protein however, shifted the ratio on paper from 7:1 to 7:2. In conclusion the ratios for the detergent phase in the GRAVY range from 0 to 0.125 were deemed to represent the same general trend for both capillary voltages.

The previously noted distinct ratio shift between the detergent and aqueous extraction phase (18 V) was confirmed in the first hydrophobic range of the 43 V distributions changing from 2:7 (C/M, X) to 5:3 (aq). A direct comparison to the 18 V ratio (4:1) was pointless due to the low protein numbers in the range.

Similar to conclusions drawn from the detergent phase the common trend of ratio-inversion between detergent and aqueous extraction phase from 0 to 0.125, independent

of instrument setting, could be an indicator for parameters influencing extraction behaviour during CPE.

The assessment of cloud point protein extracts according to the original cellular environments of the identified proteins allowed a clearer distinction of the extraction phases for both capillary voltages applied. Independent of minor variations caused by the altered electrospray ionisation conditions the respective extraction phase could instantly be identified visually from the distributions. Confirming the expected results, membrane proteins were accumulated in the detergent phase while cytoplasm related proteins were predominant in the aqueous phase.

Since the original ratio of membrane to cytoplasm related proteins within the mouse brain tissue was unknown, the resulting distribution between the extraction phases was interpreted based only on the identified proteins isolated by gel electrophoresis. The presented results can only reflect on the portion of the brain tissue proteins that fulfilled three conditions: (1) being released during the mechanical (ceramic beads) and chemical (detergent) cell disruption into the homogeneous extraction solution (4°C); (2) withstanding several extraction steps as well as the subsequent precipitation treatments without being lost in discarded fluids by irreversible denaturation and absorption to cell debris or various polymer surfaces of eppendorf tubes or pipette tips and (3) successfully redissolved in electrophoresis buffer in denatured form producing clear protein bands.

While a high number of proteins match these points the loss and exclusion of proteins due to the extraction parameters as well as during the subsequent tryptic digestion, extraction and LC/MS analysis each with their own obstacles preventing optimal detection rendered an examination and assessment of a complete set of mouse brain tissue proteins improbable. Changing merely one instrument parameter (capillary voltage 18 to 43 V) had a considerable impact on the range of proteins detected as well as their assigned original cellular locations for the aqueous phase. The same protein digest samples were subjected to both sets of mass spectroscopic experiments eliminating any influences of sample preparation procedures.

In chapter 4.3.1 it was shown that the higher capillary voltage was able to detect proteins otherwise unnoticed by the 18 V method over the observed GRAVY range. Assessment according to the cellular locations showed an improved detection of membrane proteins in the aqueous phase. The effect could again be indirectly linked to the limited detergent micelle phase volume during the extraction. Proteins listed for the aqueous phase represent all proteins remaining in the system after the extraction process. Membrane proteins may be prevented from transition into the micelle-rich phase either by sequence specific properties incompatible with the detergent environment or exclusion due to limited capacities. Peptides belonging to these membrane related proteins responded favourably to the increased capillary voltage of 43 V that previously massively improved the mass spectrometric detection of the hydrophobic amyloid β 42 protein (see chapter 4.1.2).

A relatively small effect was observed in comparison for the detergent phase (X). Cloud point extraction seemed to function as a preselection step during which protein properties that determine the transfer into hydrophobic micelles also level any positive effect of a raised capillary voltage observed for the membrane protein fraction in the aqueous phase.

The application of a higher capillary voltage was advantageous in the characterisation of protein extracts with a focus on membrane proteins. Especially for CPE extracts the additional time spend on repeating the chromatographic analysis of aqueous phase protein bands with the altered instrument settings pays off in a more comprehensive insight into the membrane related fraction.

4.3.3 Partitioning according to protein function

To complete the characterisation of the cloud point extracts functions attributed to the identified proteins were examined. Based on available information in the UniProt database each protein was assigned to one or more of 8 general categories roughly representing essential basic processes and functions in the brain (table 4-12).

Table 4-12 Function categories

category	processes/functions
[B]	biosynthesis
[C]	cytoskeleton, stability, mobility
[D]	differentiation, cell division, cell cycle, translation, DNA repair
[E]	energy
[M]	metabolism
[R]	response to stimuli
[S]	signalling
[T]	transport

Additional categories were assigned when necessary based on database information if one protein fulfilled multiple roles in the tightly knit and complex networks ensuring function and regulation of the brain. A significant part of the 502 identified proteins was exempted from categorisation (62 proteins) due to lack of detailed information or, more often, affiliation to other organisms. The majority of proteins associated with alternative organisms were found in protein bands of high concentration showing nearly analogue sequences to mouse protein sequences and were therefore mostly included in the assessment. Distributions for the extraction phases and capillary voltages as well as their cellular locations are summarised in fig. 4-40.

Apart from smaller shifts in percentages the influence of the higher capillary voltage was small. The pie chart diagrams displayed similar trends for both parameter settings. For the detergent phase only proteins involved in metabolic processes [M] were significantly affected by the higher capillary voltage (+6.5 %). The number of proteins assigned to the category increased from 9 to 14. Additional proteins originated from cytoplasmic and membrane locations, implied by the respective ratio shifts from 33.3 % to 42.9 % (cytoplasm) and 44.4 % to 50 % (membrane). Other categories did not exceed deviations of ± 3 % and were mainly attributed to minor variations between chromatographic runs. Comparing the results of both settings for the aqueous phase revealed even smaller deviations. The largest shift occurred for proteins supporting and creating the cytoskeleton [C] with a decrease of 4.7 %.

Despite minor variations in the distributions with altered capillary voltages the variations were of inferior importance for the characterisation of cloud point extracts. The main focus was put on the comparison and characterisation of the extraction phases. Pie chart diagrams in fig. 4-40 showed distinctive differences between the detergent (blue) and aqueous (yellow) phases in 4 categories – metabolism, transport, energy and biosynthesis.

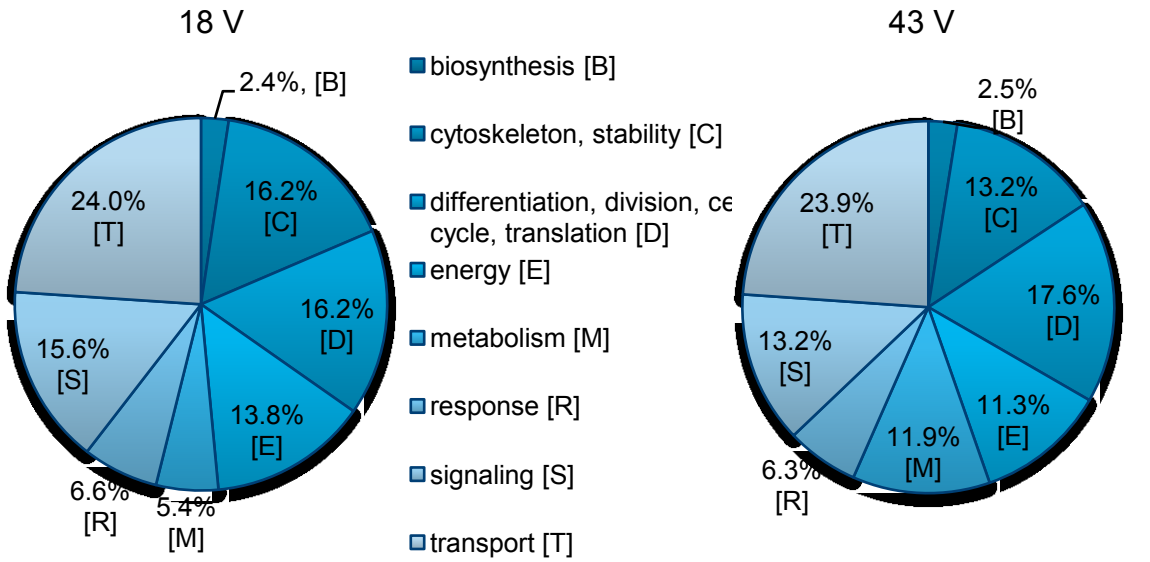

funct.	cytoplasm [% (no.)]	membrane [% (no.)]	both [% (no.)]	funct.	cytoplasm [% (no.)]	membrane [% (no.)]	both [% (no.)]
[B]	100.0 (3)	0	0	[B]	66.7 (2)	33.3 (1)	0
[C]	66.7 (16)	20.8 (5)	12.5 (3)	[C]	77.8 (14)	22.2 (4)	0
[D]	31.3 (5)	37.5 (6)	31.3 (5)	[D]	41.2 (7)	29.4 (5)	29.4 (5)
[E]	17.4 (4)	82.6 (19)	0	[E]	27.8 (5)	72.2 (13)	0
[M]	33.3 (3)	44.4 (4)	22.2 (2)	[M]	42.9 (6)	50.0 (7)	7.1 (1)
[R]	70.0 (7)	20.0 (2)	10.0 (1)	[R]	66.7 (6)	22.2 (2)	11.1 (1)
[S]	44.0 (11)	56.0 (14)	0	[S]	30.0 (6)	70.0 (14)	0
[T]	20.0 (7)	74.3(26)	5.7 (2)	[T]	22.9 (8)	74.3 (26)	2.9 (1)

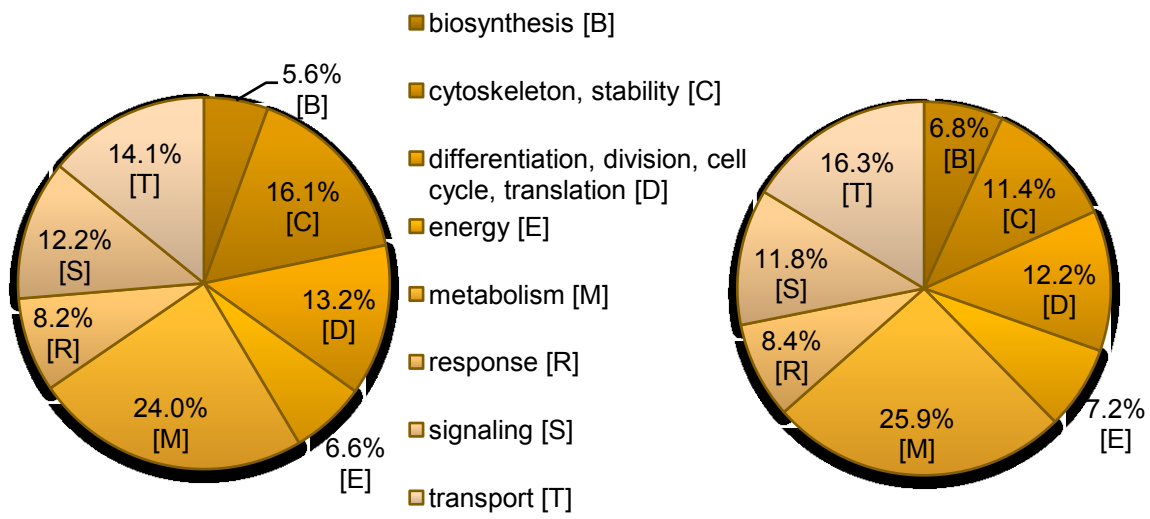

funct.	cytoplasm [% (no.)]	membrane [% (no.)]	both [% (no.)]	funct.	cytoplasm [% (no.)]	membrane [% (no.)]	both [% (no.)]
[B]	92.9 (13)	7.1 (1)	0	[B]	87.5 (14)	6.3 (1)	6.3 (1)
[C]	75.6 (34)	13.3 (6)	11.1 (5)	[C]	82.8 (24)	17.2 (5)	0
[D]	65.5 (19)	17.2 (5)	17.2 (5)	[D]	65.2 (15)	13.0 (3)	21.7 (5)
[E]	36.8 (7)	63.2 (12)	0	[E]	38.9 (7)	61.1 (11)	0
[M]	85.7 (48)	12.5 (7)	1.8 (1)	[M]	81.1 (43)	17.0 (9)	1.9 (1)
[R]	77.3 (17)	13.6 (3)	9.1 (2)	[R]	73.7 (14)	15.8 (3)	10.5 (2)
[S]	48.6 (17)	40.0 (14)	11.4 (4)	[S]	44.8 (13)	37.9 (11)	17.2 (5)
[T]	24.4 (10)	61.0 (25)	14.6 (6)	[T]	22.0 (9)	65.9 (27)	12.2 (5)

Figure 4-40 Protein distributions according to function categories ([B] to [T]) in the detergent (**blue**) and aqueous phases (**yellow**). Tables list cellular location percentages as well as total numbers for each data set

Proteins were assigned to the *biosynthesis* category if functions described in the UniProt database indicated a direct or indirect involvement in processes leading to the formation or creation of biomolecules. Detected biosynthetic proteins create important components for several essential processes, e.g. synthesis of proteins, amino acids, enzyme cofactors and nucleoside phosphates (Alberts 2002).

The fractions of [B] in the aqueous phase were significantly larger than in the micelle-rich phase (+3.2 % and +4.1 %) due to the very low number of proteins actually extracted into the detergent phase. Proteins involved in biosynthesis were predominantly found in the cytoplasm with 92.9 % compared to 7.1 % membrane-related proteins for the 18 V setting and 87.5 %, 6.3 % and additional 6.3 % found in both locations for 43 V. Category [B] showed the highest ratios of proteins originated from cytoplasm of the examined categories. The previously observed tendency for cytoplasmic proteins to prefer the aqueous phase (see chapter 4.3.2) in the cloud point extraction system was reinforced by the number of proteins found in both phases. They increased from merely 3 proteins in the detergent phase to 14 and 16, respectively in the aqueous phase.

A total of 33 proteins were assigned to category [B] covering a range from mildly hydrophobic (0.075) to highly hydrophilic (-1.233) GRAVY values. The majority of the proteins were located in the negative, hydrophilic range of the GRAVY scale. Only three exceeded the 0 value.

In direct comparison to other categories biosynthesis stood out on two points. The first was the exceptionally but logical high degree of 60.6 % (20 of 33) enzymes covering all 6 enzymatic classes. Ligases (EC 6, 6) represented the largest portion, followed by hydrolases (EC 3, 4), oxidoreductases (EC 1, 3), transferases (EC 2, 3), ligases (EC 4, 2) and isomerases (EC 5, 2). The second was the low number of additionally assigned function categories. It was often complicated to pinpoint one specific function or process for proteins assigned to the other categories as their database information often reflected multiple applications leading to the determination of a main and one or two secondary function categories. Assignment of biosynthesis proteins was often very clear. Only in 6 instances the descriptions indicated category [D] and in one each energy [E] and signalling [S].

Since a thorough discussion of all identified proteins for each category would be too elaborate within the confines of this work, representative examples were chosen to highlight essential functions and their roles within the brain.

A good example of the extraordinarily intricate and cross-linked nature of processes occurring in the brain is the amino acid serine, a non-essential amino acid synthesised in a three step process. The first step, the oxidation of 3-phosphoglycerate with NAD^+ to 3-phosphohydroxypyruvate and NADH is catalysed by D-3-phosphoglycerate dehydrogenase (Q61753, GRAVY -0.087, 56.4 kDa, pI 6.14, EC 1.1.1.95) detected in the detergent phase with 18 V capillary voltage. Serine is subsequently formed after reductive amination and hydrolysis. It serves as precursor for glycine, cysteine and tryptophane as well as a variety of metabolites and plays, as part of catalytic triads, an important role in enabling the catalytic activity of enzymes. D-serine; synthesised by serine racemase in brain, acts as neurotransmitter in synaptic signalling (Lehninger, Nelson et al. 2000).

Serine is also essential in the metabolic biosynthesis of purines and pyrimidines, nitrogeneous bases contributing 50 % of DNA (desoxyribonuleotides) and RNA (ribonucleotides) building blocks. Adenylosuccinate lyase (P54822, GRAVY -0.256, 54.7 kDa, pI 6.97, EC 4.3.2.2), detected in the aqueous phase with 43 V capillary voltage, is an essential enzyme for both purine and adenosylmonophosphate (AMP) synthesis.

The probable threonyl synthetase 2, cytoplasmic (Q8BLY2, GRAVY -0.559, 91.2 kDa, pI 7.39, EC 6.1.1.3) catalyses the ATP consuming conjugation of L-threonine to the respective tRNA molecule. Resulting L-threonyl-tRNA(Thr) molecules are subsequently available for the translation of DNA information into protein sequences by attaching the amino acid to a developing amino acid chain.

Category [C] was defined to encompass proteins contributing to the *cytoskeleton*, a system of protein structures maintaining shape, intracellular transport, cellular division and interaction with the cell membrane (Frixione 2000). Fractions corresponding to the category were similar for both extraction phases. For 18 V capillary voltage the percentage for the detergent phase (16.2 %) matches the aqueous phase's (16.1 %) despite the overall number increasing from 24 to 45. Detection seemed slightly impaired by the raised capillary voltage resulting in lower numbers (18 and 29) and percentages for both phases (13.2 % and 11.4 %). In compliance with their general function, large portions of the assigned proteins were again associated with cytoplasmic locations, in the detergent phase 66.7 % (18 V) and 77.8 % (43 V) as well as 75.6 % and 82.8 % in the aqueous phase. With significantly higher percentages in the micelle rich phase (20.8 % and 22.2 %) and aqueous phase (13.3 % and 17.2 %) more proteins were membrane related than for category [B].

The 62 proteins sorted into the cytoskeleton category were, aside from one mildly hydrophobic protein with a GRAVY index of 0.018, exclusively found in the hydrophilic GRAVY range down to -1.334. Enzymes play only a minor role for category [C], represented by only seven proteins of two enzyme classes (transferases and hydrolases). Additional function categories could be assigned to nearly half of the proteins (27). Most often the secondary function was related to category [D] (17) caused by the involvement of cytoskeletal networks in, for example, the rearrangement of chromatin into chromosomes and mitosis. Less frequent were transport (5), signalling (4), metabolism (2) and energy (1).

Cytoskeletons are composed of three types of filaments that were also identified in the extracts. Thin filaments of linear actin polymers, the microfilaments, are responsible of force generation by elongation and shrinking. Several actins and associated proteins were detected. A fitting example was fascin (Q61553, GRAVY -0.435, 54.4 kDa, pI 6.43), a protein involved in the organisation of actin filaments into bundles and of the bundles themselves (Adams 2004).

The second type of filaments are heterogeneous intermediate filaments strongly bound to the actin filament network that enable cells to bear tension and anchor organelles in the three dimensional structure of the cell. Nesprin-1 (Q6ZWR6, GRAVY -0.596, 1009.9 kDa, pI 5.43), found in the detergent phase and filamin-B (Q80X90, GRAVY -0.285, 277.8 kDa, pI 5.46), detected in the aqueous phase were identified as intermediate filaments. Nesprin-1 is a multi-isomeric modular protein that forms a linking network between cell organelles and the actin cytoskeleton to maintain the subcellular spatial organisation and connects the nucleus to the cytoskeleton. Filamin-B on the other hand connects membrane constituents to the actin network. Multiple proteins detected were associated to keratin filaments generally limited to skin, hair or nail cells. Their detection in brain tissue samples was credited to a slight contamination with mouse skin and hair during the preparation (Ausmess, Kuhn et al. 2003; Doherty and McMahon 2008; Dawe, Adams et al. 2009).

Microtubules, the third type of filament, are hollow cylinders constructed from polymers of α- and β-tubulins that enable intracellular transport of molecules. A wide range of α-

and β-tubulin chains was frequently detected in the experiments. Two proteins that are not immediate components of microtubules but are both required for their assembly were stathmin (P54227, GRAVY -1.334, 171 kDa, pI 5.76) and the microtubule-associated protein tau (P10637, GRAVY -0.858, 76.1 kDa, pI 6.34) implicated in several neurodegenerative diseases like Alzheimer's disease. Stathmin is involved in the regulation of the filament by destabilisation of microtubules and may also be required for axon formation during neurogenesis. Protein tau promotes microtubule assembly and stability and is probably involved in the establishment and maintenance of neuronal polarity (Maucuer A. 1995; Goedert and Spillantini 2006).

Proteins assigned to *category [D]* spanned a broader and looser range of cellular functions than the other categories. Processes involved in the maintenance, development, growth and regulation of the cell cycle were summarised in this group. These general functions cover the translation of DNA information into proteins, formation of tissues by creating cell-cell and cell-matrix junctions, regulation as well as processes involved in the cell cycle, namely cell division by mitosis, growth and differentiation into specific cells and ultimately apoptosis, the programmed cell death (Alberts 2002).

In contrast to the previously discussed categories biosynthesis and cytoskeleton, fractions corresponding to [D] indicated a preference for the detergent phase with a decline of 3.7 % (18 V) and 4.5 % (43 V) in the aqueous phase. An enrichment of membrane proteins extracted into the Triton X-114 phase was implied by elevated location percentages of 37.5 % (18 V) and 29.4 % (43 V) compared to the aqueous phase with 17.2 % and 13.0 % despite the lower number of proteins in the detergent phase. Extraction of cytoplasmic proteins assigned to category [D] was less favoured with approx. 65 % remaining in the aqueous phase. The number of proteins associated with both cytoplasm and membranes reached a maximum in this category in both extraction phases and parameter settings with 31.3 % and 29.4 % for the detergent and 17.2 % and 21.7 % in the aqueous phase. In addition to the separation into membrane and cytoplasm locations it was noteworthy that a high number of proteins were also associated with the nucleus (36) indicating a concentration of processes towards the organelle.

The distribution of GRAVY indices belonging to the 88 assigned proteins of category [D] also extended further into the hydrophobic range than [B] or [C], reaching from -1.28 to 0.854 and including 5 proteins with positive indices. A small portion of the proteins were enzymes (15, 17 %) consisting of transferases (EC 2, 7), hydrolases (EC 3, 4), lyases (EC 4, 2) and isomerases (EC5, 2).

The category overlapped extensively (39 of 88) with all other function categories short of biosynthesis, most frequently with signalling (15) followed by cytoskeleton (8), response (5), metabolism (5), transport (3) and energy (2). The number of neurons is generally defined prior to birth and only declines with age. The specified signalling cells generated via differentiation of stem cells (neurogenesis) explaining the link to category [S]. The connection between category [D] and the cytoskeleton already observed for category [C] mirrored the essential role of cytoskeletal elements for cell division processes.

While good and interesting examples for every aspect of this category could be found among the detected proteins, the chosen proteins focussed on neuronal development, translation and DNA maintenance. The "neuronal membrane glycoprotein M6-a" (P35802, GRAVY 0.438, 31.1 kDa, pI 5.17) is involved in the migration of stem cells and their differentiation into neurons, plays a role in neuronal plasticity, expansion of the neuronal network by neurite and filopedia outgrowth and probably synapse formation. Found only in the detergent phase, the highly hydrophobic membrane protein confirmed

the trends observed in the general distributions according to extraction phase and location. Dihydropyrimidinase-related protein 2 (O08553, GRAVY -0.267, 62.3 kDa, pI 5.95) is linked to several processes like neuron projection morphogenesis, axon growth and guidance, neuronal growth cone collapse and cell migration. The cytoplasmic protein was detected solely in the aqueous phase (Zhao, Iida et al. 2008).

To translate genetic information encoded in DNA the double helix has to be separated into single strands and transcribed into RNA that is able to leave the confines of the nucleus to be translated into proteins. The DNA-directed RNA polymerases I and III subunit (P97304, GRAVY -0.538, 15.1 kDa, pI 6.43) is the core component of two polymerases that catalyse transcription of DNA into RNA using four ribonucleoside triphosphates (guanine, adenosine, uracil and cytosine) as substrates (Willis 1993; Grummit 1999).

Other proteins included in category [D] are able to detect and repair damaged DNA strands. Among these was the endonuclease III-like protein 1 (O35980, GRAVY -0.479, 33.6 kDa, pI 9.66, EC 4.2.99.18), required for the repair of DNA damage caused by oxidative stress and spontaneous mutagenic lesions by cleaving the damaged section from the intact strand (Sarker, Ikeda et al. 1998).

A central linchpin for numerous processes in living organisms and especially the brain is the ability to harness and "store" *energy* from metabolic pathways. Biochemical energy is exchanged and transformed by breakage and formation of bonds within molecules. The major form of energy storage is adenosintriphosphate (ATP) mainly produced by mitochondrial transmembrane proteins driven by ion gradients across membranes representing a close connection to transport processes. The third phosphate group is bound only weakly to the molecule and can be easily broken by hydrolysis, releasing stored energy to form stronger bonds and drive biological processes (Berg, Tymoczko et al. 2003).

While the assignment of proteins to category [E] was less clear-cut than for other categories, they were nonetheless separated from category [T] to highlight the importance of biochemical energy for the organism and neuronal processes in the brain.

Similar to category [D] the fractions corresponding to the energy household indicated a preference for detergent phase with 13.8 % (18 V) and 11.3 % (43 V) of all proteins detected in the micelle-rich phase opposed to 6.6 % and 7.2 % in the aqueous phase. The fact that energy related processes predominantly occur in the vicinity of membranes was also reflected in the cellular location distributions. The cloud point extraction was successful in concentrating membrane related proteins sorted into category [E] increasing the respective fractions by 19.4 % (18 V) and 11.1 % (43 V) in the detergent phase. Cytoplasmic proteins on the other hand were not favourably extracted into the hydrophobic environment, indicated by the decrease from 36.8 % (18 V) and 38.9 % (43 V) in the aqueous phase to 17.4 % and 27.8 %. Unlike category [D] with a significant portion associated with cytoplasm and membranes, no protein was associated to both for [E].

The 42 proteins assigned to category [E] showed mainly hydrophobic tendencies by covering a GRAVY range from -1.066 to 0.474 and accumulating in the only slightly hydrophilic -0.3 to 0 range. Approximately a fourth possessed positive GRAVY indices (10) adding to the favourable preconditions leading to a preferred extraction into the detergent phase indicated by the nearly stable numbers of proteins assigned to both extraction phases (21/20 18 V, 18/18 43 V) in comparison to other categories where the

overall higher number of proteins translated into generally higher numbers for the aqueous phase.

Enzymes play a prominent role in the storage and release of biochemical energy and composed a large part of the category (18 of 42). Oxidoreductases (EC 1, 6), transferases (EC 2, 4) and hydrolases (EC 3, 8) were identified.

In 35 instances secondary function categories could be assigned. The dominance of category [T] with 29 proteins confirmed the co-dependence between the categories that was mirrored by a high number of proteins in [T] also assigned to [E]. Other secondary functions were metabolism (4) and category [D] (2). Proteins were sorted into category [E] if database information indicated that the storage or release of any form of biochemical energy was the primary function. Examples chosen to characterise the energy category were ultimately dependent on transport processes. Their function and importance will be discussed at this point to allow a more detailed examination of transport proteins later.

Living organisms gain energy from the consumption nutrients (sugars, proteins, fatty acids) by oxidation in a series of metabolic processes leading to the production of ATP called cellular respiration. Using oxygen as oxidizing agent the overall reaction is essentially a combustion broken down into many smaller steps to control and harness the released energy (Berg, Tymoczko et al. 2003). Several proteins incorporated into the respiratory chain located in mitochondria were identified in the extraction samples. Somatic cytochrome c (P62897, GRAVY -0.783, 11.5 kDa, pI 9.61) is one of the best known proteins in the process transferring e^- to a cytochrome oxidase complex, the final protein carrier in the mitochondrial electron transport chain. The trigged release of cytochrome c into the cytoplasm leads to apoptosis (Ruiz-Vela, Gonzalez de Buitrago et al. 2002).

A central protein complex around which the entire energy storage mechanism as well as the respiratory chain revolves is ATP synthase (EC 3.6.3.14). It is composed of two structures, the F_1 region embedded within a membrane, constructed from subunits alpha to epsilon, and the F_O region above the membrane reaching into the intermembrane matrix of the mitochondrium, constructed mainly from subunits A to C as well as additional subunits d-g, F6 and 8. Driven by a proton gradient across the inner mitochondrial membrane the F_O region on the enzyme rotates and induces a series of conformational changes leading to ATP synthesis from adenosindiphosphate (ADP) and phosphate (P_i) (Berg, Tymoczko et al. 2003). Many subunits identified in the extracts were predominantly found in the detergent phase. F_1 subunits alpha (Q03265, GRAVY -0.133, 55.3 kDa, pI 8.28), beta (P56480, GRAVY -0.004, 51.7 kDa, pI 4.99), gamma (Q91VR2, GRAVY -0.219, 30.1 kDa, pI 8.87) and delta (Q9D3D9, GRAVY 0.201, 15.0 kDa, pI 4.4) were detected frequently while F_O subunits were only rarely identified. The embedment within the membrane seemed to hinder an effective separation of protein complex and membrane resulting in its loss either to washing steps together with other impurities or to irreversible precipitation.

Not all energy related proteins detected were linked to direct transport processes. Creatine kinase B-type (Q04447, GRAVY -0.463, 42.6 kDa, pI 5.4, EC 2.7.3.2) for example reversibly catalyses the transfer of phosphate groups from ATP to various phosphogens thereby fulfilling a central role in energy transduction in tissues with large, fluctuating energy demands like the brain.

The largest number of proteins was assigned to *metabolism* [M] pathways involved in the conversion of complex biomolecules entering an organism into smaller molecules and

biochemical energy (e.g. ATP, NADH) and the construction of complex molecules (e.g. protein, polysaccharides) from precursors (e.g. amino acids, monosaccharides) under energy consumption.

Judging from phase distributions cloud point extraction with Triton X-114 was unsuitable for proteins assigned to category [M]. While some were extracted into the detergent phase, 9 proteins were detected with 18 V capillary voltage and 20 with 43 V, the majority (55 and 61) remained in the aqueous phase. The results also showed that for this category at least, application of higher capillary voltages seemed beneficial for protein detection. The effect was more noticeable for the detergent phase as the percentages increased from 5.4 % (18 V) to 11.9 % (43 V). Contributing with 24 % (18 V) and 25.9 % (43 V) metabolism was the largest fraction among the function categories in the aqueous phase.

Despite the relatively low numbers extracted into the detergent phase, a clear accumulation of membrane proteins (44.4 %, 4 and 50.0 %, 7) could be observed. Due to only 9 proteins detected in the detergent phase with the 18 V setting the percentages were carefully considered as hints towards the actual location distributions. An overwhelming majority of proteins assigned to the aqueous phase were associated to the cytoplasm, 48 (85.7 %) for 18 V and 43 (81.1 %) for 43 V. Membrane proteins were detected in 12.5 % (7, 18 V) and 17 % (9, 43 V) of all cases and just one metabolic protein was linked to both cellular locations.

In total, 97 proteins distributed over a GRAVY range from -0.788 to +0.824 were sorted into category [M]. The lion's share of the category was found on the hydrophilic side of the scale; only 12 protein sequences (12.4 %) resulted in positive hydropathy indices.

Metabolic pathways are in general series of enzymatic reaction leading to either the deconstruction of large biomolecules to gain energy or energy-consuming construction of specific complex molecules needed. Unsurprisingly, a large portion of the detected proteins were enzymes or subunits essential to the catalytic process (77 of 97). Proteins belonging to all enzyme classes were identified in the extracts to varying extents. Transferases (EC 2, 23) were the most frequent, followed by oxidoreductases (EC 1, 19) and hydrolases (EC 3, 16). Lyases (EC 4, 8), isomerases (EC 5, 6) and ligases (EC 6, 5) were less abundant.

Identified proteins assigned to category [M] were extensively linked to every other category examined in this work (61 of 97). Metabolic pathways provide energy and resources and are able to remove unfavourable byproducts resulting from other cellular functions (e.g. toxins). The overlaps to categories [D] (13), [E] (15) and [S] (13) reflected on function priorities within the examined organ as all three categories symbolise essential functions for the brain. Cell maintenance and division are necessary for the constant development of neuronal connections that lead directly to signalling processes. Constant control of bodily functions and regulation of metabolic pathways as well as the creation of new neuronal links and the memory formation and recollection require high amounts of energy provided by the metabolism in brain cells. Crossovers with biosynthesis (7), response (7), transport (4) and cytoskeleton (2) complete the picture.

A peculiarity of brain metabolism is the restricted influx of large or hydrophilic molecules due to the blood-brain-barrier (BBB) separating the cerebrospinal fluid (CSF) from the bloodstream. Only small molecules like O_2, H_2O and hormones can pass the barrier by diffusion, supplementary molecules like glucose, amino acids and other metabolic products are actively brought across the barrier by transport proteins (Ballabh, Braun et al. 2004).

Anabolic processes synthesising complex molecules from precursors imported into the brain tissue play a crucial role in supplying necessary compounds for a multitude of purposes. Few of the proteins assigned to category [M] actually possessed anabolic functions since the majority were already included in the biosynthesis category [B]. Nucleoside diphosphate kinase B (Q01768, GRAVY -0.303, 17.2 kDa, pI 7.17, EC 2.7.4.6) detected in the aqueous phase uses ATP to generate alternative nucleoside triphosphates. Cross-linking of proteins and conjugation of polyamines is catalysed by protein-glutamine gamma-glutamyltransferase 5 (Q9D7I9, GRAVY -0.246, 81.0 kDa, pI 5.48, EC 2.3.2.13), a cytoplasmic enzyme detected in the aqueous phase (43 V).

Far more proteins were involved in catabolic processes, e.g. glycolysis, citric cycle and proteolysis. Monosaccharides and especially glucose are important energy sources and are broken down along the 10 step glycolysis pathway to produce ATP, NADH and pyruvate. Several enzymes catalysing the individual steps were identified during the experiments. To convert glucose into usable energy, first it has to be activated under consumption of ATP. Hexokinase-1 (P17710, GRAVY -0.268, 108.3 kDa, pI 6.73, EC 2.7.1.1) catalyses the ATP dependent phosphorylation of D-hexoses (e.g. glucose) to D-hexose-6-phosphates during the first step of glycolysis. The resulting pyruvate is an intermediate linking several metabolic pathways and is mainly converted into acetyl-coenzyme A (acetyl-CoA) and CO_2 by enzymes like pyruvate dehydrogenase E1 component subunit beta, mitochondrial (Q9D051, GRAVY 0.049, 35.8 kDa, pI 5.39, EC 1.2.4.1), detected in the aqueous extraction phase. Acetyl-CoA is subsequently oxidised in the citric acid cycle to form H_2O and CO_2 while transferring e^- to NAD^+, storing energy as NADH (Adams, Griffin et al. 1991; Berg, Tymoczko et al. 2003).

Metabolism also encompasses the regulation of redox processes through various mechanisms. One example is the disposal of peroxides (R-O-O-R) with sulphur containing reduction equivalents (R-SH) catalysed by Peroxiredoxin-2 (Q61171, GRAVY -0.161, 21.6 kDa, pI 5.2, EC 1.11.1.15) (Rhee, Chae et al. 2005).

A fair number of proteins were involved in the cellular *response* to stress and outside stimuli. Proteins in category [R] were not preferentially extracted into the detergent phase. Similar percentages were achieved for both parameter setting for the Triton X-114 phase (6.6 % and 6.3 %) and the aqueous phase (8.2 % and 8.4 %). In all cases the fraction corresponding to cytoplasmic proteins exceeded the membrane fraction. The distributions remained at comparable levels. The detergent phase showed 70 % cytoplasmic, 20 % membrane-related and 10 % associated with both for the 18 V capillary voltage setting. Both the numbers of assigned proteins as well as the percentages for 43 V barely deviated from the 18 V values (66.7 %, 22.2 % and 11.1 %). The overall number of proteins was doubled for the aqueous phase; the distribution according to cellular location remained very similar to the detergent phase. Of all proteins detected with 18 V, 77.3 % (17) originated from the cytoplasm, 13.6 % (3) from membranes and 9.1 % (2) from both. Using a capillary voltage of 43 V resulted in slight changes to 73.7 % (14), 15.8 % (3) and 10.5 % (2), only differing in the quantity of cytoplasmic proteins.

The 35 proteins assigned to category [R] had invariably negative GRAVY indices in the range from -0.951 to -0.012. Proteins were associated with the category if they were activated or involved in the cells immediate response to stress factors. Enzymes in category [R] were important to the removal or destruction of toxic and harmful compounds. They accounted for nearly a third of the proteins (10 of 35). Only

oxidoreductases (EC 1, 5), transferases (EC 2, 2) and hydrolases (EC 3, 3) were identified.

Since a cellular response to outside stimuli like drugs, radiation or internal imbalances in redox mechanisms is dependent on certain factors and signals, the overlap to metabolic processes (13), signalling (5) and category [D] (5) was expected. Other function categories, in detail energy (2), biosynthesis (1) and transport (1), related only marginally.

Proteins sorted into category [R] illustrate to some extent the variety of stimuli causing cellular responses in order to maintain biochemical balance or defend the cell against external forces. The transmembrane protein 131 (O70472, GRAVY -0.381, 204.7 kDa, pI 8.69) may play, according to the Uniprot database, a role in the immune response to viral infection and was detected in the detergent phase at 43 V. Latexin (P70202, GRAVY -0.586, 25.5 kDa, pI 5.46) functions as a potent, hardly reversible, non-competitive inhibitor to metalloendoprotease in response to inflammation (Aagaard A. 2005).

One of the most common kinds of stress is oxidative stress caused by imbalances between reactive oxygen species as byproducts of metabolic processes and the cell's ability to counteract by detoxifying harmful intermediates like peroxides and free radicals or repair the resulting damage. Even without direct stress enzymatic antioxidants are part of the normal regulation of the redox system. Superoxide dismutase [Mn], mitochondrial (P09671, GRAVY -0.501, 22.2 kDa, pI 7.3, EC 1.15.1.1) destroys superoxide anion radicals ($\cdot O_2^-$) to form O_2 and H_2O_2 as a response to, for example, axon injuries (Rosenfeld, Cook et al. 1997; Valko, Leibfritz et al. 2007).

Consequences of oxidative stress are not only the increased need to dispose of reactive oxygen species but also to repair damaged cell components. Prolonged periods of imbalance can lead to misfolded and dysfunctional proteins or DNA lesions and are implicated in the aging process as well as in the pathogenesis of neurodegenerative diseases like Alzheimer's (Valko, Leibfritz et al. 2007).

Proteins involved in the maintenance and repair of damaged DNA strands were generally assigned to category [D]. The focus of category [R] was therefore put on the correction of protein misfolding. Proteins that assist in non-covalent folding but are not part of the final structure are called chaperones. Their normal function is the prevention of aggregation of newly synthesised protein chains and assembled structures. As the probability of misfolding increases with rising temperatures many chaperones are so-called heat shock proteins expressed in response to heat and other stresses. If a misfolded protein is detected it is pulled into the chaperone structure via hydrophilic attraction and folded correctly before being released. A characteristic example is the heat shock 70 kDa protein (Q61696, GRAVY -0.375, 70.0 kDa, pI 5.52) detected in both extraction phases and with both instrument settings. Another typical chaperone detected was the heat shock protein HSP90 (P11499, GRAVY -0.682, 83.2 kDa, pI 4.97). Additional variants of both proteins were also detected. Common to all was the presence in both extraction phases and parameter settings (Ellis 2006).

The by far most important function category was *signalling*. Proteins assigned to category [S] were directly or indirectly implicated in processes of signal transduction. Examination of the distributions according to extraction phase suggested a preference for the detergent phase with 15.9 % (18 V) and 13.8 % (43 V). Smaller fractions of the aqueous phase, 12.1 % (18 V) and 11.7 % (43 V) represented the slightly less favourable conditions in comparison to the Triton X-114 micelle environment.

With exception of the distribution for the detergent phase at the 43 V instrument setting, signalling proteins seemed to originate to fairly similar numbers from cytoplasm and membranes. For the lower capillary voltage 44.0 % (11) cytoplasmic and 56 % (14) membrane-related protein were identified in the detergent phase. In the aqueous phase the percentages shifted slightly in favour of cytoplasmic proteins with 48.6 % (10) while the fraction of membrane proteins dropped to 40.0 % (14) and four proteins (11.4 %) could occur in both locations. Repetition with the 43 V setting led to a similar distribution for the aqueous phase; 44.8 % (13) cytoplasmic, 37.9 % (11) membrane-related and 17.2 % (5) both. In the detergent phase however, the percentages shifted towards membrane locations with 70 % (14) mainly because less cytoplasmic proteins were detected with 43 V resulting in only 30 % (6).

Covering a GRAVY range from -1.198 to 0.545, with only one protein with a positive relative hydropathy index, 57 proteins possessed primary functions connected to signalling. Enzymes belonging to classes one to five accounted for 14 % (8) of the identified proteins. In three instances transferases (EC 2), in two hydrolases (EC 3) and oxidoreductases (EC 1), lyases (EC 4) and isomerases (EC 5) were identified in one each.

Protein functions of category [S] overlapped with almost every other defined category except biosynthesis. The largest crossovers were determined with category [D] (12), metabolism (9), transport (7) and cytoplasm (6). Three proteins each fulfilled secondary functions congruent with categories [E] and [R].

The survival of higher organisms is dependent on control and regulation of processes and organs through a central and peripheral nervous system (CNS). The highly complex systems composed of extensively interconnected specialised cells called neurons are “piloted” by the brain. Neurons generally contain three essential parts; the cell body or soma containing the nucleus, numerous thin and branched dendrites extending towards other neurons to receive electrical or chemical signals and one axon, a significantly longer and insulated extension from the cell body branching out into synapses to transmit signals in form of electrical impulses to dendrites of other neurons. Axons are insulated by a myelin sheath that enables electrical signals to travel rapidly while consuming less energy than non-insulated axons. The protective insulation is a specialised membrane consisting of a protein layer between two layers of lipids. Major myelin proteins frequently detected during the experiments was the sole hydrophobic membrane-related myelin proteolipid protein (P60202, GRAVY 0.545, 29.9 kDa, pI 8.72) also known as lipophilin and myelin basic protein (P04370, GRAVY -1.198, 27.2 kDa, pI 9.58) isoforms 1-3 that belong to the most abundant protein components of the myelin sheath (Trepel 1999).

Electric impulses are transferred from axon to dendrites and cell bodies of other neurons via synapses. Small knot-like axon endings form, together with the cell membrane of the connected dendrite and the cleft between them a structure called synapse. Action potentials reaching the synapse open voltage-dependent Ca^{2+} channels into the axon end and triggering the fusion of neurotransmitter filled vesicles with the membrane and their subsequent release into the synaptic cleft. Syntaxin-1B (P61264, GRAVY -0.223, 37.7 kDa, pI 5.35) is potentially involved in the docking process at presynaptic active zones while syntaxin-binding protein-1 (O08599, GRAVY -0.41, 67.6 kDa, pI 6.5) may be involved in the regulation of vesicle docking and fusion essential for neurotransmission (Bennett, Garáa-Arrarás et al. 1993). Released neurotransmitters, often glutamate (excitatory) or gamma-aminobutyric acid (GABA, inhibitory) diffuse across the cleft and activate receptors that include e.g. gamma-aminobutyric acid receptor type B subunit 2 precursor (Q80T41, GRAVY -0.138, 101.6 kDa, pI 8.87) at the post-synaptic neuron to inhibit a new action potential and stop further signal transduction. Glutamate on

the other hand would bind to its respective receptors and create a new post-synaptic action potential to continue the electrical impulse (Hughes 1958; Bennett, Garáa-Arrarás et al. 1993; Shigeri, Seal et al. 2004).

While the number of neurons is thought to be fixed even before birth only declining over a lifespan, formation and quantity of synapses increase with time and conversion of experiences and data into neuronal connections. According to the Hebbian theory memories formed during the learning process are represented by vastly interconnected networks of synapses and their plasticity. Synaptophysin (Q62277, GRAVY -0.052, 34.0 kDa, pI 4.82) is involved in both short-term and long-term synaptic plasticity modulating synapses formed by processing information so that impulses are more effectively transmitted when recalling the data (Janz, Suedhof et al. 1999).

The discussed function categories were often linked through *transport* processes. Assigned proteins were involved in endo- and exocytosis as well as transport of energy (ATP, e^-), ions, proteins, metabolites and neurotransmitters. Cloud point extraction with Triton X-114 micelles resulted in an enrichment of transport proteins in the detergent phase with 23.5 % (18 V) and 23.9 % (43 V). In the aqueous phase the fraction corresponding to transport processes amounted to just 14.1 % (18 V) and 16.3 % (43 V).

Distributions according to cellular locations followed the same trend for both extraction phases. In the aqueous phases 24.4 % cytoplasmic, 61.0 % membrane proteins and 14.6 % related to both comprised the transport fraction at 18 V capillary voltage. Detection with the higher setting led to a distribution of 22.0 %, 65.9 % and 12.2 % respectively. Membrane transport proteins were preferentially extracted into the detergent phase, indicated by their increased percentages of 74.3 % for both instrument settings. Lower numbers were observed for cytoplasmic (20.0 % and 22.9 %) and overlapping proteins (5.7 % and 2.9 %). Despite the overall lower quantity of proteins extracted into the detergent phase category [T] represented nearly equal numbers, 48 (X) to 49 (aq) for 18 V and 46 (X) to 45 (aq) for 43 V, to the aqueous phase indicating a possible phase equilibrium for transport proteins.

Category [T] covered the broad GRAVY range from -1.266 to 0.407 with 86 proteins in total. The high ratio of membrane proteins involved in transport processes were additionally illustrated by ten proteins within the positive GRAVY range. Enzymes sorted into the category were usually tightly linked to other functions requiring active transport processes to drive the catalytic reaction. Approximately 17.4 % (15) of the proteins had enzymatic function as hydrolases (EC 3, 9), oxidoreductases (EC 1, 3), transferases (EC 2, 2) and ligases (EC 6, 1).

Many transport proteins (51) were correlated to other function categories. The biggest overlaps were found for energy related processes (19), category [D] (12) and signalling (10), but transport proteins were also involved in the response to stimuli (5), metabolism (3) and cytoskeleton (2).

The crossover with energy-related processes was represented by various forms and subunits of ATPase, an enzyme catalysing the reversed reaction to ATP synthases; the release of energy by separating the weakly bound third phosphate group from ATP ($ATP \rightarrow ADP + P_i$) to drive other reactions or actively transport solutes across membranes often against concentration gradients. Frequently identified variants were the sodium/potassium-transporting ATPase (EC 3.6.3.9) subunits alpha-1 (Q8VDN2, GRAVY 0.001, 112.5 kDa, pI 5.27), alpha-2 (Q6PIE5, GRAVY -0.006, 111.7 kDa, pI 5.35) and alpha-3 (Q6PIC6, GRAVY -0.007, 111.7 kDa, pI 5.26).

The active transport of ions (ion pumps) is especially important to maintain the electrical excitability of neurons by creating a voltage base potential across membranes. An action potential reaching a synaptic end of a neuron activates transport proteins like the voltage-dependent N-type calcium channel subunit alpha-1B (O55017, GRAVY -0.227, 261.4 kDa, pI 8.85) to mediate the entry of Ca^{2+} into the synapse and trigger neurotransmitter release. Transport proteins are also involved in the termination of neuronal signal transduction. The excitatory amino acid transporter 1 (P56564, GRAVY 0.381, 59.6, pI 8.51) and 2 (P43006, GRAVY 0.407, 62.0 kDa, pI 6.24), membrane proteins detected in both extraction phases and parameter settings, are responsible for the removal of the neurotransmitter glutamate from the synaptic cleft (Shigeri, Seal et al. 2004).

The voltage-dependent anion-selective channel proteins 1 (Q60932, GRAVY -0.334, 32.4 kDa, pI 8.55), 2 (Q60930, GRAVY -0.223, 31.7 kDa, pI 7.44) and 3 (Q60931, GRAVY -0.315, 30.7 kDa, pI 8.96) form channels through outer mitochondrion membranes regulating the diffusion of small hydrophilic molecules (e.g. ATP, ADP, pyruvate) in dependence of membrane potentials. Potentials low membrane potentials result in an open protein structure that closes at potentials of 30 to 40 mV (Benz 1994; Hoogenboom, Suda et al. 2007).

A possible connection to Alzheimer's disease was found for the multiple epidermal growth factor-like domain protein 10 (Q6DIB5, GRAVY -0.442, 120.5 kDa, pI 6.8), a membrane receptor involved in phagocytosis promotes the formation of large intracellular vacuoles and may be responsible for the uptake of amyloid β peptides (Singh, Park et al. 2010).

Enzymes accounted for 34 % of all detected proteins and involved to varying degrees in all function categories. Especially for metabolism, energy, biosynthesis and response the presence of enzymes was crucial for successful processes. Figure 4-41 summarises the distribution of enzymes identified during data examination and the occurrence of the individual enzyme classes in the extraction phases.

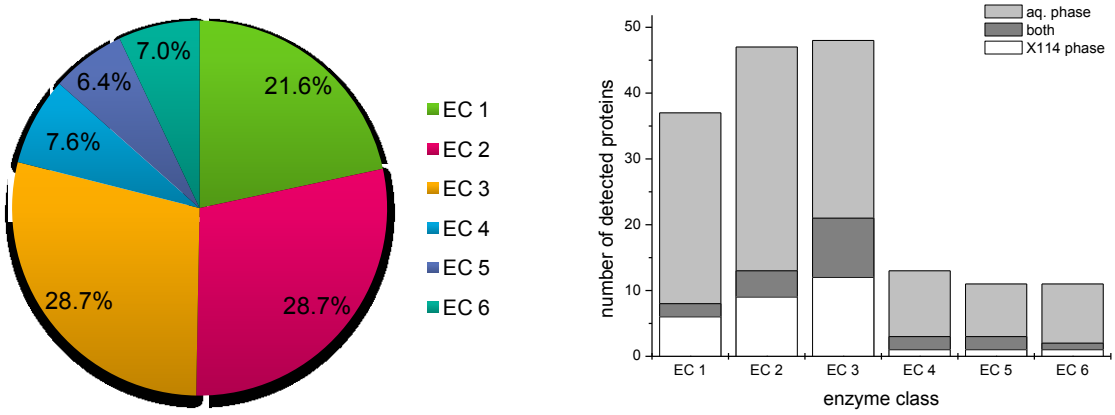

Figure 4-41 Distribution of detected enzymes according to enzyme class (**left**) and extraction phase (**right**)

The function category-independent overview revealed that major enzymatic functions were catalysis of oxidations and reductions (EC 1), transfer of functional groups between molecules (EC 2) and hydrolysis of chemical bonds. Fractions corresponding to the first

three classes alone already amounted to 79 % of the identified enzymes. The high numbers were also reflected in the extraction phase distribution in fig. 4-41. While the better part of all enzyme classes was detected in the aqueous phase, the potential of extracting enzymes into the Triton X-114 phase improved from EC 1 to EC 3 as both the number of detergent phase and overlapping proteins increased.

The remaining 21 % were split almost evenly between lyases (EC 4), isomerases (EC 5) and ligases (EC 6). They were responsible for the less often needed cleavage of bonds by alternative means to hydrolysis or oxidation often forming double bonds or ring structures, the structural rearrangement within one molecule and the combination of two molecules via covalent bonds. Cloud point extraction was, as implicated by only one enzyme detected in the detergent phase for each class, very ineffective for these enzyme classes.

The characterisation of the cloud point extracts according to their biological functions added potentially useful insights into the phase separation between the aqueous and detergent phase. Individual results for each function category indicating preferences for one extraction phase were summarised in figure 4-42 below. It showed the relative differences between the fractions corresponding to function categories in the detergent and aqueous phase. Positive percentages implicated a preferred extraction of proteins into the detergent phase. Negative values represented categories not favourably extracted into Triton X-114 micelles and were mostly found in the aqueous phase.

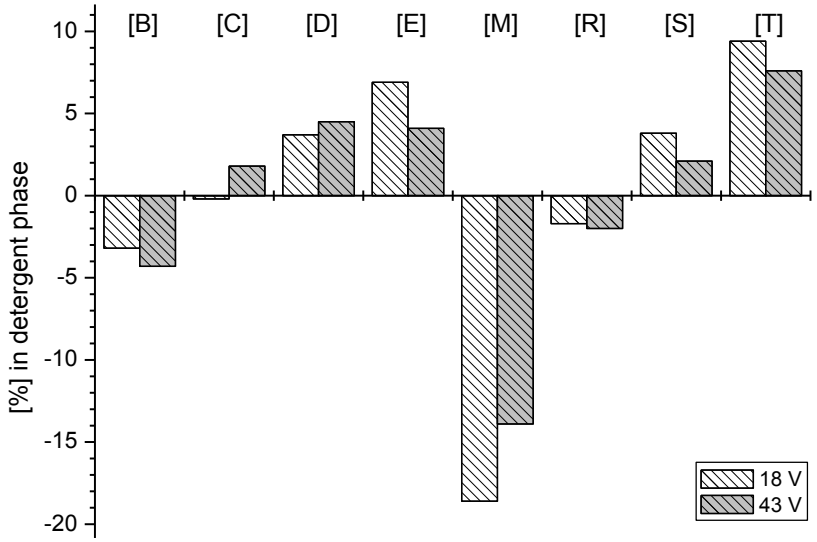

Figure 4-42 Relative protein distributions between extraction phases [% X-114] – [% aq]

Cloud point extraction was most effective for energy and transport proteins. Proteins in both categories were predominantly membrane related and confirmed the observations made in previous chapters.

Categories [D] and [S] were extracted to a lesser extent into the detergent phase. The hydrophobic extraction effect was even clearer for category [D]. Despite the high degree of cytoplasmic proteins evident in the aqueous phase, mainly membrane and dually assigned proteins were found in the detergent phase. For signalling proteins the decline was related to the relatively even location distribution in the aqueous phase. Here the numbers for the detergent phase showed a slight accumulation in membrane proteins.

The application of CPE for proteins involved in metabolism, biosynthesis and response category was an ineffective method. High numbers of cytoplasmic proteins and enzymes assigned to these categories were common to all and were not preferentially extracted into the micelle-rich phase.

In conclusion to the assessment of the detected proteins according to their general functions in the brain the probability to successfully extract a protein into the detergent phase rises not necessarily with a positive GRAVY index, but if the target protein is membrane-related and involved in cell maintenance and signalling, cell differentiation and division, energy and transport processes. The probability declines for cytoplasmic proteins and especially enzymes fulfilling roles in metabolism, biosynthesis and response.

Addition of function information, if available, to cellular location and GRAVY indices might lead to more accurate estimations of phase separation behaviour prior to the extraction and help in the decision process to extract a specific target protein via cloud point extraction with Triton X-114.

4.3.4 Interims summary III – protein partitioning in CPE

The assessment of phase partitioning of proteins extracted from mouse brain tissue was based on the grand average hydropathicity index (GRAVY) in relation to various parameters (extraction phase, capillary voltage, cellular location and function). Protein bands were subjected to tryptic in-gel digestion and identification by LC-MS/MS analysis.

- Initially expected protein distributions in the aqueous and detergent phase – distinctive trends towards the negative (aq. phase) or positive (detergent phase) GRAVY ranges – were only slightly reflected in the actual results. The majority in both phases were found in the GRAVY range of -0.750 to 0.125. Using the GRAVY index, based on the amino acid sequence, of a protein alone to estimate phase separation behaviour in a Triton X-114 cloud point extraction system was found to be unreliable.
- Adopting results from SEC-MS optimisation efforts for the hydrophobic amyloid β 42, an additional LC-MS/MS analysis incorporating a significantly higher capillary voltage (43 V) was performed. Combination of both data sets allowed a more thorough characterisation of the extraction phases.
- Phase distribution of proteins according to their cellular locations showed a clear preference of membrane proteins for the micelle-rich phase (~53 %) and of cytosol proteins for the aqueous phase (57 to 61 %). The results confirmed the favourable environment within detergent micelles for proteins normally connected to or embedded in lipid bilayer membrane structures.
- The higher capillary voltage was especially beneficial for the detection of membrane proteins in the aqueous phases, increasing by 9 %.
- Sorting identified proteins into function categories allowed assessment of relavtive phase distribution of extracted proteins. Especially proteins assigned to energy and transport and to a lesser extent signalling and cell differentiation and division were extracted into the detergent phase. Proteins related to metabolism, biosynthesis and response were predominantly found in the aqueous phase.
- Application of higher capillary voltage had only minor effects on observed distributions.

4.4 Examination of Aβ 42 related protein bands

Cloud point extraction of mouse brain tissue was orignally chosen to investigate small soluble oligomers because of the hydrophobic GRAVY index of amyloid β 42 (0.369). In order to assess excised and digested protein bands the recorded LC-MS/MS data sets were processed with BioWorks™ once more using a separate database created from sequence information collected from the online protein database of the national center for biotechnology information (www.ncbi.nlm.nih.gov) to include proteins related to amyloid β or Alzheimer's disease that were not in the general mouse database. A detailed table of the FASTA database content can be found in appendix A.8.

4.4.1 Identification of potential Aβ42 species

In theory the detection of amyloid β 42 traces in protein bands corresponding to higher molecular weights than the monomer would indicate the presence of oligomeric species in the extraction phases. Since the analysis of electrophoretically separated protein extracts was an alternative solution to using size exclusion chromatography – MS the detection of possible oligomers was primarily used to investigate the suitability of the method to extract amyloid β variants as well as their oligomeric forms.

The results of the identification process are visually represented throughout this chapter by colour-coded protein bands marked in images of prepared gels. The majority of bands was grey indicating that no truly confident match could be assigned ($P > 0.5$) to the data sets. The fact that amyloid β was very low concentrated in comparison to the whole proteome further complicated a correct and reliable identification. Protein bands containing traces of the molecule as a peptide fragment of the Aβ40 and Aβ42 form or as part of precursor proteins with probabilities $P \leq 0.5$ were included in this examination. Positively identified bands were coloured according to the protein probabilities assigned for peptides matching the amyloid β amino acid sequence. The darker the protein band the lower was the corresponding probability of a false match (table 4-13). BioWorks™ database search result are listed in detail in the supplementary digital information provided with this work.

Table 4-13 Applied colour-coded protein probabilities.

Colour	Protein probability [P]	Positive match [%]
(dark pink)	< 0.1	> 90 %
(pink)	$0.4 \geq P \geq 0.1$	60 % ≤ [%] ≤ 90%
(light pink)	= 0.5	50 %
(grey)	> 0.5	< 50 %

Boundaries were chosen based on the prevalence of protein probabilities for the 260 examined bands. A match was considered positive if a fragment of the amino acid sequence of amyloid β was identified by the SEQUEST algorithm. Figure 4-43 shows the sequence of the protein and indicates the Aβ40 and 42 variants as well as theoretical cleavage points of trypsin (R or K).

Figure 4-43 Amino acid sequence of amyloid β 40 and 42. Cleavage points for trypsin marked in blue.

The first protein bands were used to test the suitability of the established standard procedure for tryptic in-gel digests and LC-MS/MS analysis for protein identification (fig. 4-44). They were excised from the gel displaying the influence of buffer composition on extraction results (see chapter 4.2.2). Analysed protein bands included the visible bands of buffer 1 (Tris buffered PBS, 1 % X114), a high number of bands from the larger sample volume of the detergent phase of buffer 3 (pure water, 1 % X114) and a few from the aqueous phase (3 (aq), right lane).

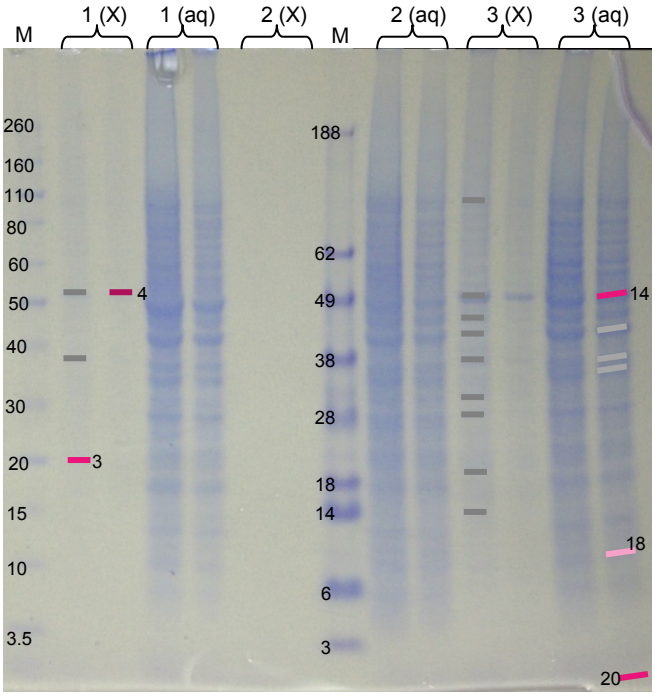

Figure 4-44 Excised protein bands analysed by LC-MS/MS **01-20 (18 V)**. Cond.: 4-12 % bis-tris, reducing cond., 75 V, SimplyBlue. Left lanes 8 µL sample volume, right lanes 4 µL

The main focus was put on the analysis of the most intensive protein bands visible for detergent phases. The Aβ40 peptide GAIIGLMVGGVV (1085.6 Da) was identified with a probability 0.057 for band no. 4 using the specialised database, representing a 94.3 % chance of a positive match.

No protein matches could be confidently identified with the general mouse database for band no. 4, showing the nessicity for a separate data processing for phase characterisation and oligomer localisation. In comparison to typical protein probabilities calculated for general data sets (down to approx. E-30) confident amyloid related matches were rarely lower than 0.001 (99.9 %). Caused mainly by the low concentration of amyloid β in the sample, extracted peptides also stood in competition to many co-extracted peptides which in turn limited the overall number of mass spectrometric scans and the amount of fragmentation data. A good representation for these unpredictable influences on the

detection of lower concentrated proteins was the lack of a positive Aβ match in the equivalent but more intensive protein band left of no.4.

Based on the position in the lane, the molecular weight was estimated as about 48.3 kDa indicating the possible presence of an oligomeric Aβ species in the detergent phase. In addition to the four protein bands for the detergent phase of buffer system 1, the most intensive bands were excised from the micelle-rich phase sample of buffer system 3 that did not result in positive matches. The combination of both observations, positive match and lack of false positives, confirmed the suitability of the cloud point extraction for further experiments.

Protein probabilities in the 0.4 to 0.1 range were interpreted as indicators for a possible Aβ match, only matches with smaller probabilities were used to draw confident conclusions on the extraction behaviour of the hydrophobic protein.

As previously discussed in chapter 4.2.2, precipitation and delipidation with method D (tributylphosphate) were repeated and detergent phases were redissolved in smaller volumes to increase their concentration. The resulting gel in figure 4-45 shows the database matches for the excised bands with 18 V (left) and 43 V (right). Fewer bands were marked for 43 V since the dual analysis with both capillary voltages was applied for protein bands from 81 upwards. Selection of protein bands was based on two conditions: (I) accordance with monomer and oligomer molecular weights or (II) thorough characterisation of the extraction phases for at least one sample (3 D and D').

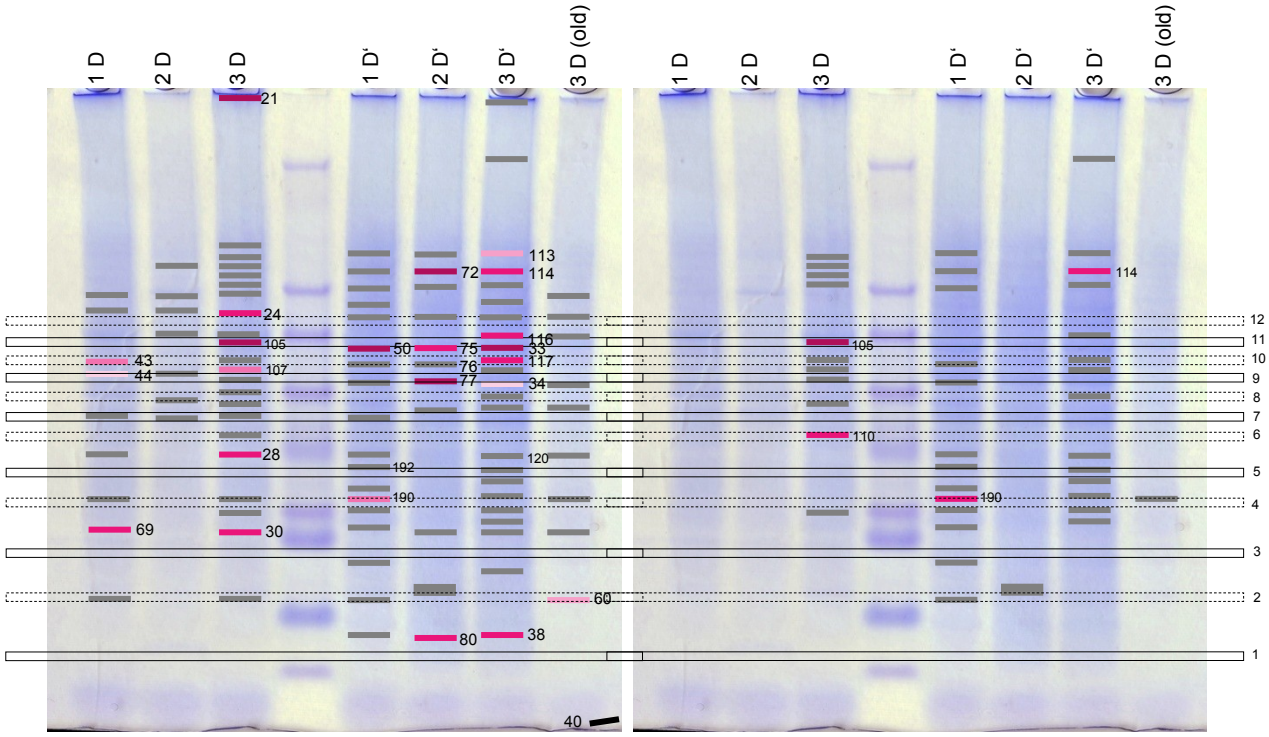

Figure 4-45 Excised protein bands analysed by LC-MS/MS. Excised bands: **(Left) 21-80, 101-120, 181-200 (18 V), (Right) 101-120, 181-200 (43 V)**. Cond.: 4-12 % bis-tris, reducing cond., 80 V, SimplyBlue

Band number 21 was excised to investigate protein residue on top of the well, caused by incompletely redissolved precipitate or proteins exceeding the capacity of the gel matrix. Amyloid β 40 was identified with a probability of 0.081 (91.9 %) and confirmed an extraction of the hydrophobic protein into the detergent phase. No amyloid related match was found for the respective band for the aqueous phase. Despite relatively mediocre

probabilities for the bands 24 (~12 mer, 0.2), 28 (~5-6mer, 0.4) and 30 (~3-4mer, 0.4) the presence of multiple Aβ species in the detergent phase was indicated.

For band no. 105 the previous Aβ40 peptide with an oxidised methionine (GAIIGLXVGGVV, 1067.7 Da, 6/22 fragment ions) was identified with a probability of 4.9E-04 translating to promising 99.951 % confidence of a positive match and a molecular weight of a 11mer of the Aβ42 species. The positive identification was confirmed by the 43 V data with a probability of 9.7E-03 (99.03 %).

Several positive matches found for the aqueous phases suggested only a partial extraction of amyloid β species into the detergent phase. The quantity of amyloid related bands was mostly attributed to the higher protein concentration in aqueous phase samples. Protein bands 50 (0.079, 92.1 %), 75 (0.1, 90 %) and 33 (0.065, 93.5 %) from aqueous phases corresponding to a similar molecular weight as band 105 confirmed the presence of an undecameric species by identifying the oxidised amyloid β 40 peptide in both phases.

Two additional good matches were found in lane 2 D' (aq. phase, PBS buffered solution), band 77 (0.038, 96.2 %) corresponding to a molecular weight of a nonamer of Aβ42 and band 72 (0.081, 91.9 %) that was significantly larger (~77.9 kDa) than the highest expected molecular weight of the often reported soluble dodecamer of Aβ42 (~52.8 kDa). Based on the molecular weight and one identified peptide alone no finite conclusions about the suspected oligomer could be drawn. Further evidence for the presence of a larger oligomer species was the identification of amyloid related peptides in band 114 with a protein probability of 0.3 (66.6 %) for both capillary voltages.

The aqueous phase also seemed to offer a better environment for the small amyloid β species. No protein bands were visible below 6 kDa in the detergent phase while for each aqueous phase protein bands corresponding to molecular weights slightly higher than a monomer were found. For extraction medium 2 and 3 low confidence matches (P = 0.2, 80 %) indicated the presence of Aβ40 species in the aqueous phase. The smallest suspected amyloid β oligomer detected in the detergent phases was excised at a molecular weight between a trimer and tetramer implied by band 30 (P = 0.4, 60 %) with a peptide derived from the precursor protein A4 (P12023, MDAEFR) and the C-terminal Aβ40 peptide in band 69 (P = 0.1). Protein bands corresponding to similar molecular weights examined for the aqueous phases led to no positive matches.

The extraction of amyloid β species into a Triton X-114 phase was less straight forward than expected. Despite the high hydrophobicity implied by GRAVY indices of the monomers only a partial extraction was observed. Furthermore, aside from the suspected undecamer (105, 50, 75, and 33) present in both phases the amyloid species implied for the detergent phase differed from the results for the aqueous phase.

To further investigate the extraction behaviour of amyloid β 42 within the cloud point system the extraction was repeated with an Aβ42 monomer standard solution as well as a spiked sample (see appendix A.1.4.2). The multi-step experiment was designed to explore the extraction of Aβ42 in a controlled blank system and in presence of the complex biological matrix (see appendix A.1.5.3). Aqueous phases of both samples were re-extracted by adding 50 µL pure Triton X-114 and repeating phase separation to explore extraction efficiency. Residual matrix material was extracted a second time with a 1 % Triton X-114 solution to observe the distribution of proteins not included the first time. Figure 4-46 shows the gel electrophoretic separation and examined protein bands for the resulting samples.

The most prominent result was the complete lack of visible protein bands for the detergent phases of the Aβ42 monomer sample. Neither cloud point extraction nor re-extraction of the aqueous phase with fresh detergent was successful in extracting

significant amounts of the protein into the micelle-rich phase. In the aqueous phases, however, one protein band representing the monomer was reliably identified (81 and 89). Contrary to previous results, another peptide was found for band 81 (LVFFAEDVGSNK, 1325.7 Da) with a probability of 4.5E-09. It was credited to the amyloid beta A4 isoform 6 precursor (Acc. 311893408) for 18 V. Repetition of the LC-MS/MS analysis with 43 V capillary voltage lowered the probability for the peptide to 2.2E-09 and added peptide matches for Aβ42 (MDAEFR, 4.9E-04) and Aβ40 (0.3). Both high confidence matches did not allow a conclusive decision on the protein ID since the sequences are identical to the last two amino acids. Since an amyloid β 42 standard was used, the protein band 81 with an estimated molecular weight of 4.1 kDa was identified as Aβ42 monomer.

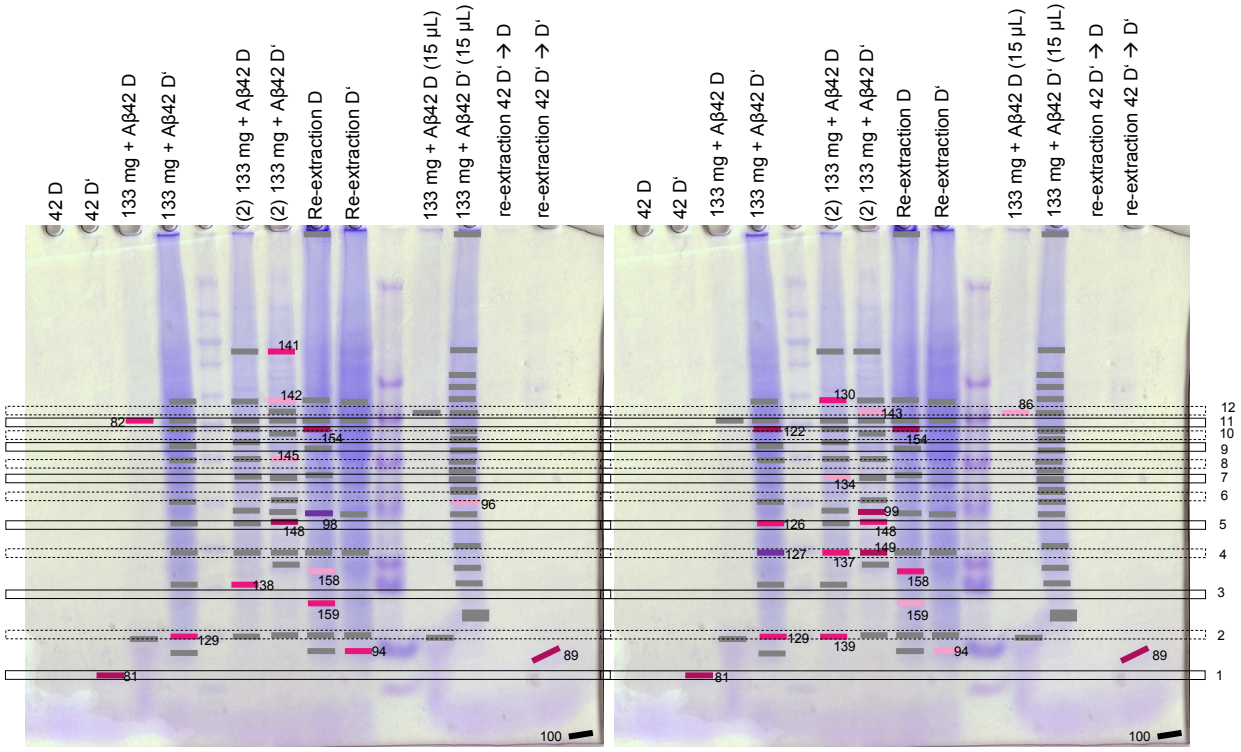

Figure 4-46 Excised protein bands analysed by LC-MS/MS. **Bands 81-100, 121-180, left: 18 V, right 43 V**. Cond.: 4-12 % bis-tris, reducing cond., 80 V, SimplyBlue

The estimated molecular mass for band 89 was slightly higher due to lane deformation caused by the location of the lane and elevated concentrations of X114 in the larger sample volumes of 15 µL in the adjoining lanes. Disturbance of the electrophoretic process was also visible in discolourations around the lowest protein band for the 15 µL detergent lane (D') and deformation of the 3 and 6 kDa marker bands. Similar to band 81 the protein probabilities for both parameter settings indicated a monomer, with 4.3E-09 (18 V) and 4.2E-09 (43 V) for LVFFAEDVGSNK.

The overall quality of the gel as well as the samples was lower than for the previous gels. Loss in sample quality was attributed to a storage period at -20 °C of the brain tissue (~2 months) between homogenisation and extraction. Protein bands were still sufficiently separated to investigate the extraction of Aβ42 in the presence of the biological matrix. Brain tissue seemed to drastically alter the observable extraction behaviour of the Aβ42 monomer. No protein bands smaller than approx. 6 kDa were visible in the gel for either extraction phase. The only protein band with a molecular weight close to the monomer

(No. 94, ~5.5 kDa) and a positive match showed protein probabilities of merely 0.4 (18 V) and 0.5 (43 V).

The first extraction of the brain tissue sample was not successful (133 mg + Aβ42 D/D'). Two protein bands and a slight distortion towards the end of the lane indicated a practically non-existent transfer of proteins into the extraction phase. The aqueous phase on the other hand (D') showed signs of overloading: an intensive blue background and deformation of several protein bands impeded a distinction between gel background and weak protein bands. Selection of protein bands from matrix-related lanes was mainly based on theoretical molecular weights of oligomeric Aβ42 species.

Analysis of the excised bands with the 18 V setting merely led to hints at amyloid species for band 82 in the detergent phase (12mer, ~52 kDa, P = 0.2) and 129 (2mer, ~8.2 kDa, P = 0.4) in the aqueous phase. Application of the higher capillary voltage led to more positive matches. In addition to band no. 129 with an equal probability to 18 V, three amyloid β related bands were detected. For band no. 122, in the range of an 11 to 12mer (~52.4 kDa), the C-terminal peptide of Aβ40 was identified by BioWorks™ with a confident probability of 0.047 (95.3 %).

The second extraction of the brain tissue with 1 % Triton X-114 in pure water ((2) 133 mg + Aβ42 D/D') resulted in a clearly better extraction of proteins into the detergent phase (D) while the concentration in the aqueous phase was visibly lower. Using residual matrix material already saturated with extraction solution and detergent micelles from the previous extraction proved advantageous. The consistent distribution of micelles throughout the tissue aided the more effective transfer of proteins into the detergent phase. It may be beneficial for cloud point extraction of homogenised and stored brain tissue to prolong the incubation time prior to phase separation.

For both extraction phases the pattern of positive amyloid β matches changed with the switch in capillary voltage. Only band 148 (~25.5 kDa, possible 5mer) from the aqueous phase was present with both settings, probability decreasing from 0.091 (90.9 %, 18 V) to 0.3 (43 V). Distribution of amyloid β species between the phases was similar to previous observations. Positive matches for the N-terminal Aβ40 peptide in the detergent phase increased from one band for 18 V (138, 0.1) to four low confidence matches for bands corresponding to the molecular weights of a dodecamer (130, P = 0.2), octamer (134, P = 0.5), tetramer (137, P = 0.2) and dimer (139, P = 0.4).

For the aqueous phase (D') band 141 (~87.4 kDa) resulted in a low probability match for the Aβ40 peptide GAIIGLMVGGVV (P = 0.2) in addition to band 148 at 18 V. The higher capillary voltage led to two high confidence matches. Amyloid β 40 was identified for band 99 with a probability of 0.019 (98.1 %) even though the estimated molecular weight (~28.4 kDa) did not directly correspond to an oligomer species. The tetramer indicated by band 137 in the detergent phase was also more confidently identified in band 149 (~20.9 kDa) excised from the aqueous phase with a protein probability of 0.06 (94 %).

Protein samples created by re-extracting the aqueous phase of the initial extraction with 50 µL Triton X-114 yielded poor quality separations in the gel. The lanes showed a high background staining as well as vertical streaking. Amyloid β related matches were predominantly found in the detergent phase for both parameter settings. Band 154, corresponding to a molecular weight of 47.1 kDa (~10mer) was the best match for both phases and settings. The protein probability for the oxidised Aβ40 peptide GAIIGLXVGGVV was calculated as 0.048 (95.2 %) for 18 V and 0.044 (95.6 %) for 43 V.

Low confidence matches for Aβ40 were found for bands 158 (~16.5 kDa, P = 0.5) and 159 (~12.4 kDa, P = 0.3) with the lower capillary voltage. The molecular weight estimated for both bands lay slightly outside of the assumed oligomer grid, just below a tetrameric (158) and trimeric species (159). The protein probabilities showed a minor change with the 43 V parameter setting, decreasing for band 158 (P = 0.2) while increasing for 159 (P = 0.5).

Re-extraction of the aqueous phase seemed to lead to an increased transition of amyloid β species into the fresh detergent phase. The suspected oligomeric species identified for band 122 (43 V) was now seemingly extracted into the detergent phase and detected in band 154. A final conclusion about phase distribution of the oligomer could not be drawn since the equivalent band in the aqueous phase was not excised and examined. The worsened separation quality and the lack of additional information gained by re-extraction suggested that an approach involving an initial extraction as well as a second extraction of the residual tissue offers a greater insight into amyloid β species.

All excised protein bands in fig. 4-47 were analysed with both capillary voltages. For this gel at least, the time-consuming extra chromatographic runs led to numerous positive matches that were not detected with the 18 V setting alone. While the protein probabilities were relatively low in comparison to the mouse-database results, they aided the assessment of the extraction behaviour of amyloid β species.

For the gel in figure 4-47 another stored, homogenised sample of brain tissue (~5 months) was spiked with the amyloid β 42 monomer and extracted. In order to test the suitability of available precipitation and delipidation methods for frozen brain tissue a sample of each extraction phase was treated according to method B (chloroform, MeOH, H_2O), C (acetone, MeOH) and D (acetone, MeOH, TBP).

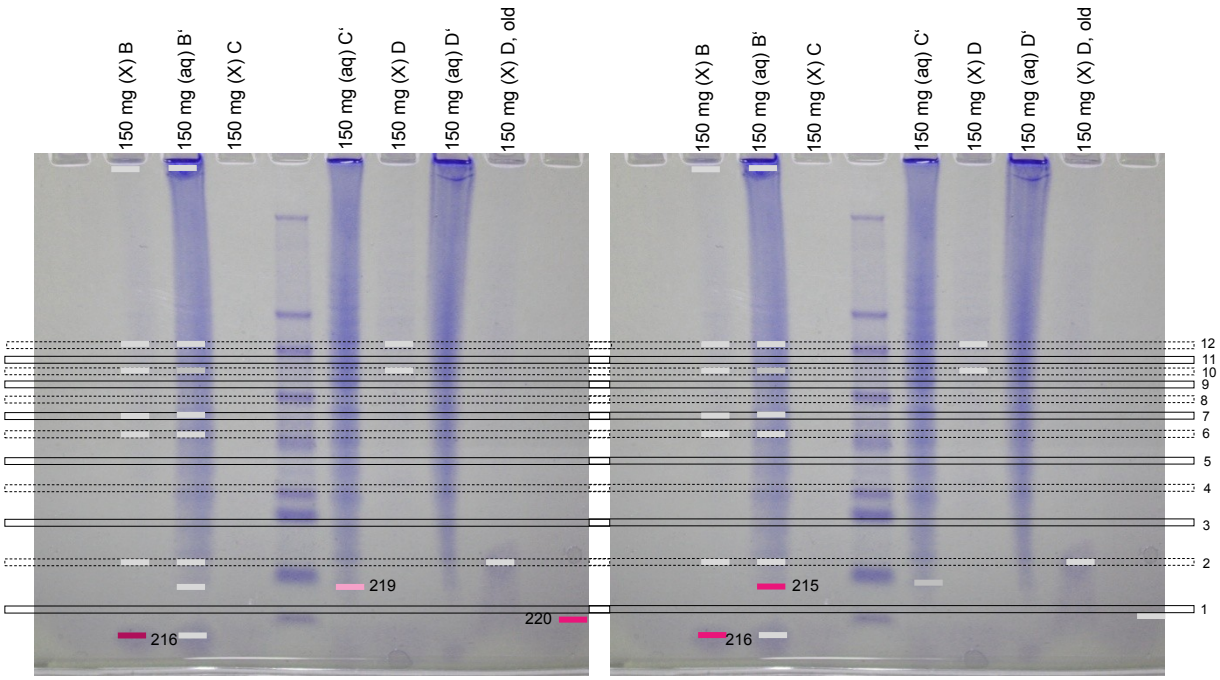

Figure 4-47 Excised protein bands analysed by LC-MS/MS. **Bands 201-220, left: 18 V, right 43 V**. Cond.: 4-12 % bis-tris, reducing cond., 80 V, SimplyBlue

The visual appearance of the gel already showed signs of sample quality deterioration caused by storage time and precipitation method. None of the chosen methods were able to produce a sufficient separation and band definition. Lanes corresponding to the

aqueous phases showed an increasing degree of vertical streaking and a decreasing resolution from (B) to (D). Very few well defined protein bands were discernable from the background stain for the aqueous phases while the protein concentration in the detergent phases was very low.

Precipitation using the chloroform/MeOH/H_2O system provided the most useful results. Despite the very low protein concentration in the detergent phase protein bands were excised and analysed. Positive matches were, in comparison to previous observations, only found below 6 kDa. None of the assigned matches fit the oligomer grid and were regarded as artefacts rather than reasonable matches. Band 216 (Aβ 40, GAIIGLMVGGVV) for example, with protein probabilities of 0.089 (91.1 %, 18 V) and 0.2 (43 V), was excised from the running front of the electrophoresis buffer of the detergent phase that normally consists of Coomassie brilliant blue and sample components to small to be retained by the gel matrix. The identification was attributed to the added monomer standard that was probably incorrectly separated during electrophoresis.

To assess the efficiency of cloud point extraction for the isolation of oligomeric amyloid β species, supernatant of a extraction of brain tissue with alkaline carbonate buffer (pH 11.5) equalized to 5 M guanidine HCl containing soluble Aβ species and non-soluble Aβ species redissolved from precipitate with 5 M guanidine HCl buffer (pH 8.0) provided by the working group of Prof. Dr. Pahnke were precipitated with method (D). Figure 4-48 shows the successful gel electrophoretic separation and excised protein bands corresponding to molecular weights of oligomers that were analysed by LC-MS/MS.

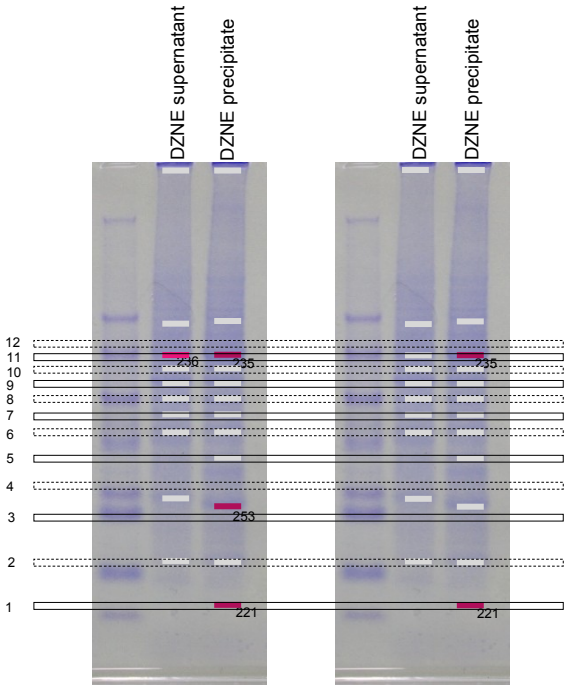

Figure 4-48 Excised protein bands analysed by LC-MS/MS. **Bands 221-240, 252/253 and 257/258, left: 18 V, right: 43 V**. Cond.: 4-12 % bis-tris, reducing cond., 80 V, SimplyBlue

The most confident match for Aβ related peptides was band no. 221 excised from the precipitate lane at an estimated molecular weight of ~3.7 kDa. With protein probabilities of 4.0E-09 (18 V) and 3.6E-09 (43 V) the search algorithm identified the C-terminal peptide LVFFAEDVGSNK common to both amyloid β 40 and 42. The peptide was previously detected with similar probabilities only for the monomer standard in bands 81

and 89. A positive identification for band no. 235 (~48 kDa) of a possible 11mer of amyloid β 40 (GAIIGLXVGGVV) was significantly less confident with 0.048 (95.2 %, 18 V) and 0.026 (97.3 %, 43 V). The distinct decrease in probability could be related to concentration ratios between monomer and oligomer.

Two additional protein bands were detected as amyloid β species using the lower capillary voltage. Band no. 236 mirrored the 11mer detected for the precipitate albeit with a relatively low probability of 0.1. The oligomer was the only amyloid related species found in both supernatant and precipitate. From the further decline in protein probability it could be postulated that while the monomer was exclusively found in the precipitate, the suspected 11mer was at least a partially soluble form of amyloid β.

The positive identification of the small peptide MDAEFR, originating from the human amyloid precursor protein (A4_HUMAN) in band no. 253 (precipitate) with a probability of 0.08 (92 %) with 18 V but not 43 V. The decision to examine the protein band was based on stain intensity rather than an exact conformance with theoretical oligomers but was closest to an Aβ42 trimer.

4.4.2 Conclusions from data re-examination with Aβ specific database

Several conclusions could be drawn from the re-examination of mass spectrometric data sets with an amyloid β specific database to assess the phase separation behaviour of amyloid β species. Cloud point extraction of mouse brain tissue was chosen based on the relative hydropathicity implied by a positive GRAVY index of 0.369 for amyloid β 42. Extraction of monomer and oligomers into the hydrophobic environment offered by Triton X-114 micelles was expected. The obtained results however indicated contradictory extraction behaviour for the monomer. Cloud point extraction of Aβ42 monomer solution led to no visible traces of the monomer in detergent phase. Added monomer in tissue samples did not appear in either extraction phase. The loss was credited to undesired adsorption to tissue components binding the small protein and preventing its extraction.

Monomers in tissue samples were identified with the highest confidence in redissolved precipitate representing insoluble Aβ species and to lesser extent for the lowest molecular weights (~5.5 kDa) for positively identified protein bands in the aqueous phases of cloud point extracts of “fresh” tissues. Homogenised tissue samples stored at -20 °C over a time period of two months lost visual protein bands smaller than 6 kDa and showed a decline in separation quality. Samples stored for longer periods (approx. 5 months) deteriorated nearly completely and were useless for cloud point extractions.

Despite the unexpected incapability of cloud point extraction with Triton X-114 to extract amyloid β monomers it proved to be a more suitable method for the examination of oligomeric species with LC-MS/MS. In samples gained through extraction with carbonate buffer (100 mM Na_2CO_3, 50 mM NaCl) and resolvation of insoluble species in 5 M guanidine HCl buffer (+50 mM Tris) positive matches were restricted to the monomer, a possible trimer and an undecamer also detected in the supernatant as a soluble species.

Taking the distribution of high confidence ($P < 0.1$) and lower confidence ($0.1 \leq P \leq 0.4$) matches for both extraction phases of CPE into account, the conclusion that cloud point extraction was the more suitable extraction method for the examination of Aβ oligomers with a high potential to provide samples containing multiple oligomer species for size-exclusion – MS examinations. The low confidence levels for the majority of positive matches were attributed to low concentrations and occasionally false positives.

For the majority of positive matches the C-terminal peptide of amyloid β 40 was detected instead of the expected 42 amino acid variant. Even for protein bands definitely corresponding to the Aβ42 monomer the identification was based on the C-terminal peptide or similar fragments of precursor proteins rather than the distinct GAIIGLMVGGVVIA peptide. Two aspects seemed to influence the detection of Aβ 42 peptide. On the one hand the fact that both amyloid β species are regularly formed in the brain and would, due to nearly identical amino acid sequences behave similarly during gel electrophoretic separations, had to be considered. The resolution achieved was not accurate enough to discern Aβ40 from Aβ42 species based on molecular weight. Detected monomer and oligomer bands could therefore correspond to either or both variants since their concentration was too low in comparison to the non-amyloid proteins in the band to produce enough fragmentation spectra for an absolutely certain identification. An indication of potential overshadowing of Aβ42 by the shorter variant was implied by the single positive identification of the C-terminal peptide for band no. 110 (P = 0.1, only 43 V) corresponding to a hexamer.

A lower concentration and the extended sequence adding isoleucine (I) and alanine (A) on the other hand might also influence the mass spectrometric detection by altering the chromatographic separation and ionisation properties of the peptide. Comparing the GRAVY indices for both variants showed an increase in hydrophobicity of +0.139 that could lead to a permanent adsorption to the apolar C18 column material, preventing a mass spectrometric detection. Premature fragmentation during the electrospray ionisation process could also have contributed to the almost non-existent detection of the N-terminal Aβ42 peptide in favour of the Aβ40 variant (-IA). The heightened hydrophobicity was observed in the retention times recorded for the respective peptides. In band 110 the longer peptide was detected at 27.3 min while the amyloid β 40 equivalent was generally found around 21 minutes. The different retention times simultaneously disproved the idea of losing isoleucine and alanine during ionisation. A possible preference of the shorter amyloid protein must have occurred during the extraction, precipitation or in-gel digestion steps of sample preparation and could not be investigated further within the timeframe of this work.

In comparison to the combination of carbonate buffer extraction and guanidine HCl resolvation of insoluble Aβ species from the precipitate with only three amyloid β species detected by LC-MS/MS (1mer, ~3mer and 11mer) cloud point extraction offered a broader variety of amyloid β oligomer species in both extraction phases. Due to limitations caused by low protein concentration and an indicated reluctance of amyloid β molecules in monomeric form to transfer into the detergent phase, confidence level and degree of oligomerisation were smaller than for the aqueous phase. Possible oligomeric species extracted into the Triton X-114 micelle-rich phase were mostly detected in the range of dimers (no. 139, 43 V), trimers (no. 138, 159), tetramers (no. 137, 43 V) and off-grid molecular masses between a 3-4mer (no. 69, 30 and 158) and a 4-5mer (no. 28). Additional species, detected with low confidence hinted towards a hexamer (no. 110, 43 V), 9-10 mer (107) and dodecamers (no. 4, 24 and 130).

Oligomer species detected in aqueous extraction phases showed a slightly altered distribution. Positive matches indicated the presence of dimers (no. 129, ~94), tetramers (no. 149, 190), nonamer (no. 77) and decamer (no. 117) also detected in the detergent phases. While no indicators for trimers were found in the aqueous phase it extended the range by adding a pentamer (no. 99, 148) as well as amyloid β related bands with molecular weights exceeding the highest expected 12mer (no. 72, 114, 141).

The majority of high confidence matches were found for protein bands with molecular weights corresponding to an undecamer of Aβ42. A positive match for the assumed oligomer was mirrored in the precipitate sample confirming the molecule as a stable form unaffected by both extraction methods. The 11mer was not only detected in the aqueous phase (bands no. 50, 75, 33 and 116) and but also extracted into the detergent phase (bands no. 105, 82 and 154).

Increasing the capillary voltage to 43 V as determined by optimisation efforts made for the intact Aβ42 monomer did not lead to an overall improvement of the detection. But occasionally the extra effort of re-running the chromatographic analysis with the altered parameter setting offered further insight into potential oligomer species within the protein bands. The biggest gain information was observed for the excised protein bands 121-140 with seven additional positive matches not detected with the 18 V setting.

Cloud point extraction of mouse brain tissue seemed to offer milder conditions for oligomeric Aβ species than the alternative extraction method and preserving less stable soluble oligomers. While positive matches were found in both extraction phases, the effect of the hydrophobic micelle environment on the extraction of amyloid β species was considerably smaller than expected. Examination of protein bands correlating to theoretical oligomer molecular weights from both extraction phases might prove to be an excellent starting point for further optimisation and investigation of amyloid β species with liquid chromatography mass spectrometry based methods.

4.4.3 Interims summary IV – examination of Aβ42 related protein bands

Using a significantly smaller, amyloid β specific protein database allowed the identification of possibly Aβ oligomer species in mouse brain tissue protein extracts based on LC-MS/MS data sets of tryptic protein digests.

- Several probable amyloid β species, monomers and oligomers, where identified in both the aqueous and detergent phases of the CPE system as well as in supernatant and precipitate of ELISA preparations.
- Sample quality of protein extracts decreased with storage time of homogenisate.
- Despite Aβ42 being a fairly hydrophobic molecule, results gained from spiked blank extraction system suggested a preference of monomeric species for the aqueous phase. The presence of brain tissue severely altered the detection of Aβ monomer.
- Slightly altered patterns of Aβ related bands were observed for aqueous and micelle-rich extraction phase.
- Common to both extraction methods and phases was an oligomeric species corresponding to a 11mer (~48 kDa), indicating a major soluble oligomeric amyloid β species unaffected by the chosen extraction method and in sufficient concentration be present in aqueous and detergent phase (phase equilibrium) as well as precipitate and supernatant.
- CPE offered a superior extraction environment than the sample preparation prior to ELISA testing in regard to the detection of oligomeric species. The detergent based system extended the limited set of Aβ species extracted into an alkaline carbonate buffer and may lead to more detailed insights into the processes of Alzheimer's disease.

5. General discussion and outlook

The connecting thread between separate sections of this work was the analysis of proteins: ranging from the general assessment of protein extracts produced by phase separation in a non-ionic detergent cloud point extraction system to the specific analytical problem posed by amyloid β species relevant in Alzheimer's disease biomarker research.

Cloud point extraction as a sample preparation method for mouse brain tissue was chosen based on two hypotheses. Research into Alzheimer's disease and amyloid β revealed the protein to be of a fairly hydrophobic nature, based on the GRAVY index of the molecule. The first hypothesis was that the protein and oligomeric species would, if exposed to the Triton X-114 micelles in the system at low temperatures, prefer the hydrophobic environment and be preferentially extracted into the detergent phase. The second hypothesis was rooted in practical considerations. For both planned analytical methods, SEC-MS and LC-MS/MS of protein bands in gels, phase separation would result in the removal of overly abundant plasma proteins like globulins and albumins from the lower concentrated hydrophobic target proteins.

Results from spiking both a system blank and a brain tissue homogenisate with amyloid β 42 monomer standard solutions contradicted the first assumption and questioned the usefulness of the second. Not even minor traces of the monomer were detected in the detergent phase of the spiked blank, while Aβ was identified with very high confidence in the aqueous phase. Addition of monomer to a tissue sample prior to phase separation had no visible effect as no protein bands corresponding to the molecular weight were present in neither the aqueous nor the detergent phases, probably lost to unintended matrix interactions.

Oligomeric species were however identified in both extraction phases with varying degrees of oligomerisation. Based on the reluctance of the monomer to be extracted into the detergent phase and overall mass ranges achieved by CPE suggested a lower mass cut-off of Triton X-114 micelles for smaller proteins or fragments. Cloud point extraction allowed, in comparison to the sample preparation pathway prior to ELISA assays, the extraction and analysis of a broader range of Aβ species. While the immune-reaction based technique delivers data regarding the overall concentration in a sample, samples prepared by CPE have the realistic potential to offer an insight into the relative distribution of soluble oligomers that are a major contributor in the progression of AD (Haass and Selkoe 2007).

A probable undecameric amyloid β species (~48 kDa) could be found in both CPE phase and in precipitate and supernatant of ELISA samples. The 11mer species was concluded to be the major soluble oligomer present in the provided mouse brain tissues as opposed to Aβ56* 12mer suggested by Lesne et al. (Lesne, Koh et al. 2006). To eventually fully validate a CPE sample preparation protocol an investigation into the effects of extraction method and medium on the distribution of oligomeric species especially in comparison to established methods will be necessary.

General characterisation of protein extracts based on GRAVY indeces, cellular location and function allowed a more thorough assessment of the process. They indicated an extraction mechanism that is less predictable by the grand average hydrophathicity index (GRAVY) calculated from amino acid sequences, but more the result of specific properties of each protein that are merely based on the AA sequence. A major factor for the extraction of a protein into detergent phase seemed to be embedment in or connection

to any kind of membrane, indicating molecular structures of micelles to emulate the bi-lipid layer membrane design in nature. The protein distribution according to cellular location reinforced observations made on CPE of mouse brain tissue by Wetterhall, Shevchenko et al. (2011).

In 2012 diagnostic guidelines for Alzheimer's disease were expanded to include not only diagnosis based on symptoms like memory loss, but also to incorporate biomarker tests that could indicate the absence or presence of the disease. Since the initial onset of the disease can predate the appearance of actual symptoms by 20 years, research into known biomarkers like Aβ and protein tau is vital to the diagnostic process and possible treatment strategies for preclinical stages of AD. Figure 5-1 shows the statistical development of major causes of death between 2000 and 2010. The most prominent fact is the increase of deaths caused by Alzheimer's disease by 68 % as opposed to declining rates for diseases with known causes, risk factors and effective treatment options that are as of today unavailable for AD patients.

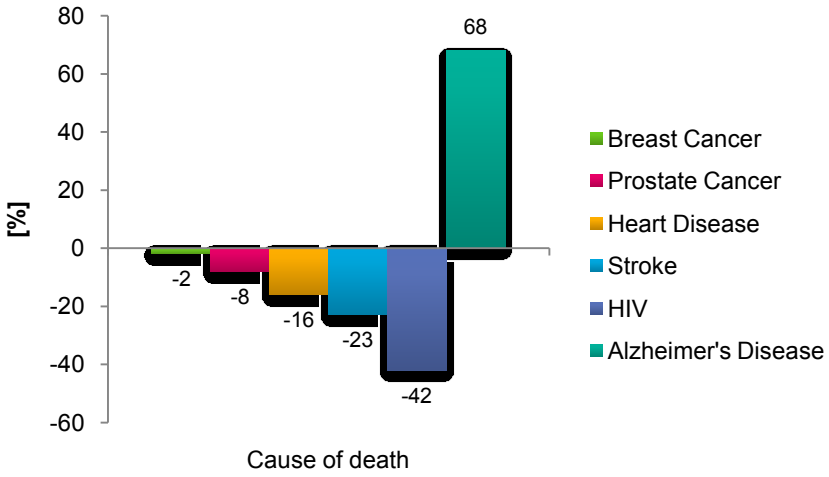

Figure 5-1 Change in number of deaths between 2000 and 2010 (taken from Alzheimer's Association 2013)

While the application of size-exclusion chromatography to the investigation of soluble amyloid β oligomers could not yet be fully realised due to the sensitive column material and time restrains, preliminary results indicated SEC coupled to mass spectrometry as a potential alternative method for the investigation of soluble oligomeric Aβ species in CPE protein samples. Using characteristic charge state distribution patterns common to monomer and oligomers detected by the mass spectrometric detector the positive identification of multiple relevant peaks corresponding to different molecular weights will be possible.

The unique extraction and phase separation properties of Triton X-114 aqueous two phase micellar systems in combination with gel electrophoresis and SEC-MS could expand the available tool set of bioanalytical and medical research laboratories. By offering an inexpensive, simple and adaptable approach to protein extraction the methods could become valuable as preliminary measures to investigate relevant marker proteins or protein complexes. The resulting data could serve to focus more extensive investigations with highly specific immunology based methods.

Further steps have to be taken to achieve the full potential of both CPE and SEC-MS of soluble amyloid β oligomers. The cloud point extraction process in itself offers multiple angles for optimisation. Two sensible possibilities were suggested by the results. First,

optimisation of incubation time (1 h at 4 °C) to prolong direct contact of the homogeneous micelle solution with the tissue sample to ideally reach phase equilibrium. Second, throughout the work it seemed as if the choice of 1 % Triton X-114 in the extraction solution had limiting effect on the extraction. Increasing the percentage during CPE may lead to improvements due to the higher concentration of micelles and volume of the detergent phase.

Next steps for SEC-MS would include a validation of the method, starting with oligomeric solutions and extending to chromatographic separations of tissue extracts. Mass spectrometric detection of amyloid β species within typical mass ranges for ion traps (max. 0 – 4000 amu) should be validated by high resolution mass detectors (FTICR or Orbitrap). The considerably higher resolutions allow the determination of actual charge states and molecular masses. A high resolution MS detector would also, if routinely implemented in SEC-MS separations of protein extract lead to significantly higher data acquisition rates and subsequently improvement of detection and mass range isolation of characteristic charge state distributions.

In comparison to ELISA assays the method could be able to detect multiple oligomer species simultaneously and eventually lead to crucial insights into the disease's mechanisms. By assessing the relative concentration levels in more accessible bodily fluids like blood and cerebrospinal fluid new and more successful treatment strategies may be developed and the diagnostic process improved to recognise the disease at earlier stages. Another notable advantage of SEC-MS analysis is the permanent form of the gained information. Data sets contain not only amyloid β relevant informations but also on every extracted protein entering the mass spectrometer and can be re-examined if new developments come to light.

Particularly in regard to the investigation of other protein-associated neurodegenerative diseases like Parkinson's or Huntington's disease CPE and mass spectrometric characterization of the extracted proteins could provide an effective, inexpensive and universal extraction approach. The ability of the method to expand the range of soluble oligomeric species extracted in comparison to the established precipitation method offers the potential to further investigate the role and interaction of known and potential biomarker proteins, independent of specific antigen-antibody reactions.

Given the fact that dementia and AD as its most frequent cause are currently the 6th leading cause of death, new pathways towards understanding the underlying biochemical causes of AD as well as potential treatments are indispensable (Alzheimer's Association 2013). Cloud point extraction providing hydrophilic and hydrophobic environments and size exclusion chromatography – mass spectrometry with a novel approach towards protein oligomer separation and detection may offer the best course towards new insights.

6. Summary

Classic approaches to the investigation of Alzheimer's disease proteins amyloid β 40 and 42 utilise specific immunology based methods. To circumvent the use of expensive assays and allow a simultaneous detection of soluble oligomer species the scope of this work was designed to examine the possibility of incorporating alternative extraction and separation techniques in analytical methods (see fig. 2-1).

- Preliminary RPLC-MS analysis of an amyloid β monomer standard solution provided essential MS data sets of Aβ42, Aβ40 and mono-oxygenated Aβ42 as basis for subsequent LC –MS method developments. Limitation of both separation mechanism and MS resolution of possible oligomeric species were observed.

- Method development of a basic SEC-MS method initially focussed on establishing compatibility between protein separation in SEC and the highly sensitive electrospray ionisation process resulting in a buffer salt free mobile phase of 80 % water and 20 % acetonitril with 0.1 % formic acid.
- Detection of Aβ required extensive optimisation of MS parameters. Manual variation of basic parameters led to minor improvements in protein detection. Software-controlled tuning of mass spectrometer settings for Aβ42 led to a nearly 700 % gain in signal intensity. Application of the developed method to CPE extracts was not yet achieved.

- CPE was successfully established as extraction method for mouse brain tissue. Based on sample quality in SDS PAGE separations a 1 % Triton X-114 extraction solution and sample precipidation/delipidation with MeOH, acetone and tri-n-butylphosphate (1:12:1) were chosen for cloud point extraction.

- Proteins in each extraction phase were characterised by RPLC-MS/MS analysis of tryptic peptides of 260 protein bands. Distributions of grand average hydro-pathicities (GRAVY indeces) in relation to extraction phase, cellular location and function were constructed.
- Phase separation behaviour reflected less on expected separation of proteins with positive (detergent phase) and negative (aq. phase) indices than the probability of proteins to be extracted into the detergent phase if it was membrane–related and fulfilled energy, transport, signalling or cell differentiation functions. Cytoplasmic proteins involved in metabolism, biosynthesis and response were predominantly found in the aqueous phase.

- Reexamination of LC-MS/MS data sets with a smaller database of proteins related to Aβ and AD led to the positive identification of several oligomeric species in both extraction phases. CPE was found to be superior to ELISA sample preparation due to the expanded range of detectable oligomers.
- A system blank and tissue samples spiked with Aβ42 monomer standard and revealed an apparent low mass cut-off of Triton X-114 micelles as well as inadvertent adsorption to matrix components.

7. References

Aagaard A., L. P., Cowieson N., Huber T., Ravasi T., Wells C.A., Flanagan J.U., Kellie S., Hume D.A., Kobe B., Martin J.L. (2005). "An inflammatory role for the mammalian carboxypeptidase inhibitor latexin relationship to cystatins and the tumor suppressor TIG1." Structure **13**: 309-317.

Adams, J. C. (2004). "Roles of fascin in cell adhesion and motility." Current Opinion in Cell Biology **16**: 590-596.

Adams, V., L. D. Griffin, et al. (1991). "Protein kinase activity of rat brain hexokinase." Biochemical and Biophysical Research Communications **177**: 1101-1106.

Aida, Y. and M. J. Pabst (1990). "Removal of endotoxin from protein solutions by phase-separation using Triton X-114." Journal of Immunological Methods **132**(2): 191-195.

Alberts, B. (2002). Molecular biology of the cell. New York, Garland Science.

Albertsson, P. A. (1956). "Chromatography and partition of cells and cell fragments." Nature **177**(4513): 771-774.

Alzheimer's-Association. (2012). "Risk Factors." Retrieved 12/4, 2012, from http://www.alz.org/alzheimers_disease_causes_risk_factors.asp.

Alzheimer's Association (2013). "Alzheimer's disease facts and figures." Alzheimers & Dementia **9**: 1-71.

Alzheimer, A. (1911). "Concerning unsual medical cases in old age." Zeitschrift Fur Die Gesamte Neurologie Und Psychiatrie **4**: 356-385.

Ausmess, N., J. R. Kuhn, et al. (2003). "The bacterial cytoskeleton: an intermediate filament-like function in cell shape." Cell **115**: 705-713.

Ballabh, P., A. Braun, et al. (2004). "The blood-brain barrier: an overview: structure, regulation and clinical implications." Neurobiology of disease **16**: 1-3.

Barker, W. C., J. S. Garavelli, et al. (1999). "The PIR-International Protein Sequence Database." Nucleic Acids Research **27**(1): 39-43.

Bennett, M. K., J. E. Garáa-Arrarás, et al. (1993). "The syntaxin family of vesicular transport receptors." Cell **74**: 863-73.

Benz, R. (1994). "Permeation of hydrophilic solutes through mitochondrial outer membranes: review on mitochondrial porins." Biochimica Et Biophysica Acta **1197**: 167-196.

Berg, J. M., J. L. Tymoczko, et al. (2003). Biochemie. Heidelberg, Spektrum Akademischer Verlag.

Berggren, K., E. Chernokalskaya, et al. (2000). "Background-free, high sensitivity staining of proteins in one- and two-dimensional sodium dodecyl sulfate-polyacrylamide gels using a luminescent ruthenium complex." Electrophoresis **21**(12): 2509-2521.

Bernstein, S. L., N. F. Dupuis, et al. (2009). "Amyloid-beta protein oligomerization and the importance of tetramers and dodecamers in the aetiology of Alzheimer's disease." Nature Chemistry **1**(4): 326-331.

Bitan, G. and D. B. Teplow (2004). "Rapid photochemical cross-linking - A new tool for studies of metastable, amyloidogenic protein assemblies." Accounts of Chemical Research **37**(6): 357-364.

Bordier, C. (1981). "Phase-separation of integral membrane-proteins in Triton X-114 solution." Journal of Biological Chemistry **256**(4): 1604-1607.

Brady, L. J., J. Valliere-Douglass, et al. (2008). "Molecular mass analysis of antibodies by on-line SEC-MS." Journal of the American Society for Mass Spectrometry **19**(4): 502-509.

Brdicka, R. and P. Nurnberg (1993). "Checking of individuality by DNA profiling." Journal of Chromatography-Biomedical Applications **618**(1-2): 167-179.

Canas, B., D. Lopez-Ferrer, et al. (2006). "Mass spectrometry technologies for proteomics." Briefings in functional genomics & proteomics **4**(4): 295-320.

Candiano, G., M. Bruschi, et al. (2004). "Blue silver: A very sensitive colloidal Coomassie G-250 staining for proteome analysis." Electrophoresis **25**: 1327-1333.

Castellanos-Serra, L., Y. Ramos, et al. (2005). "An in-gel digestion procedure that faciliates the identification of highly hydrophobic proteins by electrospray ionisation-mass spectrometry analysis." Proteomics **5**: 2729-2738.

Cech, N. B. and C. G. Enke (2001a). "Effect of affinity for droplet surfaces on the fraction of analyte molecules charged during electrospray droplet fission." Analytical Chemistry **73**(19): 4632-4639.

Cech, N. B. and C. G. Enke (2001b). "Practical implications of some recent studies in electrospray ionization fundamentals." Mass Spectrometry Reviews **20**(6): 362-387.

Choudhary, G., S. L. Wu, et al. (2003). "Multiple enzymatic digestion for enhanced sequence coverage of proteins in complex proteomic mixtures using capillary LC with ion trap MS/MS." Journal of Proteome Research **2**(1): 59-67.

Dawe, H. R., M. Adams, et al. (2009). "Nesprin-2 interacts with meckelin and mediates ciliogenesis via remodelling of the actin cytoskeleton." Journal of Cell Science **122**: 2716-2726.

Deery, M. J., E. Stimson, et al. (2001). "Size exclusion chromatography/mass spectrometry applied to the analysis of polysaccharides." Rapid Communications in Mass Spectrometry **15**(23): 2273-2283.

delaMora, J. F. (1996). "On the outcome of the coulombic fission of a charged isolated drop." Journal of Colloid and Interface Science **178**(1): 209-218.

Doherty, U. J. and H. T. McMahon (2008). "Mediation, Modulation and Consequences of Membrane-Cytoskeleton interactions." Annual Reviews of Biophysics **37**: 65-95.

Douglas, D. J., A. J. Frank, et al. (2005). "Linear ion traps in mass spectrometry." Mass Spectrometry Reviews **29**: 1-29.

Dreyer, S. and U. Kragl (2008). "Ionic liquids for aqueous two-phase extraction and stabilization of enzymes." Biotechnology and Bioengineering **99**(6): 1416-1424.

Ellis, R. J. (2006). "Molecular chaperones: assisting assembly in addition to folding." Trends in Biochemical Sciences **31**: 395-401.

English, J. A., B. Manadas, et al. (2012). "Partitioning the Proteome: Phase Separation for Targeted Analysis of Membrane Proteins in Human Post-Mortem Brain." Plos One **7**(6): 9.

Espada, A. and A. Rivera-Sagredo (2003). "Ammonium hydrogencarbonate, an excellent buffer for the analysis of basic drugs by liquid chromatography-mass spectrometry at high pH." Journal of Chromatography A **987**(1-2): 211-220.

Fazekas, S. D. S., R. G. Webster, et al. (1963). "2 new staining procedures for quantitative estimation of proteins on electrphoretic strips." Biochimica Et Biophysica Acta **71**(2): 377-&.

Feick, R. G. and J. A. Shiozawa (1990). "A high-yield method for the isolation of hydrophobic proteins and peptides from polyacrylamide gels for protein sequencing." Analytical Biochemistry **187**(2): 205-211.

Fenn, J. B., M. Mann, et al. (1989). "Electrospray ionisation for mass-spectrometry of large biomolecules." Science **246**(4926): 64-71.

Freire, M. G., C. L. S. Louros, et al. (2011). "Aqueous biphasic systems composed of a water-stable ionic liquid + carbohydrates and their application." Green Chemistry **13**: 1536-1545.

Fritz, R., W. Ruth, et al. (2009). "Assessment of acetone as an alternative to acetonitrile in peptide analysis by liquid chromatography/mass spectrometry." *Rapid Communication in Mass Spectrometry* **23**: 2139-2145.

Frixione, E. (2000). "Recurring views on the structure and function of the cytoskeleton: a 300-year epic." Cell motility and the cytoskeleton **46**: 73-94.

Gekko, K., E. Ohmae, et al. (1998). "Acetonitrile-protein interactions: amino acid solubility and preferential solvation." Biochimica Et Biophysica Acta **1387**: 195-205.

Gobom, J., E. Mirgorodskaya, et al. (1999). "Use of vapor-phase acid hydrolysis for mass spectrometric peptide mapping and protein identification." Analytical Chemistry **71**(5): 919-927.

Goedert, M. and B. Ghetti (2007). "Alois Alzheimer: His life and times." Brain Pathology **17**(1): 57-62.

Goedert, M. and M. G. Spillantini (2006). "A century of Alzheimer's disease." Science **314**(5800): 777-781.

Gordon, N. F., C. M. V. Moore, et al. (1990). "An overview of contineous-purification processes." Biotechnology Advances **8**(4): 741-762.

Granvogl, B., P. Gruber, et al. (2007). "Standardisation of rapid in-gel digestion by mass spectrometry." Proteomics **7**(5): 642-654.

Granvogl, B., M. Plöscher, et al. (2007). "Sample preparation by in-gel digestion for mass spectrometry-based proteomics." Analytical and Bioanalytical Chemistry **389**: 991-1002.

Grummit, I. (1999). "Regulation of mammalian ribosomal gene transcription by RNA polymerase I." Progress in Nucleic Acid Research and Molecular Biology **62**: 109-154.

Grundke-Iqbal, I., K. Iqbal, et al. (1986). "Microtubule-associated protein-tau - a component of Alzheimer paired helical filaments." Journal of Biological Chemistry **261**(13): 6084-6089.

Haass, C. and D. J. Selkoe (2007). "Soluble protein oligomers in neurodegeneration: lessons from the Alzheimer's amyloid beta-peptide." Nature Reviews Molecular Cell Biology **8**(2): 101-112.

Hardy, J. and D. J. Selkoe (2002). "Medicine - The amyloid hypothesis of Alzheimer's disease: Progress and problems on the road to therapeutics." Science **297**(5580): 353-356.

Hardy, J. A. and G. A. Higgins (1992). "Alzheimer-disease - the amyloid cascade hypothesis." Science **256**(5054): 184-185.

Harris, E. L. V. and S. Angal (1995). Protein purification application: a practical approach. Oxford, IRL Press.

Havlis, J., H. Thomas, et al. (2003). "Fast-response proteomics by accelerated in-gel digestion of proteins." Analytical Chemistry **75**(6): 1300-1306.

Heukeshoven, J. and R. Dernick (1985). "Simplified method for silver staining of proteins in polyacrylamide gels and the mechanism of silver staining." Electrophoresis **6**(3): 103-112.

Hinze, W. L. and E. Pramauro (1993). "A critical-review of surfactant-mediated phase separations (cloud-point extractions) - theory and applications." Critical Reviews in Analytical Chemistry **24**(2): 133-177.

Hollemeyer, K., E. Heinzle, et al. (2002). "Identification of oxidized methionine residues in peptides containing two methionine residues by derivatization and matrix-assisted laser desorption/ionization mass spectrometry." Proteomics **2**(11): 1524-1531.

Hoogenboom, B. W., K. Suda, et al. (2007). "The supramolecular assemblies of voltage-dependent anion channels in the native membrane." Journal of Molecular Biology **370**: 246-255.

Huang, Y. Y., G. C. Tseng, et al. (2008). "A data-mining scheme for identifying peptide structural motifs responsible for different MS/MS fragmentation intensity patterns." Journal of Proteome Research **7**(1): 70-79.

Hughes, J. R. (1958). "Post-tenatic potentiation." Physiological Reviews **38**: 91-113.

Hunt, D. F. (1986). "Protein sequencing by tandem mass spectrometry." Proc. Natl. Acad. Sci. USA **83**: 6233-6237.

Iavarone, A. T., J. C. Jurchen, et al. (2001). "Supercharged protein and peptide ions formed by electrospray ionisation." Analytical Chemistry **73**: 1455-1460.

Iida, J. and T. Murata (1990). "Formic-acid ammonium formate buffer system for thermospray liquid-chromatography mass-spectrometry." Analytical Sciences **6**(2): 269-272.

James, P., M. Quadroni, et al. (1993). "Protein Identification by Mass Profile Fingerprinting." Biochemical and Biophysical Research Communications **195**(1): 58-64.

Janz, R., T. C. Suedhof, et al. (1999). "Essential roles in synaptic plasticity for synaptogyrin I and synaptophysin I." Neuron **24**: 687-700.

Johnson, R. S., S. A. Martin, et al. (1988). "Collision-induced fragmentation of (M+H)+ions of peptides - side-chain specific sequence ions." International Journal of Mass Spectrometry and Ion Processes **86**: 137-154.

Jozala, A. F., A. M. Lopes, et al. (2008). "Liquid-liquid extraction of commercial and biosynthesized nisin by aqueous two-phase micellar systems." Enzyme and Microbial Technology **42**(2): 107-112.

Juan, H. F., S. C. Chang, et al. (2005). "A new application of microwave technology to proteomics." Proteomics **5**(4): 840-842.

Klein, W. L., G. A. Krafft, et al. (2001). "Targeting small A beta oligomers: the solution to an Alzheimer's disease conundrum?" Trends in Neurosciences **24**(4): 219-224.

Kyte, J. and R. F. Doolittle (1982). "A simple method for displaying the hydropathic character of a protein." Journal of Molecular Biology **157**: 105-132.

Lehninger, A. L., D. L. Nelson, et al. (2000). Principles of biochemistry. New York, W.H. Freedom.

Lesne, S., M. T. Koh, et al. (2006). "A specific amyloid-beta protein assembly in the brain impairs memory." Nature **440**(7082): 352-357.

Lewis, V., S. A. Green, et al. (1985). "Glycoproteins of the lysosomal membrane." Journal of Cell Biology **100**(6): 1839-1847.

Liu, C. L., Y. J. Nikas, et al. (1996). "Novel bioseparations using two-phase aqueous micellar systems." Biotechnology and Bioengineering **52**(2): 185-192.

Liu, S. G., R. Tobias, et al. (1997). "Removal of endotoxin from recombinant protein preparations." Clinical Biochemistry **30**(6): 455-463.

Liu, W. Y. and R. Guo (2008). "Effects of Triton X-100 nanoaggregates on dimerization and antioxidant activity of morin." Molecular Pharmaceutics **5**(4): 588-597.

Lopes, A. S., J. S. Garcia, et al. (2007). "Cloud point extraction applied to casein proteins of cow milk and their identification by mass spectrometry." Analytica Chimica Acta **590**(2): 166-172.

Lopez-Ferrer, D., J. L. Capelo, et al. (2005). "Ultra fast trypsin digestion of proteins by high intensity focused ultrasound." Journal of Proteome Research **4**(5): 1569-1574.

Mandal, A. B., B. U. Nair, et al. (1988). "Determination of the Critical Micelle Concentration of Surfactants and the Partition-Coefficient of an Electrochemical Probe by Using Cyclic Voltammetry." Langmuir **4**(3): 736-739.

March, R. E. (1997). "An introduction to quadrupole ion trap mass spectrometry." Journal of Mass Spectrometry **32**(4): 351-369.

Mast, S., L. F. Peng, et al. (2010). "Proteomic analysis of membrane preparations from developing Pinus radiata compression wood." Tree Physiology **30**(11): 1456-1468.

Masters, C. L., G. Simms, et al. (1985). "Amyloid plaques core protein in alzheimer-disease and down syndrome." Proceedings of the National Academy of Sciences of the United States of America **82**(12): 4245-4249.

Mastro, R. and M. Hall (1999). "Protein delipidation and precipitation by tri-n-butyl phosphate, acetone, and methanol treatment for isoelectric focusing and two-dimensional gel electrophoresis." Analytical Biochemistry **273**(2): 313-315.

Mathieu, E. (1868). "Memoire sur le mouvement vibratoire d'une membrane de forme elliptique." Journal de mathématiques pures et appliquées **13**: 137-203.

Maucuer A., C. J. H., Sobel A. (1995). "Stathmin interaction with a putative kinase and coiled-coil-forming protein domains." Proceedings of the National Academy of Sciences of the United States of America **92**: 3100-3104.

Maurer, K. and S. Hoyer (2006). "Alois Alzheimer revisited: differences in origin of the disease carrying his name." Journal of Neural Transmission **113**(11): 1645-1658.

Mazzola, P. G., A. M. Lopes, et al. (2008). "Liquid-liquid extraction of biomolecules: an overview and update of the main techniques." Journal of Chemical Technology and Biotechnology **83**(2): 143-157.

McIlwain, H. and H. S. Bachelard (1985). Biochemistry and the Central Nervous System. Edinburgh, Churchill Livingstone.

Merril, C. R. and M. E. Pratt (1986). "A silver stain for the rapid quantitative detection of proteins or nucleic-acids on membranes of thin-layer plates." Analytical Biochemistry **156**(1): 96-110.

Michalski, W. P. and B. J. Shiell (1999). "Strategies for analysis of electrophoretically separated proteins and peptides." Analytica Chimica Acta **383**(1-2): 27-46.

Moore, B. D., V. Rangachari, et al. (2009). "Biophysical Analyses of Synthetic Amyloid-beta(1-42) Aggregates before and after Covalent Cross-Linking. Implications for Deducing the Structure of Endogenous Amyloid-beta Oligomers." Biochemistry **48**(49): 11796-11806.

Nesatyy, V. J., A. Dacanay, et al. (2002). "Microwave-assisted protein staining: mass spectrometry compatible methods for rapid protein visualisation." Rapid Communications in Mass Spectrometry **16**(4): 272-280.

Neuhoff, V., N. Arold, et al. (1988). "Improved staining of proteins in polyacrylamide gels including isoelectric-focusing gels with clear background at nanogram sensitivity using Coomassie Brilliant Blue G-250 and R-250." Electrophoresis **9**(6): 255-262.

Neville, D. M. (1971). "Molecular weight determination of protein-dodecyl sulfate complexes by gel electrophoresis in a discontinous buffer system." Journal of Biological Chemistry **246**(20): 6328-&.

Nylander, I., K. Tanno, et al. (1995). "Processing of prodynorphin-derived peptides in stratial extracts - indentification by electrospray-ionisation mass-spectrometry linked to size-exclusion chromatography." Life Sciences **57**(2): 123-129.

O'Farrell, P. H. (1975). "High-resolution 2-dimensional electrophoresis of proteins." Journal of Biological Chemistry **250**(10): 4007-4021.

Oppermann, S., F. Stein, et al. (2011). "Ionic liquids for two-phase systems and their application for purification, extraction and biocatalysis." Applied Microbiology and Biotechnology **89**(3): 493-499.

Paizs, B. and S. Suhai (2004). "Towards understanding the tandem mass spectra of protonated oligopeptides. 1: Mechanism of amide bond cleavage." Journal of the American Society for Mass Spectrometry **15**(1): 103-113.

Paizs, B. and S. Suhai (2005). "Fragmentation pathways of protonated peptides." Mass Spectrometry Reviews **24**(4): 508-548.

Pappin, D. J. C., P. Hojrup, et al. (1993). "Rapid identification of proteins by peptide-mass fingerprinting." Current Biology **3**(6): 327-332.

Patton, W. F. (2002). "Detection technologies in proteome analysis." Journal of Chromatography B-Analytical Technologies in the Biomedical and Life Sciences **771**(1-2): 3-31.

Perkins, D. N., D. J. C. Pappin, et al. (1999). "Probability-based protein identification by searching sequence databases using mass spectrometry data." Electrophoresis **20**(18): 3551-3567.

Porath, J. and P. Flodin (1959). "Gel Filtration - Method for Desalting and Group Separation." Nature **183**(4676): 1657-1659.

Quach, T. T. T., N. Li, et al. (2003). "Development and applications of in-gel CNBr/tryptic digestion combined with mass spectrometry for the analysis of membrane proteins." Journal of Proteome Research **2**(5): 543-552.

Quina, F. H. and W. L. Hinze (1999). "Surfactant-mediated cloud point extractions: An environmentally benign alternative separation approach." Industrial & Engineering Chemistry Research **38**(11): 4150-4168.

Radde, R., T. Bolmont, et al. (2006). "A beta 42-driven cerebral amyloidosis in transgenic mice reveals early and robust pathology." European Molecular Biology Organization Reports **7**(9): 940-946.

Reinders, J., U. Lewandrowski, et al. (2004). "Challenges in mass spectrometry-based proteomics." Proteomics **4**(12): 3686-3703.

Reynolds, J. A. and C. Tanford (1970). "The gross conformation of protein-sodium dodecyl sulfate complexes." The Journal of Biological Chemistry **245**(19): 5161-5165.

Rhee, S., H. Chae, et al. (2005). "Peroxiredoxins: a historical overview and speculative preview of novel mechanisms and emerging concepts in cell signalling." Free Radic. Biol. Med. **38**: 1543-52.

Richert, S., S. Luche, et al. (2004). "About the mechanism of interference of silver staining with peptide mass spectrometry." Proteomics **4**(4): 909-916.

Roepstorff, P. and J. Fohlman (1984). "Proposal for a common nomenclature for seuqence ions in mass-spectra of peptides." Biomedical Mass Spectrometry **11**(11): 601-601.

Rosenfeld, J., J. Capdevielle, et al. (1992). "In-gel digestion of proteins for internal sequence-analysis of 1-dimensional or 2-dimensional gel-electrophoresis." Analytical Biochemistry **203**(1): 173-179.

Rosenfeld, J., S. Cook, et al. (1997). "Expression of superoxide dismutase following axotomy." Experimental Neurology **147**: 37-47.

Ruiz-Vela, A., G. Gonzalez de Buitrago, et al. (2002). "Nuclear Apaf-1 and cytochrome c redistribution following stress-induced apoptosis." FEBS Letters **517**: 133-138.

Sarker, A. H., S. Ikeda, et al. (1998). "Cloning and characterization of a mouse homologue (mNthl1) of Escherichia coli endonuclease III." Journal of Molecular Biology **282**: 761-774.

Schagger, H., W. A. Cramer, et al. (1994). "Analysis of molecular masses and oligomeric states of protein complexes by Blue Native electrophoresis and isolation of membrane-protein complexes by 2-dimensional native electrophoresis." Analytical Biochemistry **217**(2): 220-230.

Scheler, C., S. Lamer, et al. (1998). "Peptide mass fingerprint sequence coverage from differently stained proteins on two-dimensional electrophoresis patterns by matrix assisted laser desorption/ionization mass spectrometry (MALDI-MS)." Electrophoresis **19**(6): 918-927.

Schmidt, A. C., B. Fahlbusch, et al. (2009). "Size exclusion chromatography coupled to electrospray ionization mass spectrometry for analysis and quantitative characterization of arsenic interactions with peptides and proteins." Journal of Mass Spectrometry **44**(6): 898-910.

Schnier, P. D., D. S. Gross, et al. (1995). "On the maximum charge state and proton transfer reactivity of peptide and protein ions formed by electrospray ionisation." Journal of the American Society for Mass Spectrometry **6**: 1086-1097.

Schwartz, J. C., M. W. Senko, et al. (2002). "A two-dimensional quadrupole ion trap mass spectrometer." Journal of the American Society for Mass Spectrometry **13**(6): 659-669.

Shapiro, A. L., E. Vinuela, et al. (1967). "Molecular weight estimation of polypeptide chains by electrophoresis in SDS-polyacrylamide gels." Biochemical and Biophysical Research Communications **28**(5): 815-&.

Shen, M. L., L. M. Benson, et al. (2001). "Effect of enzyme inhibitors on protein quaternary structure determined by on-line size exclusion chromatography-microelectrospray ionization mass spectrometry." Journal of the American Society for Mass Spectrometry **12**(1): 97-104.

Shevchenko, G., M. O. D. Sjodin, et al. (2010). "Cloud-Point Extraction and Delipidation of Porcine Brain Proteins in Combination with Bottom-Up Mass Spectrometry Approaches for Proteome Analysis." Journal of Proteome Research **9**(8): 3903-3911.

Shigeri, Y., R. P. Seal, et al. (2004). "Molecular pharmacology of glutamate transporters." Nature **383**: 634-637.

Silva, M. E. and T. T. Franco (2000). "Liquid-liquid extraction of biomolecules in downstream processing - A review paper." Brazilian Journal of Chemical Engineering **17**(1): 1-17.

Singh, T. D., S. Y. Park, et al. (2010). "MEGF10 functions as a receptor for the uptake of amyloid-beta." FEBS Letters **584**: 3936-3942.

Sun, W., S. J. Gao, et al. (2006). "Microwave-assisted protein preparation and enzymatic digestion in proteomics." Molecular & Cellular Proteomics **5**(4): 769-776.

Tabb, D. L., L. L. Smith, et al. (2003). "Statistical characterization of ion trap tandem mass spectra from doubly charged tryptic peptides." Analytical Chemistry **75**(5): 1155-1163.

Tal, M., A. Silberstein, et al. (1985). "Why does Coomassie Brilliant Blue-R interact differently with different proteins -a partial answer." Journal of Biological Chemistry **260**(18): 9976-9980.

Taylor, J. P., J. Hardy, et al. (2002). "Biomedicine - Toxic proteins in neurodegenerative disease." Science **296**(5575): 1991-1995.

Thermo Scientific (2008). "BioWorks™ software training."
Thermo Scientific (2009). "Protein stability and storage." Tech Tip **#43**: 1-3.
Townsend, M., G. M. Shankar, et al. (2006). "Effects of secreted oligomers of amyloid beta-protein on hippocampal synaptic plasticity: a potent role for trimers." Journal of Physiology-London **572**(2): 477-492.
Trepel, M. (1999). Neuroanatomie - Struktur und Funktion. München, Urban & Fischer.
Tuinman, A. A. and G. R. Pettit (1990). "Analysis of the amino-acid-sequence of peptides by mass-spectrometry - an ion notation proposal." International Journal of Peptide and Protein Research **36**(4): 331-334.
Valko, M., D. Leibfritz, et al. (2007). "Free radicals and antioxidants in normal physiological functions and human disease." International Journal of Biochemistry and Cell Biology **39**: 44-84.
Venter, J. C., M. D. Adams, et al. (2001). "The sequence of the human genome." Science **291**(5507): 1304-+.
Vesper, H. W., L. C. Mi, et al. (2005). "Assessment of microwave-assisted enzymatic digestion by measuring glycated hemoglobin A1c by mass spectrometry." Rapid Communications in Mass Spectrometry **19**(19): 2865-2870.
Walsh, D. M., A. Lomakin, et al. (1997). "Amyloid beta-protein fibrillogenesis - Detection of a protofibrillar intermediate." Journal of Biological Chemistry **272**(35): 22364-22372.
Watanabe, H. and H. Tanaka (1978). "Nonionic surfactant as a new solvent for liquid-liquid - extraction of zinc(II) with 1-(2-pyridazolo)-2-naphtol." Talanta **25**(10): 585-589.
Weber, K. and M. Osborn (1969). "Reliability of molecular weight determinations by dodecyl sulfate-polyacrylamide gel electrophoresis." Journal of Biological Chemistry **244**(16): 4406-&.
Weckstrom, K. (1985). "The effect of salt on the critical-behaviour of non-ionic micellar solutions." Chemical Physics Letters **119**(6): 503-506.
Wessel, D. and U. I. Flügge (1984). "A method for the quantitative recovery of proteins in dilute solutions in the presence of detergents and lipids." Analytical Biochemistry **138**: 141-143.
Wetterhall, M., G. Shevchenko, et al. (2011). "Analysis of membrane and hydrophilic proteins simultaneously derived from the mouse brain using cloud-point extraction." Analytical and Bioanalytical Chemistry **400**(9): 2827-2836.
Willis, I. M. (1993). "RNA polymerase III. Genes, factors and transcriptional specificity." European Journal of Biochemistry **212**: 1-11.
Winkler, R. (2010). "ESIprot: a universal tool for charge state determination and molecular weight calculation of proteins from electrospray ionization mass spectrometry data." Rapid Communications in Mass Spectrometry **24**(3): 285-294.
Wu, C. H., R. Apweiler, et al. (2006). "The Universal Protein Resource (UniProt): an expanding universe of protein information." Nucleic Acids Research **34**: D187-D191.
Yates, J. R. (2004). "Mass spectral analysis in proteomics." Annual Review of Biophysics and Biomolecular Structure **33**: 297-316.
Zhang, T. F. and L. P. Hager (1987). "A single-step large-scale purification of pyruvate oxidase." Archives of Biochemistry and Biophysics **257**(2): 485-487.
Zhao, J., A. Iida, et al. (2008). "M6a is expressed in the murine neural retina and regulates neurite extension." Molecular Vision **14**: 1623-1630.

A. Appendix

A.1 Materials and methods

A.1.1 Materials

Table A-1 List of used chemicals

Substance	Supplier
NuPAGE® Novex© 4-12 % Bis-Tris (1 mm x 10/15 well) 10 % Bis-Tris (1 mm x 10/15 well)	Invitrogen (Germany)
NuPAGE® LDS sample buffer (4X)	Invitrogen (Germany)
MES-SDS Running buffer (20X)	Invitrogen (Germany)
NuPAGE® Reducing Agent (10X)	Invitrogen (Germany)
NuPAGE® Antioxidant	Invitrogen (Germany)
Novex® SeeBlue Prestained tandard	Invitrogen (Germany)
Novex® Sharp Unstained protein standard	Invitrogen (Germany)
SimplyBlue™ SafeStain	Invitrogen (Germany)
Pierce 660nm Assay Kit Reagent BSA; 7x3.5 mL 125-2000 µg/mL prediluted in 0.9% NaCl, 0.05% NaN_3	Thermo/Pierce
Triton® X114	Sigma
Proteomics Grade Trypsin MRFA	Sigma
Insulin β chain (bovine)	Sigma
Lysozyme from hen egg white	Sigma
Pepsin A from hog stomach	Sigma
Myoglobin	Sigma
Tributylphosphate	Sigma
Chloroform	
Methanol ChromaSolv	Sigma
Acetone Ultra Resi-analysed	J.T.Baker
Acetonitril HPLC analysed	J.T.Baker
Acetonitril with 0.1% formic acid LCMS ChromaSolv	Sigma
Water with 0.1 % formic acid LCMS ChromaSolv	Sigma
Ammoniumbicarbonate	
Ammoniumformate 99.995%	Aldrich
Ammoniumacetate HPLC analysed	J.T. Baker
Formic acid	
Sodium chloride	
Potassium chloride	
Sodium hydrogenphosphate · 2 H_2O	
Potassium dihydrogenphosphate	
Tris pro analysi	Merck
Protease inhibitor cocktail (DZNE)	

Table A-2 List of used laboratory equipment

Equipment	Supplier
LCQ Advantage	Finnigan MAT
LCQ Advantage MS detector	
TSP Autosampler	
TSP P4000 pump	
Column oven	
LTQ (built 2005)	Thermo
Finnigan LTQ MS detector	
Autosampler Plus – Finnigan Surveyor	
MS Pump Plus – Finnigan Surveyor	
PDA Plus – Finnigan Surveyor	
BioBasic C18 300 Å column (2.1 x 150 mm, 5 µm)	Thermo
BioSEC-3 150 Å column (4.6 x 300 mm, 3 µm)	Agilent
Photometer Specord2000	Analytik Jena
Vertical Mini-Gel System, Single Unit	Sigma
ZOOM Dual Power Supply	Invitrogen
Mars Xpress microwave	CEM
Centrifuge 5810 R	Eppendorf
Centrifuge Mikro 22R	Hettich
Sonic bath Sonorex TK52	Bandelin
Mini-Vap Evaporator/Concentrator	Supelco
Reacti-Therm Dry Block	Thermo
Thermomixer Comfort PHMT Grant-bio	Eppendorf
Vortex VWR VV3 S40	VWR
Pipettes Research	Eppendorf
0.5 – 10 µL, 10 – 100 µL, 100 – 1000 µL, 100 – 5000 µL	
Geloader epT.I.P.S 20 µL	Eppendorf
Gel knife	Invitrogen
Ceramic scalpel	
Protein LoBind tubes 1.5 mL, 2 mL	Eppendorf
Siliconized glass vials 1.8 mL	
Siliconized glass inserts µL	
Disposable cuvettes	

Table A-3 Amyloid β related samples provided by working group of Prof. Jens Pahnke

Amyloid β related samples	**Source**
Synthetic Aβ1-42 standard, 1000 ng/mL	hAmyloid β42 Brain ELISA Kit, The Genetics Company
Protein extracts from mouse brain tissue, prepared for ELISA	Working group of Prof. Dr. Dr. Jens Pahnke
Supernatant: 1.74 mg/mL protein content, 470.76 ng Aβ42 per mg protein	
Precipitate: 1.92 mg/mL protein content, 1264.7 ng Aβ42 per mg protein	
Synthesised Aβ1-42 standard, > 95 %, 2 mg/mL HFIP (1 mL)	Genscript
Mouse brain tissue samples (3 mice)	Working group of Prof. Dr. Dr. Jens Pahnke, preparated by Dr. Markus Krohn
Transgenic mouse model (Radde, Bolmont et al. 2006), APPPS1 (mutated amyloid precursor protein KM670/671NL and mutated presinilin-1 L166P)	
kept in specific pathogen free environment, 12 h day/night cycle, 21 °C	
age: approx. 6.5 months, gender: male, healthy	

A.1.2 Reversed phase chromatography – MS

A.1.2.1 Sample dilution

To investigate concentration ranges detectable with various separation techniques a dilution scheme was developed to create diluted protein samples for proteins as well as a series of amyloid β 42 monomer standard solutions.

Proteins used as references in reversed-phase and size exclusion experiments were diluted from a 1 mg/mL solution in pure water. The amyloid β 42 standard provided by the working group of Prof. Dr. Pahnke was a 1 mg/mL solution in hexa-fluoroisopropanol to preserve the monomeric form and prevent undesired oligomerisation due to the high concentration. The solvent was evaporated at room temperature to leave a film of Aβ42 monomers in the reaction tube. It was then resolvated by adding 500 µL DMSO and the 2 mg/mL Aβ42 monomer solution was split into five aliquots to be stored at -20 °C. The dilution procedure and resulting sample concentration are summarised in table A-4 below.

Table A-4 Dilution procedure and sample concentrations

level	dilution	concentration [protein]	concentration [Aβ42]
Stock	-	1 mg/mL	2 mg/mL
A	50 µL stock + 50 µL H_2O	0.5 mg/mL	1 mg/mL
B	10 µL A + 90 µL H_2O	0.05 mg/mL	0.1 mg/mL
C	10 µL B + 90 µL H_2O	5 µg/mL	10 µg/mL
D	10 µL C + 90 µL H_2O	0.5 µg/mL	1 µg/mL
E	10 µL D + 90 µL H_2O	0.05 µg/mL	0.1 µg/mL

A.1.2.2 Basic RP HPLC-MS instrument method

Apart from the analysis of tryptic digests described elsewhere (see chapter A.1.5.5.) reversed-phase chromatography was used to perform preliminary examinations of amyloid β 42 samples. The following tables display the initial HPLC and MS detector settings for a data dependent analysis of a sample using gradient elution with a flow rate of 150 µL/min.

Table A-5 Mobile phase composition I

t [min]	H_2O + 0.1 % FAC [%]	acetone [%]
0	95	5
10	95	5
50	20	80
55	20	80
60	95	5
70	95	5

Table A-6 HPLC parameter settings I

parameter	setting
needle height	4 mm
syringe speed	2.0 µL/min
flush volume	4000 µL
source	bottle
needle wash	4000 µL
flush speed	250 µL/s
injection method	Partial Loop
Injection volume	5 µL
tray temperature	20 °C
oven temperature	25 °C

Initial chromatographic separation of amyloid β related samples was detected using a data dependent Top4 method. Parameters defined in table A-7 determine the selection of the four most intensive mass signals in a FullScan for further MS/MS analysis.

Table A-7 MS detection parameter settings data dependent method I (LTQ)

parameter	setting
ionisation	ESI
modus	positive
run time	70 min
tune method	tune524_06.10.2009
capillary voltage	3 kV
capillary temperature	275 °C
scan events	3
scan event 1	FullScan
mass range	300 – 2000 m/z
scan event 2	ZoomScan
scan event 3	data dependent MS^2

Table A-8 Data dependent MS^2 settings I

data dependent parameter	setting
dependent reject masses	low 1.5 amu/ high 3.5 amu
Zoom mass range width	low 5.0 amu/ high 5.0 amu
MS^2 settings	
Default charge state	+2
Charge state screening	enabled
Manual reject masses	339.6; 663.47; 685.57; 741.33; 943.94; 1347.28

A.1.2.3 FullScan detection with varying column temperatures

To investigate the temperature dependent retention of Aβ42 monomer on a BioBasic C18 column, a simplified FullScan detection method was developed. Now containing only one scan event the instrument methods were further modified to include varying column oven temperatures and a reduced sample volume of 3 µL (table A-9).

Table A-9 Modified parameter settings. FullScan instrument methods with varying column temperatures

modified parameter	setting
Sample volume	3 µL
Tray temperature	15 °C
Oven temperature	25 °C; 40 °C; 70 °C
Scan events	2
Scan event 1	FullScan (positive mode)
Mass range	300 – 2000 m/z
Scan event 2	FullScan (negative mode)
Mass range	300 – 2000 m/z

A.1.2.4 Time controlled UltraZoom scan analysis of Aβ42

Based on chromatograms recorded with the FullScan methods previously described the 25 °C column temperature method was modified to include high resolution UltraZoom scans of the most prominent m/z signal observed for the Aβ42 monomer standard. The higher resolution was applied in an attempt to discern possible Aβ42 species corresponding to the two peaks observed in the chromatograms. HPLC and basic mass spectrometer parameter settings were identical to the previous methods, the time frame dependent scan events are summarised in table A-10.

Table A-10 Time controlled UltraZoom scan method (LTQ)

parameter [time frame]	setting
scan events	5
scan event 1 [0 – 31 min]	FullScan (+)
scan event 2 [31 – 34 min; Peak 1]	UltraZoom (+)
center mass	903.8 m/z
mass width	5.0 m/z
scan event 3 [34 – 59 min]	FullScan (+)
scan event 4 [59 – 62 min]	UltraZoom (+)
center mass	903.8 m/z
mass width	5.0 m/z

A.1.3 Size exclusion chromatography – MS

A.1.3.1 Mobile phase composition

For size exclusion chromatography – MS experiments, two mobile phase systems were explored. The first system contained a volatile buffer salt and the second was based on the available LCMS solvents H_2O and ACN with 0.1 % formic acid. Ammonium formate was chosen as buffer salt for the buffered system and was prepared offline by dissolving 315.5 mg in 500 mL solvent to achieve a final concentration of 10 mM. Several buffered mobile phases with varying ACN content were tested: 5 % (25 mL ACN), 10 % (50 mL ACN) and 20 % (100 mL ACN). Manually prepared mobile phases were degassed by sonification for 3 min to prevent damage to the column material by air bubbles.

A.1.3.2 Determination of optimal flow rate

The optimal separation performance range for the BioSEC-3 column (150 Å, 4.6 x 300 mm) used was given in pressure units (137 bar) rather than flow rate. To determine the corresponding flow rate for the used LCQ LC-MS system and the 10 mM ammonium formate, 20 % ACN mobile phase the flow rate was increased in 0.05 mL/min increments over the range of 0.1 to 0.4 mL/min and resulting pressures observed.

A.1.3.3 Basic SEC-MS instrument method (LCQ)

Size exclusion chromatography requires isocratic elution. Buffered mobile phases replaced solvent C (H_2O + 0.1 % FAC) and provided 100 % of the mobile phase over the run time of 30 min at a flow rate of 0.27 mL/min. Instrument parameter settings are summarised in table 7-11. The basic HPLC parameter settings like needle height and flush volume were adopted from the LTQ methods (see table A-6).

Table A-11 SEC-MS parameter settings

parameter	**setting**
injection method	FullLoop
injection volume	5 µL
column/tray temperature	room temperature (~25°C)
run time	30 min
segments	1
scan events	2
scan event 1	FullScan (+)
Mass range	200 – 2000 m/z
scan event 2	FullScan (-)
Mass range	200 – 2000 m/z
tune method	tune1422_06.10.2009

A brief deviation from the basic parameters was expressed in the instrument method defining an alternative mobile phase to the 80/20 H_2O/ACN with 0.1 % FAC. The new mobile phase composition was set as 70 % H_2O with 0.1 % FAC and 30 % ACN with 0.1 % FAC.

A.1.3.4 Manual optimisation of ESI parameters (LCQ)

Three parameter settings were changed to manually create tune methods regulating the electrospray ionisation process. To increase ionisation efficiency and accommodate the high water content (mobile phase 80 % H_2O, 20 % ACN with 0.1 % FAC) and flow rate, gas flow rates of sheath and auxiliary gas as well as capillary temperature were adjusted using a piece of capillary instead of the analytical column. The general tune method "tune524_06.10.2009" was modified from a capillary temp. of 275 °C, sheath gas flow rate of 30 units and auxiliary flow rate of 5 units to create a method with 275 °C, 40 units and 20 units, respectively (method 2). Another method kept the higher flow rates (40 and 20 units) and implemented a higher capillary temperature of 300 °C (method 3).

The modified tune methods were used in FullScan instrument methods identical to the method described in chapter A.1.3.3 with the exception of acquisation time decreased to 10 min and alternative tune methods. The effect on the ionisation of proteins in the buffered mobile phase (10 mM ammonium formate, 20 % ACN) was tested by injecting haemoglobin and BSA solutions and assessment of MS data quality.

A.1.3.5 Modified SEC-MS method (LCQ)

Conclusions drawn from preliminary protein separations with the buffered mobile phase as well as optimisation efforts for the ionisation process led to a modification of the basic SEC-MS instrument method. Parameter settings remained mainly unchanged, but the tune method was exchanged for method 3 (300 °C, 40 units sheath gas, 20 units auxiliary gas) and the mobile phase was switched from 10 mM ammonium formate in 20 % ACN to an inline mixed isocratic 80 % H_2O with 0.1 % formic acid and 20 % ACN with 0.1 % formic acid. The method was applied to dilution series (see chapter A.1.2.1) of myoglobin, lysozyme and an amyloid β 42 standard.

A.1.3.6 Analyte specific tune methods (LCQ)

Using the direct injection of Aβ42 solution (infusion) into the mobile phase shortly before the ESI capillary offers the possibility of a software controlled optimisation of a tune method based on a chosen m/z signal of amyloid β 42 under experiment conditions (flow rate 0.27 mL/min). For the injection 20 µL of 0.1 mg/mL Aβ42 standard were diluted with 80 µL mobile phase (80/20 H_2O/ACN with 0.1 % FAC) to a final concentration of 0.02 mg/mL. The syringe (500 µL) was flushed thrice with the mobile phase, filled with 100 µL Aβ42 solution, fastened into the syringe pump attachment of the MS detector, connected to the regular mobile phase towards the ESI capillary via a fused silica capillary and a T-piece adapter.

The optimised tune method 3 was opened in the Tune Plus programme provided by the manufacturer for the direct control of MS detection parameters. With the tool “define scan box” center masses with a width of 2.0 m/z were selected in positive ionisation mode (three microscans, max. injection time 200 ms, centroid profile). After starting the forced injection of amyloid β 42 into the ESI source, a center mass was entered and the software controlled optimisation of ionisation and MS detection parameters was initiated. The improved parameter settings for 1505.5 m/z and 903.8 m/z were saved as new tune files for the application in amyloid β 42 specific instrument methods (table A-12).

Table A-12 Adapted method parameter for Aβ42 specific FullScan methods (LCQ)

method	**parameter**	**setting**
“Abeta1505”	tune file	Tune524_Abeta1505
	aquire time	60 min
“Abeta903.8”	tune file	Tune524_903.8
	aquire time	60 min

A.1.4 Cloud point extraction

A.1.4.1 Preconcentration of Triton X-114

Prior to its application in the cloud point extraction Triton X-114 was pre-concentrated following a procedure published by Bordier. Essentially a cloud point phase separation, 10 g Triton X-114 were dissolved in 490 g 10 mM Tris-HCl buffer (+ 150 mM NaCl, pH 7.4) at 4 °C. Phase separation was induced by incubating the solution overnight at 35 °C. The aqueous phase was discarded and 490 g fresh buffer was added to repeat phase separation overnight. After removing the aqueous phase the micelle-rich phase was used as stock solution for subsequent extractions. Photometric examination of a 1:1000 dilution at 275 nm and 18 °C suggested a Triton X-114 content of approx. 14 %.

A.1.4.2 Cloud point extraction procedure

Three genetically altered mice were chosen from the live stock provided by the working group of Prof. Dr. Pahnke and the preparation of the brains was performed by Dr. Markus Krohn. The brains were severed in half and filled into 2 mL eppendorf tubes. Three halves were directly frozen (liquid N_2) and the other three halves were chilled on ice, homogenised without the addition of extraction solution using ceramic beads and stored at -20 °C.

Extraction solutions with different compositions containing a protease inhibitor cocktail were added to conform to the ratio of 1.0 mL for 100 mg brain tissue and the sample was homogenised with ceramic beads (table A-13).

Table A-13 Extraction of fresh brain tissue. Medium composition and extraction volume

extraction medium	composition	m_{tissue} [mg]	V [µL]
1	10 mM Tris, 150 mM NaCl, PBS	~140	1400
2	10 mM Tris, 150 mM NaCl	~157	1570
3	ultrapure H_2O	~160	1600

The fresh sample solutions were incubated for 1 h at 4 °C under mild agitation and separated from solid tissue components by centrifugation at 4 °C (10000 x g, 30 min). The supernatant was transferred into a fresh tube upon a 100 µL sucrose cushion solution (6 %). Sucrose solutions were prepared with the respective extraction media by dissolving 60 mg in 1 mL solution. Cloud point phase separation was induced by incubation at 37 °C for five minutes. The turbid solutions were separated into two phases by centrifugation at 37 °C (2800 x g, three min); supernatants transferred into new eppendorf tubes and stored at 4 °C. Cool extraction solution (500 µL, without X114) were added to the detergent phases, cooled to 4 °C, and brought again to cloud point phase separation by incubation at 37 °C for five minutes. Following centrifugation (2800 x g, 37 °C) the supernatant is pooled with the aqueous phase of the first cloud point. Cooled buffer solution (without X114) is then added to equalize the volume of both extraction phases.

The homogenised tissue samples stored at -20 °C were thawed and extracted at later points in time. Two samples were spiked with Aβ42 monomer standard to investigate its extraction behaviour. After thawing the tissue samples, defined amounts of monomer standard were added (table A-14). Simultaneously to the extraction of the 133 mg tissue sample a reference extraction of monomer standard was performed.

Table A-14 Spiked brain tissue samples (stored at -20 °C)

m_{tissue} [mg]	$V_{Aβ42, 2\ mg/mL}$ [µL]	time lapse
133 mg	25 µL	+ 2 months
- (reference)	25 µL	-
150 mg	42 µL	+ 5 months

For the extractions the volume of extraction medium (H_2O with protease inhibitor cocktail) was set to 1 mL to create an equivalent basis for the comparison between reference and tissue samples. Prior to incubation at 4 °C tissue sample were thoroughly mixed by Vortex to re-homogenise the solution. Cloud point extraction was performed as described.

Additional extractions were performed to explore the extraction behaviour of amyloid β species. The aqueous phase of both the spiked 133 mg sample and the reference were re-extracted by adding 50 µL Triton X-114, vortexing, cooling to 4 °C and causing cloud point phase separation (37 °C, 5 min). After centrifugation (2800 x g, 37 °C) the extraction phases were separated and brought to equivalent volume.

The tissue of the 133 mg sample was extracted a second time after adding 1 mL extraction solution (1 % X114 and protease inhibitor cocktail) following the general procedure.

A.1.4.3 Precipitation/delipidation methods

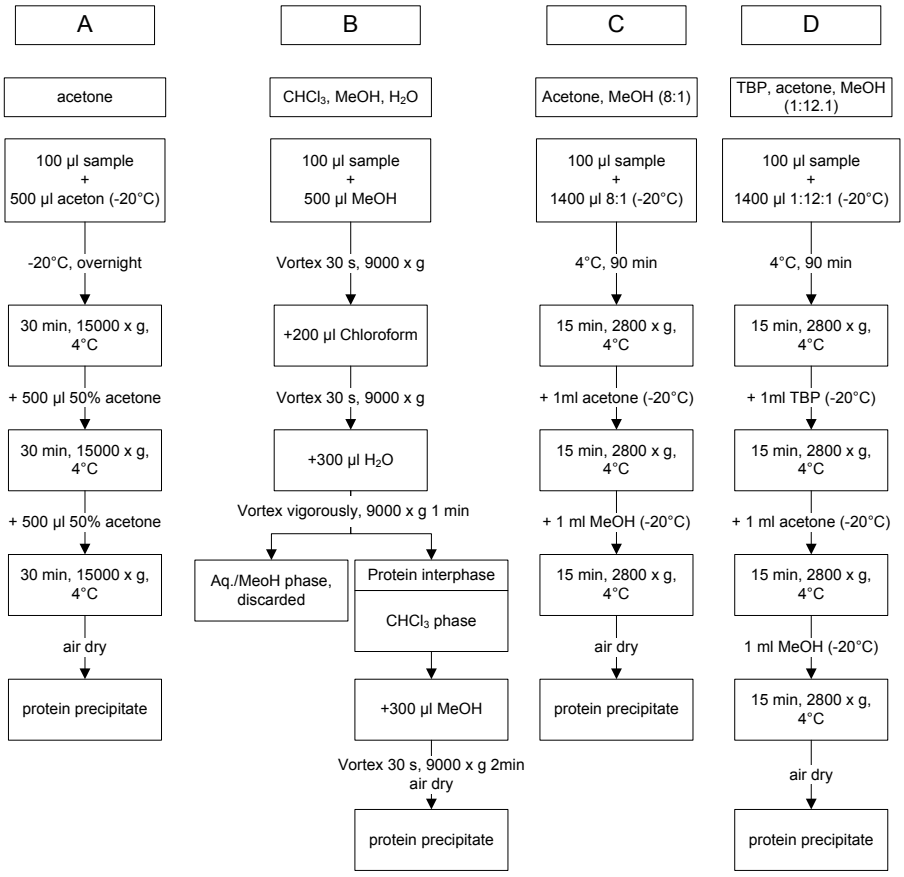

Figure A-1 Protein precipitation/delipidation methods

The precipitation and delipidation methods are summarised in figure A-1. They were applied for the aqueous (A'-D') and detergent (A-D) phases of tissue and reference samples.

A.1.5 Protein analysis

A.1.5.1 660 nm protein assay

The Pierce 660 nm assay is a dye-based photometric method to determine protein concentrations. Calibrations were performed with provided pre-diluted BSA standard solutions at 10.5 °C. To accommodate for Triton X-114 in extract solutions 33.3 µL standard solution and 33.3 µL extraction medium 2 (1 % Triton X-114, 10 mM Tris, 150 mM NaCl) were combined to a final sample volume of 66.6 µL. The reaction was initiated by adding 1000 µL assay reagent. After incubation at room temperature for five min, the extinction of the sample at 660 nm was recorded.

Extraction phase samples were also diluted with a 10 mM Tris, 150 mM NaCl solution (33.3 µL sample + 33.3 µL solvent) to reach non-interfering detergent contents < 1 %.

A.1.5.2 Denaturing gel electrophoresis (SDS PAGE)

Protein precipitates were redissolved in electrophoresis sample buffer. Precipitates were initially redissolved in a final volume of 100 µL and incubated at 70 °C for ten min prior to electrophoresis. Due to decreased protein concentrations in the detergent phases the sample volume for electrophoresis was lowered to 40 µL. Sample composition is summarised in table A-15.

Table A-15 Electrophoresis sample compositions for 40 µL and 100 µL

component	**$V_{40\ \mu L}$ [µL]**	**$V_{100\ \mu L}$ [µL]**
LDS sample buffer (4X)	10	25
Reducing agent (10X)	4	10
ultrapure H_2O	26	65

Of each prepared solution, up to 15 µL were loaded into the gel wells of pre-cast mini-gels (8 x 8 cm, 1 mm) to be separated. Lanes that were not used were filled with 10 µL of diluted LDS sample buffer (1X). In addition to the protein samples one or two lanes were used for protein standards. To prevent reoxidation of reduced proteins 187 µL antioxidant were added to the upper reservoir (75 mL MES SDS running buffer). Voltages of 75 V or 80 V were applied over a period of ~2 hours until the running front indicated by a blue band of Coomassie brilliant blue molecules reached the contact opening of the gel cassette.

Gels were then stained using the accelerated microwave staining method with SimplyBlue SafeStain. Removed from the gel cassette, the gel is washed thrice by adding 100 mL ultrapure H_2O and heating the solution by microwaving for 45 s at 950 W, gently rinsed on an orbital shaker for one min. The water was discarded after each step except for the last incubation. Instead, 20 mL SimplyBlue SafeStain were added and the solution

heated again. Excessive background staining was removed by rinsing the gel with 100 mL ultrapure water for five and ten minutes. In the last step 20 mL of a 20 % (w/v) NaCl solution are added. The gel can be stored in the solution at 4 °C.

A.1.5.3 Determination of theoretical Aβ 42 related protein bands

One objective of the work was the investigation of soluble oligomeric amyloid β species. To determine protein bands corresponding to theoretical molecular weights a calibration using the relative distance travelled by standard proteins was performed. Digital images of each gel were opened with the graphic manipulation programme GIMP 2.6 and the distances for the running front as well as for the standard proteins were determined in pixels. The logarithmic molecular weight ($\log_{10}$MW) was plotted against quotient of both distances (R_f). Theoretical multimers of the approximated Aβ42 (human) molecular mass of 4.6 kDa were entered into the calibration function to determine the respective R_f factors and subsequently the positions of theoretical bands within the gel.

A.1.5.4 In-gel digestion of protein bands

In order to identify proteins in the individual bands an in-gel digestion with trypsin was performed to produce LC-MS/MS mass range compatible peptides. Protein bands corresponding to theoretical oligomer molecular weights were carefully excised with a ceramic scalpel, cut into cubes (~1x1 mm) and placed in a LoBind eppendorf tube. The bands were destained by incubating the pieces in 50 % ACN in 25 mM ammonium-bicarbonate at 30 °C for 30 min. Destaining was repeated until the blue stain was completely removed. The gel cubes were dehydrated in 100 % ACN for 5 – 10 min at room temperature.

Activated trypsin solution (35 µL per band), prepared from a 0.2 µg/µL stock solution in 1 mM HCl by a 1:20 dilution with a 40 mM ammonium bicarbonate and 9 % ACN, was added to the gel pieces and incubated on ice for one hour. The fully rehydrated cubes were incubated overnight at 37 °C to digest the proteins within the gel matrix. Peptides were extracted in two steps. First, the gel pieces were incubated with 25 µL of 5 % formic acid for 30 min at room temperature. After centrifugation (14000 x g, 1 min) the collected fluid was transferred into a siliconised glass insert in a 1.8 mL vial. The second extraction was performed with 25 µL 5 % formic acid in 50 % ACN and the fluid added to the vial.

The pooled peptide solutions were evaporated under argon using a MiniVap apparatus and redissolved in 30 µL of the initial mobile phase of the C18 gradient (see chapter A.1.5.5), generally 95 % H_2O with 0.1 % FAC and 5 % ACN with 0.1% FAC.

A.1.5.5 Instrument method for RPLC-MS/MS analysis (LTQ)

Peptide solutions produced by in-gel disgestion were analysed using the basic parameter settings described in chapter A.1.2.2. The organic component in the mobile phase was switched from acetone to acetonitrile with 0.1 % formic acid (table A-16). In addition to the established instrument method implementing the general tune524 file with a capillary voltage of 18 V a second instrument method was created by transferring observations won by method optimisation for amyloid β 42 on the LCQ to the LTQ. Using the Tune Plus programme the tune file created by the yearly calibration focussing on 524 m/z was

modified. The capillary voltage was raised from 18 V to 43 V, the capillary temperature raised to 300 °C and saved as a separate file. Data dependent parameter settings excluding reject masses are summarised in table A-17.

Table A-16 Mobile phase composition II, flow rate 150 µL/min

t [min]	H_2O + 0.1 % FAC [%]	ACN + 0.1 % FAC [%]
0	95	5
10	95	5
50	20	80
55	20	80
60	95	5
70	95	5

Table A-17 Data dependent parameter settings II (LTQ)

data dependent parameter	setting
dependent reject masses	low 1.5 amu/ high 3.5 amu
Zoom mass range width	low 5.0 amu/ high 5.0 amu
MS^2 settings	
Default charge state	+2
Charge state screning	enabled

A.1.5.6 BioWorks™ database search settings

Two FASTA format protein databases were used to identify proteins from mass spectrometric fragmentation data sets of peptides; a general database containing proteins associated with the mouse proteome and a specific amyloid β related database. Sequest search parameter settings defining the database search process are summarised in table A-18.

Table A-18 SEQUEST search parameters

SEQUEST parameter	setting
modifications	none
precursor and fragment masses	monoisotopic
enzyme	trypsin (KR)
enzyme limits	fully enzymatic, cleaves at both ends
missed cleavage sites	2
peptide tolerance	1.5 amu
fragment ions tolerance	1.0 amu
number results scored	250
ions	B ions, Y ions
peptide matches reported	10

The mouse database was extracted with the FASTA database utility tool from the UniProt Swissprot database published in November 2011. Entries were selected for the sub-database if they contained the word [mus] and saved as a separate FASTA database

(mouse_Nov2011).Using protein sequences published on the national center for biotechnology information (NCBI) homepage relating to amyloid β, a number of sequences (e.g. Aβ40, Aβ42, APP, A4) were combined in a small FASTA database (NCBI_fasta, see appendix A.8).

A.1.5.7 Additional protein properties

Several protein properties and specific information about their function and cellular location were not included in FASTA sequence data sets used for identification with BioWorks™. Relative hydropathicity indices were determined by entering the UniProt identification assigned to the protein matches into the ProtParam tool on web.expasy.org. The tool calculated various sequence specific properties like pI, molecular weight, statistical distribution of amino acids and the GRAVY index for the selected chain. For all proteins the expressed and functional protein sequences separated from precursor proteins were included in the assessed data sets.

For protein function, enzyme classifications and cellular location the vast pool of information contained in the UniProt Swissprot online database. Specific data sets were again accessed using the Uniprot Ids and protein properties and cellular locations were added to the assessed data sets if available.

Table A-19 Source for additional protein property data

source	website	properties	accessed
ProtParam tool	web.expasy.org/protparam/	GRAVY, pI, MW	2011 – 2013
UniProt database	www.uniprot.org/uniprot	cellular location, function, EC	Jan – Apr 2013

A.2 Molecular weight determination with ESIprot 1.0

Table A-20 Mass spectrometric data entered into ESIprot to determine molecular weight of peaks in fig. 4-1

retention time [min]	selected [M+H$^+$]	MW [Da] (ESIprot)	charge states
23.20 (1)	770.18	8458.81 ± 1.93	+11
	847.14		+10
	940.86		+9
	1058.29		+8
	1209.15		+7
	1410.46		+6
23.20 (2)	781.17	8585.44 ± 4.06	+11
	859.80		+10
	955.32		+9
	1074.53		+8
	1227.72		+7
	1430.84		+6
23.20 (3)	799.89	8788.24 ± 1.05	+11
	879.97		+10
	977.62		+9
	1099.45		+8
	1256.32		+7
	1465.66		+6
24.02	798.83	8773.19 ± 2.16	+11
	878.57		+10
	975.93		+9
	1097.59		+8
	1254.11		+7
	1462.75		+6
	1755.31		+5
26.09	814.6	8947.55 ± 2.09	+11
	896.03		+10
	995.23		+9
	1119.37		+8
	1278.98		+7
	1491.82		+6
27.6 – 29.8	1193.19	14305.68 ± 0.51	+12
	1301.57		+11
	1431.57		+10
	1590.45		+9
	1789.19		+8
31.36	556.28	3886.49 ± 0.29	+7
	648.75		+6
	778.27		+5
	972.58		+4
33.3 – 35.9 (1)	1213.24	66602.04 ± 77.10	+55
	1232.38		+54
	1258.69		+53
	1281.06		+52
	1307.30		+51
	1331.61		+50
	1362.99		+49
	1388.31		+48
	1417.03		+47
33.3 – 35.9 (2)	1482.36	66631.72 ± 49.77	+45
	1515.98		+44

	1548.77		+43
	1588.84		+42
	1625.25		+41
	1666.86		+40
33.3 – 35.9 (3)	1666.86	66613.67 ± 31.75	+40
	1709.80		+39
	1752.86		+38
	1801.15		+37
	1852.27		+36
	1903.08		+35
	1960.57		+34
37.48	1287.91	66921.86 ± 56.64	+52
	1314.28		+51
	1340.97		+50
	1367.29		+49
	1393.39		+48
	1423.35		+47
	1455.18		+46
	1489.22		+45
	1521.67		+44
47.37 (1)	520.42	1038.60 ± 0.31	+2
	1039.39		+1
47.37 (2)	542.36	1072.54 ± 14.34	+2
	1063.39		+1
47.92	inconclusive		
48.79	inconclusive		
50.55	438.83	2737.78 ± 164.14	+6
	578.64		+5
	718.07		+4
	856.93		+3

Table A-21 Molecular weight determination of peaks in chromatogram of supernatant solution (soluble Abeta peptides isolated from brain matter for ELISA analysis)

retention time [min]	**selected [M+H$^+$]**	**MW [Da] (ESIprot)**	**charge states**
20.09	621.68	4964.17 ± 1.22	+8
	710.31		+7
	828.43		+6
	993.67		+5
	1241.64		+4
20.27	633.97	5062.57 ± 0.96	+8
	724.27		+7
	844.73		+6
	1013.29		+5
21.38	inconclusive		
25.42	674.09	14206.64 ± 81.74	+21
	704.41		+20
	750.41		+19
	791.78		+18
	838.33		+17
	890.66		+16
	943.36		+15
	1017.59		+14
	1104.71		+13
27.21-28.4	1139.04	12725.92 ± 216.09	+11

	1301.48		+10
	1431.54		+9
	1590.36		+8
	1789.14		+7
29.39 (1)	714.88	8562.62 ± 8.17	+12
	779.73		+11
	857.67		+10
	952.74		+9
	1071.69		+8
	1221.86		+7
29.39 (2)	705.4	8448.64 ± 4.92	+12
	768.6		+11
	846.27		+10
	940.04		+9
	1056.39		+8
29.65	723.06	8663.09 ± 1.49	+12
	788.65		+11
	867.41		+10
	963.67		+9
	1083.86		+8
	1238.35		+7
	1444.47		+6
31.57	845.38	14926.43 ± 393.72	+17
	915.35		+16
	998.45		+15
	1098.14		+14
	1188.17		+13
	1258.00		+12
	1372.03		+11
	1451.81		+10
32.93	1102.76	14322.26 ± 2.08	+13
	1194.79		+12
	1302.93		+11
	1433.31		+10
	1592.35		+9
	1790.90		+8
35.65	1367.18	68252.72 ± 116.79	+50
	1394.82		+49
	1423.35		+48
	1449.56		+47
	1483.89		+46
	1513.22		+45
	1554.41		+44
	1589.72		+43
	1629.30		+42
39.4	inconclusive only 1 mass		
44.4	inconclusive		
44.7	inconclusive		
47.54	507.50	7673.23 ± 57.77	+15
	551.46		+14

	595.48		+13
	639.43		+12
47.86	419.34	5989.06 ± 89.63	+14
	463.45		+13
	507.46		+12
	551.44		+11
	595.48		+10
50.02	582.50	2828.56 ± 95.42	+5
	721.99		+4
	943.81		+3
	1348.16		+2
50.51	inconclusive		

Table A-22 Molecular weight determination of peaks in chromatogram of resolvated protein pellet (insoluble Abeta peptides isolated from brain matter for ELISA analysis)

retention time [min]	**selected [M+H$^+$]**	**MW [Da] (ESIprot)**	**charge states**
20.00 (shoulder)	776.58	24054.19 ± 57.18	+31
	799.05		+30
	830.11		+29
	862.48		+28
	892.71		+27
	925.12		+26
	965.74		+25
	1003.64		+24
20.17	621.74	4964.63 ± 0.87	+8
	710.23		+7
	828.38		+6
	993.78		+5
20.36	634.02	5062.98 ± 0.99	+8
	724.36		+7
	844.76		+6
	1013.38		+5
21.48	699.69	9159.24 ± 42.71	+13
	766.04		+12
	835.42		+11
	918.77		+10
	1020.65		+9
24.46	646.53	17498.88 ± 59.02	+27
	675.85		+26
	697.96		+25
	731.85		+24
	763.73		+23
	794.32		+22
	837.87		+21
	875.13		+20
25.33	615.79	14135.32 ± 5.8	+23
	643.67		+22
	674.24		+21
	708.01		+20

	745.05		+19
	786.41		+18
	831.72		+17
	884.14		+16
	943.35		+15
26.16	660.37	13830.68 ± 13.89	+21
	693.41		+20
	728.74		+19
	770.14		+18
	814.18		+17
	864.14		+16
	922.55		+15
	988.32		+14
27.29	840.74	10076.32 ± 1.31	+12
	917.22		+11
	1008.56		+10
	1120.56		+9
	1260.38		+8
29.08 (1)	714.96	8566.07 ± 0.79	+12
	779.77		+11
	857.62		+10
	952.77		+9
	1071.67		+8
	1224.63		+7
29.08 (2)	705.44	8449.01 ± 5.71	+12
	768.06		+11
	846.17		+10
	940.00		+9
	1057.36		+8
	1208.14		+7
29.44	723.05	8644.51 ± 47.36	+12
	788.76		+11
	867.44		+10
	963.58		+9
	1069.49		+8
	1238.43		+7
30.8	753.08	9893.72 ± 106.34	+13
	823.15		+12
	905.35		+11
	1005.82		+10
	1093.24		+9
31.53	784.84	10979.90 ± 17.29	+14
	844.82		+13
	915.43		+12
	1001.98		+11
	1098.26		+10
34.97	764.06	13130.36 ± 154.43	+17
	826.39		+16
	877.09		+15
	947.98		+14
	1032.70		+13

	1083.23		+12
	1188.04		+11
	1302.01		+10
36.69	740.99	9620.50 ± 0.81	+13
	802.63		+12
	875.62		+11
	963.13		+10
	1069.93		+9
	1203.70		+8
40.54	1200.09	16795.24 ± 16.41	+14
	1292.48		+13
	1403.40		+12
	1527.32		+11
	1679.84		+10
	1866.42		+9
44.45	Inconclusive		
44.70	Inconclusive		
48.74	Inconclusive		
50.55	578.66	2817.56 ± 87.68	+5
	717.85		+4
	941.95		+3
	1347.28		+2

A.3 Amino acids

Table A-23 Amino acids – structure, 3-letter, 1-letter codes and molecular weights

name	structure	AAA	A	M (amu)
glycine	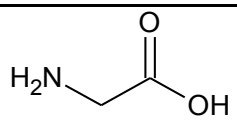	Gly	G	57.0
alanine	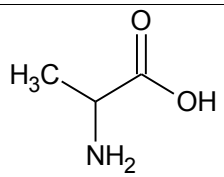	Ala	A	71.0
serine	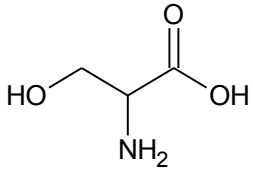	Ser	S	87.0
proline	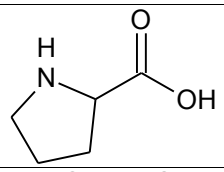	Pro	P	97.1
valine	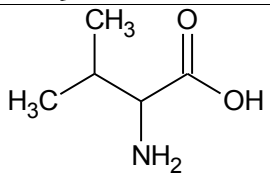	Val	V	99.1
threonine	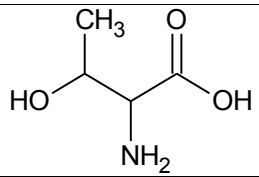	Thr	T	101.1
cysteine	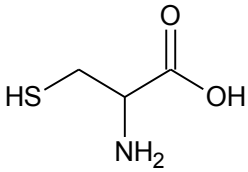	Cys	C	103.0
leucine	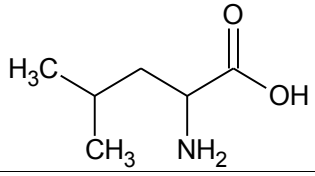	Leu	L	113.1
isoleucine	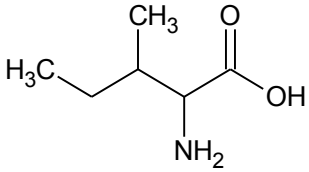	Ile	I	113.1
asparagine	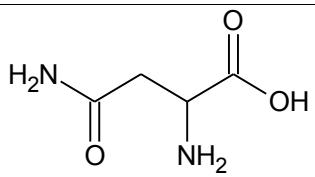	Asn	N	114.0

aspartic acid	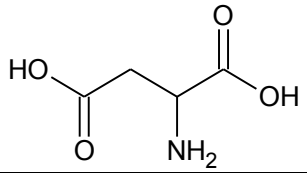	Asp	D	115.0
glutamine	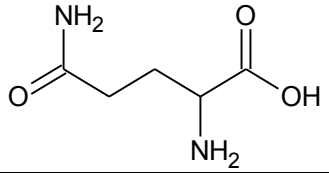	Gln	Q	128.1
glutamic acid	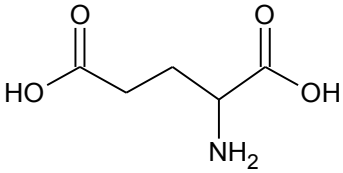	Glu	E	129.04
lysine	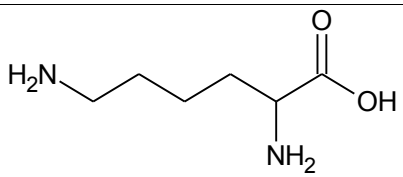	Lys	K	128.1
methionine	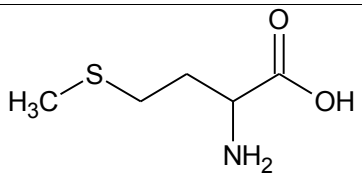	Met	M	131.0
histidine	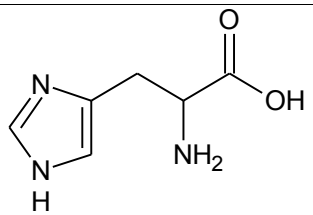	His	H	137.1
phenylalanine	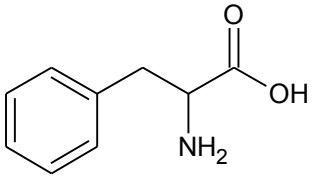	Phe	F	147.1
arginine	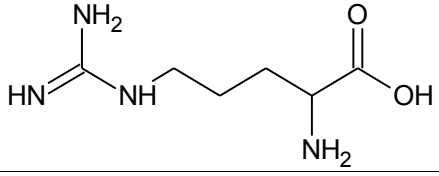	Arg	R	156.1
tyrosine	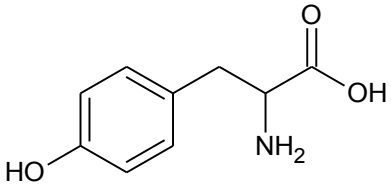	Tyr	Y	163.1
tryptophane	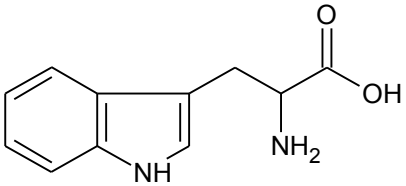	Trp	W	186.1

A.4 Supplementary chromatographic data

A.4.1 ELISA Aβ42 charge state determination

Additional chromatographic data for the determination of the charge state of amyloid β 42 in ELISA Aβ42 standard solution separated by RPLC. Previously observed peaks were further analysed by applying the highest available mass spectrometric resolution in form of time controlled UltraZOOM Scans. Figure A-2 shows the FullScan chromatogram and the UltraZOOM analysed portions. A representative mass spectrum for the 60.5 min peak is depicted in fig. A-3.

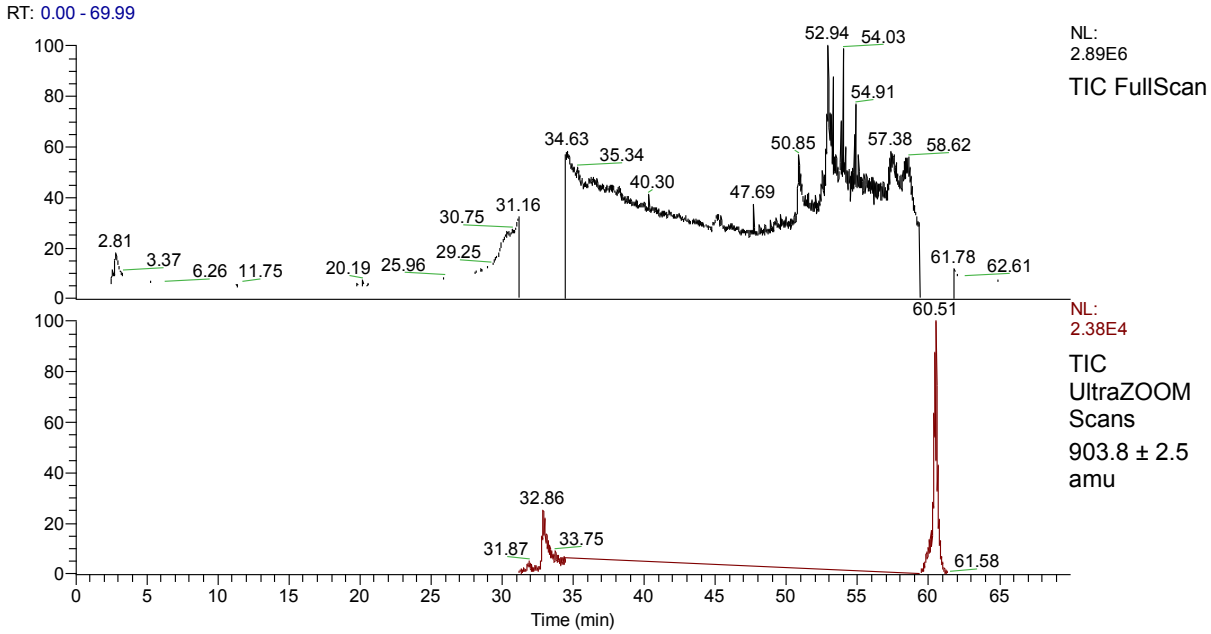

Figure A-2 Chromatogram of Aβ42 ELISA standard, FullScan with time window controlled UltraZOOM scans of the mass signal 903.8 ± 2.5 amu

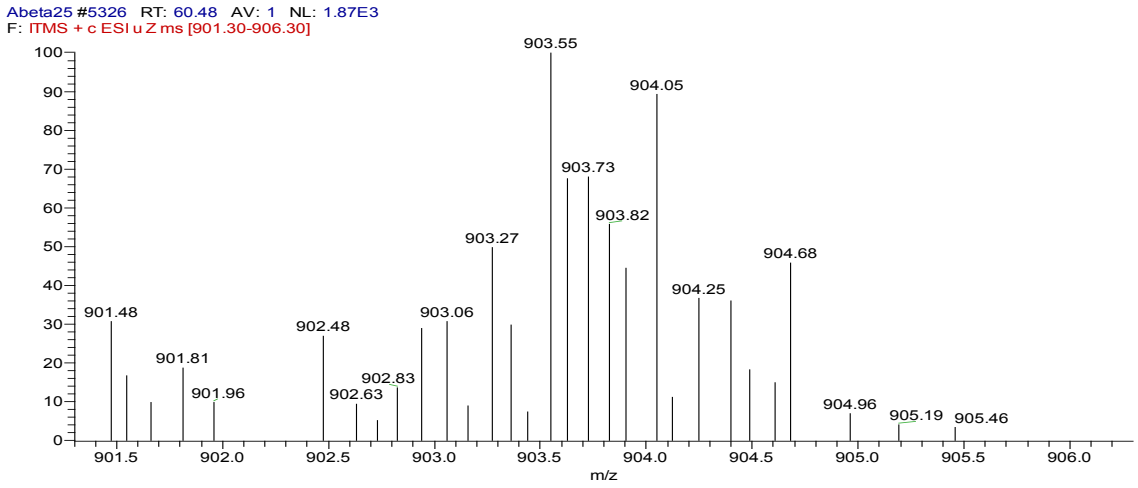

Figure A-3 UltraZOOM scan of amyloid β 42 species in 60.5 min peak of RPLC-MS chromatogram

A.4.2 Flow rate determination (SEC-MS)

Table A-23 summarizes the backpressure data recorded to establish the optimal flow rate for SEC-MS experiments using the LCQ mass spectrometer.

Table A-24 Backpressure in relation to flow rate of 20 % ACN, 80 % H_2O with 0.1% FAC

flow [µL/min]	p [bar]	p [bar]	p [bar]
100	58	57	
150	81	80	80
200	104	102	102
250	126	125	124
300	148	148	148
350	170	170	169
400	192	191	

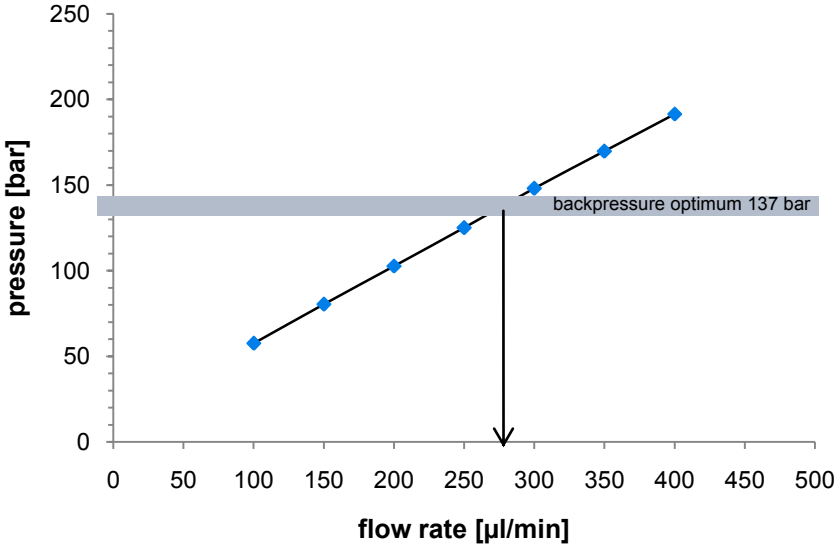

Figure A-4 Plot of backpressure p in bar vs flow rate in µL/min for SEC separation using the LCQ mass spectrometer. Grey area indicates optimum backpressure. Mobile phase: 10 mM NH_4COOH with 20% ACN

A.4.3 Tune method optimisation

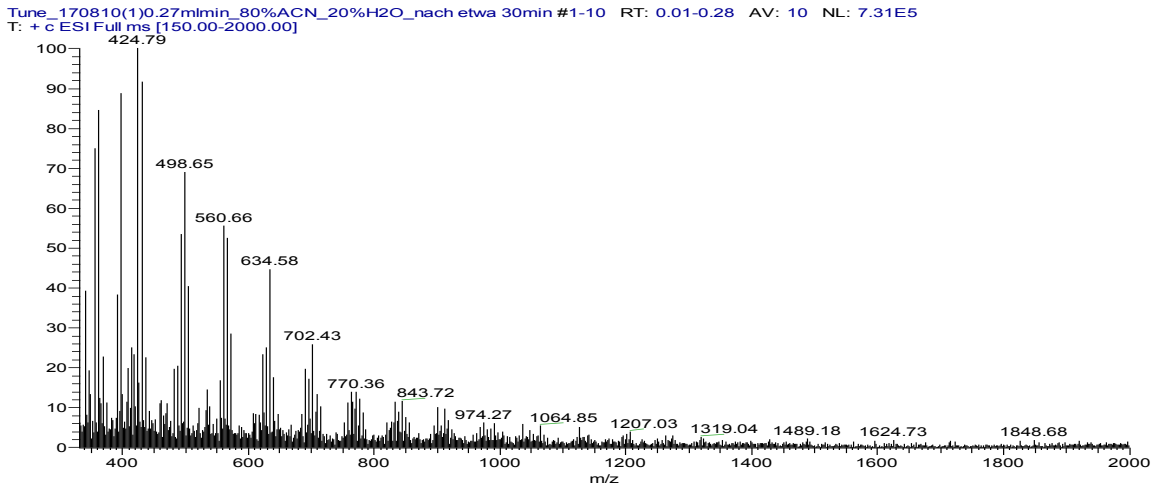

Figure A-5 Tune data method 1 – capillary temp. 275 °C, sheath gas 30 units, sweep gas 5 units. FullScan [331-2000 amu]

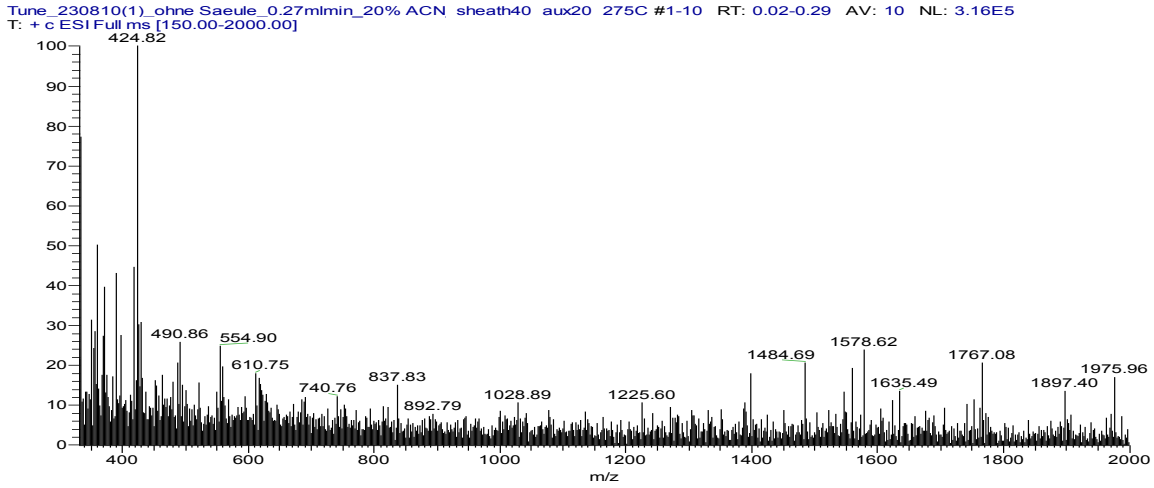

Figure A-6 Tune data method 2 – capillary temp. 275 °C, sheath gas 40 units, sweep gas 20 units. FullScan [331-2000 amu]

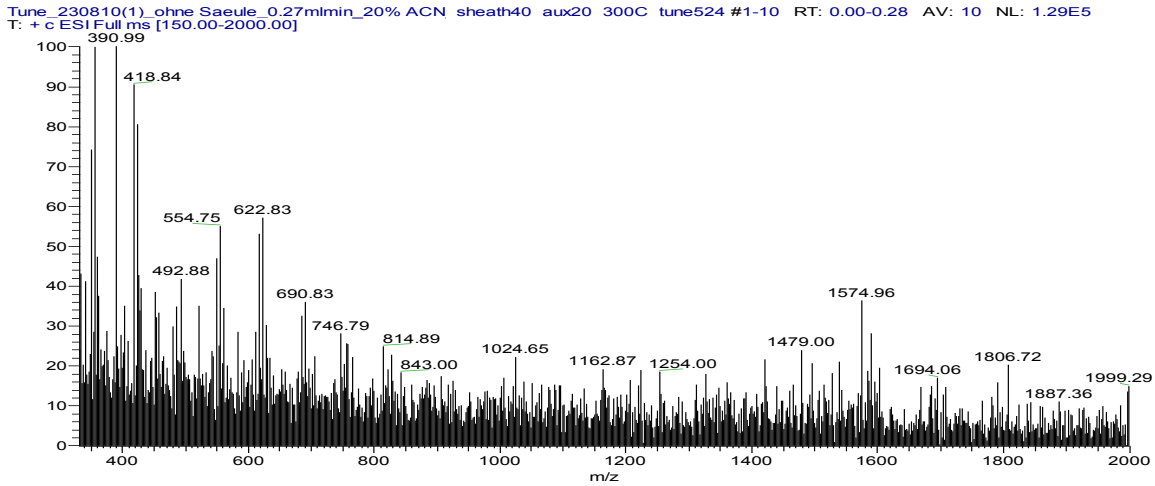

Figure A-7 Tune data method 3 – capillary temp. 300 °C, sheath gas 40 units, auxillary gas 20 units. FullScan [331-2000 amu]

A.4.4 Dilution series of myoglobin and lysozyme (SEC-MS)

Chromatographic and mass spectrometric data for myoglobin dilution series on BioSEC-3 column are shown in fig. A-8 and A-9.

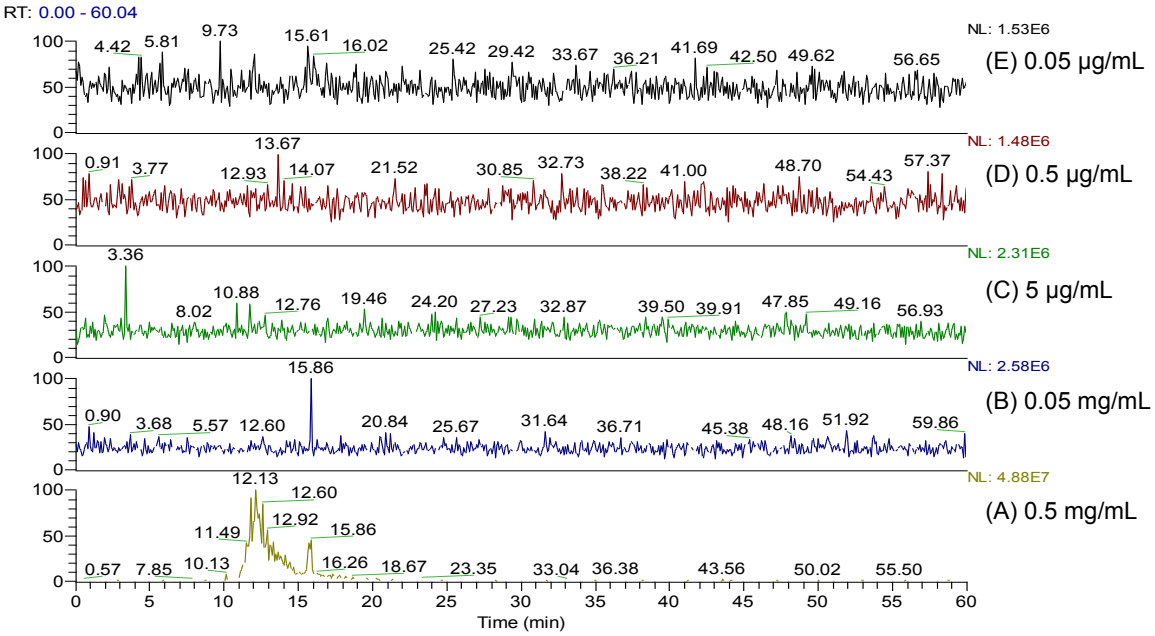

Figure A-8 SEC-MS chromatograms of myoglobin dilutions (E) 0.05 µg/mL to (A) 0.5 mg/mL. Base peak view chromatograms

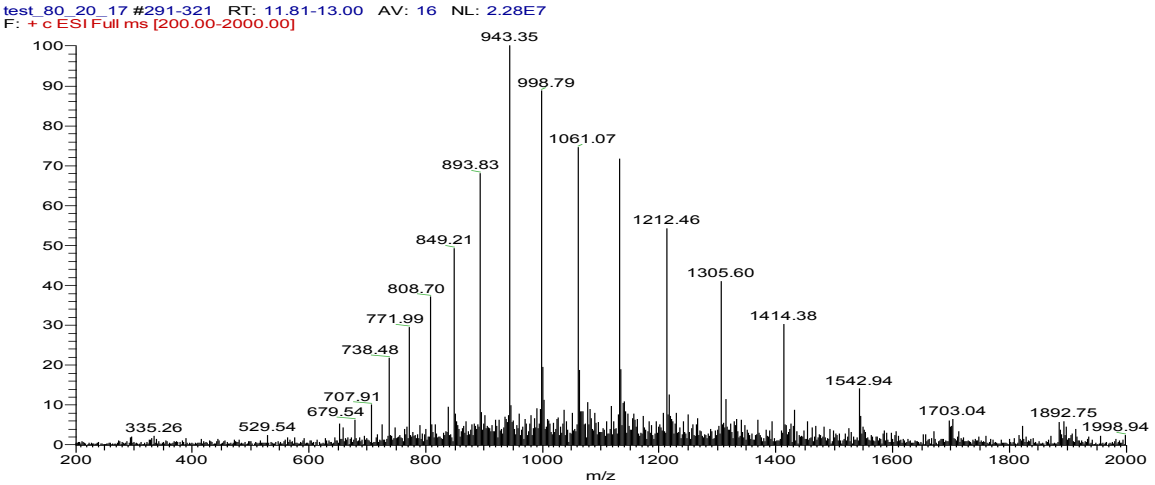

Figure A-9 Mass spectrum (averaged) correlating to myoglobin peak (11-14 min) in Fig A-8. FullScan [200-2000 amu]. Moleculare weight (ESIprot) [808.7 to 1305.6]: 16961.67 ± 1.5 Da (+21 to +13)

Chromatographic and mass spectrometric data for lysozyme dilution series on BioSEC-3 column are shown in fig. A-10 and A-11.

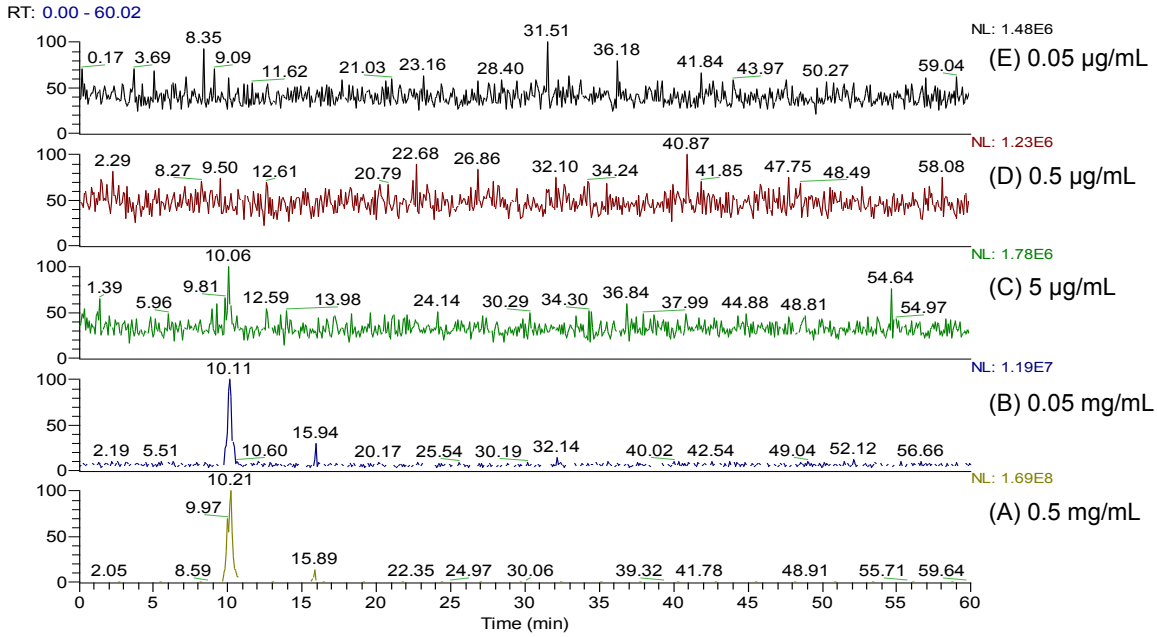

Figure A-10 SEC-MS chromatograms of lysozyme dilutions (E) 0.05 µg/mL to (A) 0.5 mg/mL. Base peak view chromatograms

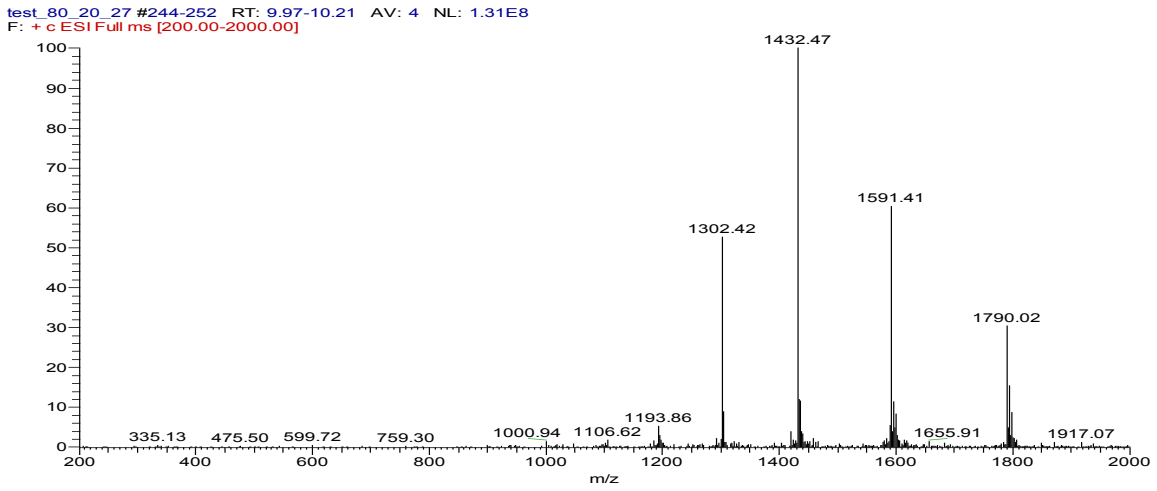

Figure A-11 Mass spectrum (averaged) correlating to lysozyme peak (10.21 min) in Fig A-10. FullScan [200-2000 amu]. Molecular weight (ESIprot) [1193.86 to 1790.02]: 14314.02 ± 1.28 Da (+12 to +8)

A.5 Supplementary photometric data

A.5.1 Pierce 660 nm photometric assay

To accommodate the strong effects the detergent has on the Pierce 660 nm assay, a calibration was performed with standard protein solutions (BSA, prediluded provided with kit) at 0.5 % Triton X-114.

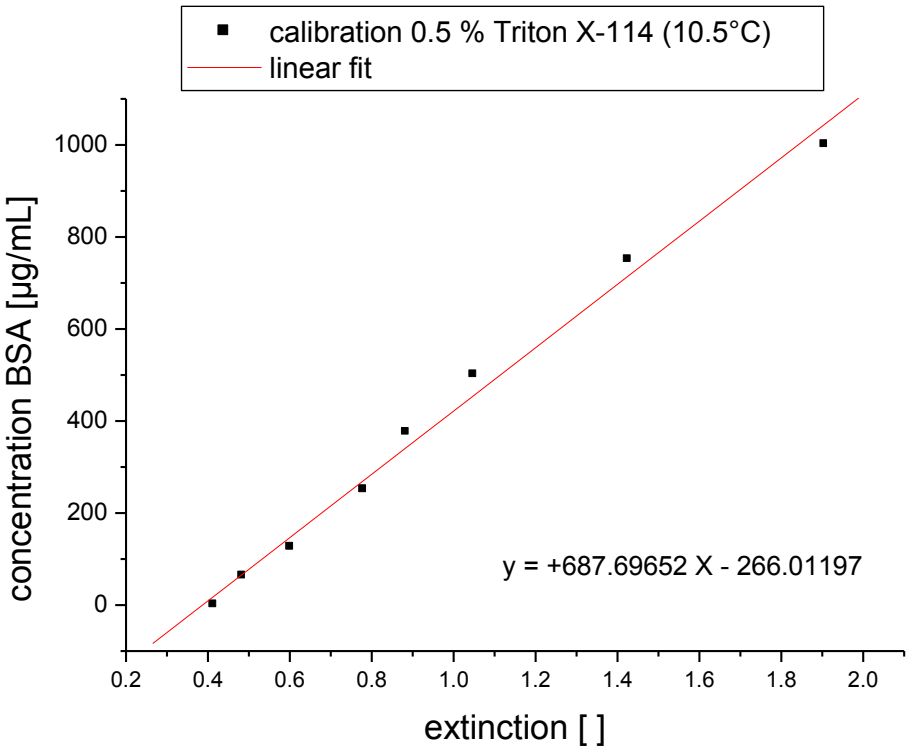

Figure A-12 Calibration of 660 nm assay for BSA standard solutions containing 0.5 % Triton X-114. 0-1000 µg/mL. Temp: 10.5°C

The calibration was used to estimate the total protein content of mouse brain extract solutions. Detergent (X) and aqueous (aq) phases were analysed without performing further precipitation steps prior to the assay. Results are summarized in table A-25.

Table A-25 Protein concentration of detergent (X) and aqueous (aq.) phases of cloud point extracts with varying buffer compositions

buffer system	tissue mass [wet]	extinction I	extinction II	extinction III	MW	c (1:1) [µg/mL]	C [µg/mL]
buffer 1, X	140 mg	1.2172	1.2174	1.2165	1.2170	570.94	1141.88
buffer 2, X	157 mg	1.1657	1.1647	1.1636	1.1647	534.93	1069.85
buffer 3, X	160 mg	1.2071	1.2059	1.2049	1.2060	563.33	1126.65
buffer 1, aq	140 mg	2.3230	2.3242	2.3243	2.3238	1332.08	2664.16
buffer 2, aq	157 mg	2.3586	2.358	2.3594	2.3587	1356.03	2712.07
buffer 3, aq	160 mg	2.6366	2.6368	2.6367	2.6367	1547.24	3094.47

A.6 Digested protein bands – overview

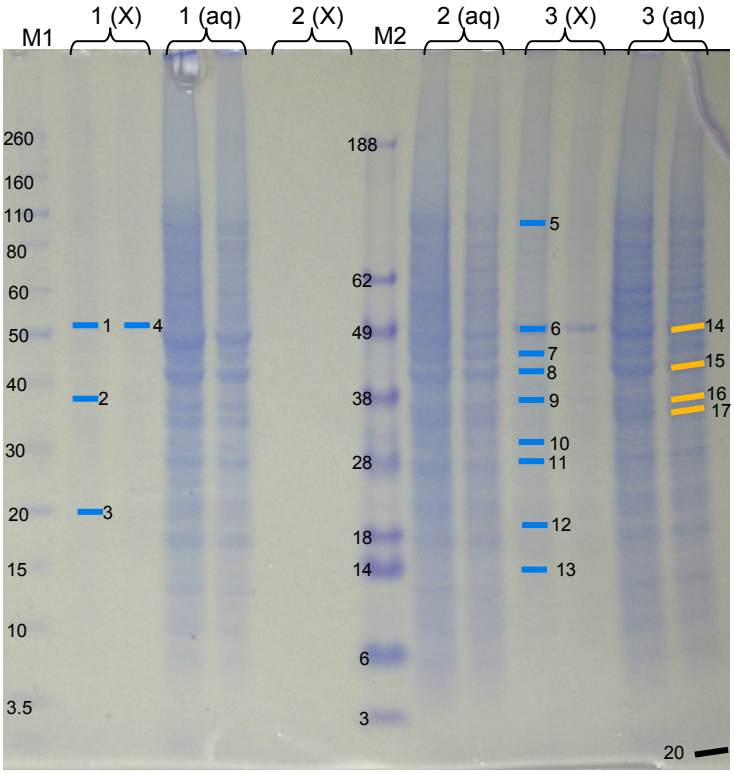

Figure A-13 SDS-PAGE (4-12 %, reducing cond.) of protein extracts using buffer systems 1-3. M1 – Novex Sharp unstained marker, M2 – SeeBlue marker. Sample volume 8 µL (**left**) and 4 µL (**right**) for each phase respectively. Indicated protein bands were analysed by LC-MS/MS

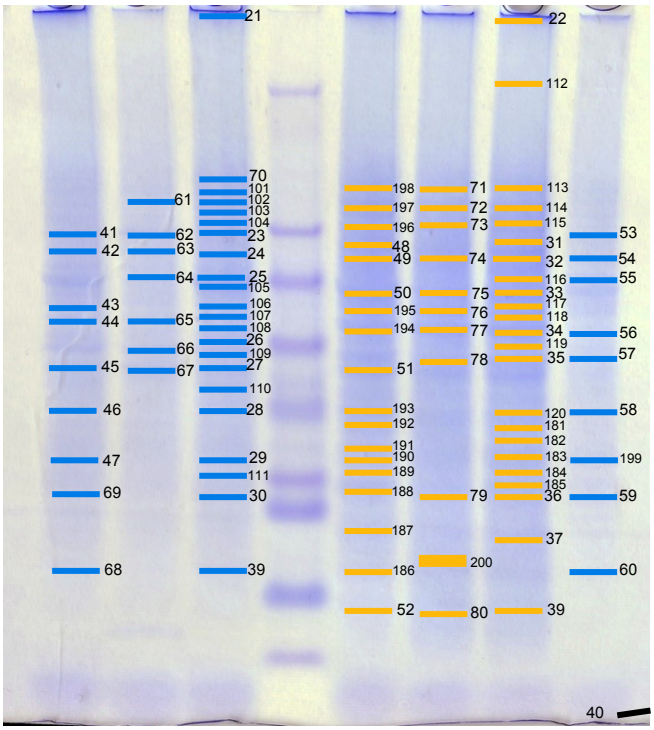

Figure A-14 SDS-PAGE (4-12 %, reducing cond.) of protein extracts using buffer systems 1-3. M2 – SeeBlue marker. Detergent phases (**left of marker**) 40 µL resolvation solution, aqueous phases (**right**) 100 µL. Indicated protein bands were analysed by LC-MS/MS

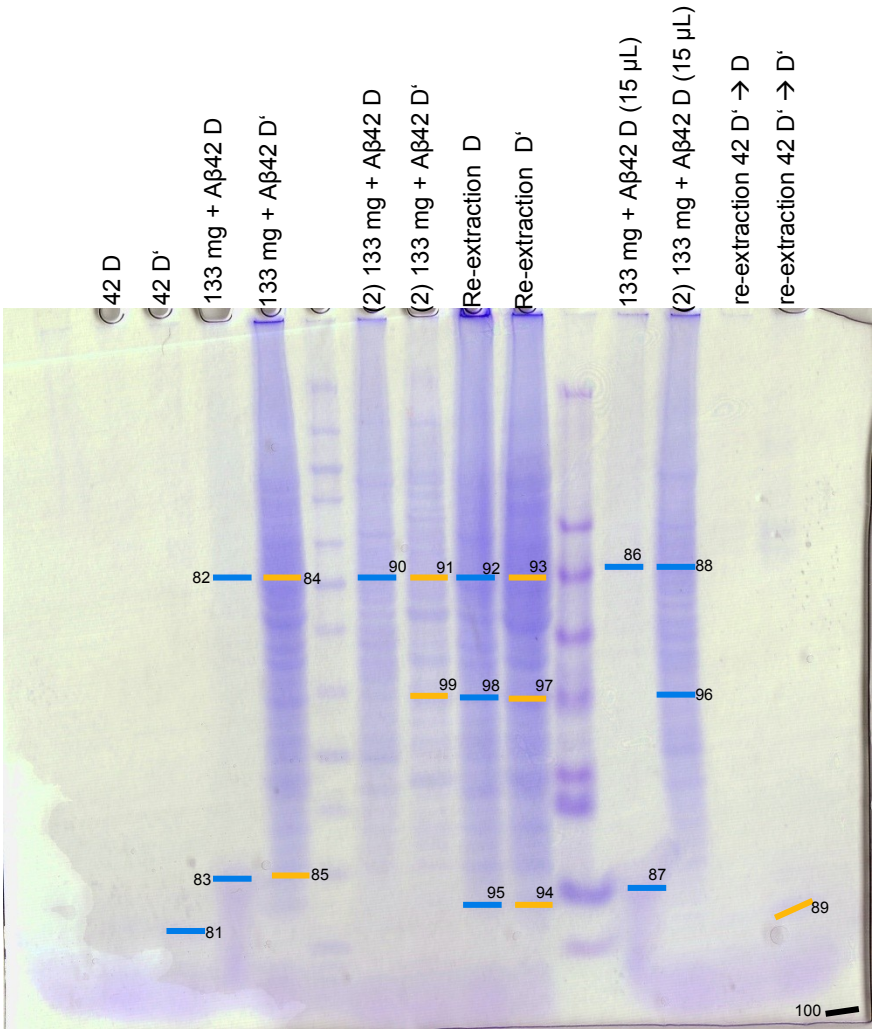

Figure A-15 SDS PAGE (4-12 %, reducing cond., 80 V) of Aβ42 phase distribution experiments. Resolvation volume detergent phase precipitates 40 µL, 100 µL for aqueous phases. Indicated protein bands were analysed by LC-MS/MS

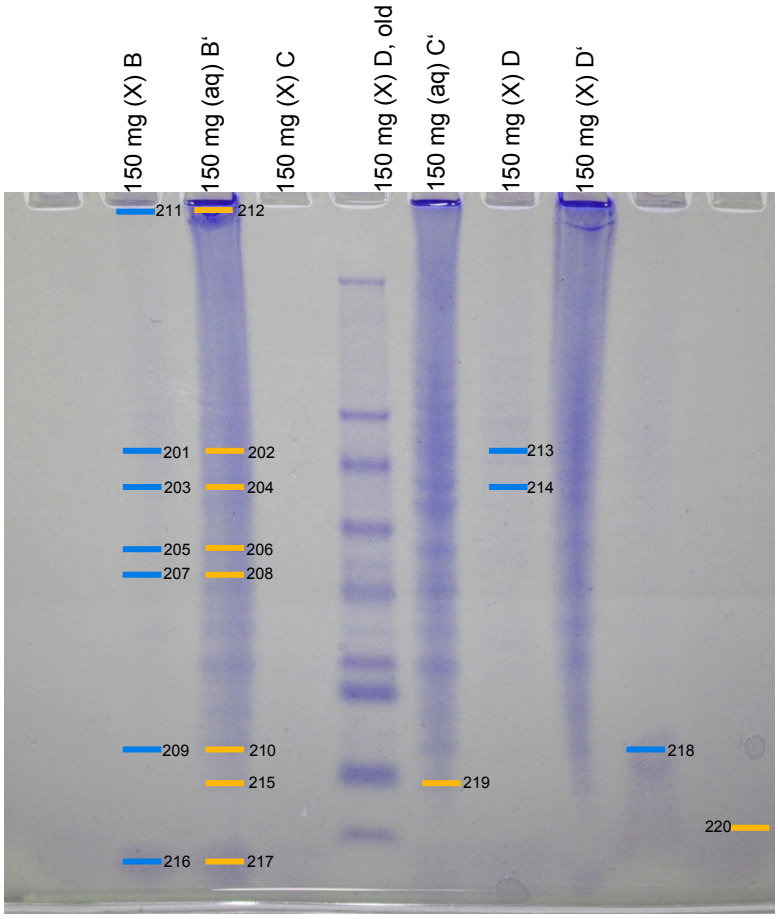

Figure A-16 SDS PAGE (4-12 %, reducing cond., 80 V) with protein extracts of a spiked mouse brain sample (Aβ42), precipitated with methods B-D. Indicated protein bands were analysed by LC-MS/MS

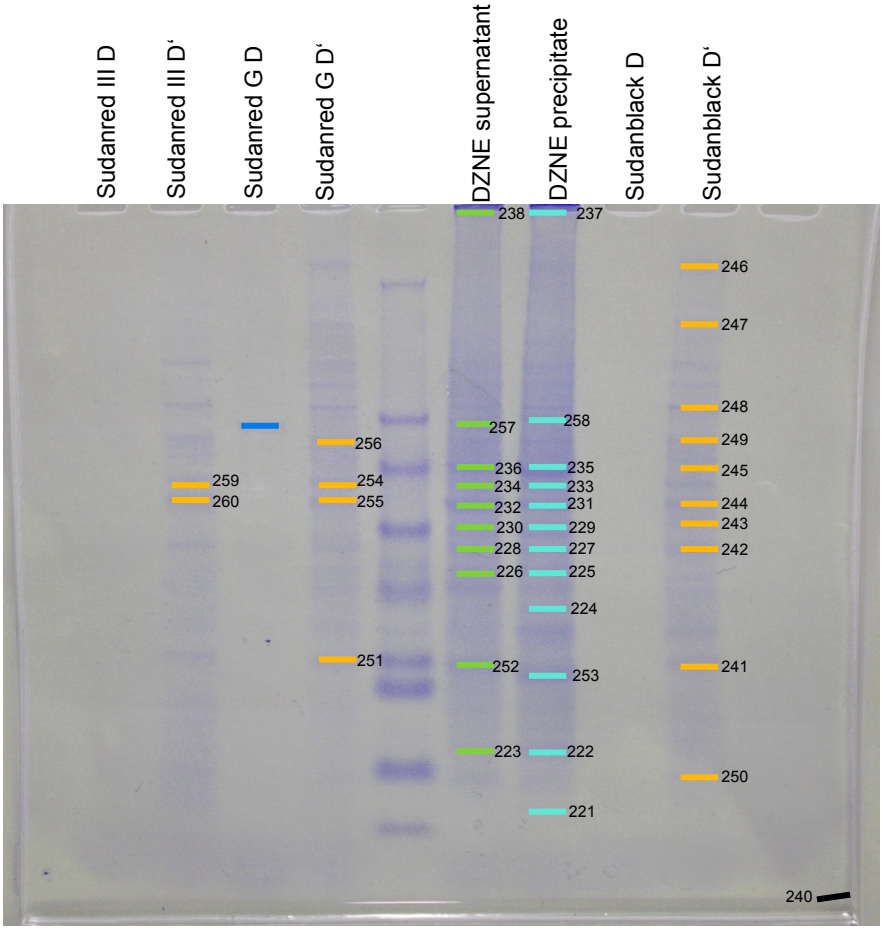

Figure A-17 SDS PAGE (4-12 %, reducing cond., 80 V) with protein extracts provided by Pahnke et al. (DZNE) and samples resulting from reextraction of CP extracts using lipophilic dyes to stain the detergent phase. Indicated protein bands were analysed by LC-MS/MS

A.7 Supplementary protein distribution data

The following figures display the distribution data composing the overview figures in chapter 4.3.1. Additionally, the distribution of protein pI in relation to their GRAVY index is shown for both 18 V and 43 V capillary voltage.

A.7.1 Aqueous phases, 18 V

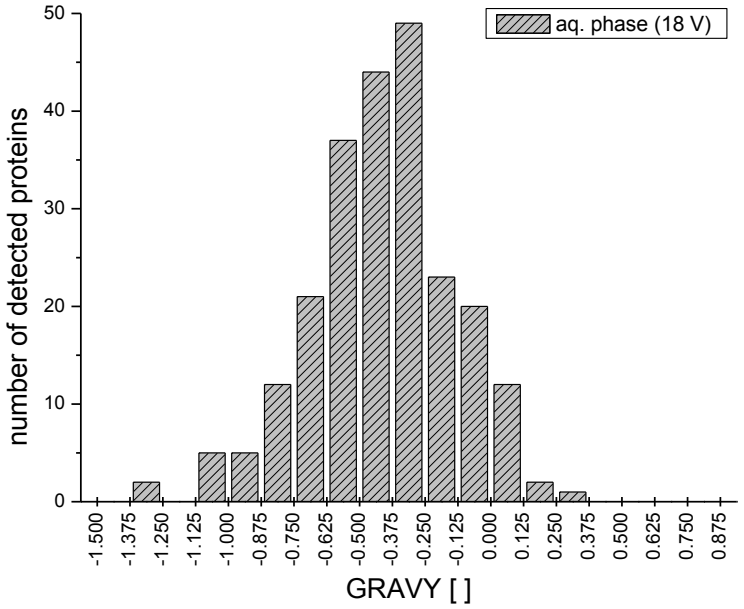

Figure A-18 Plot number of proteins found in the aqueous phases over GRAVY index ranges of [0.125], 18 V

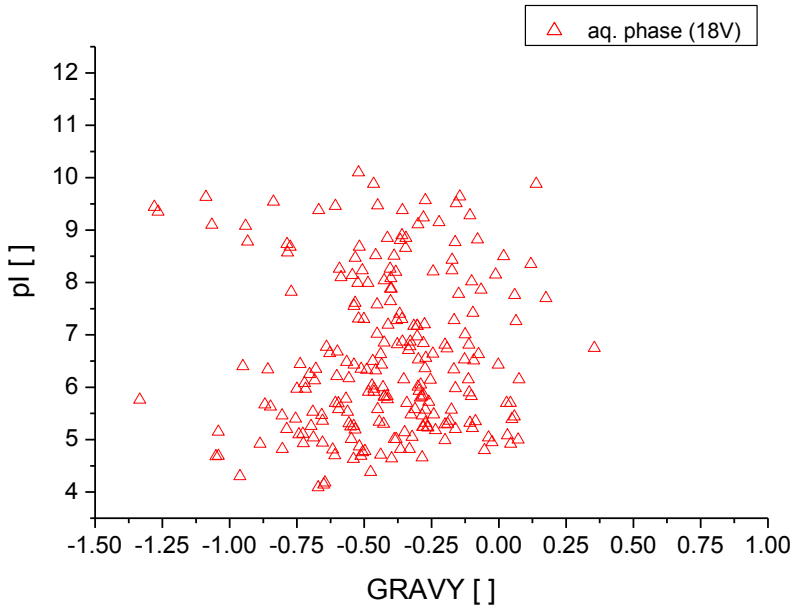

Figure A-19 Plot isoelectric points (pI) of proteins found in the aqueous phase over GRAVY indices, 18 V

A.7.2 Detergent phases, 18 V

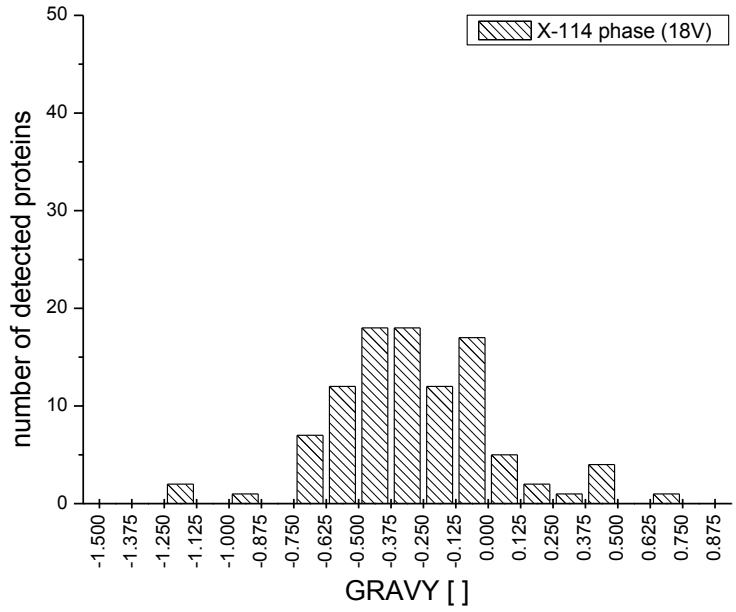

Figure A-20 Plot number proteins found in the detergent phases over GRAVY index ranges of [0.125], 18 V

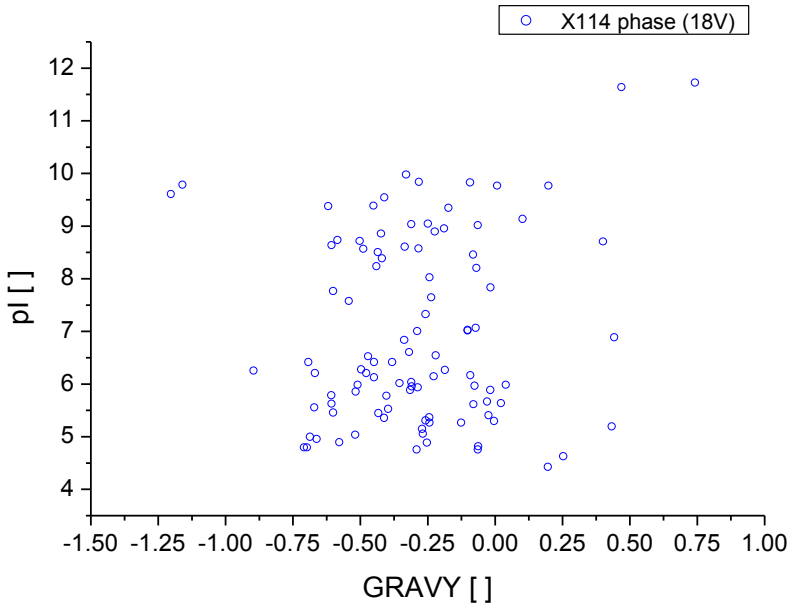

Figure A-21 Plot isoelectric points (pI) of proteins found in the aqueous phase over GRAVY indices, 18 V

A.7.3 Aqueous and detergent phases, 18 V

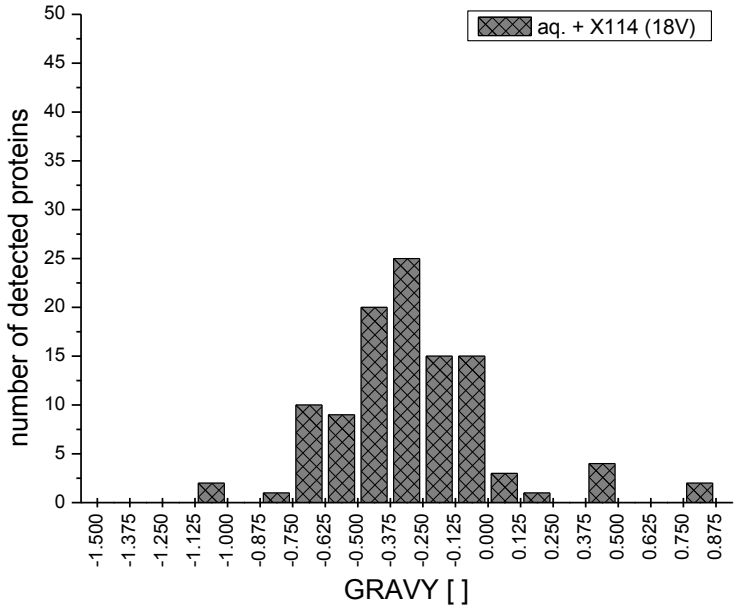

Figure A-22 Plot number proteins found in both the aqueous and detergent phases over GRAVY index ranges of [0.125], 18 V

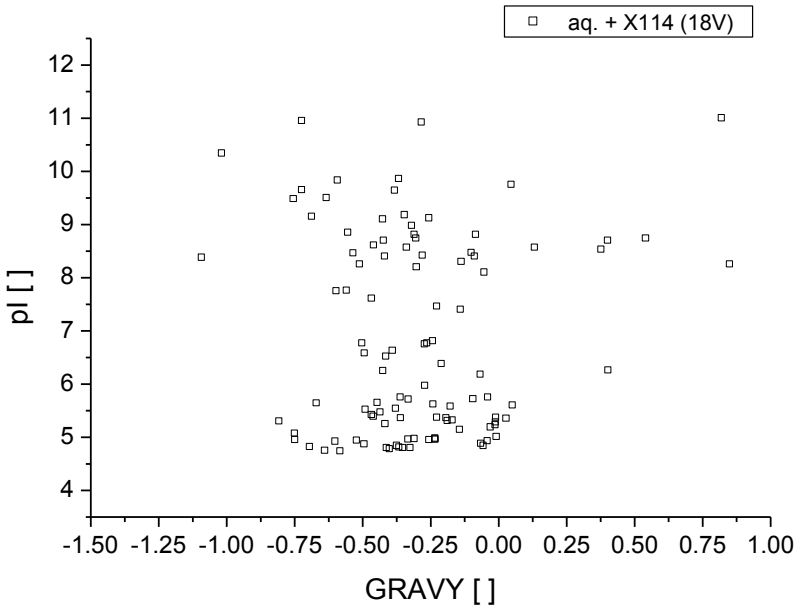

Figure A-23 Plot isoelectric points (pI) of proteins found in the aqueous phase over GRAVY indices, 18 V

A.7.4 Aqueous phases, 43 V

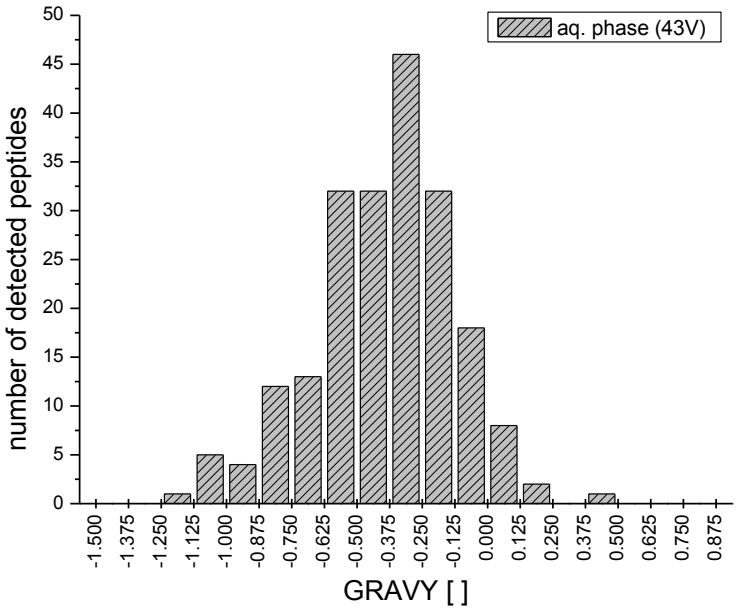

Figure A-24 Plot number proteins found in the aqueous phases over GRAVY index ranges of [0.125], 43 V

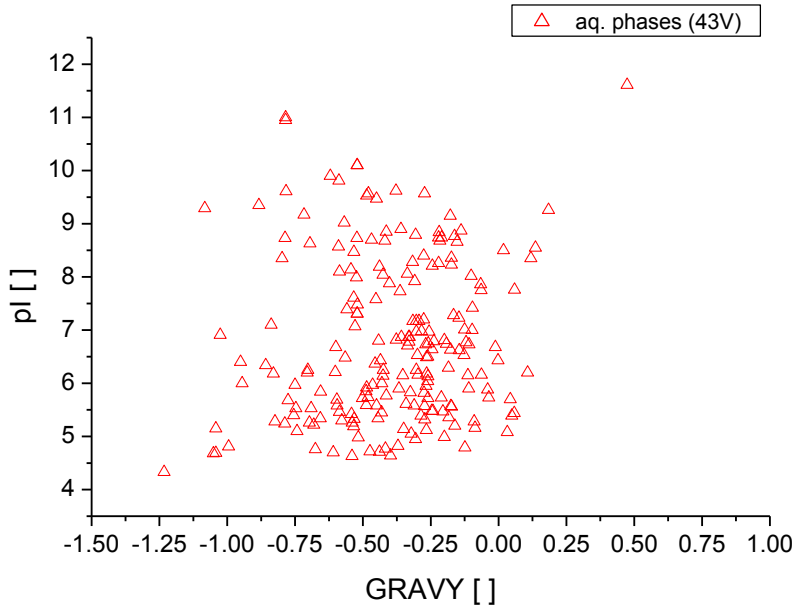

Figure A-25 Plot isoelectric points (pI) of proteins found in the aqueous phase over GRAVY indices, 43V

A.7.5 Detergent phases, 43 V

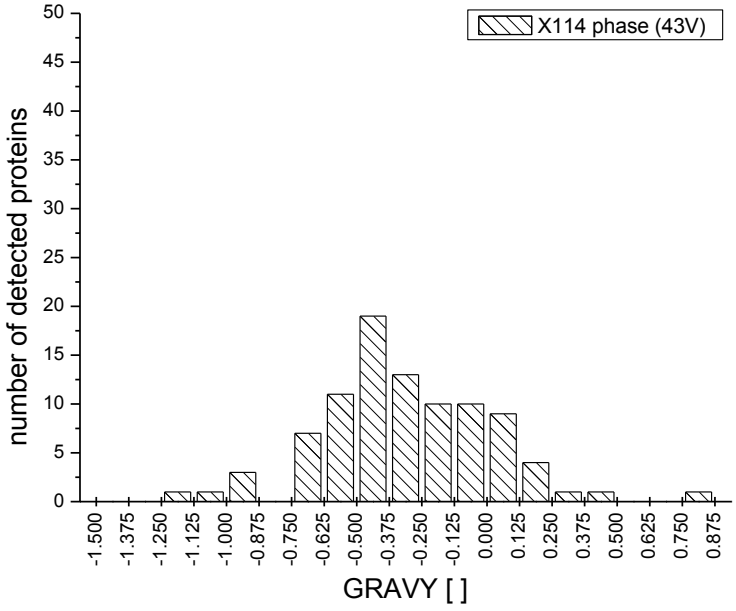

Figure A-26 Plot number proteins found in the detergent phases over GRAVY index ranges of [0.125], 43 V

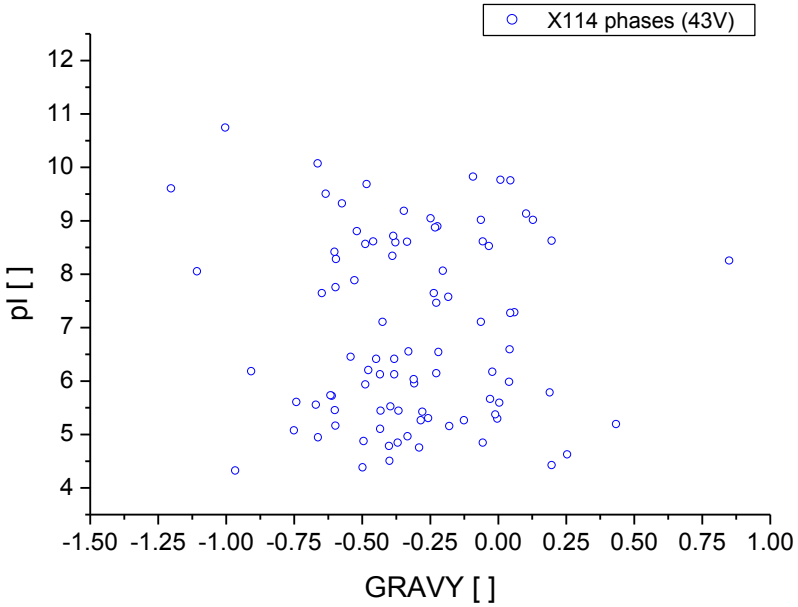

Figure A-27 Plot isoelectric points (pI) of proteins found in the aqueous phase over GRAVY indices, 43V

A.7.6 Aqueous and detergent phases, 43 V

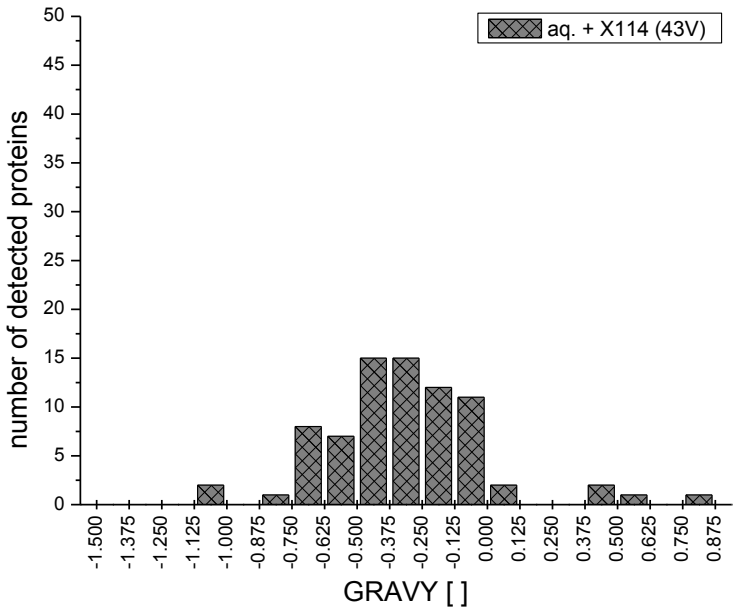

Figure A-28 Plot number proteins found in the aqueous and detergent phases over GRAVY index ranges of [0.125], 43 V

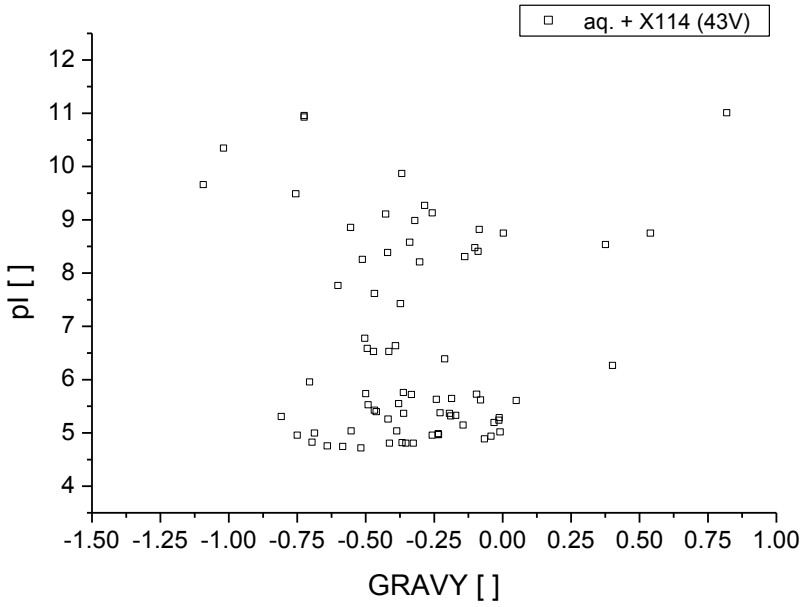

Figure A-29 Plot isoelectric points (pI) of proteins found in the aqueous and detergent phase over GRAVY indices, 43V

A.8 Amyloid β specific FASTA database

Table A-26 Protein sequences included in the amyloid β specific FASTA database (NCBI)

Name	Acc. number	protein sequence
amyloid beta A4 protein isoform 6 precursor [Mus musculus]	311893408	MLPSLALLLLAAWTVRALEVPTDGNAGLLAEPQIAMFCGKLNMHMNVQN GKWESDPSGTKTCIGTKEGILQYCQEVYPELQITNVVEANQPVTIQNWC KRGRKQCKTHTHIVIPYRCLVGEFVSDALLVPDKCKFLHQERMDVCETH LHWHTVAKETCSEKSTNLHDYGMLLPCGIDKFRGVEFVCCPLAEESDSV DSADAEEDDSDVWWGGADTDYADGGEDKVVEVAEEEEVADVEEEEAD DDEDVEDGDEVEEEAEEPYEEATERTTSTATTTTTTTESVEEVVREVCS EQAETGPCRAMISRWYFDVTEGKCVPFFYGGCGGNRNNFDTEEYCMA VCGSVSTQSLLKTTSEPLPQDPDKLPTTAASTPDAVDKYLETPGDENEH AHFQKAKERLEAKHRERMSQVMREWEEAERQAKNLPKADKKAVIQHFQ EKVESLEQEAANERQQLVETHMARVEAMLNDRRRLALENYITALQAVPP RPHHVFNMLKKYVRAEQKDRQHTLKHFEHVRMVDPKKAAQIRSQVMTH LRVIYERMNQSLSLLYNVPAVAEEIQDEVDELLQKEQNYSDDVLANMISE PRISYGNDALMPSLTETKTTVELLPVNGEFSLDDLQPWHPFGVDSVPAN TENEGSGLTNIKTEEISEVKMDAEFGHDSGFEVRHQKLVFFAEDVGSNK GAIIGLMVGGVVIATVIVITLVMLKKKQYTSIHHGVVEVDAAVTPEERHLSK MQQNGYENPTYKFFEQMQN
amyloid beta A4 protein isoform 1 precursor [Mus musculus]	311893401	MLPSLALLLLAAWTVRALEVPTDGNAGLLAEPQIAMFCGKLNMHMNVQN GKWESDPSGTKTCIGTKEGILQYCQEVYPELQITNVVEANQPVTIQNWC KRGRKQCKTHTHIVIPYRCLVGEFVSDALLVPDKCKFLHQERMDVCETH LHWHTVAKETCSEKSTNLHDYGMLLPCGIDKFRGVEFVCCPLAEESDSV DSADAEEDDSDVWWGGADTDYADGGEDKVVEVAEEEEVADVEEEEAD DDEDVEDGDEVEEEAEEPYEEATERTTSTATTTTTTTESVEEVVREVCS EQAETGPCRAMISRWYFDVTEGKCVPFFYGGCGGNRNNFDTEEYCMA VCGSVSTQSLLKTTSEPLPQDPDKLPTTAASTPDAVDKYLETPGDENEH AHFQKAKERLEAKHRERMSQVMREWEEAERQAKNLPKADKKAVIQHFQ EKVESLEQEAANERQQLVETHMARVEAMLNDRRRLALENYITALQAVPP RPHHVFNMLKKYVRAEQKDRQHTLKHFEHVRMVDPKKAAQIRSQVMTH LRVIYERMNQSLSLLYNVPAVAEEIQDEVDELLQKEQNYSDDVLANMISE PRISYGNDALMPSLTETKTTVELLPVNGEFSLDDLQPWHPFGVDSVPAN TENEVEPVDARPAADRGLTTRPGSGLTNIKTEEISEVKMDAEFGHDSGF EVRHQKLVFFAEDVGSNKGAIIGLMVGGVVIATVIVITLVMLKKKQYTSIHH GVVEVDAAVTPEERHLSKMQQNGYENPTYKFFEQMQN
amyloid beta A4 protein isoform 2 precursor [Mus musculus]	47271504	MLPSLALLLLAAWTVRALEVPTDGNAGLLAEPQIAMFCGKLNMHMNVQN GKWESDPSGTKTCIGTKEGILQYCQEVYPELQITNVVEANQPVTIQNWC KRGRKQCKTHTHIVIPYRCLVGEFVSDALLVPDKCKFLHQERMDVCETH LHWHTVAKETCSEKSTNLHDYGMLLPCGIDKFRGVEFVCCPLAEESDSV DSADAEEDDSDVWWGGADTDYADGGEDKVVEVAEEEEVADVEEEEAD DDEDVEDGDEVEEEAEEPYEEATERTTSTATTTTTTTESVEEVVRVPTTA ASTPDAVDKYLETPGDENEHAHFQKAKERLEAKHRERMSQVMREWEE AERQAKNLPKADKKAVIQHFQEKVESLEQEAANERQQLVETHMARVEA MLNDRRRLALENYITALQAVPPRPHHVFNMLKKYVRAEQKDRQHTLKHF EHVRMVDPKKAAQIRSQVMTHLRVIYERMNQSLSLLYNVPAVAEEIQDE VDELLQKEQNYSDDVLANMISEPRISYGNDALMPSLTETKTTVELLPVNG EFSLDDLQPWHPFGVDSVPANTENEVEPVDARPAADRGLTTRPGSGLT NIKTEEISEVKMDAEFGHDSGFEVRHQKLVFFAEDVGSNKGAIIGLMVGG VVIATVIVITLVMLKKKQYTSIHHGVVEVDAAVTPEERHLSKMQQNGYEN PTYKFFEQMQN
amyloid beta A4 protein isoform 5 precursor [Mus musculus]	311893406	MLPSLALLLLAAWTVRALEVPTDGNAGLLAEPQIAMFCGKLNMHMNVQN GKWESDPSGTKTCIGTKEGILQYCQEVYPELQITNVVEANQPVTIQNWC KRGRKQCKTHTHIVIPYRCLVGEFVSDALLVPDKCKFLHQERMDVCETH LHWHTVAKETCSEKSTNLHDYGMLLPCGIDKFRGVEFVCCPLAEESDSV DSADAEEDDSDVWWGGADTDYADGGEDKVVEVAEEEEVADVEEEEAD DDEDVEDGDEVEEEAEEPYEEATERTTSTATTTTTTTESVEEVVREVCS EQAETGPCRAMISRWYFDVTEGKCVPFFYGGCGGNRNNFDTEEYCMA VCGSVFPTTAASTPDAVDKYLETPGDENEHAHFQKAKERLEAKHRERM SQVMREWEEAERQAKNLPKADKKAVIQHFQEKVESLEQEAANERQQLV ETHMARVEAMLNDRRRLALENYITALQAVPPRPHHVFNMLKKYVRAEQK DRQHTLKHFEHVRMVDPKKAAQIRSQVMTHLRVIYERMNQSLSLLYNVP AVAEEIQDEVDELLQKEQNYSDDVLANMISEPRISYGNDALMPSLTETKT TVELLPVNGEFSLDDLQPWHPFGVDSVPANTENEGSGLTNIKTEEISEVK MDAEFGHDSGFEVRHQKLVFFAEDVGSNKGAIIGLMVGGVVIATVIVITLV MLKKKQYTSIHHGVVEVDAAVTPEERHLSKMQQNGYENPTYKFFEQMQ N
amyloid beta A4 protein isoform 3 precursor [Mus	311893404	MLPSLALLLLAAWTVRALEVPTDGNAGLLAEPQIAMFCGKLNMHMNVQN GKWESDPSGTKTCIGTKEGILQYCQEVYPELQITNVVEANQPVTIQNWC KRGRKQCKTHTHIVIPYRCLVGEFVSDALLVPDKCKFLHQERMDVCETH

musculus]		LHWHTVAKETCSEKSTNLHDYGMLLPCGIDKFRGVEFVCCPLAEESDSV DSADAEEDDSDVWWGGADTDYADGGEDKVVEVAEEEEVADVEEEEAD DDEDVEDGDEVEEEAEEPYEEATERTTSTATTTTTTTESVEEVVREVCS EQAETGPCRAMISRWYFDVTEGKCVPFFYGGCGGNRNNFDTEEYCMA VCGSVFPTTAASTPDAVDKYLETPGDENEHAHFQKAKERLEAKHRERM SQVMREWEEAERQAKNLPKADKKAVIQHFQEKVESLEQEAANERQQLV ETHMARVEAMLNDRRRLALENYITALQAVPPRPHHVFNMLKKYVRAEQK DRQHTLKHFEHVRMVDPKKAAQIRSQVMTHLRVIYERMNQSLSLLYNVP AVAEEIQDEVDELLQKEQNYSDDVLANMISEPRISYGNDALMPSLTETKT TVELLPVNGEFSLDDLQPWHPFGVDSVPANTENEVEPVDARPAADRGL TTRPGSGLTNIKTEEISEVKMDAEFGHDSGFEVRHQKLVFFAEDVGSNK GAIIGLMVGGVVIATVIVITLVMLKKKQYTSIHHGVVEVDAAVTPEERHLSK MQQNGYENPTYKFFEQMQN
APP protein [Homo sapiens]	13325112	MLPGLALLLLAAWTARALEVPTDGNAGLLAEPQIAMFCGRLNMHMNVQN GKWDSDPSGTKTCIDTKEGILQYCQEVYPELQITNVVEANQPVTIQNWC KRGRKQCKTHPHFVIPYRCLVGEFVSDALLVPDKCKFLHQERMDVCETH LHWHTVAKETCSEKSTNLHDYGMLLPCGIDKFRGVEFVCCPLAEESDNV DSADAEEDDSDVWWGGADTDYADGSEDKVVEVAEEEEAEVEEEEADD DEDDEDGDEVEEEAEEPYEEATERTTSIATTTTTTT ESVEEVVREKWYKEVHSGQARWLML
H2-Ab1 protein [Mus musculus]	14198219	MALQIPSLLLSAAVVVLMVLSSPGTEGGDSERHFVHQFKGECYFTNGTQ RIRLVTRYIYNREEYLRFDSDVGEYRAVTELGRHSAEYYNKQYLERTRAE LDTACRHNYEETEVPTSLRRLEQPNVAISLSRTEALNHHNTLVCSVTDFY PAKIKVRWFRNGQEETVGVSSTQLIRNGDWTFQVLVMLEMTPHQGEVY TCHVEHPSLKSPITVEWRAQSESARSKMLSGIGGCVLGVIFLGLGLFIRH RSQKGPRGPPPAGLLQ
App protein [Mus musculus]	13529548	NLHDYGMLLPCGIDKFRGVEFVCCPLAEESDSVDSADAEEDDSDVWWG GADTDYADGGEDKVVEVAEEEEVADVEEEEADDDEDVEDGDEVEEEAE EPYEEATERTTSTATTTTTTTESVEEVVREVCSEQAETGPCRAMISRWY FDVTEGKCVPFFYGGCGGNRNNFDTEEYCMAVCGSVSTQSLLKTTSEP LPQDPDKLPTTAASTPDAVDKYLETPGDENEHAHFQKAKERLEAKHRER MSQVMREWEEAERQAKNLPKADKKAVIQHFQEKVESLEQEAANERQQL VETHMARVEAMLNDRRRLALENYITALQAVPPRPHHVFNMLKKYVRAEQ KDRQHTLKHFEHVRMVDPKKAAQIRSQVMTHLRVIYERMNQSLSLLYNV PAVAEEIQDEVDELLQKEQNYSDDVLANMISEPRISYGNDALMPSLTETK TTVELLPVNGEFSLDDLQPWHPFGVDSVPANTENEVEPVDARPAADRG LTTRPGSGLTNIKTEEISEVKMDAEFGHDSGFEVRHQKLVFFAEDVGSNK GAIIGLMVGGVVIATVIVITLVMLKKKQYTSIHHGVVEVDAAVTPEERHLSK MQQNGYENPTYKFFEQMQN
A Chain A, Aqueous Solution Structure Of The Alzheimer's Disease Abeta Peptide (1-42)	109156948	DAEFRHDSGYEVHHQKLVFFAEDVGSNKGAIIGLMVGGVVIA
A Chain A, The Solution Structure Of Rat Ab-(1-28) And Its Interaction With Zinc: Insights Into The Scarity Of Amyloid Deposition In Aged Rat Brain	28374079	XAEFGHDSGFEVRHQKLVFFAEDVGSNX
A Chain A, Solution Structure Of The Methionine-Oxidized Amyloid Beta-Peptide (1-40). Does Oxidation Affect Conformational Switching? Nmr, 10 Structures	159162104	DAEFRHDSGYEVHHQKLVFFAEDVGSNKGAIIGLXVGGVV
D Chain D, 3d Structure Of Alzheimer's Abeta(1-	83754393	DAEFRHDSGYEVHHQKLVFFAEDVGSNKGAIIGLMVGGVVIA

42) Fibrils		
PSN1_HUMAN RecName: Full=Presenilin-1	1709856	MTELPAPLSYFQNAQMSEDNHLSNTVRSQNDNRERQEHNDRRSLGHP EPLSNGRPQGNSRQVVEQDEEEDEELTLKYGAKHVIMLFVPVTLCMVVV VATIKSVSFYTRKDGQLIYTPFTEDTETVGQRALHSILNAAIMISVIVVMTIL LVVLYKYRCYKVIHAWLIISSLLLLFFFSFIYLGEVFKTYNVAVDYITVALLIW NFGVVGMISIHWKGPLRLQQAYLIMISALMALVFIKYLPEWTAWLILAVISV YDLVAVLCPKGPLRMLVETAQERNETLFPALIYSSTMVWLVNMAEGDPE AQRRVSKNSKYNAESTERESQDTVAENDDGGFSEEWEAQRDSHLGPH RSTPESRAAVQELSSSILAGEDPEERGVKLGLGDFIFYSVLVGKASATAS GDWNTTIACFVAILIGLCLTLLLLAIFKKALPALPISITFGLVFYFATDYLVQP FMDQLAFHQFYI
A Chain A, A Partially Folded Structure Of Amyloid-Beta(1 40) In An Aqueous Environment	340780221	DAEFRHDSGYEVHHQKLVFFAEDVGSNKGAIIGLMVGGVV
A Chain A, Alzheimer's Disease Amyloid-Beta Peptide (Residues 10-35)	13096318	YEVHHQKLVFFAEDVGSNKGAIIGLM
A Chain A, The Solution Structure Of Amyloid Beta-Peptide (1-40) In A Water-Micelle Environment. Is The Membrane-Spanning Domain Where We Think It Is? Nmr, 10 Structures	159162102	DAEFRHDSGYEVHHQKLVFFAEDVGSNKGAIIGLMVGGVV
A4_HUMAN RecName: Full=Amyloid beta A4 protein	112927	MLPGLALLLLAAWTARALEVPTDGNAGLLAEPQIAMFCGRLNMHMNVQN GKWDSDPSGTKTCIDTKEGILQYCQEVYPELQITNVVEANQPVTIQNWC KRGRKQCKTHPHFVIPYRCLVGEFVSDALLVPDKCKFLHQERMDVCETH LHWHTVAKETCSEKSTNLHDYGMLLPCGIDKFRGVEFVCCPLAEESDNV DSADAEEDDSDVWWGGADTDYADGSEDKVVEVAEEEEVAEVEEEEAD DDEDDEDGDEVEEEAEEPYEEATERTTSIATTTTTTTESVEEVVREVCSE QAETGPCRAMISRWYFDVTEGKCAPFFYGGCGGNRNNFDTEEYCMAV CGSAMSQSLLKTTQEPLARDPVKLPTTAASTPDAVDKYLETPGDENEHA HFQKAKERLEAKHRERMSQVMREWEEAERQAKNLPKADKKAVIQHFQE KVESLEQEAANERQQLVETHMARVEAMLNDRRRLALENYITALQAVPPR PRHVFNMLKKYVRAEQKDRQHTLKHFEHVRMVDPKKAAQIRSQVMTHL RVIYERMNQSLSLLYNVPAVAEEIQDEVDELLQKEQNYSDDVLANMISEP RISYGNDALMPSLTETKTTVELLPVNGEFSLDDLQPWHSFGADSVPANT ENEVEPVDARPAADRGLTTRPGSGLTNIKTEEISEVKMDAEFRHDSGYE VHHQKLVFFAEDVGSNKGAIIGLMVGGVVIATVIVITLVMLKKKQYTSIHH GVVEVDAAVTPEERHLSKMQQNGYENPTYKFFEQMQN